

University of Warsaw
Faculty of Physics

Jan Henryk Kwapisz

Beyond the Standard Model of particle physics, beyond the cosmological standard model: A Quantum Gravity Perspective.

Supervisor:
prof. dr hab. Krzysztof A. Meissner
Institute of Theoretical Physics
Department of Theory of Particles
and Elementary Interactions

Warsaw, December 2021

Acknowledgements

First and foremost, I would like to express my gratitude to my advisor Krzysztof Meissner for supporting me throughout the years, from the start of my career, and helping me to develop both as a researcher and a human being. His provocative questions and answers, which I often understood years after he phrased them, often challenged my viewpoints and helped me understand more. Thank you!

The second thank you goes to Astrid Eichhorn for hosting me for almost two years at CP3-Origins in Denmark and providing me with a stimulating scientific atmosphere there. Thank you for having your doors always open and answering my questions about science and life.

I want to thank all of the members of the Astrid group not only for doing science together but also for helping me survive the pandemic! Special “thank you” to the CP3-Origins *squad*: Martin, Marc, Christopher, Ludivine, Héloïse, Rafael, Gustavo, Philipp, João, Esben and Juan.

I want to express my thanks to Hermann Nicolai, Piotr Żuchowski and Vahe Gurzadyan for inviting me for scientific stays and allowing me to discover what lies beyond.

I would like to thank all of my current and past collaborators: Sebastian, Rafał, Kamil, Mariusz, Stanisław, Krzysztof, Leszek, Frederic, Michał, Jan, Julia, Oskar, Artur, Tomasz, Zygmunt, Marek, Astrid, Marc, Aaron, Lohan and Przemek. Without you this thesis cannot be written.

I want to thank Astrid, Marc, Aaron, Jan, Lohan, Krzysztof, and Piotr for reading (parts of) this thesis and providing valuable insights which made the text better. Special thanks to Jan Chojnacki and Marc Schiffer for the help with plots and some derivations.

A special thank you goes to Edward for helping me make up my mind towards a Ph.D. To Lucjan for giving me my first ideas on quantum theory. To Piotr for insightful discussions throughout the years and providing his unique notes on QFT, which helped me to understand the essence of renormalization.

Finally, I would like to thank my parents, family, and friends for making this Enterprise possible and to encourage me *to boldly go where no physicist has gone before!*

To all of you: *live long and prosper!*

To my parents

The text below presents my viewpoint on quantum gravity and related topics, yet it is primarily based on published material resulting from collaborations with other scientists. The way the published work is presented expresses my current view on the matter, which significantly changed from when those articles were published. These publications are listed in reversed chronological order, and the sections in which they are discussed are referred to:

- [1] Aaron Held, Jan H. Kwapisz, Lohan Sartore, to appear in 2022, in Sec. 4.1.
- [2] Astrid Eichhorn, Jan H. Kwapisz, Marc Schiffer, The weak-gravity bound in asymptotically safe gravity-gauge systems, 2021, arXiv: 2112.09772, in Sec. 4.3.
- [3] Aaron Held, Jan H. Kwapisz, Lohan Sartore, to appear in 2022, in Chapter 3 and App. A.
- [4] Tomasz Krajewski, Jan H. Kwapisz, Zygmunt Lalak, Marek Lewicki, Stability of domain walls in models with asymmetric potentials, Phys. Rev. D 104, 123522, in Sec. 3.4.
- [5] Jan Chojnacki, Jan H. Kwapisz, Finite Action Principle and Hořava-Lifshitz Gravity: early universe, black holes, and wormholes, Phys. Rev. D 104, 103504, in Ch. 6.
- [6] Jan Chojnacki, Julia Krajecka, Jan H. Kwapisz, Oskar Słowik, Artur Strag, Is asymptotically safe inflation eternal?, JCAP, Volume 2021, April, in Chapter 5.
- [7] Jan H. Kwapisz, Krzysztof A. Meissner, Asymptotic safety and quantum gravity amplitudes, 2021, Nuclear Physics B Vol 965, 115341, in Sec. 2.4.
- [8] Jan H. Kwapisz, Asymptotic safety of gravity, the Higgs boson mass and beyond the Standard Model physics, 2019, Phys. Rev. D 100, 115001, in Sec. 4.2.2.
- [9] Frederic Grabowski, Jan H. Kwapisz, Krzysztof A. Meissner, Asymptotic safety and Conformal Standard Model, 2018, Phys. Rev. D 99, 115029, in Sec. 4.2.2.
- [10] Jan H. Kwapisz, Krzysztof A. Meissner Conformal Standard Model and Inflation, 2018 Acta Physica Polonica B, in Sec. 5.2.1.
- [11] Sebastian M. Dawid, Rafał Gonsior, Jan H. Kwapisz, Kamil Serafin, Mariusz Tobolski, Stanisław D. Głazek Renormalization group procedure for potential $-g/r^2$ 2018, Physics Letters B, in Sec 2.1.3.

I am also author of the following articles, preprints and conference proceedings:

- [12] Jan Chojnacki, Jan H. Kwapisz, Finite Action Principle and wormholes, 2021, proceedings of 16th Marcel Grossmann Meeting, accepted, to be published in International Journal of Modern Physics D.
- [13] Jan H. Kwapisz, Leszek Stolarczyk, Applications of Hückel-Su-Schrieffer-Heeger method. I. Carbon-carbon bond lengths in polycyclic benzenoid hydrocarbons, Structural Chemistry 2021.
- [14] Frederic Grabowski, Jan Kwapisz, Asymptotic safety, cosmology and Conformal Standard Model, proceedings of 15th Marcel Grossmann Meeting.

Abstract

We study the quantum gravity imprint on particle physics and cosmological phenomena. We show that combining particle physics and cosmology with quantum gravity results in non-trivial conditions on the low energy theories and quantum gravity models.

We discuss how the Grand Unified Theories can be UV-completed by quantum gravity at the Planck scale in a model-independent way. This results in a set of conditions that constrain the possible parameter space stemming from UV-completion by quantum gravity. We find that within the studied model the deepest minima are either non-Standard Model like or require large threshold corrections to realize the Standard Model as low energy theory. For models with multiple vacua, we study the domain walls' evolution depending on the initial conditions and shape of the potential.

In the cosmological setting, we elaborate on the path integral formulation of quantum gravity. We show that for the Hořava-Lifshy gravity, the non-flat and non-homogenous cosmologies do not contribute to the Euclidean path integral. On the other hand, we show that Hořava-Lifshy gravity satisfies the finite-action selection principle, that has been proposed as a model independent solution of the black hole singularities.

Our study of Grand Unified Theories within the asymptotically safe approach points out towards “transplanckian” breaking and hence proton stability under certain assumptions. On the other hand, in the Standard Model, the asymptotic safety constrains the Higgs mass to take the smallest value such that the electroweak vacuum is stable. Considering the current top quark mass measurements, this value is $m_H \approx 130$ GeV, five GeV above the experimental value. Here we consider the predictions of the Higgs mass in various Beyond Standard Model scenarios, where this prediction can be improved. As we show, the inclusion of new $U(1)$ symmetry can potentially give the correct prediction for this mass.

Then we discuss the Weak Gravity Bound in the Abelian vector field system, limiting the gravitational fluctuations' strength. We find that the bound does not restrict the number of vector species, unlike the scalar case. We investigate the gauge invariance of the results.

The (no) eternal inflation principle has been put forward based on swampland considerations in string theory. The natural question arises whether similar conditions hold in other approaches to quantum gravity. We consider asymptotic safety models with and without gravity in the context of eternal inflation. The existence of UV fixed point generically flattens the potential, and our findings suggest no tension between eternal inflation and asymptotic safety in contradistinction to string theory.

Within the text, we also discuss various caveats of the formulation of asymptotically safe gravity, provide specific examples for asymptotic safety in quantum mechanics and discuss the possible connections between asymptotic safety and string theory.

Tytuł pracy w języku polskim

Fizyka poza Modelem Standardowym Cząstek Elementarnych, poza Standardowym Modelem Kosmologicznym: Perspektywa kwantowo-grawitacyjna.

Streszczenie

W tej pracy omawiamy wpływ grawitacji kwantowej na fizykę cząstek elementarnych i kosmologię. Połączenie grawitacji kwantowej z modelami fizyki cząstek elementarnych i kosmologicznymi skutkuje nietrywialnymi warunkami na niskoenergetyczne teorie i teorie kwantowo grawitacyjne.

Teorie Wielkiej Unifikacji połączone z grawitacją kwantową, muszą spełnić zaproponowanych przez nas zestaw warunków, które ograniczają przestrzeń parametrów wynikającą z tego połączenia. Jak pokazaliśmy na przykładzie najgłębsze minima albo nie prowadzą do Modelu Standardowego, albo wymagają dużych poprawek progowych. Dla modeli o wielu możliwych wartościach oczekiwanych próżni zbadaliśmy ewolucję ścian domenowych w zależności od warunków początkowych i kształtu potencjału.

Następnie analizujemy teorie wielkiej unifikacji w połączeniu z asymptotycznie bezpieczną grawitacją. Jak pokazujemy potencjał teorii staje się niestabilny poniżej skali Plancka, co wskazuje na stabilność protonów. Z drugiej strony w Modelu Standardowym asymptotyczne bezpieczeństwo ogranicza masę bozonu Higgsa w Modelu Standardowym. Jak pokazujemy wartość ta wynosi $m_H \approx 130$ GeV, jest zatem wyższa od wartości eksperymentalnej. W pracy rozważamy przewidywania masy Higgsa w ramach fizyki poza Modelem Standardowym, w ramach asymptotycznego bezpieczeństwa. Wprowadzenie nowej grupy $U(1)$ skutkuje poprawnym przewidywaniem masy Higgsa. Połączenie grawitacji z materią nakłada ograniczenia na siłę oddziaływanego grawitacyjnego, tak zwane ograniczenie słabej grawitacji (WGB). W pracy pokazujemy, że to ograniczenie nie wpływa na liczbę cząstek wektorowych sprzężonych do grawitacji. Pokazujemy niezmienność cechowania otrzymanych wyników.

W pracy zadajemy pytanie, czy zaproponowaną w oparciu o rozważania w teorii strun zasadę (nie)-wiecznej inflacji można wprowadzić w innych podejściach do grawitacji kwantowej. Jak pokazujemy w modelach asymptotycznie bezpiecznych istnienie punktu stałego spłaszcza potencjał, co sugeruje brak sprzeczności między wieczną inflacją a asymptotycznym bezpieczeństwem.

Następnie omawiamy wnioski ze sformułowania grawitacji kwantowej w ramach całek po trajektoriach. Pokazujemy, że dla grawitacji Hořavy-Lifszycza w układach kosmologicznych kosmologie niepaskie i niejednorodne nie dają wkładu do euklidesowej całki po trajektoriach. Z drugiej strony udowadniamy, że grawitacja Hořavy-Lifszycza spełnia zasadę selekcji skończonego działania, która została zaproponowana jako rozwiązanie problemu osobliwości czarnych dziur w ramach całki po trajektoriach.

W tekście omawiamy również różne problemy dotyczące sformułowania asymptotycznie bezpiecznej grawitacji, przedstawiamy przykłady asymptotycznego bezpieczeństwa oraz omawiamy możliwe związki między asymptotycznym bezpieczeństwem a teorią strun.

Contents

Synopsis of the results	6
I The quantum gravity perspective	9
1. Introduction	11
1.1. Singularities and quantum theory	11
1.1.1. General Relativity and singularities	12
1.2. Quantum gravity approaches	15
1.2.1. Hořava-Lifshyc gravity	15
1.2.2. String-theory	17
1.2.3. Asymptotic safety programme	18
1.3. Standard Model and beyond	18
1.3.1. Overview of the Standard Model	18
1.3.2. Beyond the Standard Model	23
1.4. Λ -CDM and beyond	26
1.4.1. Λ -CDM model	26
1.4.2. Inflation	28
II Renormalization and quantum gravity	33
2. Renormalization group techniques and the asymptotic safety program	35
2.1. The renormalization group	35
2.1.1. Perturbative renormalization	35
2.1.2. Renormalisation group	38
2.1.3. Wilsonian renormalization	40
2.1.4. Functional renormalization Group	45
2.2. Asymptotic safety in quantum gravity	46
2.3. Scale identification for μ and k	50
2.3.1. Dimensionless couplings	50
2.3.2. Scale identification in asymptotic safety	51
2.4. Is string-theory asymptotically safe?	52
2.4.1. Running in terms of amplitudes.	52
2.4.2. Veneziano amplitude	52
3. Quantum Gravity as an UV completion	54
3.1. Quantum gravity as UV completion	54
3.2. Analysis of the model: minimal SO(10)	55

3.2.1. SO(10) with fermionic $\mathbf{16}_F$ and scalar $\mathbf{45}_H \oplus \mathbf{16}_H$	55
3.3. The Results	57
3.3.1. The results: The $\mathbf{45}_H$ model	57
3.3.2. The Results: The $\mathbf{16}_H \oplus \mathbf{45}_H$ model	60
3.4. Degeneracy of minima and Domain Walls formation	63
3.4.1. Domain walls formation	63
3.4.2. The potential and dynamics	63
3.4.3. Simulation and results	65
4. Asymptotically safe quantum gravity phenomenology	69
4.1. Unified Asymptotic Safety	69
4.1.1. A minimal SU(5) model	69
4.1.2. The asymptotic safety fixed points and potential breaking	70
4.2. Asymptotic safety and Higgs mass	73
4.2.1. Higgs mass prediction in the Standard Model	73
4.2.2. Higgs mass prediction Beyond the Standard Model	74
4.2.3. The θ_{QCD} and asymptotic safety	77
4.3. U(1) vector bosons and Weak Gravity Bound	78
4.3.1. Weak gravity bound	78
4.3.2. Single gauge system	79
4.3.3. Weak gravity bound for more than one gauge field	81
4.3.4. Gauge dependence	82
III Quantum gravitational cosmology	85
5. Eternal Inflation	87
5.1. Eternal Inflation	87
5.1.1. How inflation becomes eternal?	87
5.1.2. Tunelling and eternal inflation	90
5.1.3. Starobinski eternal inflation	92
5.2. Eternal inflation beyond the Standard Model	93
5.2.1. Inflation in Conformal Standard Model	93
5.2.2. Alpha-attractors	95
5.3. Can Asymptotically Safe Inflation be eternal?	96
5.3.1. Renormalisation group improved Starobinski	96
5.3.2. Inflation in the Veneziano limit	98
6. Finite Action Principle	102
6.1. Cosmological Singularities and Finite Action Principle	103
6.2. Black holes and Finite Action Principle	106
6.2.1. Singular black holes	106
6.2.2. Regular black holes	108
6.3. Wormholes and Finite Action Principle	108
7. Conclusions, future directions	110
7.1. Conclusions	110
7.2. Outlook	112

Appendices	114
A. Effective potential and the breaking scale	114
A.1. Renormalisation group-improved 1-loop potential	114
A.2. Minimisation of the RG-improved potential	116
A.3. Breaking patterns triggered by the RG-flow	118
B. $SO(10)$ appendix	119
B.1. Conventions	119
B.2. Potential for $\mathbf{10}_H \oplus \mathbf{16}_H \oplus \mathbf{45}_H$ model	120
C. Beta functions	120
C.1. Beta functions of the $SO(10)$ $\mathbf{10}_H \oplus \mathbf{45}_H \oplus \mathbf{16}_H$ model	120
C.2. Beta functions of the $SU(5)$ model	121
Bibliography	122

List of Figures

1.1.	Running of couplings in the Standard Model	22
1.2.	Breaking steps of the $SO(10)$	25
1.3.	Quantum jumps in eternal inflation	32
2.1.	Limit cycle for $1/r^2$ potential	42
2.2.	Dependence on l	43
2.3.	The position of the gravitation fixed point depending on N_V for $\beta_h = 1$	49
3.1.	The deepest minima of the $\mathbf{45}_H$ potential.	58
3.2.	The depths of the minimas given $\lambda_1(M_P), \lambda_2(M_P)$	59
3.3.	The scale of breaking towards $SU(5) \times U(1)$ vacua.	60
3.4.	The viable vs non-viable parameter space for $\mathbf{45}_H \oplus \mathbf{16}_H$ model.	61
3.5.	Breaking directions in $\mathbf{45}_H \oplus \mathbf{16}_H$	62
3.6.	Shape of potentials to be studied in the domain wall evolution.	65
3.7.	Dependence of the decay time $\eta_{dec} - \eta_{start}$ on δV and $d3V$	66
3.8.	Dependence of the decay time $\eta_{decay} - \eta_{start}$ on δV	67
3.9.	Dependence of the decay time $\eta_{decay} - \eta_{start}$ on $d3V$ and the mean value	68
4.1.	Asymptotic safety and $SU(5)$	71
4.2.	Asymptotic safety and $SO(10)$	72
4.3.	$\lambda(M_{\text{top}})$ for KSVZ model	76
4.4.	Higgs mass in the Z' model.	78
4.5.	The weak gravity bound for the one-gauge system.	81
4.6.	The weak gravity bound for the systems with increasing number of gauge fields.	82
4.7.	The WGB in a function of N_V and β_h	83
4.8.	WGB in the $\beta_h = 0$ case.	84
5.1.	Eternal inflation and tunnelling	91
5.2.	Starobinski model and eternal inflation	93
5.3.	Alpha attractors and eternal inflation	96
5.4.	RG improved Starobinski and eternal inflation	97
5.5.	Eternal inflation and Veneziano limit	99
5.6.	Tunnelling in eternal inflation: parameter dependence.	100
5.7.	Tunnelling in eternal inflation: probabilities.	101

List of Tables

3.1.	Stability conditions for the model $\mathbf{45}_H \oplus \mathbf{16}_H$	56
3.2.	Summary of the considered breaking chains for SO(10) group.	57
4.1.	Stability of the SU(5) potential at the Planck scale.	71
5.1.	Minimal values of the radial part of inflation potential.	94

Synopsis of the results

There are no prospects to find quantum gravity directly in scattering experiments¹. The particle accelerator obtaining center-of-mass energies of the order of Planck mass is far beyond reach². Does it mean that quantum gravity research cannot be successful?

In this thesis, we shall argue that quantizing gravity profoundly impacts “what can happen” within the realm of particle, black holes, and cosmological physics. On the other hand “matter and cosmology matters” [22] for the consistency of the quantum gravity approaches. In string theory, the swampland program investigates the possible set of low-energy theories, so-called effective field theories (EFTs), which can be embedded into string theory as UV completion. While this program is currently heavily developed within the stringy community³, other approaches “stayed behind”. The purpose of this dissertation is to “bridge the gap” and investigate the realm of possible EFTs coupled to quantum gravity from the perspective of other approaches and the agnostic, model-independent way. Finally we are interested to what degree the swampland criteria stemming from string theory are robust for other quantum gravity approaches. In the thesis on top of string theory we consider Hořava-Lifshyc gravity and asymptotic safety.

In Part I, we point out that quantum gravity, cosmology, and particle physics are “three friends in need”. The arguments stemming from quantum gravity approaches can narrow down the possible EFT space, while particle physics and cosmology combined with quantum gravity can give unique signatures for various approaches. Together with gathering experimental data, this strategy seems feasible to find quantum gravity imprints. In Sec. 1.1 we review the singularities of classical gravity and point out difficulties when quantizing gravity. We review the arguments against the standard perturbative quantization of general relativity. Then we discuss three quantum gravity approaches that appear in the thesis: Hořava-Lifshyc gravity, string theory, and asymptotic safety. In Sec. 1.3 we review the Standard Model and its problems, pointing out the quantum gravity perspective on solving some of them. In Sec. 1.4 we discuss the Λ -CDM cosmology and its initial conditions in the context of inflation. Then we discuss eternal inflation and possible quantum gravity perspective on the matter.

In Part II we discuss the concept of the renormalization group, its consequences for quantum gravity, and possible particle physics phenomenology stemming from the behavior of the renormalization group flow. In Chapter 2 we discuss the renormaliza-

¹In this thesis, we do not discuss the quantum gravity at electroweak scale stemming from extra dimensions or the UV-IR correspondence, see [15, 16, 17, 18, 19, 20].

²It would probably cost more than one Death Star, which cost has been estimated as 10^{21} \$[21].

³By 31/03/2021 the 394 articles have been released with swampland in the title or abstract[23].

tion group techniques, the notion of effective action and effective potential, as well as the asymptotic safety program, which would prove crucial for Chapters 3 and 4. In Sec. 2.1.1 we discuss the origin of the requirement of renormalization in the perturbative QFT and its connection to the S-matrix. The complementary, Wilsonian approach is illustrated in the example of $1/r^2$ potential in Sec 2.1.3. The modern formulation of the asymptotic safety program via Functional renormalization is discussed in Sec. 2.2. In Sec. 2.3.1 we review the essential concept of the scale identification and renormalization group improvement of the effective potential, which would be crucial in Chapter 3. The more detailed discussion on the Renormalization Group improvement in the context of Grand Unified Theories will be provided in [3] and Appendix A, where we introduce a new algorithm for “optimal” renormalization group improvement. The discussion of the connection between the renormalization scale and physical scales in Sec. 2.3.2 and the recent critique of the asymptotic safety program [24] bring us to the cross approaches question: *Can string-theory be asymptotically safe?* discussed in Sec. 2.4. In Sec. 2.4 we provide a set of conditions on the S matrix amplitudes that asymptotically safe theories should satisfy and show that string theory satisfies those. On the other hand, checking the discussed four graviton amplitudes haven’t been calculated in the asymptotic safe approach and it is important for the development of the program to understand the UV behavior of the graviton amplitudes, as Weinberg postulated [25, 25, 26].

In Chapter 3 we discuss the model-independent viewpoint on quantum gravity and its constraints on particle physics. We assume that any quantum gravity theory should set the couplings’ values at the Planck scale. Then we impose the minimalistic requirements: stability of the potential at the Planck scale, lack of Landau poles in the renormalization group flow, and the emergence of the Standard Model as the low-energy theory. Those requirements significantly restrict the possible space of couplings. We introduce a general blueprint of how to study Grand Unified Theories (GUT) within our paradigm. Then we illustrate our idea on the example of SO(10) GUT with $\mathbf{16}_H \oplus \mathbf{45}_H$ having admissible breaking chains towards the Standard Model. We show that the deepest minima of the potential are either non-viable or require large threshold corrections to reproduce the Standard Model. Our work is the first to study the non-viable minima beyond the tree level in the literature and the first one to construct the renormalization group improved potential for the GUT, for related studies see [27, 28, 29]. In Sec. 3.4 we discuss the domain-wall formation depending on the properties of the potential and initial conditions. In particular, we show that, when the minima of a theory, such as GUT, are degenerate, they can form long-living domain walls that tend to dominate the Universe.

In Chapter 4 we extend the conditions from Chapter 3 by the requirements stemming from the asymptotic-safety paradigm. We show that those pose further constraints on the EFT space of models. In Sec. 4.1 we look again at GUTs from the asymptotic safety perspective. We discuss the possibility of “transplanckian breaking” of the GUT gauge group and proton stability within the asymptotic safety framework. Then, due to “transplanckian breaking”, we shift our focus towards the minimalistic models. In particular, we discuss the possible minimal Standard Model extensions that are consistent with the asymptotic safety, can solve the other mysteries of the Standard Model, and give the correct Higgs mass prediction. Out of the three models we study, we show that gauging the $U(1)_{B-L}$ symmetry might be sufficient to reproduce the correct Higgs

mass in the asymptotically safe paradigm. The other studied models are Conformal Standard Model and the model with uncharged quarks. In Sec. 4.2.3 we briefly discuss the possible resolution of the strong CP problem within asymptotic safety. In Sec. 4.3 we investigate consequences of coupling matter to asymptotically safe gravity resulting in restricting the gravitational parameter space as well as the possible particle content. We will show that when coupling vector fields to AS quantum gravity the gravity has to be sufficiently weak and its fixed points have to lie below the Weak Gravity Bound. We show that for any number of U(1) gauge bosons the gravity fixed points are compatible with this bound. In particular, we discover that systems with 12 gauge fields (like the Standard Model) are compatible with the Weak Gravity Bound within the background approximation. Furthermore, we test the gauge invariance of our results in Sec. 4.3.4. This is a crucial result since the calculations rely on gauge-dependent effective action.

In Part III we address questions of fundamental importance: detection of quantum gravity signatures in the context of (eternal) inflation and the fate of singularities in quantum gravity. In string theory, the no-eternal eternal inflation principle has been proposed [30]. Here we study its robustness across the quantum gravity approaches. In Chapter 5 we discuss (eternal) inflation stemming from BSM scenarios and eternal inflation in the context of asymptotic safety. In particular, we investigate eternal inflation for exemplary models: Starobinski inflation, the models with non-minimal couplings to gravity, as well as the alpha-attractors. In Sec. 5.3 we discuss the question: *Can Asymptotically Safe Inflation be eternal?* on two models: the RG-improved Starobinski action and the $SU(N)$ Yang-Mills theory in the Veneziano limit. We show that the existence of UV fixed point generically flattens the potential, and our findings suggest no tension between eternal inflation and asymptotic safety. In Sec. 5.1.2 we introduce a new type of eternal inflation scenario for the multi-minima models: eternal inflation by tunneling and illustrate that for the $SU(N)$ Yang-Mills theory in the Veneziano limit in Sec 5.3.2. In this chapter also we discuss a bunch of popular inflationary models, in particular we introduce the non-minimal couplings within the Conformal Standard Model, providing a successful inflationary scenario.

In Chapter 6 we deduce the fate of singularities from the path-integral approach, assuming that action is fundamental instead of the metric. Resulting Finite Action Principle [31, 32, 33] proposes that only finite action metrics should “matter”. In the cosmological context, in Sec 6.1, we show that the requirement of the Finite Action provides an isotropic, flat, and accelerating early universe for the Hořava-Lifszyc (H-L) gravity⁴. Furthermore, in Sec 6.2 we discuss that requirement of finite action for the H-L gravity selects only the regular black-hole spacetimes, thus resolving the singularity issue for black holes. In Sec. 6.3 we comment on the possibility of traversable wormholes in theories with higher curvature invariants. Our results reveal that Finite Action Principle predictions are robust for various quantum gravity approaches [31, 32, 33].

⁴Asymptotic safety calculations deal with the effective action thus reconstructing the microscopic action (by microscopic we mean the action in the exponent of the path integral) is highly non-trivial [34]. On the other hand H-L gravity has a well-defined microscopic action and is unitary.

Part I

The quantum gravity perspective

Chapter 1

Introduction

Where we discuss the broader context for our work. We discuss how the singularities of classical theories had been resolved in the past. We discuss the singularities within general relativity together with (non)-renormalizability properties of the theory. We discuss three approaches towards quantizing gravity: Horava-Lifshyc, asymptotic safety, and string theory.

We review the problems of the current fundamental physics, both in particle and cosmological physics. We offer a quantum gravity perspective on that matter.

1.1. Singularities and quantum theory

Around 1899 all of the physics (now called classical) fell under paradigms of mechanics, electrodynamics, and statistical physics. Most problems seemed to be solved, and “only what is left is to use physics for engineering”. Nevertheless, a couple of issues remained: the stability of atoms and ultraviolet catastrophe in the black body spectrum were among those. At the time, they seemed marginal and “will be solved within a decade at most”. However, as it turned out, “There is Plenty of Room at the Bottom” [35]. Below, we briefly discuss the stability of atoms and ultraviolet catastrophe, how they pose problems to classical physics due to singular behavior, and how quantum physics has overcome them.

Ultraviolet catastrophe The black body is an idealized object that absorbs all the electromagnetic radiation. In thermal equilibrium, it emits black body radiation. The radiation properties of most of the materials and the Sun approximates as black body spectrum. Based on arguments stemming from classical physics [36, 37] the Rayleigh-Jeans law has been derived connecting the frequency ν , temperature T and power emitted per unit surface $f(\nu, T)$:

$$f(\nu, T) = 2 \frac{\nu^2}{c^2} k_B T, \quad (1.1)$$

where k_B is the Boltzmann constant, and c is the speed of light. The law well approximates the black-body spectrum for low frequencies. On the other hand, the law predicts that the maximum of the spectrum should be at far UV, where the frequencies become large, and the power becomes infinite as $\nu \rightarrow \infty$. This behavior was in clear contradistinction with experiment and has been called ultraviolet catastrophe since the radiation cannot be infinite. To solve this problem, in 1900, Max Planck modeled

the black body as oscillators in a cavity and proposed that those oscillators can only change their energy by the multitude of $h\nu$, where h is now called Planck constant [38]. He then derived the law (now called the Planck law):

$$f(\nu, T) = \frac{2h\nu^3}{c^2} \frac{1}{e^{h\nu/(k_B T)} - 1}. \quad (1.2)$$

The (1.2) not only fitted the experimental data perfectly but also resolved the UV catastrophe problem. The described mechanism is one example of how quantum theory tamed singularity. Later developed quantum theory reproduced the Planck law utilizing Bose-Einstein statistics for photon gas.

Stability of atoms At the dawn of the XX century, Thompson [39]. Then Rutherford experiments [40] established that atoms do consist of subatomic entities: negatively charged electrons, orbiting around positively charged tiny nuclei. Based on that observations, a new puzzle arises. Why are the atoms stable? From the point of view of classical electrodynamics, the electron should fall onto the nucleus radiating away all of the energy, such that the time of fall estimate is

$$t_{\text{fall}} \approx 1.6 \times 10^{-11} \text{s}. \quad (1.3)$$

Furthermore, the classical theory predicts that the atoms seemed to radiate their energies in the discrete lines, characteristic for a given atom, rather than continuous spectra. As a remedy, Niels Bohr proposed his famous planetary model [41]. Bohr assumed that electrons could move only on certain orbits (geostationary orbits) such that the angular momentum is quantized $L = n\hbar$, where n is the natural number and $\hbar = h/(2\pi)$. On that orbits, electrons do not radiate. They only radiate when they switch between the orbits. That model solved the stability question for the hydrogen atom. Later, to describe other atoms, the full formalism of the quantum theory has been developed based on de-Broglie [42], Heisenberg [43] and Schrödinger works [44]. In particular, the solution to the Schrödinger equation for the hydrogen atom for the 1s orbital is given by

$$\psi_{1s}(r) = \frac{1}{\sqrt{\pi a_0^{3/2}}} e^{-r/a_0}, \quad (1.4)$$

and the probability density is

$$P(r)dr = 4\pi r^2 |\psi_{1s}(r)|^2 dr \quad (1.5)$$

the maximum is at $r = a_0$ the Bohr radius of the first orbit! On the other hand, the probability distribution for the electron in classical electrodynamics will quickly approximate Dirac delta peaked at 0. Once again, the quantum theory saved us from singularities!

1.1.1. General Relativity and singularities

The singularities also occur in General Relativity, the classical theory of spacetime. The spacetime, a collection of reparametrization equivalent Lorentzian manifolds [45], is bounded to obey Einstein equations

$$R_{\mu\nu} - \frac{1}{2}g_{\mu\nu}R = \frac{8\pi G}{c^4}T_{\mu\nu}, \quad (1.6)$$

where $T_{\mu\nu}$ is the energy momentum tensor of matter [45]. The gravitational part of the equations stems from the Einstein-Hilbert action:

$$S = \frac{1}{8\pi G} \int d^4x \sqrt{-g} (R - 2\Lambda), \quad (1.7)$$

Λ being the cosmological constant. The two most celebrated solutions: the black hole and the solution for the whole Universe, the FLRW metric, both contain singularities. Let us take a closer look into those.

Singularities in black holes The Schwarzschild solution is:

$$ds^2 = - \left(1 - \frac{r_s}{r}\right) dt^2 + \left(1 - \frac{r_s}{r}\right)^{-1} dr^2 + r^2 d\theta^2 + r^2 \sin \theta^2 d\phi^2, \quad (1.8)$$

where we use $c = 1$ and $r_s = 2GM$, M is the mass of the central object. The metric has singularities at $r = r_s$ and at $r = 0$. The singularity at $r = 2GM$ is so called *coordinate singularity* [46] and can be removed with a proper coordinate transformation, for example:

$$dt_{PG} = dt + \frac{\sqrt{2Mr}}{r - 2M} dr. \quad (1.9)$$

The resulting Painleve-Gullstrand metric is regular at $r = r_s$:

$$ds^2 = -dt_{PG}^2 + \left(dr - \sqrt{\frac{2M}{r}} dt_{PG} \right)^2 + r^2 d\Omega^2, \quad (1.10)$$

On the other hand, the singularity at $r = 0$ represents a *physical singularity*, since (some of) the curvature invariants, like Kretschmann invariant:

$$R_{\mu\nu\rho\sigma} R^{\mu\nu\rho\sigma} = \frac{48G^2 M^2}{r^6} \xrightarrow[r \rightarrow 0]{} \infty, \quad (1.11)$$

become divergent. The Schwarzschild solution is a final state of spherical gravitational collapse [47, 48] and according to Hawking-Penrose theorems, a black hole state is generic for gravitational collapse such that the singularity forms [45, 49, 50]. Nevertheless, the singularity at $r = 0$ is hidden beyond the event horizon; hence it does not affect any outside observer. It has been proposed that Nature always hides the singularities; hence the “naked” singularity can never be observed [51]. The other black hole solutions in General Relativity, like the Kerr, Reissner-Nordstrom, or Kerr-Newman metric, are singular at $r = 0$.

Singularities in cosmology The other famous solution of Einstein gravity is the Friedman-Lemaître-Robertson-Walker [52, 53, 54, 55] metric describing the homogeneous and isotropic Universe

$$ds^2 = [dt^2 - a^2(t)h_{ij}dx^i dx^j]. \quad (1.12)$$

The non-vanishing components of h_{ij} are:

$$h_{11} = \frac{1}{1-kR^2}, \quad h_{22} = R^2, \quad h_{33} = R^2 \sin^2 \theta \quad (1.13)$$

and k denotes the spatial curvature of the metric. On the FLRW background the Einstein equations (1.6) reduces to the Friedman equations

$$H^2 = \left(\frac{\dot{a}}{a}\right)^2 = \frac{8\pi G}{3}\rho - \frac{k}{a^2}, \quad \frac{\ddot{a}}{a} = -\frac{4\pi G}{3}(\rho + 3p) \quad (1.14)$$

for energy-momentum tensor of perfect fluid $T_{\mu\nu} = \rho u_\mu u_\nu + p(u_\mu u_\nu + g_{\mu\nu})$ with ρ energy density, p pressure and u_μ the velocity, satisfying the continuity equation

$$\nabla^\mu T_{\mu\nu} = \dot{\rho} + 3H(\rho + p) = 0. \quad (1.15)$$

It was shown by Stephen Hawking in [56] that the Universe evolved back according to (1.14), similarly as for black holes, results in the initial singularity as long as $\Lambda = 0$ and the strong energy condition holds

$$\rho + 3p > 0. \quad (1.16)$$

If $\rho = wp$, the proportionality coefficient w is called barotropic parameter. For (1.16) to hold one requires

$$w > -\frac{1}{3}. \quad (1.17)$$

Quantum gravity and renormalization The quantization of physical theory introduces another source of infinities. In quantum field theories, when using the “bare”, classical Lagrangian, the calculations of Feynman diagrams are plagued with infinities. The Lagrangian has to be connected to the measurable quantities to restore predictivity. The procedure to achieve it is called renormalization, which we shall discuss in detail in Chapter 2. Within the perturbative loop expansion, the counterterms are introduced order by order. For the theories containing only relevant or marginal couplings, such that their mass dimension is non-negative $4 \geq [c_i] \geq 0$, the number of counterterms is finite; furthermore, they are proportional to the original action. This is not the case for the Einstein-Hilbert action, where $[R] = 2$ and hence the coupling has negative dimension $[G_N] = -2$. By this argument, quantum gravity is the theory with an infinite number of counterterms (if there are no cancellations), which has been confirmed by the explicit Feynman diagrams calculations showing that General Relativity requires counterterms not proportional to R at the one-loop level when coupled to matter [57, 58] (which disappear in the matter free case by the equations of motions) and at two loops in the matter free case [59, 60]:

$$\delta\lambda_2 C_{\mu\nu}^{\kappa\lambda} C_{\kappa\lambda}^{\rho\sigma} C_{\rho\sigma}^{\mu\nu}, \quad (1.18)$$

In higher orders, one expects further counterterms to appear; however, one cannot make an infinite number of experiments to determine the theory’s predictions. Hence it seems that General Relativity, when quantized within the perturbative approach, cannot have predictions at all energy scales¹.

Similarly to quantum mechanics, we expect the quantum theory of gravity to resolve the singularities both in the classical theory and those associated with renormalization and counterterms. Various approaches have been proposed modifying assumptions usually considered for general relativity and quantum theories

¹General Relativity can be nevertheless quantized as effective field theory below the Planck scale, yielding finite quantum corrections to the scattering amplitudes and Newtonian potential [61, 62, 63, 64].

- Diffeomorphism invariance
- Continuous spacetime
- Quantum field theory formalism
- Microcausality
- Perturbative renormalizability and unitarity

Below we present some of the approaches. Our discussion will not be exhaustive since we shall concentrate on the approaches utilized in this thesis. In particular, we shall omit supergravity, causal sets, causal dynamical triangulations, and other approaches.

1.2. Quantum gravity approaches

1.2.1. Hořava-Lifshy gravity

The Stelle gravity [65] considers additionally to the E-H action the R^2 and $R_{\mu\nu}R^{\mu\nu}$ terms:

$$S = S_{EH} + \int d^4x \sqrt{-g} [aR^2 + bR_{\mu\nu}R^{\mu\nu}] . \quad (1.19)$$

The presence of those terms allows for perturbative quantization of the theory; furthermore, the theory can be asymptotically free [66]. On the other hand, the presence of higher than second-order time derivatives in action changes the spectrum of the theory. On top of spin-2 gravity, there is a massive spin-zero particle 0 and a massive 2 particle with the negative norm. Putting it differently as the consequence of the Ostrogradsky Theorem [67] the Hamiltonian is not-bounded from below manifesting in those instabilities.

Various solutions have been proposed, such as the addition of new particles and extra symmetry [68], giving up the micro-causality and changing the propagator prescriptions [69, 70] or taking into account infinitely many derivatives [71], see also the discussion [72] on possible resolution in the context of asymptotic safety.

Here, we explore yet another possibility, where *the Lorentz Invariance (LI)* is broken at the fundamental level. In the Hořava-Lifshy (H-L) gravity [73] diffeomorphism invariance is broken by the foliation \mathcal{F} of the 4-dimensional spacetime into 3-dimensional hypersurfaces of constant time, called leaves. Kinetic terms are first order in the time derivatives. At the same time, higher spatial curvature scalars regulate the UV behavior of the gravity, making the theory power-counting renormalizable (see also the renormalization group studies of the subject [74, 75, 76, 77]) and avoiding the instabilities related to the Ostrogradsky theorem. The remaining symmetry respects transformations:

$$t \rightarrow \xi_0(t), \quad x^i \rightarrow \xi^i(t, x^k), \quad (1.20)$$

and is often referred to as the foliation-preserving diffeomorphism, denoted by $\text{Diff}(M, \mathcal{F})$. The four-dimensional metric may be expressed in the Arnowitt-Deser-Misner (ADM) [78] variables:

$$(N, N^i, {}^{(3)}g_{ij}), \quad (1.21)$$

where N , N^i , ${}^{(3)}g_{ij}$ denote respectively the lapse function, shift vector, and 3-dimensional induced metric on the leaves. The theory is constructed from the following quantities:

$${}^{(3)}R_{ij}, \quad K_{ij}, \quad a_i, \quad {}^{(3)}\nabla_i, \quad (1.22)$$

where ${}^{(3)}R_{ij}$ is the 3-dimensional Ricci curvature tensor, ${}^{(3)}\nabla_i$ is the covariant derivative constructed from the 3-dimensional metric ${}^{(3)}g_{ij}$, and $a_i := \frac{N_{,i}}{N}$. Extrinsic curvature K_{ij} is the only object, invariant under general spatial diffeomorphisms containing exactly one time derivative of the metric tensor ${}^{(3)}g_{ij}$:

$$K_{ij} = \frac{1}{2N} \left(\frac{\partial {}^{(3)}g_{ij}}{\partial t} - {}^{(3)}\nabla_i N_j - {}^{(3)}\nabla_j N_i \right). \quad (1.23)$$

Quantities (1.21) are tensor/vectors with respect to $\text{Diff}(M, \mathcal{F})$ possessing the following mass dimensions:

$$[{}^{(3)}R_{ij}] = 2, \quad [K_{ij}] = 3, \quad [a_i] = 1, \quad [{}^{(3)}\nabla_i] = 1. \quad (1.24)$$

Following [79, 80] the action of the H-L gravity takes the form:

$$S_g = \zeta^2 \int dt dx^3 N \sqrt{{}^{(3)}g} (\mathcal{K} - V), \quad (1.25)$$

where $\mathcal{K} = K_{ij}K^{ij} - \lambda K^2$ with $K = K_{ij}{}^{(3)}g^{ij}$, ${}^{(3)}g$ denotes the determinant of the 3-dimensional metric and $\zeta^2 = 1/16\pi G$. The potential V built from (1.22) can contain over 100 terms up to the 0th order in mass dimension [79]. Yet, the immense number of invariants is limited by imposing further symmetries. One possible restriction for the potential comes from the projectability condition $N = N(t)$, then terms proportional to $a_i \equiv 0$ vanish. The potential compatible with power counting renormalizability restricted by the projectability condition is given by:

$$\begin{aligned} V = & 2\Lambda\zeta^2 - {}^{(3)}R + \frac{1}{\zeta^2} (c_2 {}^{(3)}R^2 + c_3 {}^{(3)}R^{ij} {}^{(3)}R_{ij}) \\ & + \frac{1}{\zeta^4} (c_4 {}^{(3)}R^3 + c_5 {}^{(3)}R {}^{(3)}R^{ij} {}^{(3)}R_{ij} + c_6 {}^{(3)}R_j^i {}^{(3)}R_k^j {}^{(3)}R_i^k), \\ & + \frac{1}{\zeta^4} (c_7 {}^{(3)}R \nabla^2 {}^{(3)}R + c_8 (\nabla_i {}^{(3)}R_{jk})(\nabla^i {}^{(3)}R^{jk})) , \end{aligned} \quad (1.26)$$

where Λ is the cosmological constant and c_i are the coupling constants. On top of that the *detailed balance condition* can be imposed [73], resulting in $c_4 = c_5 = c_6 = 0$ and $c_7 = 1/8c_8$. One should also mention that this *minimal theory* [81] suffers from the existence of spin 0 graviton, which is unstable in the IR, see [82, 83, 84, 85]. Various solutions to this problem have been proposed. One can impose the additional local $U(1)$ symmetry [79, 86]. Then by the introduction of new fields prevents the zero-mode from propagating. On the other hand, one can drop the projectability condition $a_i = 0$ and include the terms containing a_i in the potential term:

$$V = 2\Lambda\zeta^2 - {}^{(3)}R - \beta_0 a_i a^i + \sum_{n=3}^6 \mathcal{L}_V^{(n)}, \quad (1.27)$$

then for the spin-0 mode to be stable one requires $0 < \beta_0 < 2$ [87, 88].

Finally, let us comment on the famous Gibbons-Hawking-York (GHY) [89, 90] term in

the context of H-L gravity. Namely, the variational principle with Dirichlet boundary condition requires a variation of the action to be zero when fixing the boundary metric [91]. However, this is not satisfied for the Einstein Hilbert action, and hence the famous Gibbons-Hawking-York (GHY) term [89, 90] has to be added². On the other hand, the action possesses higher spatial derivatives for H-L gravity. The variational principle requires $\delta\gamma_{ij}$ along with its derivatives to be zero at the spatial boundary; hence the variation is well defined without the boundary term [93]. Furthermore, the absence of the boundary term has been recently proven for the mimetic H-L gravity, see [94, 95].

1.2.2. String-theory

String theory takes a different route and postulates that *strings are fundamental entities* instead of point particles and hence abandons the quantum field theory framework [96, 97, 98]. Together with requirements of Weyl (conformal) invariance, diffeomorphism symmetry on the worldsheet and global Poincare invariance, one can write Polyakov action as

$$S = \frac{1}{4\pi\alpha'} \int d^2\sigma \sqrt{-g} g^{\alpha\beta} \partial_\alpha X^\mu \partial_\beta X^\nu \eta_{\mu\nu}, \quad (1.28)$$

where $\alpha, \beta \in 1, 2$ are the worldsheet indices, while $\mu, \nu \in 1, \dots, d$ are the target space indices. The quantum Weyl invariance (vanishing of worldsheet Weyl anomaly) leads to $d = 10$ for the superstrings and $d = 26$ for the bosonic strings, which we identify with physical dimensions. The massless spectrum of the string consist of spin-2 symmetric graviton $G_{\mu\nu}$, spin 0 scalar dilaton ϕ and spin-2 antisymmetric torsion $B_{\mu\nu}$. The quantisation with the use of conformal field theory methods gives general prescription for the string S-matrix amplitude on the target space as correlation function on the two dimensional worldsheet, expanded as a sum over the topologies with the growing genus. In particular, the genus 0 four graviton amplitude is given by

$$A(p_1, p_2, p_3, p_4) = 2g_D^2 K_{cl} C(s, t, u), \quad (1.29)$$

where $C(s, t, u)$ is

$$C(s, t, u) = -\pi \frac{\Gamma(-s/8)\Gamma(-t/8)\Gamma(-u/8)}{\Gamma(1 + \frac{s}{8})\Gamma(1 + \frac{t}{8})\Gamma(1 + \frac{u}{8})} \quad (1.30)$$

and K_{cl} is a lengthy kinematic (cross-symmetric) and polarization factor polynomial in s, t, u . Varying s and keeping t fixed, the amplitude has infinite number of simple poles [96] on a real line at $s = 8n$, with $n \geq 0$. This can be understood as summing over infinite number of particles with growing masses in the s -channel, that tame the singularities occurring for the Einstein-Hilbert action. The similar conclusion can be drawn if we keep s fixed and vary t . This property is called duality, discovered by Veneziano [99]. Due to modular symmetry on the worldsheet string theory is conjectured to be finite to all orders [96, 97, 98].

Furthermore string theory can also be quantised on non-trivial backgrounds of massless fields: $G_{\mu\nu}$, ϕ and $B_{\mu\nu}$. Then the requirement of Weyl invariance (encoded in vanishing of the beta functions of a 2-dimensional QFT [100]) puts constraints on the evolution of the background. In particular for $\phi = \text{const}$ and $B_{\mu\nu} = 0$ the equations reduce to

$$R_{\mu\nu} + \mathcal{O}(\alpha') = 0, \quad (1.31)$$

²The GHY term is crucial for the finiteness of the action, see [92].

thus recovering the vacuum Einstein equations (1.6)! The calculations of the corrections stemming from higher stringy modes turns out to be quite involved. Nevertheless in certain cases an all order expression can be given [101, 102], using constraints stemming from T-duality [68, 103, 104].

Dualities relate five consistent superstring string theories [96, 97, 98], connected by the web of dualities tying together these five and 11-dimensional supergravity. Those are supposed to be the facets of one unified M-theory [105, 106, 107]. Yet, the amount of possible compactifications is far more extensive, hence the low-energy theories. The collection of possible false vacua in string theory is called the string theory landscape, and the amount of vacua is estimated as 10^{500} , significantly reducing the predictability of the theory, whether the Standard Model is within one of those remains unknown.

1.2.3. Asymptotic safety programme

General relativity, treated as quantum field theory, has an infinite number of (counter)-terms. However, this doesn't necessarily mean that the theory is un-predictive at arbitrary scales. Steven Weinberg [108, 25] noticed that quantum gravity (QG) could be predictive if almost all of the counterterms (and the associated couplings) could be determined in terms of the finite subset of couplings. Requiring the scale-invariant in the UV imposes relations between the couplings [108, 25, 109, 110]. The term asymptotic safety has been coined due to resemblance to the asymptotic freedom, where all of the interactions vanish for large momenta [111, 112]. Yet, General Relativity does not admit a well-defined perturbative expansion. Within asymptotic safety, the couplings are supposed to stem from a regime where they scale canonically.

In the early days, this mechanism was found in 2-dimensions and its vicinity [113, 114, 115, 116] by means of the $2 + \epsilon$ dimensional expansion. Similar claims were also made with the $1/N_F$ expansion approach [117].

However, only after applying the Wilsonian inspired exact Wetterich-Morris-Ellwanger equation [118, 119, 120] to tackle this problem the approximate fixed point was found in seminal Reuter article [121], see also [122, 123], and then explored in various truncations. We shall discuss that in detail in Sec. 2.2.

Here let us note that this program shares similarity with loop quantum gravity, causal dynamical triangulations (CDT) and euclidean dynamical triangulations (EDT). All of them claim that “gravity can stand on its feet” when properly quantized. In particular, both EDT and CDT are another methods for testing Weinberg's claim using lattice simulations instead of the use of the Functional renormalization group. On the other hand, it was conjectured [124] that loop quantum gravity utilizing canonical quantization with Ashtekhar variables [125] is supposed to reduce to asymptotic safety within the semiclassical limit.

1.3. Standard Model and beyond

1.3.1. Overview of the Standard Model

Contradictory to the common belief in the early XXI century, the Large Hadron Collider hasn't discovered any particles beyond the Glashow-Weinberg-Salam model [126, 127, 128], now called the Standard Model. Here we review the model's basic features and point out possible connections to the quantum gravity realm. The Standard

Model [129, 130, 27] is given by (i) its gauge group

$$\mathcal{G}_{\text{SM}} = SU(3)_c \times SU(2)_L \times U(1)_Y \quad (1.32)$$

and their gauge bosons. (ii) The three generations of fermionic matter. The fermionic content of the model in terms of representations of the SM gauge groups is given by:

$$\mathcal{F}_{\text{SM}} = \underbrace{\left(\mathbf{3}, \mathbf{2}, +\frac{1}{6}\right)}_{q_L^{(i)} = (u_L^{(i)}, d_L^{(i)})} \oplus \underbrace{\left(\mathbf{1}, \mathbf{2}, -\frac{1}{2}\right)}_{(e_L^{(i)}, \nu_L^{(i)})} \oplus \underbrace{\left(\bar{\mathbf{3}}, \mathbf{1}, -\frac{2}{3}\right)}_{u_R^{c,(i)}} \oplus \underbrace{\left(\bar{\mathbf{3}}, \mathbf{1}, +\frac{1}{3}\right)}_{d_R^{c,(i)}} \oplus \underbrace{(\mathbf{1}, \mathbf{1}, +1)}_{e_R^{(i)}}, \quad (1.33)$$

where $i \in \{1, 2, 3\}$. (iii) The scalar sector. In the Standard Model it contains a complex $SU(2)_L$ doublet, the Higgs field H :

$$\mathcal{S}_{\text{SM}} = (\mathbf{1}, \mathbf{2}, 1/2). \quad (1.34)$$

(iv) The Lagrangian, consisting of kinetic terms of the fields, the scalar potential and Yukawa interaction (responsible for generating the masses of elementary particles):

$$\mathcal{L} = \mathcal{L}_{\text{kin}} + \mathcal{L}_Y - V. \quad (1.35)$$

Within the Standard Model, the Higgs potential is given by:

$$V = \frac{\lambda}{4} (H^\dagger H - v^2)^2, \quad (1.36)$$

where $v \approx 246$ GeV is the Higgs vacuum expectation value and $m_H^2 = -2\lambda v^2$ is the Higgs mass. The non-trivial vacuum configuration of the Higgs doublet

$$H = \begin{pmatrix} 0 \\ v \end{pmatrix} \quad (1.37)$$

triggers the spontaneous symmetry breaking (SSB) giving masses to the three out of four gauge bosons of the $SU(2)_L \times U(1)_Y$ and the electroweak group is broken to $U(1)_{\text{em}}$. The B^0 of $U(1)_Y$ and W^0 of $SU(2)_L$ are mixed during the SSB such that

$$\begin{pmatrix} Z^0 \\ \gamma \end{pmatrix} = \begin{pmatrix} \cos \theta_W & \sin \theta_W \\ -\sin \theta_W & \cos \theta_W \end{pmatrix} \begin{pmatrix} W^0 \\ B^0 \end{pmatrix}. \quad (1.38)$$

The θ_W is called the Weinberg angle and is measured to be $\theta_W \approx 30^\circ$. The electric charge is given by

$$Q = Y + T_3, \quad (1.39)$$

where T_3 is the 3-rd component of weak isospin, $T_3 = \pm 1/2$ for doublets and 0 for singlets of $SU(2)_l$. The Yukawa interaction term is:

$$\mathcal{L}_Y = \bar{L}^i H Y_{ij}^E E^j + \bar{Q}^i H Y_{ij}^D D^j + \bar{Q}^i \epsilon H^* Y_{ij}^U U^j + \text{h.c.}, \quad (1.40)$$

where $\epsilon = i\sigma_2$. The three generations of the fermionic matter differ only by respective the couplings to the Higgs, resulting in different masses after spontaneous symmetry breaking. The Yukawa matrices are three 3×3 complex matrices; after considering the redefinitions and symmetries, we obtain 13 free parameters: nine masses, three angles, and one phase. So in total, the model has 19 parameters, since we take into account three couplings of the gauge groups g_3, g_2, g_1 , Yukawa couplings, the θ QCD term, Higgs expectation value v and Higgs self-coupling λ .

Anomaly cancelation. The charges of $SU(3)_c$ and $SU(2)_L$ are fixed in terms of representations of the field. The hypercharges, in principle, could have assigned arbitrary values. Later it was found that the proposed hypercharges assignments are those required for gauge anomaly to vanish. The anomaly breaks the symmetry of classical Lagrangian broken at the quantum level. While the anomalies of the global symmetries can occur, in particular, the chiral anomaly of quantum chromodynamics is responsible for generating the proton mass, the anomalies of the gauge symmetries make the theory non-unitary, hence have to be canceled. Calculation of the anomalies stems from the triangle diagrams with gauge bosons on external lines and matter on internal ones. For example, the mixed $SU(2)^2 U(Y)$ anomaly is

$$B^\mu \sim \sim \sim \quad f^i \quad f^j \quad W^{\nu,a} \quad W^{\lambda,b}$$

$$\propto \sum_{\mathcal{F}_{SM}} \text{Tr } T^a T^b Y \propto \delta^{ab} \sum_{l,q} Y = 0 \quad (1.41)$$

For the Standard Model the non-vanishing expressions are [131]

$$\begin{aligned} U(1)_Y^3 : \quad & (2Y_l^3 - Y_e^3) + 3(2Y_q^3 - Y_u^3 - Y_d^3) = 0, \\ SU(3)_C^2 U(1)_Y : \quad & (2Y_q - Y_u - Y_d) = 0, \\ SU(2)_L^2 U(1)_Y : \quad & (Y_l + 3Y_q) = 0. \end{aligned} \quad (1.42)$$

By plugging the hypercharge values one can indeed check that the Standard Model is anomaly free [132]. One can ask the opposite question: is the assignments of charges within the Standard Model unique? The equations (1.42) have actually infinitely many solutions. However, this assignment is further constrained by coupling SM with gravity

$$\text{grav}^2 U(1)_Y : \quad (2Y_L - Y_e) + 3(2Y_q - Y_u - Y_d) = 0, \quad (1.43)$$

the constraints (1.42, 1.43) reduces to two solutions

$$2Y_l = Y_e = -6Y_q = -\frac{3}{2}Y_u = 3Y_d, \quad (1.44)$$

$$Y_u = -Y_d, \quad Y_l = Y_q = Y_e = 0. \quad (1.45)$$

Finally once the Standard Model is UV extended by Grand Unified Theory (GUT) only the (1.44) is possible, see Sec. 1.3.2.

Higgs mass On the quantum level the Higgs mass acquires corrections from the matter loops

$$H \dashrightarrow \text{loop} \dashrightarrow H \sim m_{f_i}^2, \quad (1.46)$$

with the top quark, the heaviest particle gives the dominant contribution. One could expect that the particles with masses far above the Standard Model one can also contribute to this mass, and hence the Higgs mass should be proportional to the scale of new physics. Naively, the Planck scale is a natural cutoff for the Standard Model; thus, one could argue that Higgs mass should be of the order of the Planck mass. This huge separation of scales $M_{\text{EW}} \ll M_P$ called the **hierarchy problem**. The hierarchy problem for gravity is a subtle issue. In particular, gravitons are massless particles. We shall come back often to that issue in the text.

Three mysteries The nineteen couplings of the Standard Model can be measured experimentally in the scattering experiments. The couplings values depend on the renormalization scale, which can be associated with the energy of the processes. They evolve (“run”) according to the renormalization group equations (RGE) ³:

$$\mu \frac{\partial c_i}{\partial \mu} = \beta_i(\{c_j\}). \quad (1.47)$$

We depict their behavior in Fig. 1.1. The depicted results provide us with three coincidences or “mysteries”:

- (i) **Perturbativity:** The running of the couplings remain within the perturbative regime, without any Landau poles up to the Planck scale ⁴.
- (ii) **(Meta)-Stability:** Around 10^9 – 10^{10} GeV, the Higgs coupling becomes negative, and the vacuum becomes unstable.
- (iii) **Unification:** The values of three gauge couplings are nearly the same at the scale around 10^{15} GeV, so they roughly unify.

Concerning (ii), the running of λ is very sensitive to the value of the top Yukawa value (and hence the associated mass of the top quark). At the same time, the interactions with other particles have a marginal impact on the running, see [8, 135]. The value of the top Yukawa coupling is known with large error bars. Yet, the central value indicates that for the Standard Model, the Higgs potential develops a deeper minimum around 10^{10} GeV. In principle, this might not be the fatal flaw as long as the longevity of the EW vacuum exceeds the age of the Universe, which seems to be the case [135]. Lowering the error bars is undoubtedly crucial for our understanding of the Standard Model [135, 136, 137, 138]. Hence, to amend the Higgs stability, the results (i), (ii) imply that new physics should occur below / around the scale $\sim 10^{10}$. On the other hand, because of no pathologies in the different sectors, the new physics sector can be relatively small, and Standard Model “can remain roughly as it is” [139, 140, 141, 142] with only a few new particles introduced. However, evolving the couplings beyond the Planck scale leads to the Landau pole in the hypercharge sector. Therefore, the Abelian hypercharge sector of SM is not UV-complete and suffers a divergence at some finite scale, which is estimated to lie far beyond the Planck scale. In this regime, however, quantum gravitational effects might alter the scale dependence of the gauge coupling

³The concept of the renormalization group in both perturbative and Wilsonian approaches will be discussed in Sec. 2.1.

⁴For the running of the Yukawa parameters see, e.g., [133, 134].

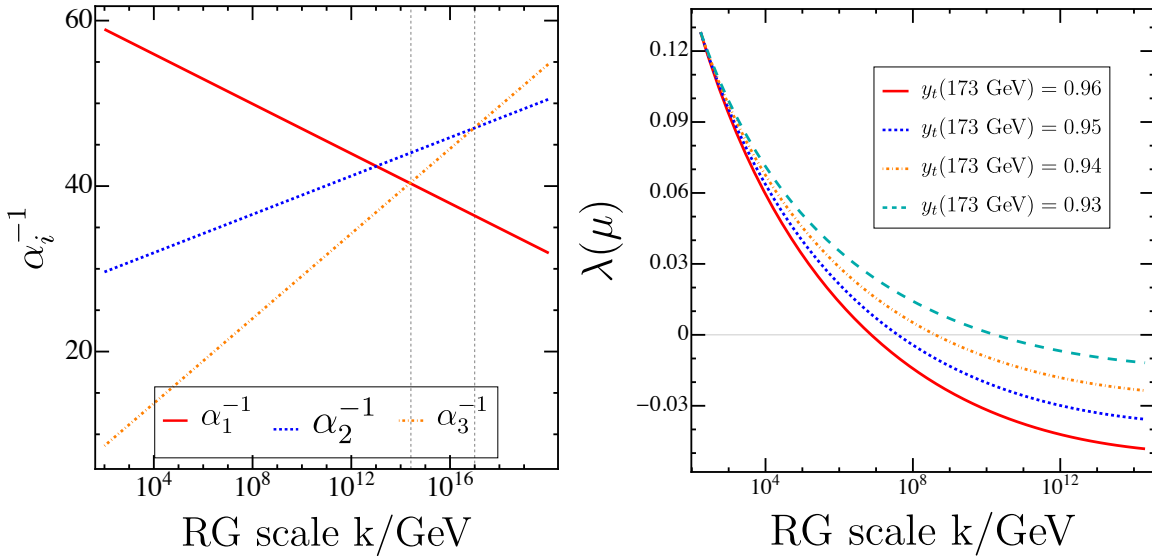


Figure 1.1: Running of couplings in the Standard Model.

To the left: The one-loop gauge couplings running, $\alpha_i = \frac{g_i^2}{4\pi}$. The grey lines denote a possible unification scale between two of the three couplings.

To the right: The λ self-coupling one-loop running depending on the value of the top Yukawa coupling. The result presented here will be discussed for the two-loops running and matching in Sec 4.2.2.

and induce a UV-completion of the gauge sector, which we shall discuss in Sec. 2.2 and Sec. 4.3.

On the other hand around 10^{15} GeV the couplings have almost the same value, cf. Fig. 1.1. Thus (iii) points out towards unification of forces into one gauge group, resolving the Landau pole problem as long as the corresponding GUT is asymptotically free in the gauge sector.

Neutrino masses On top of the discussed issues, the Standard Model does not explain certain phenomena that have been observed. In its minimalistic version the all the neutrinos are massless. On the other hand, the experiments with neutrino oscillations revealed that neutrinos are massive. Yet, the gauge invariance forbids both Dirac and Majorana mass terms. To tackle this question, various approaches have been proposed. In the minimalistic approach, the right-handed Majorana neutrinos are added to the model in the representation

$$\mathcal{F}_{\text{SM}} \oplus \underbrace{(\mathbf{1}, \mathbf{1}, 0)}_{\nu_R^{(j)}}. \quad (1.48)$$

Their number is not constrained since they do not enter into the triangle diagrams corresponding to the gauge anomalies. If they are heavy enough, then their masses can trigger the see-saw mechanism explaining the smallness of left-handed neutrino masses, see, and references therein [143, 144, 145, 146, 147].

Baryon asymmetry If the Universe is neutral concerning all of the possible charges, then the observed dominance of matter over antimatter should be the result of some

physical process triggered during the cosmical evolution. The sufficient conditions for that to happen are encoded in the Sakharov conditions [148]:

- (1) Baryon number violation
- (2) C and CP violations
- (3) Departure from thermal equilibrium

For a suitable choice of coupling, the Standard Model electroweak phase transition could fulfill all of these conditions. However, neither the CP-violations [149, 150] in the Standard Model is strong enough, nor the electroweak phase transition is of the first order - out of equilibrium [151, 152, 153, 154, 155, 156, 157]. The EW phase transition would be of first order for the Higgs mass smaller than ~ 70 GeV [152, 153, 158, 159].

1.3.2. Beyond the Standard Model

To overcome the issues discussed in Sec 1.3.1⁵ there has been a plethora of possible extensions of the Standard Model proposed. They vary in their complexity, scales of new physics, and new particles introduced. There are, in general, two types of models, which rely on a different philosophy of building such an extension. The first type is the theories where the SM structure is UV extended by another more extensive view. A good example is a supersymmetry (SUSY) concept. The main idea is that each particle has its super-partner. Due to the breaking of this symmetry, a super-partner of a given particle is much heavier. The most popular is the Minimal Supersymmetric Standard Model (MSSM) and its descendants. Yet in this thesis, due to lack of experimental confirmation for low-energy SUSY in LHC, we focus on the non-SUSY extensions of the SM⁶.

Another good example of such a theory are Grand Unified Theories (GUT). They assume that the initial symmetry of the theory is some single “big” gauge group such that $\mathcal{G}_{\text{GUT}} \supset \mathcal{G}_{\text{SM}}$. On a certain large scale a spontaneous symmetry breaking scenario occurs, which is supposed to reproduce the Standard Model in the low energies. GUTs could provide an explanation for the seemingly coincidental near-equality of SM gauge couplings at the high-energy scale $M_{\text{GUT}} \sim 10^{15}$ GeV [163]; the fermionic representations are unified into one or two GUT representations [164]; in some GUTs, the unified fermionic representation naturally accounts for heavy right-handed sterile neutrinos [27] which could trigger a see-saw mechanism [27, 165] and thereby leptogenesis [27]. In particular, for the $SU(5)$ unified theory the fermionic representations of the SM fits into two $SU(5)$ representations:

$$\begin{aligned} \bar{\mathbf{5}} &= \left(\bar{\mathbf{3}}, \mathbf{1}, +\frac{1}{3}\right) \oplus \left(\mathbf{1}, \mathbf{2}, -\frac{1}{2}\right), \\ \mathbf{10} &= (\mathbf{5} \otimes \mathbf{5})_A = \left(\bar{\mathbf{3}}, \mathbf{1}, -\frac{2}{3}\right) \oplus \left(\mathbf{3}, \mathbf{2}, +\frac{1}{6}\right) \oplus (\mathbf{1}, \mathbf{1}, +1). \end{aligned} \quad (1.49)$$

⁵See also the discussion of inflation and dark matter in Sec 1.4.

⁶This choice is also dictated by the fact that supersymmetric models (also the GUT models) are usually embedded into superstring theory, where they have been studied extensively as the low-energy limit, and none other approach relies on subplanckian supersymmetry so heavily as string theory does. On the other hand, in the $N = 8$ supergravity, the supersymmetry can be broken at the Planck scale such that the Standard Model is reconstructed if taking into account the E_{10} generator, see [160, 161]. Furthermore, asymptotically safe quantum gravity seems to prefer the non-supersymmetric matter [22, 162].

Let us now look into the hypercharge of the Standard Model representations. The most generic hypercharge generator compatible with $SU(3)_c$ and the $SU(5)$ embedding is [27]:

$$Q = \text{diag}(a, a, a, -3a, -b), \quad (1.50)$$

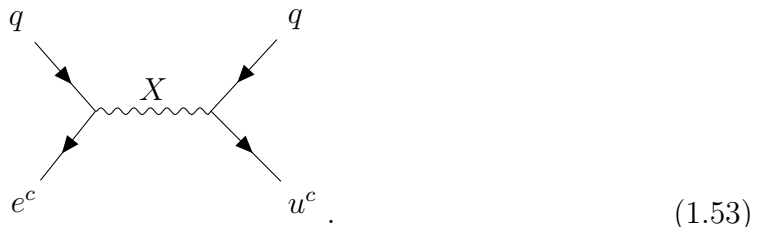
wherein order for the anomaly to vanish, we require $\text{Tr } Q = 0$, which uniquely specifies the hypercharge assignments of the Standard Model as

$$Y_{e^c} = -Y_e = \frac{3}{2}Y_u = -\frac{3}{2}Y_{u^c} = -3Y_d = 3Y_{d^c} = b, \quad (1.51)$$

together with $Y_\nu = 3a + b = 0$. The most profound prediction (a signature-mark) of the Grand Unified Theories is the possibility of proton decay towards the π^0 meson and positron. In the low-energies this process originates from the $d = 6$ operators suppressed by the unification scale M_{GUT}

$$\mathcal{O}_1^{d=6} \propto \frac{1}{M_{\text{GUT}}^2} \bar{e}^c \bar{u}^c q q, \quad \mathcal{O}_2^{d=6} \propto \frac{1}{M_{\text{GUT}}^2} \bar{d}^c \bar{u}^c q l \quad (1.52)$$

mediated by the X bosons stemming from the gauge sector of the GUT (see also discussion of the other possible channels here [27]). In particular, the second process is depicted below



The inclusion of the operators (1.52) in the low-energy EFT results in the bound

$$\frac{1}{\tau(p \rightarrow \pi^0 e^+)} \sim \alpha_{\text{GUT}}^2 \frac{m_p^5}{M_{\text{GUT}}^4}, \quad (1.54)$$

with α_{GUT} being the coupling of the unified group and M_{GUT} being the unification scale. Plugging in $\alpha_{\text{GUT}}^{-1} = 40$, one gets

$$M_{\text{GUT}} > 2.3 \times 10^{15} \text{ GeV}. \quad (1.55)$$

Hence proton decay is the highest energy process we can measure in particle physics. Experiment bounds on the proton unification and the lack of exact one-step Unification, c.f. Fig 1.1 have ruled out the $SU(5)$ [166] model. Hence more complicated models have been considered, such as $SO(10)$ model [167], see also [168, 164]. The $SO(10)$ model possesses a plethora of viable multistep breaking chains towards the Standard Model. In particular, in Fig. 1.2 we depict the viable possibilities for the $SO(10)$ model⁷. The unified gauge group gets broken towards the SM is via spontaneous symmetry breaking in a suitable scalar potential. To date, most GUT analyses assume that all suitable breaking chains can be realized by some – possibly complicated – scalar potential. Oftentimes, the latter remains to be explicitly specified. On top of scalar representations, the breaking directions depend on the couplings of those

⁷Bear in mind that there are also non-SM breakings, see Tab. 3.2.

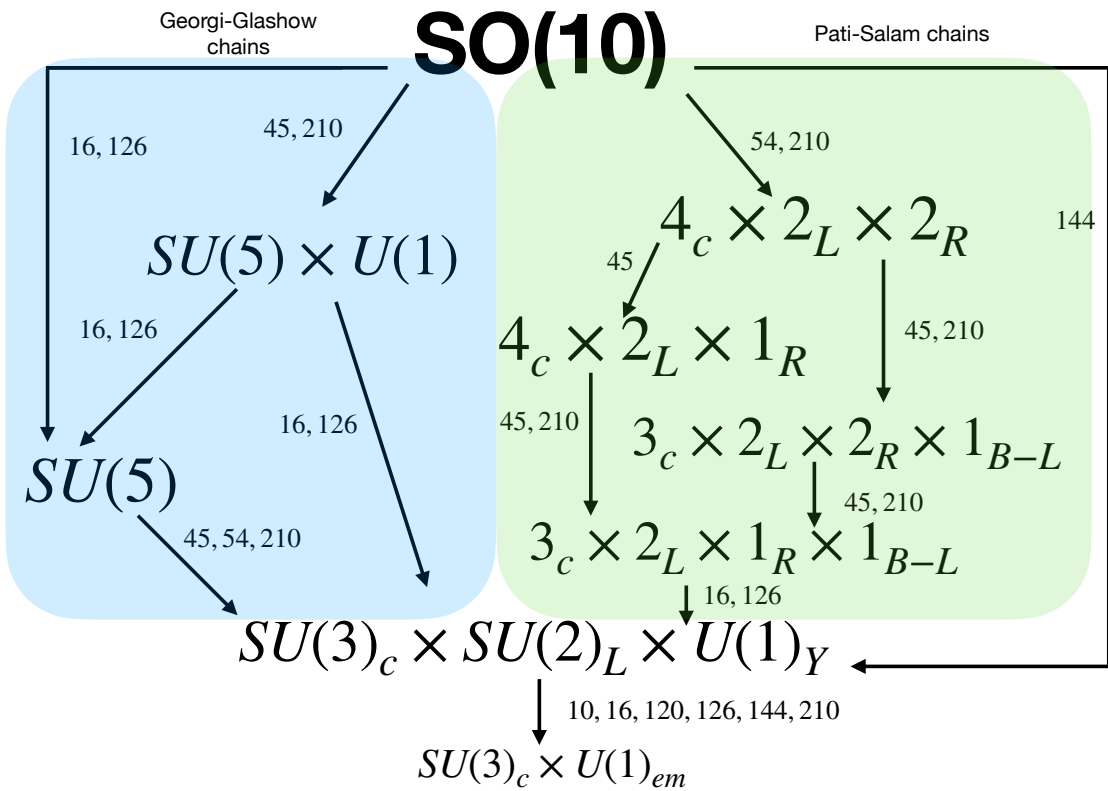


Figure 1.2: Breaking steps of the $SO(10)$ [27]. For the Pati-Salam breakings we adopt the notation $SU(N)_I = N_I$ and $U(1)_I = 1_I$.

potentials. Hence, to be viable, GUTs have many free parameters⁸. Furthermore, unlike the Yukawa and gauge couplings, the couplings entering the GUT potential are largely arbitrary and are not constrained by the current data.

In the lack of new experimental data, we also study the second type of model, minimal extensions. They propose only a slight extension of SM, where $\mathcal{G}_{\text{model}} = \mathcal{G}_{\text{SM}} \oplus \dots$, $\mathcal{F}_{\text{model}} = \mathcal{F}_{\text{SM}} \oplus (\mathbf{1}, \mathbf{1}, 0)$. They not only solve problems of SM but can be, in principle, valid up to the Planck scale with no new intermediate scales and give possible candidates for dark matter. The ν SM is such an extension, where only right chiral neutrinos and one scalar singlet are added [141]. Another one is Conformal Standard Model [169], relying on solving the hierarchy problem via conformal symmetry instead of supersymmetry [170, 171, 172]. Some recent experimental hints support some of the minimal models, see the recent results in the flavor sector, see, e.g., [173, 174, 175] and possible discrepancy of the muon anomalous magnetic momenta [176, 177]. Yet those are not conclusive and may go away⁹.

We shall study both models: Grand Unified Theories and minimalistic models. Both classes of models can solve the baryogenesis problems, have mechanisms giving correct neutrino masses, and possess candidates for dark matter. In this thesis, we focus on the other issues of SM, such as Higgs mass prediction, stability of the vacua, absence of Landau poles, and the number of vector species. Considering quantum gravity, some

⁸In particular, the minimal viable $SO(10)$ with $\mathbf{10}_H \oplus \mathbf{126}_H \oplus \mathbf{45}_H$ possess roughly 20 couplings in the scalar potential only, which is more than the SM itself

⁹In the past, there has been particular interest in the LHC run-1 750 GeV excess, speculated to be a second scalar particle, which then faded away.

of the problems of the Standard Model and Beyond Standard Model physics can be tackled. On the other hand, we will show that quantum gravity can constrain the Beyond Standard Model scenarios that seem otherwise perfectly reasonable.

In string theory constraining matter models by quantum gravity is called the swampland program [178, 179]. The program studies which effective (low-energy) field theories can be combined with quantum gravity (understood as string theory) at high energies. For an effective field theory to be a low-energy approximation of string theory, it must meet all the conditions of not being in a swampland (so-called swampland conjectures), see [178, 179]. Thanks to this approach, it turned out that the number of correct theories (landscape) is much smaller than the total number of possible effective theories. Moreover, it has been suggested that the so-called KKLT construction of the de-Sitter vacuum [180], which is based on the idea of a multiverse, may contradict these conditions [181]. This means that string theory does not have a de Sitter vacuum, which has far-reaching consequences in [182] cosmology.

1.4. Λ -CDM and beyond

1.4.1. Λ -CDM model

The Copernicus Principle or Cosmological Principle, saying: *The Universe is homogeneous and isotropic in large scales* is fundamental for physical cosmology. Homogeneity means that the Universe has the same matter distribution everywhere. Isotropy means that the Universe looks the same in every direction. The observable Universe is of order 3000 Mpc¹⁰, while the data suggest that Universe is homogeneous and isotropic for scales larger than 100 Mpc [183]. Certainly, over the smaller scales, the Universe ceases to be so due to galaxies, clusters, and ultimately us, humans.

The evolution of the homogeneous and isotropic metric according to Friedman equations (1.14) implies that expansion is determined by the type of matter that is within the universe. Let ρ_c denote the current energy density of all species, then by (1.14):

$$\rho_c = \frac{3}{8\pi G} H_0^2, \quad (1.56)$$

where $H_0 \approx 70 \frac{\text{km/s}}{\text{Mpc}}$ is the current value of the Hubble parameter¹¹. For species i we define the fractional quantities: ρ_i , p denoting their relative fraction in the total ρ , p etc. The critical density ρ_{cr} is defined as the density of a species i required to obtain Hubble parameter H without any other contributions from other fractions. The relative scale-dependent density is defined as:

$$\Omega_i(a) = \frac{\rho^i}{\rho_{\text{cr}}} \quad (1.57)$$

and measure of relative curvature contribution as:

$$\Omega_k(a) = -\frac{k}{a^2 H^2(a)}. \quad (1.58)$$

¹⁰1 Mpc $\simeq 3.26 \cdot 10^6$ light-years $\simeq 3.08 \times 10^{24}$ cm.

¹¹For the discussion of different Hubble measurements and the so called H_0 tension, see [184, 185, 186, 187, 188, 189].

At present time (t_0) one sets $a(t_0) = a_0 = 1$. Then

$$\sum_i \Omega_i(a_0) + \Omega_k(a_0) = 1. \quad (1.59)$$

Dark energy, dark matter The paradigm where the Universe evolution is described by FLRW metric with Friedmann equations coupled to matter and dark energy is called Λ -CDM cosmology, where Λ comes from dark-energy and CDM states for cold dark matter. The respective critical densities of species are [190]:

- (1) Dark-energy $\Omega_{DE} = 0.69$, such that ρ_{DE} stays almost constant during evolution.
- (2) Non-relativistic matter: $\Omega_M = 0.31$, scaling as $\frac{1}{a^3(t)}$.
 - (a) Dark matter: $\Omega_{DM} = 0.26$.
 - (b) Usual, baryonic matter $\Omega_B = 0.049$.
- (3) Relativistic matter (Radiation)¹² $\Omega_{rad} = 9.1 \cdot 10^{-5}$, scales as $\frac{1}{a^4(t)}$.

The Standard Model particles make up about 5% of all matter and energy in the cosmos. Hence the lack of dark matter candidates within the SM is one of the principal reasons to extend the model. Within this thesis, we adopt the BSM scenarios possessing dark matter candidates. In particular, one can constrain various dark matter models from both quantum gravity perspective as well as from the dark matter one, see for example [191].

The value of dark energy density is $\rho_{DE} = (2 \cdot 10^{-3} \text{eV})^4$, which is completely different from any physical scale we observe in the physical models'¹³. The most economical description is to identify dark energy with the cosmological term from the EH action (1.7), then $\rho_\Lambda = \rho_{DE}$, such that $\rho_\Lambda = -p_\Lambda$ and at the late time expansion the Universe resembles de-Sitter space.

It may appear that the cosmological constant should play a principal role in quantum gravity research. Most of the approaches can accommodate the cosmological constant experimental value, but this value is not a specific prediction. This is the case for loop quantum gravity [193], asymptotic safety [194, 195] and causal dynamical triangulations [196, 197, 198, 199, 200]. The Causal Sets predicts cosmological constant very close to the experimental value [201]. Within string theory the prevailing opinion is that de-Sitter vacua can be at least meta-stable [181] and cosmological constant should be replaced with quintessence [182], yet see the KKLT construction [180] and the constructions within the $O(d, d)$ formalism [68, 101, 102, 103, 104]. On the other hand, anti-de-Sitter vacua with $\Lambda < 0$ are quite common within the strings compactifications, and famous Maldacena gauge/gravity duality is formulated on the $AdS_5 \times \mathbb{S}^5$ compactification of IIB string theory [18].

¹²Counting neutrinos as massless.

¹³There is a usually raised EFT argument that cosmological constant should be proportional to the cutoff $\Lambda \propto M_P^4$, due to zero-point energy calculations. However, as recently showed [192] the cosmological constant is NOT the subject to the zero-point energy contribution, making the issue of quantum corrections less severe.

The flatness problem Observationally the Universe is almost flat [190]:

$$\frac{|k|}{a_0^2} < 0.007H_0^2. \quad (1.60)$$

The spatial curvature just after the Planck era is subject to a condition:

$$\Omega_k(a) = 1 - \sum_i \Omega_i(a) < 10^{-56} \quad (1.61)$$

The question arises: can such a small value be dynamically achieved? It turns out it is quite the opposite [183, 202]. Assume we have Universe dominated by some matter with the equation of state $\rho = wp$, then by (1.14) we get

$$\frac{\partial \Omega_k}{\partial \log a} = \Omega_k(1 + 3w). \quad (1.62)$$

The $\Omega_k = 0$ is the repelling fixed point of the evolution as long as $w > -1/3$ and the fractional curvature density grows with time.

Homogeneity problem Another fine-tuning of the Early Universe is related to homogeneity and anisotropy. As we have mentioned, currently our Universe is homogeneous on large scales where the domain scale is comparable to the present horizon scale, $l_0 = ct_0 \sim 10^{26}$ m according to [183]. Yet, the sizes of domains change with time according to the scale factor, a_i/a_0 . Then from the Planck time $t_i \sim 10^{-43}$, the Universe has growth roughly: $l_i \sim l_0 \frac{a_i}{a_0}$. It is natural to compare it to a size of a causal region $l_c \sim ct_i$: $\frac{l_i}{l_c} \sim \frac{t_0}{t_i} \frac{a_i}{a_0}$. Using the relation $a = 1/T$ and

$$a_i/a_0 \sim T_0/T_{\text{PL}} \sim 10^{-32}. \quad (1.63)$$

Then a rough estimate of causally disconnected patches at the Planck time is:

$$\left(\frac{l_i}{l_c}\right)^3 \sim \left(\frac{\dot{a}_i}{\dot{a}_0}\right)^3 \sim (10^{28})^3 \quad (1.64)$$

with energy variation of order $\frac{\delta\rho}{\rho} \sim 10^{-4}$. It is an extreme fine tuned value. Moreover, approximating: $a/t \sim \dot{a}$ one gets:

$$\frac{l_i}{l_c} \sim \frac{\dot{a}_i}{\dot{a}_0}, \quad (1.65)$$

such that homogeneity scale in Λ -CDM has always been larger than the causality scale. The fact that the Universe remains homogenous despite being causally disconnected is called the *horizon* or *homogeneity* problem.

Yet, on top of that, the small inhomogeneities have to be generated in order to create stars, galaxies, etc. A possible resolution lies in dropping the strong energy condition and assuming a quasi de-Sitter stage $\rho \approx -p$ at the Early Universe when the accelerated expansion occurred.

1.4.2. Inflation

In this section, we inspect how the inflation theory explains fine-tuning problems mentioned in the previous section. Roughly speaking, inflation is a stage of accelerated

expansion of the Universe at its beginning, when gravity was repulsive. For the $k = 0$ case the Friedmann equation (1.14) is:

$$\ddot{a} = -\frac{4\pi}{3}G(\rho + 3p)a. \quad (1.66)$$

The $\ddot{a} > 0$ occurs if and only if $(\rho + 3p) < 0$, i.e. when the strong energy condition is violated. In inflationary cosmology, starting with small causally connected spacetime that grows rapidly results in causally disconnected very homogeneous Universe we observe today. The pure de-Sitter solution “cannot do the trick” since the Universe will be accelerating forever. So in the inflationary cosmology model there has to be a moment when acceleration solution turns into decelerated Friedmann solution. That moment is called the graceful exit. A scalar field called the inflaton is the natural candidate for a source term in FLRW equations providing the desired graceful exit. The action characterizes the classical homogenous scalar field:

$$S = \int_{\Omega} d^4x \sqrt{-g} \left(\frac{1}{2}\dot{\varphi}^2 - V(\varphi) \right), \quad (1.67)$$

Satisfying the Klein-Gordon equation in FLRW background:

$$\ddot{\varphi} + 3H\dot{\varphi} + V_{,\varphi} = 0. \quad (1.68)$$

together with Friedmann equation as a constraint:

$$H^2 = \frac{8\pi M_P^2}{3} \left(\frac{1}{2}\dot{\varphi}^2 + V(\varphi) \right), \quad (1.69)$$

The energy density is given by:

$$\rho = \frac{1}{2}\dot{\varphi}^2 + V(\varphi), \quad p = \frac{1}{2}\dot{\varphi}^2 - V(\varphi). \quad (1.70)$$

The equation of state is:

$$w = \frac{p}{\rho} = \frac{\frac{1}{2}\dot{\varphi}^2 - V(\varphi)}{\frac{1}{2}\dot{\varphi}^2 + V(\varphi)}, \quad (1.71)$$

for $\dot{\varphi}^2 \ll V(\varphi)$, the $\rho \approx -p$ is satisfied such that strong energy condition gets violated when the barotropic parameter $w \approx -1 < -1/3$, resulting in accelerated expansion. Then two conditions on the inflationary evolution can be put forward. They both translate into the conditions on the potential and when either gets violated the inflationary evolution stops. Because the second time derivative term in KG equation is suppressed by the Hubble term those are called the slow-roll conditions.

Slow roll condition 1: *Violation of strong energy condition $\dot{\varphi}^2 \ll V(\varphi)$, which can be controlled by*

$$\epsilon = -\frac{\dot{H}}{H^2} \simeq \frac{1}{2} \left(\frac{V_{,\varphi}}{V} \right)^2, \quad (1.72)$$

as long as $\epsilon \approx 0$ the condition is satisfied.

Slow roll condition 2: *Staying on attractor trajectory* $\ddot{\varphi} \ll 3H\dot{\varphi}$. From this condition we get:

$$3H\dot{\varphi} + V_{,\varphi} \simeq 0. \quad (1.73)$$

The second slow-roll parameter is

$$\eta = \frac{\ddot{\varphi}}{H\dot{\varphi}} \ll 1, \quad (1.74)$$

These conditions can be replaced as a condition for the potential:

$$\epsilon \simeq \frac{1}{2} \left(\frac{V_{,\varphi}}{V} \right)^2, \quad \eta \simeq \left| \frac{V_{,\varphi\varphi}}{V} \right|. \quad (1.75)$$

The inflation ends when approximately: $\epsilon \simeq 1$.

How long does Inflation last? The measure for the time of accelerated expansion is a number of e-folds, where one e-fold is the era when the Universe grows by e . In a slow-roll regime the number of e-folds (duration of inflation) is by its definition:

$$N = \int_{t_i}^{t_{end}} H dt = \int_{\varphi_i}^{\varphi_{end}} \frac{H}{\dot{\varphi}} d\varphi \simeq \int_{\varphi_{end}}^{\varphi_i} \frac{V(\varphi)}{V_{,\varphi}(\varphi)} d\varphi, \quad (1.76)$$

where in the last equality the slow-roll conditions were used. Then the equation for the scale factor can be solved in the integral form:

$$a(\varphi) \simeq a_i \exp \left(8\pi \int_{\varphi}^{\varphi_i} \frac{V}{V_{,\varphi}} d\varphi \right). \quad (1.77)$$

For example the power-law potential $V = (1/n)\lambda\varphi^n$, which satisfies both conditions at $|\varphi| \gg 1$, the scale factor is given by:

$$a(\varphi(t)) = a_i \exp \left(\frac{4\pi}{n} (\varphi_i^2 - \varphi^2(t)) \right). \quad (1.78)$$

Quantum Fluctuations The Planck CMB data clearly shows that Universe is almost homogeneous with $\delta T/T \sim 10^{-5}$. Inflationary cosmology allows to predict their origin and calculate their spectrum, while in the Λ -CDM model, they are postulated as initial conditions. According to inflation, primordial perturbations originated from quantum fluctuations. These fluctuations started to arise on scales close to Planckian length. Inflation causes them to stretch to massive (galactic) scales with almost unchanged amplitudes. Since the number of inhomogeneities is enormous, they are treated as random fields. In particular, one assumes that the Fourier components have random Gaussian¹⁴ distribution with variance:

$$\sigma_k^2 \equiv |\Phi_k|^2, \quad (1.79)$$

given by the amplitude of a two point function:

$$\langle f_k f'_k \rangle = \sigma_k^2 \delta(k + k'). \quad (1.80)$$

¹⁴One has to stress that gaussianity of inhomogeneities is an assumption coming from the measurements [203, 204]. The higher point functions can also be of interest, and they originate predominantly in multi-inflaton models. The Planck collaboration results puts an upper bound on the non-Gaussianities [203, 204].

The calculation is standard and relies on quantizing quadratic perturbations of a scalar field(s) and metrics around the classical inflationary background. We shall just sketch the relevant results. For the full derivation of this two-point function, we refer the reader towards [205] and [183, 206] and references therein. One defines the power spectrum as:

$$\mathcal{P}(k) = \frac{|\Phi_k|^2 k^3}{2\pi^2}, \quad (1.81)$$

and introduce the spectral index:

$$n - 1 = \frac{d \ln \mathcal{P}}{d \ln k}. \quad (1.82)$$

The flat spectrum gives $n_s = 1$. For the scalar perturbations one gets

$$\mathcal{P}_s(k) = A_s \left(\frac{k}{k_*} \right)^{n_s - 1}, \quad (1.83)$$

which agrees with the profile measured by Planck, where $k^* = 0.05 \text{ Mpc}^{-1}$ is the reference scale. Both $A_s = 9 \times 10^{-9}$ and $n_s \approx 0.96$ have been measured. In principle, it is possible to recover further informations about the shape of the potential from the CMB, for details see [207]. Amplitude of the scalar power spectrum fixes the value of the potential at k_* , via the relation:

$$V(\phi_*) = 24\pi^2 M_P^4 \epsilon(\phi_*) A_s. \quad (1.84)$$

During inflation the quantum fluctuations of metric are also present. Yet those, have not been measured yet. The upper bound on the relative amplitude is given by

$$r = \frac{A_t}{A_s} < 0.07, \quad (1.85)$$

where A_t is the amplitude of the tensorial modes. Both r and n_s can be related to the slow roll parameters

$$n_s - 1 \approx (-6\epsilon_* + 2\eta_*), \quad r \approx 16\epsilon_* \quad (1.86)$$

These primordial gravitational waves, if detected that would be a detection of quantum gravity itself! This is making inflationary dynamics so exciting from the Quantum Gravity perspective.

Eternal inflation The quantum fluctuations leads to another effect: the random walk of a field and a diffusion process on top of the classical motion [208, 209], which can result in inflation being eternal. Indeed, the quantum fluctuations of the inflaton field produce changes in the rate on top of classical, slow roll background. Then, the regions with a higher value of inflaton expand exponentially and dominate the universe, despite the natural tendency of inflation to end classically in the minimum of the potential. This makes inflation to continue forever, see also the further discussions on the subject of eternal inflation [209, 210, 211, 212, 213, 214, 215, 216, 101, 102, 217, 218].

Recently widely discussed is so-called de-Sitter conjecture [181, 182], which states that string theory cannot have de-Sitter vacua. In line of this swampland criteria the no eternal inflation principle¹⁵ has been put forward [30]. Namely, the de-Sitter conjecture states that any scalar potential has to satisfy:

$$M_P \frac{|V'|}{V} > c \sim \mathcal{O}(1), \quad (1.87)$$

¹⁵See further discussions about possible tensions between inflation and string theory in [219, 220].

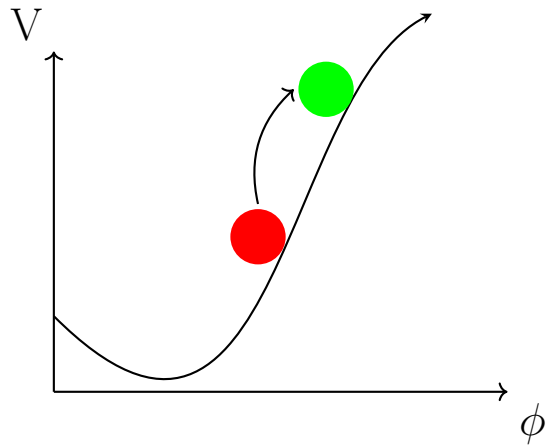


Figure 1.3: The schematic picture of the quantum jumps responsible for eternal inflation.

while the eternal inflation condition is given by:

$$\frac{V'}{V^{3/2}} < \frac{\sqrt{2}}{2\pi M_P^3}. \quad (1.88)$$

Hence c being large enough, there is a tension between those two. In Part III we investigate whether this (no) eternal inflation principle carries over to other approaches, in particular asymptotic safety.

Part II

Renormalization and quantum gravity

Chapter 2

Renormalization group techniques and the asymptotic safety program

Where we sharpen our tools by reviewing and discussing the notion of the renormalization group that is central to this thesis. We discuss how the renormalization group stems from the S-matrix in the perturbative quantum field theory. Then we turn to the complementary Wilsonian approach of integrating out the high momenta modes in the path integral. We illustrate it on the $1/r^2$ potential model in quantum mechanics. We briefly review the functional renormalization group techniques in the context of asymptotic safety in quantum gravity. We discuss when the renormalization scale can be identified with the energy scale of the process. We propose criteria for running in terms of amplitudes. We show that string theory satisfies those criteria. We point out that, studying the physical momentum dependence processes stemming from asymptotically safe theories is crucial.

2.1. The renormalization group

2.1.1. Perturbative renormalization

Quantum Field Theory (QFT) is a successful theoretical framework unifying special relativity and quantum mechanics principles. To discuss QFT, we follow closely [221, 222]. QFT in its mature form originated from the description of the scattering experiments, where initially non-interacting particles collide and interact. Results of such collisions are then measured far away from the scattering instance. These predictions of the measurements are encoded in S-matrix, an array of amplitudes between the free β_0 and α_0 states (forming two complete bases of Hilbert space):

$$S_{\beta\alpha} = \langle \beta_0 | S_0 | \alpha_0 \rangle, \quad (2.1)$$

where the α_0 represents a free prepared state of particles, and the β_0 represents free state measured on the detector. The probability for the process $\alpha_0 \rightarrow \beta_0$ to occur is then simply $|S_{\alpha\beta}|^2$, where the rate of interaction is $|S_{\beta\alpha} - \delta(\alpha - \beta)|^2$. To ensure the quantum mechanics and special relativity principles, the S matrix has to satisfy certain properties [221, 222]: unitarity, Lorentz invariance (and gauge invariance) and cluster decomposition principle ¹. In the Heisenberg picture, the quantum evolution of any

¹Distant experiments have to give uncorrelated results.

state is associated with the Hamiltonian operator H :

$$|\Psi(t)\rangle = e^{-iHt}|\Psi(0)\rangle =: U(t,0)|\Psi(0)\rangle. \quad (2.2)$$

To ensure cluster decomposition, Hamiltonian can be of the form $H = \int d^3\mathbf{x}\mathcal{H}$, where \mathcal{H} is built from local operators². The Hamiltonian can be split into $H = H_0 + H_{int}$, where the energy spectrum of H_0 is known exactly $H_0|\psi_\alpha\rangle = E_\alpha|\psi_\alpha\rangle$. Assume that³

- (i) Spectrum of H_0 is particle-like.
- (ii) Spectra of H and H_0 coincide (masses of particles are the same).

The evolution operator is

$$U(t_2, t_1) = e^{iH_0t_2}e^{-iH(t_2-t_1)}e^{-iH_0t_1}. \quad (2.3)$$

The transition operator S_0 can be defined as

$$S_0 = \lim_{t_1 \rightarrow -\infty} \lim_{t_2 \rightarrow +\infty} U(t_2, t_1). \quad (2.4)$$

Differentiating $U(t_2, t_1)$ and using $[H_0, S_0] = 0$ we get that:

$$S_0 = T \exp \left(-i \int_{-\infty}^{+\infty} d^4x H_{int}(t) \right). \quad (2.5)$$

This representation of S_0 is often used as the basis for a perturbative expansion. By virtue of the LSZ reduction [223], the processes described by S -matrix can be reconstructed from the vacuum Greens functions - the matrix elements of chronologically ordered fields

$$G_{l_1, \dots, l_n}^n(x_1, \dots, x_n) = \langle \Omega | T[\phi(x_1) \dots \phi(x_n)] | \Omega \rangle. \quad (2.6)$$

Their Fourier transformed counterparts are $G_c^n(q_1, \dots, q_n)$ and their inverse are called the n -point functions and are given by $\Gamma^{(n)}(q_1, \dots, q_n) = (G_c^n(q_1, \dots, q_n))^{-1}$. Within the perturbative expansion the Greens functions are represented graphically by Feynman diagrams. To calculate the amplitude of a process one has to find all the possible Feynman diagrams and calculate their respective contributions from Feynman rules of constructing diagrams. Let us now discuss the loop diagrams on the example of the scalar field theory with Hamiltonian density

$$\mathcal{H} = \frac{1}{2}\partial_\mu\phi_B\partial^\mu\phi_B + \frac{1}{2}m_B^2\phi_B^2 + \frac{\lambda_B}{4!}\phi_B^4. \quad (2.7)$$

Naively $\mathcal{H}_0 = \frac{1}{2}\partial_\mu\phi_B\partial^\mu\phi_B + \frac{1}{2}m_B^2\phi_B^2$ and $\mathcal{H}_{int} = \frac{\lambda_B}{4!}\phi_B^4$. Then the interactions introduce corrections to the two point Greens function (propagator)

$$G(p, p) := G(p) = \frac{i}{p^2 - m^2} (1 + \Sigma(p^2) + \dots) = \text{---} + \text{---} \text{---} \text{---} + \dots,$$

$$\Sigma(p^2) = \frac{\lambda}{2} \int \frac{d^4\mathbf{k}}{(2\pi)^4} \frac{i}{k^2 - m^2 + i0}. \quad (2.8)$$

²This is the main reason why we can perform quantization of the classical theory described by lagrangian density and hope for a sensible QFT [221, 222].

³For the Green's function approach to the QFT, where these assumptions are alleviated, see [222]. Still, to recover the finite S matrix, the self-interactions have to be subtracted for the asymptotic states.

In particular, this correction is infinite! Within our current split into \mathcal{H}_0 and \mathcal{H}_{int} , the asymptotic states receives corrections from the virtual particles circulating in the loops, such as 2.8 and hence condition (ii) is violated. Therefore, we should split the \mathcal{H} in such a way that the asymptotic states are free states and are not affected by the virtual particles to ensure condition (ii) and tie couplings to the observed quantities. At every loop order, we reformulate the \mathcal{H}_0 and \mathcal{H}_{int} in terms of measurable quantities, then the infinite corrections stemming from “wrong” splitting are not there. This procedure is called renormalization and results in a finite S-matrix.

It is often more convenient to split the renormalization procedure into three parts. In the first step, often called regularization, one extracts the parts of the diagrams that diverge when removing the regularization. This can be done by introducing a momentum cutoff in the loop integrals, or by Dimensional Regularization (DIMREG), where the theory is formulated in d dimensions and the loop integrals have poles in $d = 4$. DIMREG is much more convenient when dealing with gauge theories since then the gauge symmetry is preserved in every step of the calculation⁴.

Then in the second step, often imprecisely called renormalization, one defines new, renormalized couplings g_R and fields $\phi_B = Z^{1/2}\phi_R$, where Z is called wave-function renormalization in such a way that all of the elements of S-matrix are finite. The renormalized couplings are often split as $g_R = g_B - \delta g$, where the bare parts g_B are independent of regularization, and all the regularization dependence goes into the counterterms. The choice of counterterms is called the renormalization scheme. For example, in the on-shell scheme, the counterterms are such that the renormalized couplings are equal to the measurable quantities. On the other hand, in the minimal subtraction (MS) scheme⁵ one introduces counterterms that subtract only the divergent poles in the DIMREG procedure.

In principle, one should write all the possible counterterms respecting the symmetries of the theory. However, if a classical Lagrangian has only couplings of non-negative mass dimension, then by power counting arguments, one can show that only the n -point interactions with $n \leq 4$ can be divergent. In that case, the counterterms will have the same structure as the original terms of bare lagrangian. In particular, for ϕ^4 theory one introduces $\delta\lambda$, δm^2 counterterms and wavefunction renormalization Z .

The calculations can be done with the Feynman rules derived from (2.7) supplemented by counterterm rules, such that their summed contributions give finite physical quantities, even though they are separately divergent. In particular, the regularisation introduces the renormalization scale μ ⁶.

In the last step, called matching, one connects the resulting theory with observables such that its experimental predictions are independent of the renormalization scheme, regularisation procedure, and scale μ . This independence is automatic for the on-shell scheme, and scale dependence drops out from cross-sections or decay rates, while for other schemes, matching has to be done loop-by-loop. Typically at n loop order, one does matching at $n - 1$ loops.

⁴For studies of Yang-Mills theories with cutoff regularization, see [224].

⁵In the MS scheme, one subtracts only the divergent contributions in the $d \rightarrow 4$ limit, while in the MS one additionally subtracts the contributions that are d independent.

⁶In the cutoff regularisation, the cutoff scale is usually denoted as Λ , while the renormalization scale in DIMREG is denoted as μ . Here we adapt the Functional renormalization group convention and denote k as the renormalization scale in the Wilsonian approach, and μ is the renormalization scale/cutoff in the perturbative method. The Λ denotes cutoff in the Wilsonian approach.

2.1.2. Renormalisation group

For the schemes other than the on-shell one, such as $\overline{\text{MS}}$, in order to compensate for the possible changes of the renormalization scale μ one has to assume that the renormalized parameters of the theory depend implicitly on μ . When changing μ one has also to change the numerical values of renormalized coupling that the measurable quantities do not change. We say that couplings “run” with scale μ . The notion of the “running” couplings can be formalized by the Callan-Symanzik equation [225, 226]. In particular, the bare n-point functions are μ independent

$$\frac{\partial}{\partial \mu} \Gamma^B(p_1, \dots, p_n) = 0. \quad (2.9)$$

Since

$$\frac{\partial}{\partial \mu} \Gamma^B(p_1, \dots, p_n) = \frac{\partial}{\partial \mu} \left(Z^{-n/2} \Gamma_R^{(n)}(p_1, \dots, p_n, \{g_i\}\mu) \right) = 0, \quad (2.10)$$

we get the Callan-Symanzik equation for $\Gamma_R^{(n)}$, where $\{g_i\}$ are the couplings. In particular, for the ϕ^4 theory the resulting Callan-Symanzik equation is

$$\left(\mu \frac{\partial}{\partial \mu} + \beta_\lambda \frac{\partial}{\partial \lambda} + \gamma_m \frac{\partial}{\partial m} + n\gamma \right) \Big|_{\lambda_B, m_B} \Gamma_R^{(n)}(p_1, \dots, p_n, m_R, \lambda_R, \mu) = 0, \quad (2.11)$$

where

$$\beta_\lambda = \mu \frac{\partial \lambda_R}{\partial \mu}, \quad \gamma_m = \mu \frac{\partial m_R}{\partial \mu}, \quad \gamma = \mu \frac{\partial \log Z^{1/2}}{\partial \mu}. \quad (2.12)$$

The change (“running”) of renormalized couplings with scale μ can be read off from the renormalization group equations (RGE) ⁷:

$$\mu \frac{\partial g_R}{\partial \mu} = \beta_g, \quad \gamma = 0, \quad (2.13)$$

where the beta functions can be extracted from amplitudes or calculated within the background field method ⁸. Let us take an example of ϕ^4 theory, which beta function reads

$$\beta_\lambda = \frac{3}{16\pi^2} \lambda^2 + \mathcal{O}(\lambda^3), \quad (2.14)$$

and (2.13) can be then solved exactly

$$\lambda(\mu) = \frac{\lambda(\mu_0)}{1 - \lambda(\mu_0) \frac{3}{16\pi^2} \log \left(\frac{\mu}{\mu_0} \right)}. \quad (2.15)$$

The Eq. (2.15) can be expanded around the arbitrary reference scale μ_0

$$\lambda(\mu) = \lambda(\mu_0) + \lambda(\mu_0)^2 \frac{3}{16\pi^2} \log \frac{\mu}{\mu_0} + \lambda(\mu_0)^3 \left(\frac{3}{16\pi^2} \right)^2 \left(\log \frac{\mu}{\mu_0} \right)^2 + \dots, \quad (2.16)$$

⁷The term renormalization group comes from the fact that transitions between various renormalization scales are satisfying the axioms of a group.

⁸For simplicity from now on we drop the subscript R , keeping in mind that the renormalised coupling are discussed below.

where the first term is the tree-level scale-independent vertex, the remaining terms, stem from the momentum loop integrals. In particular, n loop diagram involves $n + 1$ vertices, giving factor $\lambda^{n+1}(\mu_0) \log^n(\mu/\mu_0)$. Then, the notion of running couplings effectively resums a sub-class of the diagrams to all orders. This resummation improves the perturbative expansion significantly for the scales departing from the scale μ_0 . Indeed, without the RG resumation at the 1-loop level the effective coupling is no longer λ but $\lambda \log(\mu/\mu_0)$. Hence, even if λ is small at the scale μ_0 , the $\lambda \log(\mu/\mu_0)$ might become big constituting the so called large logarithm problem [26], that is alleviated by the renormalization group. The resummation of geometric series provide us then with a better expansion parameter λ instead of $\lambda \log(\mu/\mu_0)$. In particular, the equation 2.15 implies that $\lambda(\mu)$ becomes infinite at some finite scale exemplifying the break-down of perturbative expansion, the so called Landau pole.

Fixed points In general, the solutions of (2.13) are not analytical, and the qualitative study of the solutions is performed. Given coupling g and its beta function β_g the fixed points (FP) are the values $g_*^{(i)}$, $i \in \{1, \dots, n\}$ at which the $\beta(g_*^{(i)}) = 0$, depending on the fixed point properties various scenarios are possible. The coupling diverges in the UV and towards IR if there is no FP. In particular, if the fixed points are complex, the running exhibits the limit cycle. We investigate such an example in Sec. 2.1.3. For the real fixed points, there are various possibilities. At the FP $g_*^{(i)}$ we define

$$\theta^{(i)} = - \left. \frac{d\beta}{dg} \right|_{g=g_*^{(i)}} , \quad (2.17)$$

such that for $\theta^{(i)} < 0$ ($\theta^{(i)} > 0$) the fixed point $g_*^{(i)}$ is is IR (UV) attractive. Thus trajectories in the vicinity of the fixed point would lead to the IR (UV) fixed point ⁹. If $g_*^{(i)} \equiv 0$ we call such a point a Gaussian fixed point (GFP). Theories with the GFP in the UV are called asymptotically free (AF). Most famously, the Yang-Mills theories with $SU(N_c)$ gauge group coupled to N_F Dirac fermions and N_s real scalars can be asymptotically free due to the existence of attractive GFP. Their beta function at one loop reads [227]:

$$\beta(g) = \frac{g^3}{16\pi^2} \left(\frac{-11}{6} N_c + \frac{4}{3} N_F + \frac{1}{6} N_S \right) . \quad (2.18)$$

In particular, for $N_S = 0$ as long as $N_c > \frac{4}{11} N_F$ the AF is achieved. This is the case of the QCD sector of the Standard Model [111, 112].

On the other hand, when $g_* \neq 0$ we call such fixed point non-Gaussian/interacting and theories where the UV non-Gaussian FP is realized are called asymptotically safe (AS).

Let us now discuss the physical implications for various behaviors. First, the theory to be UV fundamental, i.e., having predictions at all scales, must possess a UV fixed point. This requirement narrows down the set of IR values of the couplings. In particular, if the equation for running of the coupling g possesses a UV repulsive fixed points at UV scale, then there is only one low energy initial condition $g(\mu_0)$ stemming from that FP. In particular, when a theory to be UV fundamental requires $g(\mu) = 0$ for all scales,

⁹Discussion below can be naturally extended to the multiple couplings case, In particular, critical exponents are defined as minus eigenvalues of the stability matrix.

then such theory is non-interacting at all scales, i.e., *trivial*. This is the case of ϕ^4 theory, where to avoid the Landau pole, one requires $\lambda(\mu) = 0$ at all scales. On top of ϕ^4 theory, this is the case of the matter charged under Abelian gauge group [228], where Abelian gauge coupling g_Y scale dependence is given by

$$\beta_{g_Y} = \#_1 g_Y^3 + \mathcal{O}(g_Y^5) \quad (2.19)$$

where $\#_1$ is the positive one-loop coefficient of the perturbative expansion [228], resulting in a Landau pole behavior.

The argument above relies on the perturbative studies of the scale dependence of g_Y . Yet, the non-perturbative studies using lattice [229] or functional methods [230] suggest that the divergence of the gauge coupling persists beyond perturbation theory. It seems that the existence of the Landau pole carries over to the Abelian gauge sector of the Standard Model [135]. There, it results in the so-called *triviality problem*, since the Abelian hypercharge is measured to be non-zero. We discuss a possible solution within the asymptotic safety framework in Sec. 4.3.

2.1.3. Wilsonian renormalization

The Wilsonian renormalization conceptually differs from the perturbative approach discussed above. In the momentum space, the general set-up is the following¹⁰. One introduces a cutoff Λ and “effective” theory at scale $k \ll \Lambda$, such that all the fluctuations with momenta bigger than k are integrated out. Unlike the perturbative renormalization, the Wilsonian procedure does not express the theory’s parameters in terms of observables. Instead, the counterterms are found by demanding that the theory at k cannot depend on Λ . At the same time, processes in the effective theory occurring at energies much smaller than k cannot depend on k because the cutoff k is merely a mathematical boundary between the implicit degrees of freedom above and explicit degrees of freedom below k . Namely, in the complete theory that ranges up to Λ , the arbitrary splitting of degrees of freedom into above and below k must be of no physical consequence.

To illustrate this view-point, let us study example of $1/r^2$ potential [11] in 3 dimensions. Eigenvalue problem for Hamiltonian

$$H = \frac{\vec{p}^2}{2m} - \frac{g}{\vec{r}^2}, \quad (2.20)$$

provides a well-known example of a singular Schrödinger equation that requires regularization and produces a limit cycle [232, 233, 234, 235, 236, 237, 238, 239]. On the other hand, the Hamiltonian of Eq. (2.20) is of broad interest phenomenologically e.g. describing a charge interacting with a point dipole. From the theoretical side, the potential is providing an example of scaling-symmetry breaking through dimensional transmutation [240], associated with renormalization. Renormalization of $1/r^2$ is described in the position representation by several authors [236, 233, 234, 236, 241] as well as in the momentum representation using the ultraviolet cutoff μ on the particle momentum. Yet, those procedures are justified *a posteriori*. Namely, one hypothesizes a corrected Hamiltonian and derives solutions of the Schrödinger equation to verify the

¹⁰In the position space, one averages out over patches of space, in particular for the Ising model, one average over squares and derives the block spin RG, see [231]. Discussion of it is beyond the scope of this work.

hypothesis.

On the other hand, we use here a well-defined procedure, introduced in Refs. [242, 243, 244, 245]. The renormalization procedure starts with regulating it in a scheme called the “triangle of renormalization” [246]. Introducing the cutoff Λ we regularize theory and introduce H_Λ , from which we evaluate the effective Hamiltonians H_k with cutoffs $k \ll \Lambda$. We demand that matrix elements of H_k with finite k in the subspace of states limited by k do not depend on Λ , such that the limit $\Lambda \rightarrow \infty$ is well defined. This condition allows us to determine the structure of counterterms needed in H_Λ , which is done in a sequence of successive approximations that improves the counterterms put in H_Λ until all matrix elements in H_k in the subspace of states limited by k become independent of Λ . As a result, we obtain a family of Hamiltonians H_k whose predictions for all eigenvalues much smaller than k are by construction independent of k . In momentum representation the Eq. (2.20) reads as

$$\frac{p^2}{2m}\phi(\vec{p}) - \frac{g}{4\pi} \int d^3q \frac{\phi(\vec{q})}{|\vec{p} - \vec{q}|} = E\phi(\vec{p}). \quad (2.21)$$

We use the spherical harmonics decomposition and introduce the wave-functions with definite angular momentum, $\phi(\vec{p}) = \psi_l(p)Y_{lm}(\Omega_p)$. The problem then reduces to

$$p^2\psi_l(p) + \int_0^\infty dq q^2 V_l(p, q) \psi_l(q) = \mathcal{E}\psi_l(p), \quad (2.22)$$

where $\mathcal{E} = 2mE$ and $V_l(p, q)$ given by

$$V_l(p, q) = -\frac{\alpha}{2l+1} \left[\frac{\theta(p-q) q^l}{p^{l+1}} + \frac{\theta(q-p) p^l}{q^{l+1}} \right]. \quad (2.23)$$

The $\alpha = 2mg$ is the dimensionless coupling constant and θ is the Heaviside step function. We regulate the (2.22) by posing a bound on momenta $p, q \leq \Lambda$. We now eliminate the high momentum modes proceeds in infinitesimal steps: to $\Lambda - d\Lambda$,

$$p^2\psi_l(p) + \int_0^{\Lambda-d\Lambda} dq q^2 V_l(p, q) \psi_l(q) - \frac{\alpha}{2l+1} \frac{p^l}{\Lambda^{l+1}} \psi_l(\Lambda) d\Lambda = \mathcal{E} \psi_l(p). \quad (2.24)$$

The $\psi_l(\Lambda)$ is expressed in terms of values of $\psi_l(p)$ with $p < \Lambda - d\Lambda$ by setting $p = \Lambda$ in Eq. (2.24). For eigenvalues $\mathcal{E} \ll \Lambda^2$ and neglecting $\mathcal{O}(d\Lambda^2)$ terms

$$\psi_l(\Lambda) = \frac{\alpha}{(2l+1)\Lambda^2} \int_0^{\Lambda-d\Lambda} dq q^2 \frac{q^l}{\Lambda^{l+1}} \psi_l(q). \quad (2.25)$$

For $\Lambda - d\Lambda$ being the new-cutoff k , we have

$$p^2 \psi_l(p) + \int_0^k dq q^2 [V_l(p, q) + \gamma_k q^l p^l] \psi_l(q) = \mathcal{E} \psi_l(p), \quad \gamma_k = -\frac{\alpha^2 d\Lambda}{(2l+1)^2 \Lambda^{2l+2}}. \quad (2.26)$$

Further reduction of the cutoff k to $k - dk$ results in

$$p^2 \psi_l(p) + \int_0^{k-dk} dq q^2 [V_l(p, q) + \gamma_{k-dk} q^l p^l] \psi_l(q) = \mathcal{E} \psi_l(p), \quad (2.27)$$

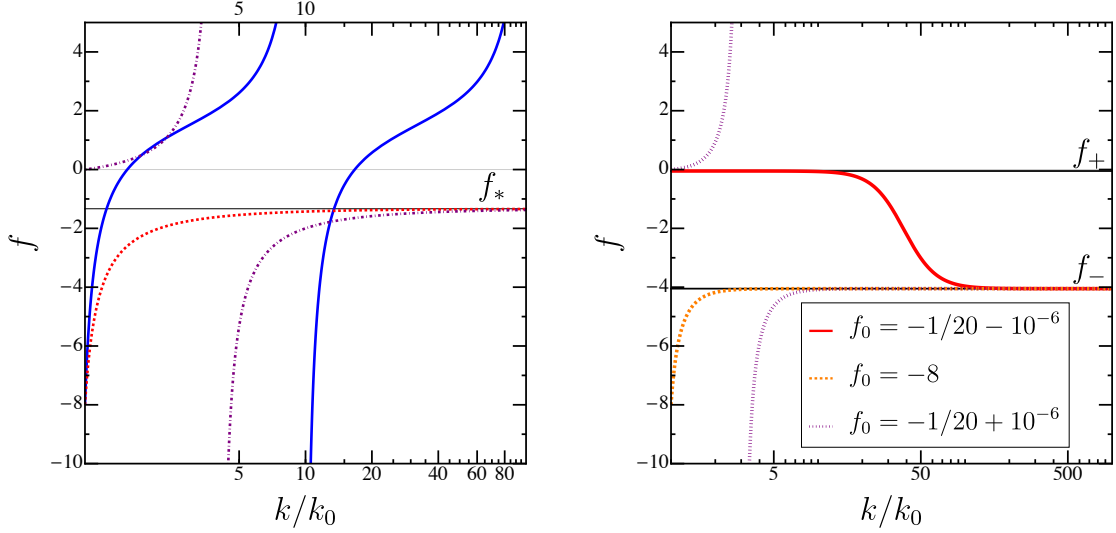


Figure 2.1: Limit cycle for $1/r^2$ potential.

Left: The evolution for $\alpha = 2$. The blue line represents $f(k_0) = -8$, $l = 0$ and runs according to the limit cycle behaviour. The red, dashed line represents $f(k_0) = -8$, $l = 1$ and converges to the attractive fixed point f_* . The purple dot-dashed line denotes the Landau pole behaviour for $f(k_0) = 0$ and $l = 1$.

Right: the running for $\alpha = \alpha_{lc}$ and $l = 2$. There are two fixed points present $f_- = -4.05$ and $f_+ = -0.05$. The fixed point f_- is attractive such that both trajectories starting at $f_0 = -1/20 - 10^{-6}$ and $f_0 = -8$ evolve towards f_- . On the other hand the f_+ is repulsive. This is illustrated by the Landau pole behaviour for the purple line $f_0 = -1/20 + 10^{-6}$.

where

$$\gamma_{k-dk} = \gamma_k - \left[\gamma_k k^l - \frac{\alpha}{(2l+1)k^{l+1}} \right]^2 dk. \quad (2.28)$$

Now no new terms appear and the coupling constant $\gamma_k \rightarrow \gamma_{k-dk}$. Hence the infinitesimal scale transformation of $\gamma_k \rightarrow \gamma_{k-dk}$ obeys the Riccati equation

$$\frac{d\gamma}{dk} = \left[\gamma k^l - \frac{\alpha}{(2l+1)k^{l+1}} \right]^2. \quad (2.29)$$

For $l = 0$ our results reproduce those found in [237]. There is also second equation on scale dependence of α :

$$\frac{d\alpha}{dk} = 0, \quad (2.30)$$

hence α is not-scale dependent. In order to solve Eq. (2.29) we make an ansatz $\gamma_k = f(k)/k^{2l+1}$ and obtain the β -function for $f(k)$

$$k \frac{\partial f}{\partial k} = \beta(f) = (f - A)^2 + B^2, \quad A = \frac{2\alpha - (2l+1)^2}{2(2l+1)}, \quad B = \sqrt{\alpha - \frac{(2l+1)^2}{4}}. \quad (2.31)$$

For $B \neq 0$, the solution for the dimensionless coupling is

$$f(k) = \left[B \tan \left(\varphi + B \ln \frac{k}{k_0} \right) + A \right], \quad \varphi = \arctan \left(\frac{f_0 - A}{B} \right). \quad (2.32)$$

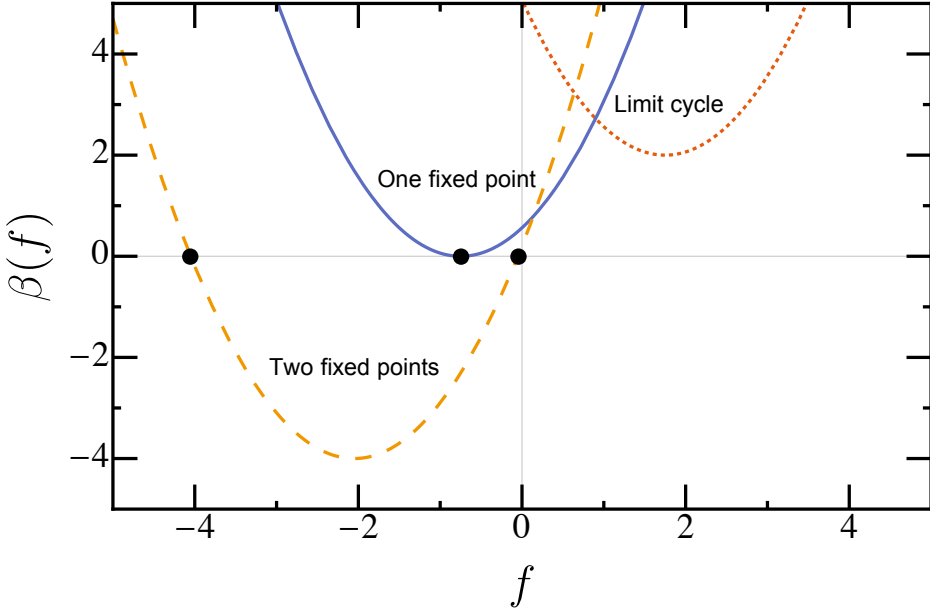


Figure 2.2: Dependence on l . Plot done for $\alpha = \alpha_{lc} = (1 + 1/2)^2$. Increasing l the situation changes the qualitative behaviour of the system. For $l = 0$ the fixed points are complex and the limit cycle occurs, for $l = 1$ there is one fixed point, for $l = 2$ the two fixed points emerges. The fixed points are the same as in the right panel of Fig. 2.1, f_- is attracting and the f_+ is repulsive.

At scale k_0 the value $f_0 = f(k_0)$ can be matched to the physical energy value of a partial wave. When B is real, which occurs when the coupling constant $\alpha > \alpha_{lc} = (l + 1/2)^2$, the theory posses a limit cycle for $l' \leq l$, in particular see left panel in the Fig. 2.1. Then, the H_∞ does not exists, due to oscillations of f with k there is no UV FP. On the other hand, when B is purely imaginary, *i.e.* $\alpha < \alpha_{lc}$, the constant f tends to f_* , for $k \rightarrow \infty$ resulting in asymptotic safety. For $l = 0$, the well-known critical-value condition is recovered at $\alpha_{0c} = 1/4$. For $\alpha = \alpha_{lc}$ one gets

$$f - A_c = \frac{f_0 - A_c}{1 - (f_0 - A_c) \ln \frac{k}{k_0}}, \quad (2.33)$$

with $A_c = -(2l + 1)/4$ and the asymptotically safe fixed point at $f = A_c$ is the edge of the basin of attraction. Thus, asymptotic safety is reached for $f_0 < A_c$ and the theory hits the Landau pole for $f_0 > A_c$. Finally, $B \rightarrow 0$ results in period growing to infinity, hence our result demonstrates connection between renormalization group limit cycle, asymptotic safety and asymptotic freedom [247]. Finally let us note that as long as $\mathcal{E} \ll k$ our results are exact and catches all possible terms that are generated along the renormalization group flow. This won't be possible for more general theories, in particular for QFTs.

Wilsonian procedure and the path integral So far we have discussed the Wilsonian procedure for Hamiltonians. Now we turn our attention to the path integral approach [248] and Lagrangians. Consider a general action

$$S[\phi] = \int d^4x \left[\frac{1}{2} \partial^\mu \phi \partial_\mu \phi + \sum_i \bar{g}_{i,0} \mathcal{O}_i(x) \right], \quad (2.34)$$

where $\mathcal{O}_i(x)$ are some local operators of dimension $d_i > 0$ and $\bar{g}_{i,0}$ are the corresponding couplings. Then the Wick rotated path integral for the action (2.34) is

$$\mathcal{Z}[J] = \int_{\phi \in C^\infty(M)} \mathcal{D}\phi e^{-S[\phi] + \int d^4x J[\phi] \cdot \phi}, \quad (2.35)$$

where $J[\phi]$ is some external source. The path integral (2.35) can be used to calculate the Green's functions (2.6)

$$\frac{\langle \Omega_J | T[\phi(x_1) \dots \phi(x_n)] | \Omega_J \rangle}{\langle \Omega_J | \Omega_J \rangle} = \frac{\int \mathcal{D}\phi(x_1) \dots \phi(x_n) e^{-S[\phi] + \int d^4x J[\phi] \cdot \phi}}{\mathcal{Z}[J]}, \quad (2.36)$$

similarly to the previous case this expression also have to be renormalized. From now on, in this paragraph we shall assume $J \equiv 0$. We start by regularizing 2.34

$$S_\Lambda[\phi] = \int d^4x \left[\frac{1}{2} \partial^\mu \phi \partial_\mu \phi + \sum_i \Lambda^{4-d_i} g_{i0} \mathcal{O}_i(x) \right], \quad (2.37)$$

where we define the dimensionless couplings as $\bar{g}_{i,0} = \Lambda^{d-d_i} g_{i0}$. We call 2.37 the microscopic action and define regularized partition function as

$$\mathcal{Z}_\Lambda(g_{i0}) = \int_{\phi \in C^\infty(M)_{\leq \Lambda}} \mathcal{D}\phi e^{-S_\Lambda[\phi]}, \quad (2.38)$$

the integration is taken over those ϕ that within the Fourier decomposition $p \leq \Lambda$. Similarly as before we introduce the renormalization scale k and split field $\phi(x) = \varphi(x) + \chi(x)$ such that $\chi(x) \in C^\infty(M)_{[k,\Lambda]}$ and $\varphi \in C^\infty(M)_{\leq k}$. The measure splits as $\mathcal{D}\phi = \mathcal{D}\varphi \mathcal{D}\chi$. Performing the integral over the χ results in a Wilsonian effective action (playing the same role as the effective Hamiltonians) at scale k , resulting in the following equation

$$S_k^{\text{eff}}[\phi] = -\log \left[\int_{C^\infty(M)_{[k,\Lambda]}} \mathcal{D}\chi \exp(-S_\Lambda[\varphi + \chi]) \right], \quad (2.39)$$

for the low-energy modes. Similarly as before the process can be iterative and we can obtain new Wilsonian effective action at even lower scale k'

$$S_{k'}^{\text{eff}}[\phi] = -\log \left[\int_{C^\infty(M)_{[k',k]}} \mathcal{D}\chi \exp(-S_k^{\text{eff}}[\varphi + \chi]) \right]. \quad (2.40)$$

Note that

$$\mathcal{Z}_k(g_i(k)) = \int_{C^\infty(M)_{\leq k}} \mathcal{D}\phi \exp(-S_k^{\text{eff}}[\phi]) \quad (2.41)$$

is the same as

$$\mathcal{Z}_k(g_i(k)) = \mathcal{Z}_\Lambda(g_{i0}), \quad (2.42)$$

hence \mathcal{Z} should be independent of k :

$$k \frac{d\mathcal{Z}_k(g)}{dk} = \left(k \frac{\partial}{\partial k} \Big|_{g_i} + k \frac{\partial g_i(k)}{\partial k} \frac{\partial}{\partial g_i} \Big|_k \right) \mathcal{Z}_k(g_i) = 0, \quad (2.43)$$

such that

$$k \frac{\partial g_i(k)}{\partial k} = d_i g_i + \eta(g_i). \quad (2.44)$$

Starting from S_Λ along the renormalization group trajectory, all of the possible terms respecting symmetries of the microscopic action are generated. In particular, for the ϕ^4 theory, we expect the $\phi^{(2n)}$ terms to be generated. Despite the notational simplicity of the Callan-Symanzik equation, the Wilsonian approach starts from a different philosophy and results in the other organizing principles of the expansion. In particular, the renormalization group equation 2.43 is often called Exact Renormalization Group (ERG) ¹¹ since the couplings do not have to lie within the perturbative regime.

2.1.4. Functional renormalization Group

In the Functional renormalization Group (FRG), for reviews see e.g.[194, 250, 251, 252, 253, 254], instead of studying the path integral one studies its Legendre transform - the Euclidean effective action ¹²

$$\Gamma_E[\Phi] = -\log \mathcal{Z}[J] + \int d^4x J(x) \cdot \Phi(x), \quad \Phi(x) = \frac{\delta \mathcal{Z}[J]}{\delta J(x)}, \quad (2.45)$$

where we define “classical” field Φ as being generated by external source J . The Φ can be a field of any spin and internal indices. In the discussion below we assume those only implicitly. The Γ_E is the effective action for the classical field Φ , satisfying quantum-corrected equations of motions in presence of sources

$$\frac{\delta \Gamma_E[\Phi]}{\delta \Phi} = J[\Phi], \quad \left. \frac{\delta \Gamma_E[\Phi]}{\delta \Phi} \right|_{J=0} = 0. \quad (2.46)$$

From now on we drop the subscript E . Solving above equations for Γ results in the full interacting quantum field theory. For constant vacuum expectation value (vev) $\Phi = \varphi_c$ the above equation reduces to a *c*-number equation

$$\frac{dV(\varphi_c)}{d\varphi_c} = 0 \text{ and } \Gamma[\varphi_c] = -V_{\text{eff}}(\varphi_c) \left(\int d^4x \right). \quad (2.47)$$

The effective potential $V_{\text{eff}}(\varphi_c)$ is sufficient when studying the momenta independent minimas of the theory.

Following the considerations from the previous Section, one can integrate the quantum fluctuations momentum wise. In order to do so one introduces an mass IR-cutoff $\Delta S_k[\phi]$ such that

$$\mathcal{Z}_k[J] = \int D\phi e^{-S[\phi] - \Delta S_k[\phi] + \int J \cdot \phi}, \quad (2.48)$$

and

$$\Gamma_k[\Phi] = -\log \mathcal{Z}_k[J] + \int d^4x J(x) \cdot \Phi(x) + \Delta S_k[\Phi] \quad (2.49)$$

with

$$\Delta S_k(\phi) = \frac{1}{2} \int d^4q \phi(-q) R_k(q) \phi(q), \quad (2.50)$$

the regulator $R_k(q)$ satisfies the following properties:

¹¹For the smooth cutoff implementation see [249].

¹²This is often more convenient, since the effective action removes the redundant vacuum non-connected diagrams.

- (i) it suppresses the IR modes with $z < k$ and leaves modes with $z > k$ unchanged. Two popular regulators are exponential: $R_k(q) = \alpha q^2 e^{q^2/k^2} - 1$) and the theta one $R_k(q) = \alpha(k^2 - q^2)\theta(k^2 - q^2)$, where α is parameter of order of unity.
- (ii) It vanishes in the limit $k \rightarrow 0$ such that the full effective action is restored: $R_k(k^2/q^2 \rightarrow 0) = 0$ such that $\Gamma_k \rightarrow \Gamma$.
- (iii) The fundamental action is restored in the limit $k \rightarrow +\infty$: $R_{k \rightarrow \infty}(q^2) \rightarrow \infty$.

Then the exact equation for Γ_k can be derived [118, 119]:

$$k\partial_k \Gamma_k = \frac{1}{2} \text{STr} \left(\frac{\delta^2 \Gamma_k}{\delta \phi \delta \phi} + R_k \right)^{-1} \frac{k\partial R_k}{\partial k} \quad (2.51)$$

the super-trace STr involve an integration over 4-dimensional space as well as the summation internal indices for the fields with such. The flow equation 2.51 is in principle exact, but cannot be solved exactly in practice. Therefore the effective action is truncated to given set of operators ¹³

$$\Gamma_k[\Phi] = \sum_i g_i(k) \mathcal{O}_i(\Phi). \quad (2.52)$$

The beta-functions of couplings, which parameterize the different \mathcal{O}_i in Γ_k , can be extracted from the flow equation by projecting onto the corresponding field monomials. The form of regulator satisfying (i), (ii), (iii) results in the calculation of the effective action in a momentum shell wise fashion, since at scale k , the dominant contributions come from the modes $q \approx k$, due to the form of $\frac{dR_k}{dk}$. Furthermore, $\frac{dR_k}{dk}$ serves also as a UV cutoff making the expression free from UV divergences. The construction above can be generalized to gauge theories and gravity, see, e.g., [194, 250, 251, 252, 254].

2.2. Asymptotic safety in quantum gravity

As we have discussed in Sec. 1.1.1, gravity, to be quantized, requires the addition of new counterterms at each loop, which means an infinite number of counterterms with different operator structures than R . However, an infinite number of experiments cannot be performed to find all the couplings of the theory, so gravity is nonrenormalizable perturbatively. To solve this problem, various approaches have been proposed.

First, an additional interaction/symmetry can be introduced to remove all higher counterterms. For example, in the supergravity theory [255], by introducing supersymmetry as local symmetry, the theory becomes renormalizable (at least up to 8 loops for $N = 8$ supergravity [256]), and possibly even finite [257] which seems to be indicated by the amplitude calculations [258, 259, 260] and the double copy conjecture [261, 262]. In the (super) string theory, Weyl symmetry (along with supersymmetry) is introduced, which, together with the assumption that at the fundamental level, the components of matter are strings, not point particles, makes this theory capable of describing quantum gravity at every scale [97, 98].

Second, one can accept that gravity indeed can possess an infinite number of couplings. However, the theory is nevertheless predictive as long as the values of (almost) all couplings can be calculated theoretically, such that they are functions of finite number of

¹³For the other expansions schemes, such as derivative expansions see [254].

experimental values¹⁴. This is, for example, the case of asymptotic safety in quantum gravity (ASQG) proposed by Weinberg [108, 25, 26], where one requires the scale symmetry in the UV, such that

$$k \frac{\partial g_i}{\partial k} \Big|_{g_{i,*}} = 0. \quad (2.53)$$

As we have discussed, this is necessary for the theory to be UV-fundamental [25, 109, 110] such that the limit $\Lambda \rightarrow \infty$ is meaningful. For the dimensionless counterpart of Newton coupling $G = \bar{G}k^2$ the beta function is:

$$\beta(G) = 2G + \gamma G^2 + \mathcal{O}(G^3). \quad (2.54)$$

If $\gamma < 0$ the Newton coupling possesses an asymptotically safe fixed point. The Functional renormalization Group (FRG) [118, 119] techniques adapted to quantum gravity indicate towards $\gamma < 0$ and such a tentative fixed point was found [121, 122, 264, 265] (previously conjectured by other considerations [113, 114, 115, 116, 117]). Given the theory, the number of free parameters is the number of UV-attractive directions in the flow of all possible couplings, since all the others become the function of the relevant directions. For the theory to be predictive, one requires the amount of UV-attractive directions to be finite. This is called the finite *hypersurface requirement*. In particular, most of the calculations indicate that there are 3 relevant directions associated with monomials R , Λ and relevant direction in the R^2 , $R_{\mu\nu}R^{\mu\nu}$ plane [266] and review [194], yet see [267] for the other possible FP. On the other hand, the FP for G_N at 0 is UV-repulsive. This is why the perturbation expansion collapses (the expansion around the zero fixed point) and why gravity appears nonrenormalizable at first glance. When applied together to gravity, scale symmetry and finite hypersurface conditions constitute the asymptotic safety program. Let us now briefly discuss the setup for calculations within the FRG framework.

Functional renormalization group calculations The truncation of the gravitational system is of the form [194]

$$\Gamma_k = -\frac{1}{16\pi G k^{-2}} \int d^4x \sqrt{g} (R - 2\Lambda k^2) + \Gamma_{k,\text{higher-order}} + S_{\text{gf},h} + S_{\text{ghost}} + \Gamma_{k,\text{matter}}, \quad (2.55)$$

where the dimensionless versions of the Newton coupling G and of the cosmological constant Λ are introduced. The gauge-fixing action is given by

$$S_{\text{gf},h} = \frac{1}{32\pi\alpha_h G k^{-2}} \int d^4x \sqrt{\bar{g}} \mathcal{F}^\mu \bar{g}_{\mu\nu} \mathcal{F}^\nu. \quad (2.56)$$

and α_h is one of two gauge parameters. The second, β_h enters the definition of \mathcal{F}^μ , with

$$\mathcal{F}^\mu = \left(\delta^{\mu\kappa} \bar{D}^\lambda - \frac{1+\beta_h}{4} \delta^{\kappa\lambda} \bar{D}^\mu \right) h_{\kappa\lambda}. \quad (2.57)$$

¹⁴In string theory, there are symmetries of the amplitude (and of the corresponding effective action) like $O(d, d)$ symmetry in string theory [68, 103] that tie together many terms in the lagrangian – for example a 4-graviton amplitude involves many higher curvature terms that are uniquely fixed by the symmetry [104, 263].

The gauge fixing also introduces Fadeev-Popov ghosts, see [268, 269]. In the background-field method the full metric is decomposed into a background metric and a fluctuation field, according to

$$g_{\mu\nu} = \bar{g}_{\mu\nu} + h_{\mu\nu}. \quad (2.58)$$

Note that $h_{\mu\nu}$ does not have to be a small fluctuation.

The matter degrees of freedom impact gravity and hence change position of the fixed point. In this thesis in Sec. 4.3 we study the impact of gravity on the N_V system of $U(1)$ gauge bosons. Through this thesis we choose the regulator as

$$R_k = \Gamma_k^{(2)} \Big|_{\Lambda=0} r_k(p^2/k^2), \quad (2.59)$$

with the shape-function r_k , see discussions on the regulator [270, 250, 271, 272]. For the shape-function r_k we choose a Litim-type cutoff [273]

$$r_k(p^2/k^2) = \left(\frac{k^2}{p^2} - 1 \right) \theta(1 - p^2/k^2), \quad (2.60)$$

resulting in analytic expressions for the beta-functions. In the Landau gauge ($\alpha_h = 0$, $\beta_h = 1$) the beta functions for Λ , G are given by ¹⁵:

$$\begin{aligned} \beta_G &= 2G - \frac{1}{6\pi(1-2\Lambda)^2} (56\Lambda^2 + 4(1-2\Lambda)^2 N_V - 68\Lambda + 29) G^2, \\ \beta_\Lambda &= -2\Lambda + \frac{G}{6\pi(1-2\Lambda)^2} (\Lambda + 3(-1+N_V) - 16\Lambda N_V - 8\Lambda^3(7+2N_V) + 4\Lambda^2(5+7N_V)), \end{aligned} \quad (2.61)$$

with the non-trivial solution

$$G_{N,*} = \frac{12(1-2\Lambda_*)^2\pi}{29 + 4N_V + 8(\Lambda_*)^2(7+2N_V) - 4\Lambda_*(17+4N_V)}, \quad (2.62)$$

such that as $N_V \rightarrow +\infty$ the non-trivial fixed point reaches the limit of vanishing interaction: $G_{N,*}$, $\Lambda_* \rightarrow (0, \frac{3}{8})$, see Fig. 2.3. This result is coinciding with the studies of AS in the large N_F expansion [117]. The calculations have been done for various choices of α_h , β_h , regulators and performed within various truncations and in various setting give compelling evidence for the existence of the UV fixed point, see reviews [194, 254, 278, 279]. In particular it has been shown that the 2-loop counterterm is also asymptotically safe [280].

Interactions with matter As much as matter degrees of freedom influence the position of the gravitational fixed point, gravity can alter the running of the matter coupling. For the couplings of dimension $d = 4$ this is schematically given by

$$\beta_g = -f_g g + \beta_g^{\text{matter}} \quad (2.63)$$

where f_g is the quantum gravitational contribution, which depends explicitly on the gravitational couplings. In the context of asymptotically safe quantum gravity, the dimensionless counterparts of the gravitational couplings have constant FP values above

¹⁵We use the results from [274] together with [275, 22]. For the results in the other gauges see [276, 277], see also the discussion in [272].

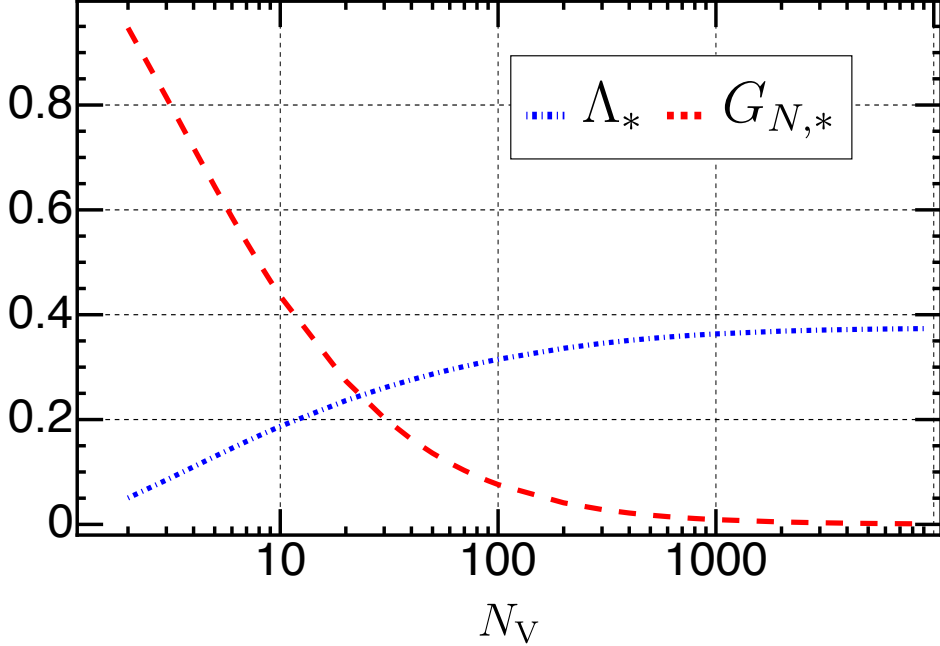


Figure 2.3: The position of the gravitation fixed point depending on N_V for $\beta_h = 1$.

the Planck scale. Below the Planck scale, the Newton coupling approaches zero quickly. Therefore, the gravitational contribution can be approximated as

$$f_g = \begin{cases} f_g^* & \text{as } k > M_P \\ 0 & \text{as } k \leq M_P. \end{cases} \quad (2.64)$$

For the gauge coupling the explicit computations using the FRG techniques yield $f_g \geq 0$ [281, 282, 283, 284, 285, 286, 287, 288]. For the Yukawa coupling the sign of the contribution can vary throughout the parameter space [289, 290, 291]. For the scalar couplings one gets $f_g < 0$ [292, 293, 294, 295]. The corrections from gravity interpolating between the transplanckian and the subplanckian regimes are given as [292]:

$$\beta_{\text{grav}}(g, \mu) = \frac{a_i}{8\pi} \frac{k^2}{M_P^2 + 2\xi_0 k^2} g, \quad (2.65)$$

where $M_P = 2.4 \times 10^{18}$ GeV is the low energy Planck mass, $\xi_0 \approx 0.024$. Depending on the sign of a_i one gets repelling / attracting GFP for a given coupling. Following [292] we choose $a_\lambda = +3$, $a_{y_t} = -0.5$, $a_{g_i} = -1$. The low-energy values stemming from the repelling fixed points becomes predictable. Since $a_\lambda = +3$, then Higgs self coupling has a repelling fixed point at zero, and becomes a prediction of a theory rather than being a free parameter.

This results in the rich phenomenological behavior, such as prediction of Higgs mass in Standard Model [292] and in various extensions [8, 9], prediction of masses of various quarks [296, 297], properties of dark matter [191, 298] and resolution of the Landau pole in the U(1) sector ¹⁶. We shall discuss those in Chapter 4.

¹⁶Since the gravitational couplings are not marginal, the gravitational contribution f_g is not universal and scheme-dependent. Studies using dimensional regularization within perturbation theory indicate that $f_g = 0$ [299, 300, 301, 302, 303], but neglect the contribution of higher-order couplings to the scale dependence of g_Y [285].

2.3. Scale identification for μ and k

So far, we have not discussed whether the scales μ and k can be attributed to some physical processes. In this Section, we fill this gap.

2.3.1. Dimensionless couplings

For dimensionless couplings, the n -point functions are symmetric under the exchange of momenta. In particular, the 4-point functions exhibit the *crossing* symmetry [24, 303], i.e. permutation symmetry in the Mandelstam variables $s = (p_1 + p_2)^2$, $t = (p_1 + p_3)^2$, $u = (p_1 + p_4)^2$ [304]. For dimensionless couplings, the counterterms are proportional to the couplings themselves, and the sign of the loop correction is not channel dependent (*universality*)¹⁷. These two facts mean that the renormalization scale μ can be attributed to the energy scale (*scale identification*) of the processes. Then the energy dependence of the S -matrix processes can be “packed” into the renormalization group equations (RGE), such that dominant logarithmic corrections are resumed (*renormalization group improvement*). Then studying the renormalization group equations results in studying the energy dependence of the theory.

This scale identification can be used to study the minimas of the quantum effective potential (2.66) [240]. In particular, for (2.7) coupled to scalar electrodynamics with $m_B = 0$, classically the potential has minimum only at $\varphi_c = 0$. The one-loop effective potential is given by

$$V(\phi) = V^0(\phi) + V^1(\phi, \mu) \approx \frac{\lambda}{4!} \phi^4 + \frac{3e^4 \phi^4}{64\pi^2} \left(\log \frac{\phi^2}{\mu^2} - \frac{25}{6} \right). \quad (2.66)$$

Since μ is an arbitrary scale it can be identified with the value of the field as

$$\mu = \varphi_c. \quad (2.67)$$

At the minimum of V one has

$$0 = V'(\varphi_c) = \left(\frac{\lambda}{6} - \frac{11e^4}{16\pi^2} \right) \varphi_c^3, \quad (2.68)$$

such that the expression for the potential is

$$V(\phi) = \frac{3e^4}{64\pi^2} \phi^4 \left(\log \frac{\phi^2}{\varphi_c^2} - \frac{1}{2} \right). \quad (2.69)$$

Furthermore, the theory possesses non-trivial minima generated radiatively. This mechanism is called the Coleman-Weinberg mechanism [240] and would be crucial for our discussion in Chapter 3. The technicalities together with the renormalization-group improvement of these results are discussed in App. A, where we introduce novel ways to calculate the effective potential. Here let us note that (2.67) is not always the “best choice” of the scale identification. In particular, in the case of multiple fields, there are multiple physical scales that can be identified with μ . However, as we shall argue, there exists an “optimal” choice for the theory with multiple scalar fields that allows for all order resummation, which will be discussed in App. A. In that approach the renormalization scale μ is chosen such that the quantum corrections vanishes $V^1(\phi, \mu) = 0$.

¹⁷Note that also until two loops, the beta functions are scheme independent in the mass-independent schemes.

[305].

Finally, let us note that both effective action and effective potential are not gauge independent quantities. This is why they should be used with caution, and the gauge dependence of the results has to be checked. This is the case, e.g., for the Higgs stability bound [306, 307], yet the ambiguities are too small to “make a difference”. Study of gauge dependence of the results in asymptotic safety will be discussed in Sec. 4.3.4.

2.3.2. Scale identification in asymptotic safety

The scale identification for k is more subtle¹⁸. As we have discussed, within the asymptotic safety approach, one computes the dependence of couplings on k , such that the effective action Γ is obtained in the limit $k \rightarrow 0$. For a coupling g the renormalization group flow interpolates between the fixed point value $\lim_{k \rightarrow \infty} g(k) = g_*$ and $\lim_{k \rightarrow 0} g(k) = g$, where the latter limit is often problematic to be taken [195].

On the other hand, in GR the gravitons’ amplitudes are not universal and not crossing symmetric [24, 308] and depend on several independent scales. Hence, identifying the k scale with some physical momentum scale, such as one of the Mandelstam variables, is ambiguous. The resulting map between various amplitudes and the k -dependent coupling is not bijective¹⁹.

Below the Planck scale, quantum gravity can be treated perturbatively utilizing effective field theory [61]. In that regime, the predictions of asymptotic safety and the perturbative approach should coincide [24]. It is then crucial to extract the momentum dependence of the amplitudes from FRG calculations. Currently, several approaches are on the way to achieving it. The vertex expansion [314] associates distinct couplings to distinct vertices²⁰. So far, the fully momentum-dependent propagator of the graviton was obtained in [318], together with the three [319] and four-point functions [315, 316] calculated at momentum symmetric points, see also calculations in the gravity-matter setting [286] as well as calculations on non-trivial backgrounds [320, 321].

Recently within the form factor approach [308, 322, 323, 324, 325] the finite four-scalar graviton mediated scattering satisfying the Froissart bound [326] has been obtained [308, 323]. Nevertheless, the current calculations are far from obtaining the desired 4-graviton amplitude. If obtained, such an amplitude has to behave well in the UV. Below, in Sec. 2.4, we propose three criteria that have to be satisfied by the set of amplitudes such that the theory is described by the “running” of a finite number of parameters and the map between amplitudes and generalized “running” couplings is bijective. In our approach, the running is not tied to any individual coupling of a given monomial but the “collective behavior” of the amplitudes. We illustrate that by the 4-graviton string theory amplitude.

¹⁸In general, the Wilsonian and perturbative approaches give the same results for the one-loop beta functions of the action truncated to containing only the dimensionless couplings. Reconstruction of the 2-loop beta functions from the Wilsonian calculations has not been achieved fully; see [195] and references therein.

¹⁹In the systems of enhanced symmetry, such as black holes or cosmological settings, such scale identification can be performed and sometimes is even unique [309]. In particular, such RG-improvements could solve classical black hole singularity problem [310, 311], gives finite entanglement entropy [312] and generates inflationary regime in quantum gravity [194, 313, 309]. For inflation, we shall study one such model in Chapter 5.

²⁰See the discussion of effective universality of the different vertices for quantum gravity [315, 316, 277, 317].

2.4. Is string-theory asymptotically safe?

2.4.1. Running in terms of amplitudes.

Motivated by the original Weinberg notion of asymptotic safety, we propose three criteria in terms of the UV behavior of amplitudes. First, specifying a finite number of amplitudes is sufficient to derive the theory predictions. Second, all the amplitudes should possess a scale-invariant regime for very large energies (near the cutoff) [327]:

$$A(p_1, p_2, \dots) = \lambda^{-d} A(\lambda p_1, \lambda p_2, \dots), \quad (2.70)$$

where d is the dimension of A . In terms of quantum field theory this corresponds to the massless limit. Third, we demand the $E \rightarrow +\infty$ limit to be unambiguous for the ‘running’ part of amplitude A' , i.e. the amplitude without the polarizations’ contractions. In particular for the 4 identical particle elastic scattering this means that

$$\lim_{s \rightarrow \infty, t \text{-fixed}} A'(s, t, u) = \lim_{t \rightarrow \infty, s \text{-fixed}} A'(s, t, u). \quad (2.71)$$

We call this asymptotic crossing symmetry²¹. In particular, the first and second conditions ensure finiteness and UV-fundamentality of the theory. The second condition ensures the scale symmetry in the UV. Furthermore, suppose we do not assume the asymptotic crossing symmetry. In that case, there is no universal notion of running governing the high energy behavior of the theory, and the map between amplitudes and “running” parts of amplitudes is bijective. The amplitude defined in that way satisfies both *crossing* and *universality* properties by construction, meeting the criteria posed in [24].

In the context of quantum gravity, one should require that the theory has a graviton in its spectrum and the four graviton amplitude is not trivial. Another reason for the asymptotic crossing symmetry is that a single coupling G_N describes the low energy limit, which we then match to high energy physics.

Given these criteria, we identify the “running” in quantum gravity with the change of the “scalar” part (multiplying the polarization tensors kinematics part) of the 4-graviton amplitude in the entire theory.

2.4.2. Veneziano amplitude

Actually the crossing symmetry was the main motivation for the Veneziano amplitude [99], which gave birth to the string theory [328]. In Type II superstring theory the Virasoro-Shapiro amplitude (closed string analog for Veneziano amplitude for four gravitons) takes the following form [97]

$$A(p_1, p_2, p_3, p_4) = 2g_D^2 K_{cl} C(s, t, u), \quad (2.72)$$

where $C(s, t, u)$ is given by

$$C(s, t, u) = -\pi \frac{\Gamma(-s/8)\Gamma(-t/8)\Gamma(-u/8)}{\Gamma(1 + \frac{s}{8})\Gamma(1 + \frac{t}{8})\Gamma(1 + \frac{u}{8})} \quad (2.73)$$

²¹Without this assumption, the amplitudes can still be well behaved, but the relation between amplitudes and generalized couplings will not be bijective. Let us also note that the LSZ reduction requires a weaker form of crossing symmetry $s \leftrightarrow u$.

and K_{cl} is a lengthy kinematic (cross-symmetric) and polarization factor polynomial in s, t, u . If we vary s and keep t fixed, then this amplitudes has infinite number of simple poles [96] on a real line at $s = 8n$, with $n \geq 0$. This can be understood as summing over infinite number of particles with growing masses in the s -channel. The similar conclusion can be drawn if we keep s fixed and vary t . This property is called duality. Due to existence of poles, the large energy limit cannot be taken ($s \rightarrow \infty$, s/t fixed) along the real line. In order to take the limit we shift s slightly in the imaginary direction ²². As a result we get the exponential fall-off:

$$C(s, t, u) \propto \exp\left(-\frac{1}{4}(s \log s + t \log t + u \log u)\right), \quad (2.74)$$

satisfying our criteria. Our conditions are also satisfied beyond the tree level amplitude, since this behavior is also present for the resumed loop amplitude in this limit [329, 330, 331] (string theory preserves generally the crossing symmetry at the loop level [332]). On the other hand in the low-energy limit the Veneziano amplitude can be matched with tree-level graviton amplitude, since $C(s, t, u) \sim \frac{1}{stu}$ with $\kappa = \frac{1}{2}\alpha'g^2$ for heterotic strings [97], where $g \approx 1$ and $\alpha' \approx M_P^2$.

It should be emphasized that the fact that the amplitude (2.74) asymptotically vanishes does not say anything about the individual contributions from the interaction vertices in the lagrangian, in particular, whether the Newton's constant G_N asymptotically vanishes or not. The low-energy effective action calculated within the non-linear sigma model approach [333, 334], when truncated to finite order in α' cannot reproduce the amplitude Eq. (2.72). Furthermore, the finiteness of string amplitudes and hence behavior (2.74) is tied to the modular invariance that cannot be reproduced using a lagrangian of any conventional QFT with a finite amount of operators. This points to an important and far-reaching change of perspective concerning the usual approach where only Newton's constant and its running are taken into account. The necessity of considering the infinite numbers of operators might also be crucial to the understanding of the unitarity in asymptotic safety [72]. In [72] it is discussed that only specific types of propagators calculated within the truncated effective action can result in unitary quantum field theory for the full effective action.

²²Ultimately, the poles are anyway shifted off the real axis making the $s \rightarrow \infty$ limit well defined because massive states are unstable in the interacting theory, hence their amplitudes possess non-trivial imaginary part.

Chapter 3

Quantum Gravity as an UV completion

Where we discuss how the requirement of quantum gravity as UV completion constrains the theories. Working in a minimal SO(10) model, we explicitly demonstrate that the condition of successful radiative symmetry-breaking below the Planck scale to the SM-like vacuum expectation value provides strong constraints on the underlying microscopic dynamics. Given GUT model, the EFT parameter space is significantly constrained by demanding a viable breaking chain to be realized radiatively without assumptions about dynamics beyond the Planck scale.

In the case of multiple minima of the potential, such as for GUTs, the domain walls may form. Here, we calculate the decay rates of the domain wall networks depending on the potential shape and initial conditions. We show that the potential shape around the maximum has little effect on stability.

3.1. Quantum gravity as UV completion

The studies of quantum gravity phenomenology usually rely on the specified microscopic dynamics such as string theory or asymptotic safety. One can then study their respective swamplands and landscapes using the criteria stemming from those approaches and check whether they overlap. Following [3], we propose a new model-independent set of constraints for the below Planckian dynamics.

We assume that up to the Planck scale, the QFT accurately describes the particle physics phenomena, such that the cutoff scale is $\Lambda = M_P$. At the Planck scale, an EFT is specified. In particular, for the Grand Unified Theories, EFT (GUEFT) is determined by its symmetry group \mathcal{G}_{GUT} , the set of fermionic as well as scalar representations \mathcal{F}_{GUT} and \mathcal{S}_{GUT} and the values of the couplings g_i . In the following, we omit the canonically irrelevant terms and the masses, so the breaking is realized radiatively [335]. The scalar sector is chosen such that the Standard Model is one of the possible vacua. In this setup, we introduce a set of necessary constraints for the scalar sector [3].

- (I.a) We demand tree-level stability at $\Lambda = M_P$.
- (I.b) We demand the absence of Landau poles between the first symmetry-breaking scale M_{GUT} and $\Lambda = M_P$.

- (I.c) We demand that the deepest vacuum expectation value (vev) induced by radiative symmetry breaking, is admissible, i.e., remains invariant under the Standard Model gauge group $\mathcal{G}_{\text{SM}} \subset \mathcal{G}_{\text{GUT}}^{(\text{local})}$.

On top of these constraints on the scalar potential, one may apply more commonly addressed phenomenological constraints on the gauge-Yukawa sector [27, 336, 337]. More precisely:

- (II.a) We demand gauge unification and a sufficiently long proton lifetime to avoid experimental proton-decay bounds.
- (II.b) We demand a viable Yukawa sector.

The conditions (I) and (II) are not independent. In general, to combine those, there are two possible strategies. First, one may also randomize the gauge and Yukawa couplings and look for viable phenomenology subspace for a combined set of couplings. In the following, we adopt a different strategy. Since gauge and Yukawa are constrained experimentally, we fit them to the phenomenological values¹. The above two sets of constraints can be viewed as necessary consistency constraints for a GUEFT to be a viable UV extension of the SM.

In addition, one may specify an underlying quantum gravity theory and typically results in additional constraints. This is discussed within the asymptotic safety context in Sec. 4.1.

3.2. Analysis of the model: minimal $\text{SO}(10)$

In this section, we present the specific GUEFT for the group $SO(10)$ to be investigated. Therein, we also briefly review the phenomenology of this model.

3.2.1. $\text{SO}(10)$ with fermionic $\mathbf{16}_F$ and scalar $\mathbf{45}_H \oplus \mathbf{16}_H$.

In this paragraph we closely follow [27]. For the $SO(10)$ -GUT the fermionic content of the Standard Model (together with right handed neutrinos) nicely fits into one, unifying $\mathbf{16}_F$ spinor representation. Minimal scalar content to reproduce the Standard Model electroweak theory is $\mathbf{45}_H \oplus \mathbf{16}_H$. In terms of its group-theoretic specification, the model reads

$$\left(\mathcal{G}_{\text{GUT}}, \mathcal{F}_{\text{GUT}}^{(i)}, \mathcal{S}_{\text{GUT}} \right) = (\text{SO}(10), \mathbf{16}_F, \mathbf{45}_H \oplus \mathbf{16}_H), \quad (3.1)$$

where $i \in (1, 2, 3)$ is the family index. The Lagrangian is given by

$$\mathcal{L} = \mathcal{L}_K + \mathcal{L}_Y - V, \quad (3.2)$$

where the \mathcal{L}_K is the fermionic, scalar and gauge kinetic part and V is the $\mathbf{45}_H \oplus \mathbf{16}_H$ potential. Additionally in order to break the electroweak symmetry the $\mathbf{10}_H$ representation is introduced. Its full form is given in the App. B together with the spinor conventions and the potential for the $\mathbf{10}_H \oplus \mathbf{45}_H \oplus \mathbf{16}_H$ representation. To simplify our analysis of the radiative minimas we shall assume stability in the $\mathbf{10}_H$,

¹We are allowed to do so since the values of the scalar couplings influence the running of g only at 3-loops and the Yukawa couplings at two loops, see discussion on the smallness of that effect in[27].

which is required for viable phenomenology. We report the beta functions for $\mathbf{10}_H \oplus \mathbf{45}_H \oplus \mathbf{16}_H$ in the App. C.1. Despite the model consisting of $\mathbf{10}_H$, $\mathbf{16}_H$ and $\mathbf{45}_H$ does not correctly reproduce the Yukawa couplings of the Standard Model [338]² it can result in the breaking towards the Standard Model. The possible first breaking of the breaking chains are summarized in the Tab. 3.2 and the stability conditions are summarized in the Tab. 3.1³. The Table 3.2 infers the $\mathbf{45}_H$ has to break first and $\mathbf{16}_H$

Table 3.1: Stability conditions for the model $\mathbf{45}_H \oplus \mathbf{16}_H$.

	$\mathbf{45}_H$	$\mathbf{16}_H$	$\mathbf{45}_H \oplus \mathbf{16}_H$
$\text{SO}(10) \rightarrow \text{SU}(5) \times \text{U}(1) \rightarrow \mathcal{G}_{\text{SM}}$	$\lambda_1 + \frac{13}{20}\lambda_2 > 0$		$\lambda_8 + \frac{1}{20}\lambda_9 + \sqrt{\lambda_6(\lambda_1 + \frac{13}{20}\lambda_2)} > 0$
$\text{SO}(10) \rightarrow 3_C 2_L 2_R 1_{B-L} \rightarrow \mathcal{G}_{\text{SM}}$	$\lambda_1 + \frac{7}{12}\lambda_2 > 0$	$\lambda_6 > 0$	$\lambda_8 + \frac{3}{4}\lambda_9 + \sqrt{\lambda_6(\lambda_1 + \frac{7}{12}\lambda_2)} > 0$
$\text{SO}(10) \rightarrow 4_C 2_L 1_R \rightarrow \mathcal{G}_{\text{SM}}$	$\lambda_1 + \frac{1}{2}\lambda_2 > 0$		$\lambda_8 + \frac{1}{2}\lambda_9 + \sqrt{\lambda_6(\lambda_1 + \frac{1}{2}\lambda_2)} > 0$
$\text{SO}(10) \rightarrow \text{SU}(5) \times \text{U}(1) \rightarrow \text{SU}(5)$	$\lambda_1 + \frac{13}{20}\lambda_2 > 0$	$\lambda_6 > 0$	$\lambda_8 + \frac{5}{4}\lambda_9 + \sqrt{\lambda_6(\lambda_1 + \frac{13}{20}\lambda_2)} > 0$
$\text{SO}(10) \rightarrow \text{SO}(8)$	$\lambda_1 + \frac{1}{4}\lambda_2 > 0$	/	/

to be responsible for subsequent breaking, hence $\langle \mathbf{16}_H \rangle < \langle \mathbf{45}_H \rangle$. If $\langle \mathbf{16}_H \rangle = \langle \mathbf{45}_H \rangle$ we would have (forbidden phenomenologically) one-step breaking towards the Standard Model ($3_C 2_L 1_Y$)⁴. Furthermore, the $\text{SU}(5) \times \text{U}(1)$ and $3_C 2_L 1_R 1_{B-L}$ require the fine-tuning of the masses of scalar representations after the symmetry breaking to match the phenomenological data⁵, see [337]. Hence, phenomenologically the most interesting is the so-called Pati-Salam breakings $3_C 2_L 2_R 1_{B-L}$ and $4_C 2_L 1_R 1_{B-L}$.

A series of articles in the 1970-1980s studying the $\mathbf{45}_H \oplus \mathbf{16}_H$ model [28, 339, 340, 341, 342] pointed that the only minima of the potential are in the direction of flipped $\text{SU}(5) \times \text{U}(1)$ for $\mathbf{45}_H$ breaking, which require big threshold corrections to be viable [337] or the excluded standard $\text{SU}(5)$ GUT for the $\mathbf{16}_H$ vev. The other possible vev's in the Pati-Salam direction are not the minima of the potential but saddle points. Hence the model has been disregarded for 30 years.

²The general structure of the Yukawa couplings is given by

$$\mathcal{L}_Y = \mathbf{16}_F(Y_{10}\mathbf{10}_H + Y_{120}\mathbf{120}_H + Y_{126}\overline{\mathbf{126}}_H)\mathbf{16}_F + \text{h.c.}, \quad (3.3)$$

where $\mathbf{10}_H$ and $\mathbf{120}_H$ are real representations of the $\text{SO}(10)$ and $\mathbf{10}_H$ is identified with the SM Higgs boson. To correctly reproduce the Yukawa sector, the $\mathbf{10}_H \oplus \mathbf{120}_H \subset \mathcal{S}_{\text{GUT}}$ or $\mathbf{10}_H \oplus \mathbf{126}_H \subset \mathcal{S}_{\text{GUT}}$ has to hold. Since $(\mathbf{16}_H \otimes \mathbf{16}_H)_S = \mathbf{126}_H$ the breaking chains triggered by those two representations are similar [27], yet $\mathbf{16}_H$ possess far less possible couplings.

³In Table it is implicitly understood that in the definition of S_3 , S_1 and S_2 must be satisfied.

⁴To reclaim the breaking at the electroweak scale one additionally requires $\langle \mathbf{10}_H \rangle \ll \langle \mathbf{45}_H \rangle, \langle \mathbf{16}_H \rangle$. In particular, if $\langle \mathbf{10}_H \rangle \gg \langle \mathbf{45}_H \rangle, \langle \mathbf{16}_H \rangle$, the model would break towards the non-SM $\text{SO}(9)$ vacua. This can be investigated by the beta functions given in the App. C.1 and is left for future work.

⁵To be more precise, the running of g require large threshold effect. In the \overline{MS} type of scheme, the decoupling of heavy particles is not straightforward and relies on the matching of amplitudes in the low and high energy theory. This results in the discontinuity of the coupling at the scale where the theories are matched. The size of the corrections relies on the differences in the masses of the particles that are integrated out. In particular in the formalism introduced in App. A.1 those can be calculated and compared with the values required for successful unification [337].

Recently it has been pointed out that one-loop quantum corrections to the potential can turn the phenomenologically preferable saddle points into minima [27]. Hence, the models containing the $\mathbf{45}_H$ have been recently revived. In our work, we confirm the formation of the Pati-Salam minima using the leading logarithm resummation techniques, discussed in A. Nevertheless, by considering the non-SM minima, we find that these are never the deepest minima.

Breaking chain	Representation	Admissible?	Viable ?
$SU(5)$	$\mathbf{16}_H$	Yes	No
$SU(5) \times U(1)_X$	$\mathbf{45}_H$	Yes	Yes, if fine tuning
$3_C 2_L 2_R 1_{B-L}$	$\mathbf{45}_H$	Yes	Yes
$4_C 2_L 1_R 1_{B-L}$	$\mathbf{45}_H$	Yes	Yes
$3_C 2_L 1_R 1_{B-L}$	$\mathbf{45}_H$	Yes	Yes, if fine tuning
$3_C 2_L 1_Y$	$\mathbf{45}_H \oplus \mathbf{16}_H$	Yes	No
$SO(8) \times U(1)$	$\mathbf{45}_H$	No	No
$SO(7)$	$\mathbf{45}_H \oplus \mathbf{16}_H$	No	No
$SU(4) \times U(1)^2$	$\mathbf{45}_H \oplus \mathbf{16}_H$	No	No
$SU(4) \times U(1)$	$\mathbf{45}_H \oplus \mathbf{16}_H$	No	No

Table 3.2: Summary of the considered breaking chains for $SO(10)$ group. The considered breaking chains are called admissible if they can recreate the Standard Model and viable if they obey the proton stability and unification constraints. We do not include so called non-observable breaking chains, see [3]. Note that λ_7 does not enter any of the stability conditions.

3.3. The Results

Let us start by noting that the value of $SO(10)$ gauge coupling g_{10} is heavily constrained experimentally. We assume $g_{10}(M_P) = 0.435$, yet the results are robust throughout the discussed region ⁶.

3.3.1. The results: The $\mathbf{45}_H$ model

We first state the results for the model consisting of $\mathbf{45}_H$ only, but keeping the g_{10} running as in the $\mathbf{45}_H \oplus \mathbf{16}_H$. Hence, effectively we assume vanishing portal interactions between the scalar representations. As shown in the Tab. 3.2 the $\mathbf{45}_H$ can break towards $SU(5) \times U(1)$, $4_C 2_L 1_R 1_{B-L}$, $3_C 2_L 2_R 1_{B-L}$ and non-viable $SO(8) \times U(1)$ ⁷.

In the Fig. 3.1 we depict the deepest minima by regions in the couplings λ_1, λ_2 at the Planck scale. The deepest minima are either $SO(8) \times U(1)$ for $\lambda_2 \gtrapprox 0$ or $SU(5) \times U(1)$ for $\lambda_2 \lessapprox 0$. In presence of scalar mass terms and the sign of λ_2 determines the ordering of the depths of the vacua [28], see (C.1) for conventions. Our results confirm that this

⁶In the $\mathbf{45}_H$ case analysis we have scanned over the values of the allowed range of the couplings $g_{10}(M_P) \in (0.4, 0.45)$ see [27, 336, 337]. In particular, for $3_C 2_L 2_R 1_{B-L}$ the fits give $g_{10}(M_P) = 0.406$ and for $4_C 2_L 1_R 1_{B-L}$ one has $g_{10}(M_P) = 0.443$ [27]. This range takes into account the possible from the quantum gravity effects, the higher loops corrections and various unification paths. In particular, if not otherwise specified

⁷There is also the $3_C 2_L 1_R 1_{B-L}$ breaking which is equivalent to the $SU(5) \times U(1)$ breaking for the $\mathbf{45}_H$ model.

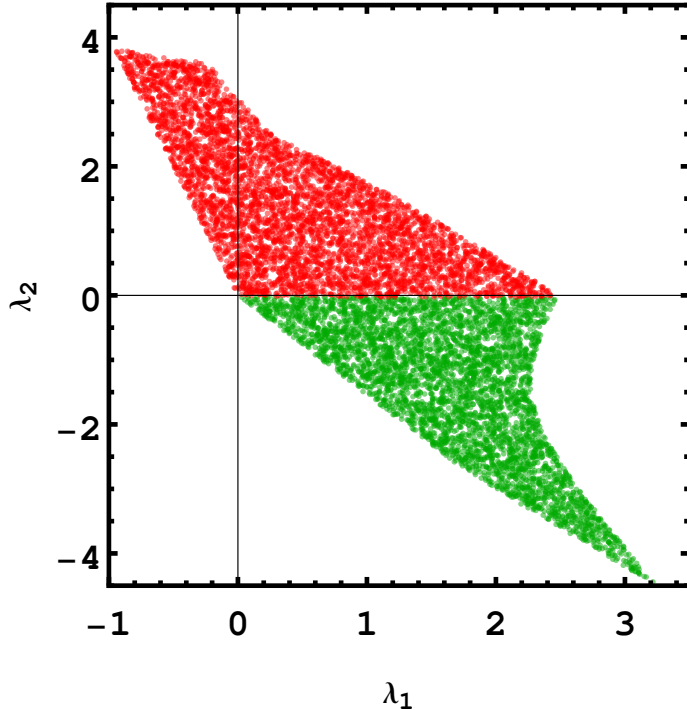


Figure 3.1: The deepest minima of the $\mathbf{45}_H$ potential. The green points depicts the $SU(5) \times U(1)$ and red the non-SM $SO(8) \times U(1)$, the other regions either have diverging couplings or have unstable potential at M_P . The simulation has been done for the 10000 points, such that the $(\lambda_1, \lambda_2) \in [-5, 5]^2$ for $g(M_P) = 0.435$.

ordering this is preserved at 1-loop.

In Fig. 3.2 we explicitly demonstrate the relative depth of the respective vacua on the exemplary hypersurfaces of fixed $\lambda_i(M_P)$. The top row depicts $\lambda_2(M_P)$ fixed, while the bottom one the $\lambda_1(M_P)$ fixed. Disregarding the $SO(8) \times U(1)$ breaking the Pati-Salam vacua can be the deepest minima for some parts of the parameter space while enjoying the radiative corrections stabilization [27], see Fig. 3.2a. However, after taking into account the $SO(8) \times U(1)$ vacua, the Pati-Salam ceases to be the deepest vacua of the model.

The vacua at $\lambda_2 \approx 0$ become degenerate. Since $\lambda_2(M_P) = 0$ results $\lambda_2(\mu) \approx 0$ along the flow, then all of the vacua have the same stability condition, namely $\lambda_1(\mu) > 0$ and the long-living domain walls may form, see Sec. 3.4.

Phenomenological constraints Having established the parameter space of $\lambda_1(M_P)$, $\lambda_2(M_P)$ leading towards the admissible $SU(5) \times U(1)$, let us now apply the remaining criteria. Depending on the initial values for λ_1 , λ_2 different breaking scale will be realized, as depicted on Fig 3.3. In particular, parts of the parameter space will not be phenomenologically viable. The proton decay bounds as well as the unification constrain result in the bound

$$\langle \mathbf{45}_H \rangle > 10^{15} \text{ GeV}, \quad (3.4)$$

with best fit, being $\langle \mathbf{45}_H \rangle = 10^{15.84}$ GeV [337]. Note, that assuming $\langle \mathbf{45}_H \rangle = 10^{15.84}$ results in the reduction of the parameter space by one. In the Figure 3.3 we plot the $\lambda_1(\lambda_2)$ line, such that the breaking scale matches the unification scale. Furthermore

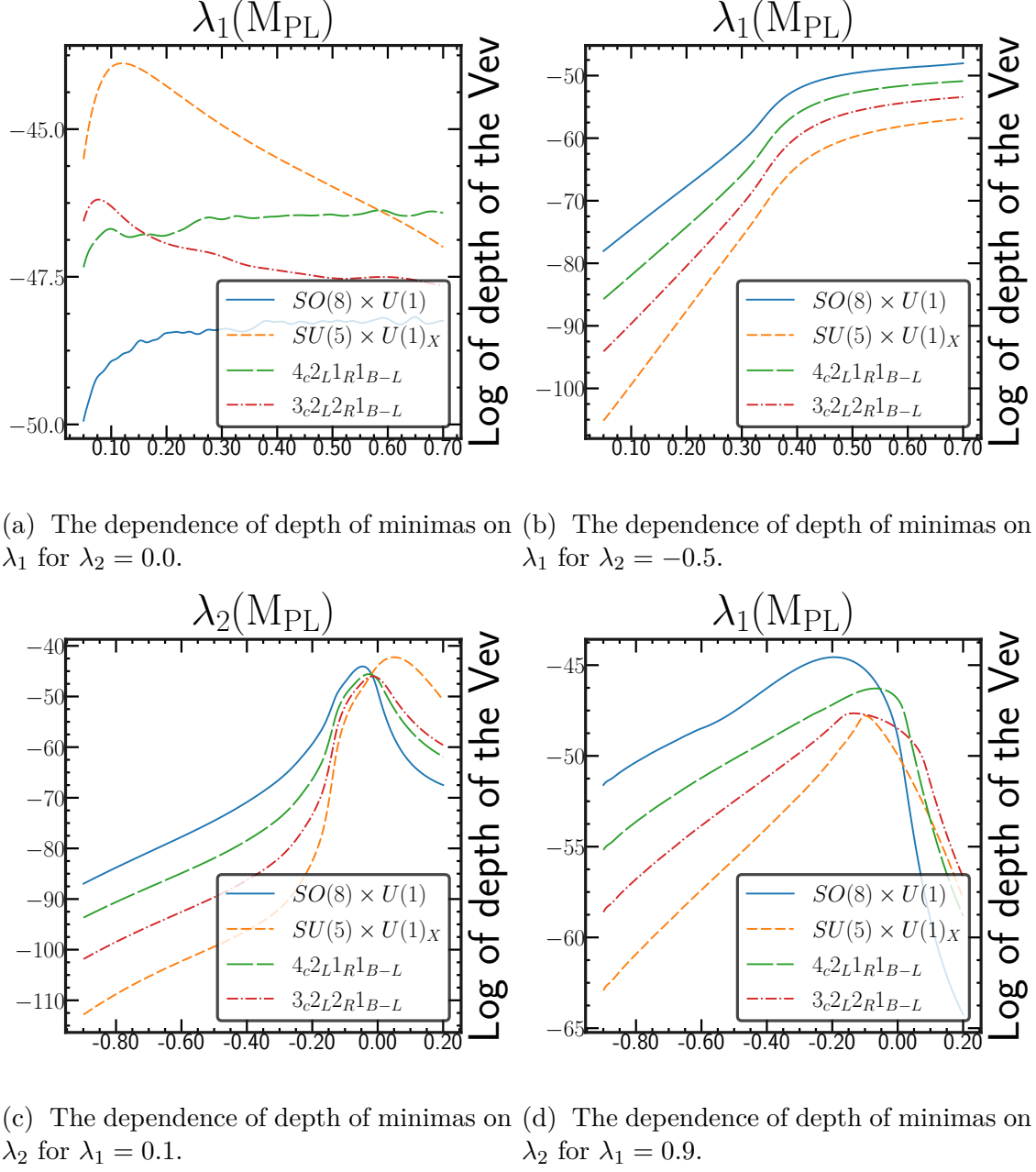


Figure 3.2: The depths of the minimas given $\lambda_1(M_P)$, $\lambda_2(M_P)$.

we find the analytic relation between the couplings realising the unification.

$$\lambda_2 = -1.350\lambda_1 + 0.367\lambda_1^2 + \mathcal{O}(\lambda_1^3) \quad (3.5)$$

The intermediate $SU(5) \times U(1)$ stage contains the lepto-quarks that can also mediate the proton behaviour, hence for that representation the $\langle \mathbf{16}_H \rangle > 10^{15}$. To understand the further consequences of $\mathbf{16}_H$ let us now analyze the $\mathbf{16}_H \oplus \mathbf{45}_H$ model.

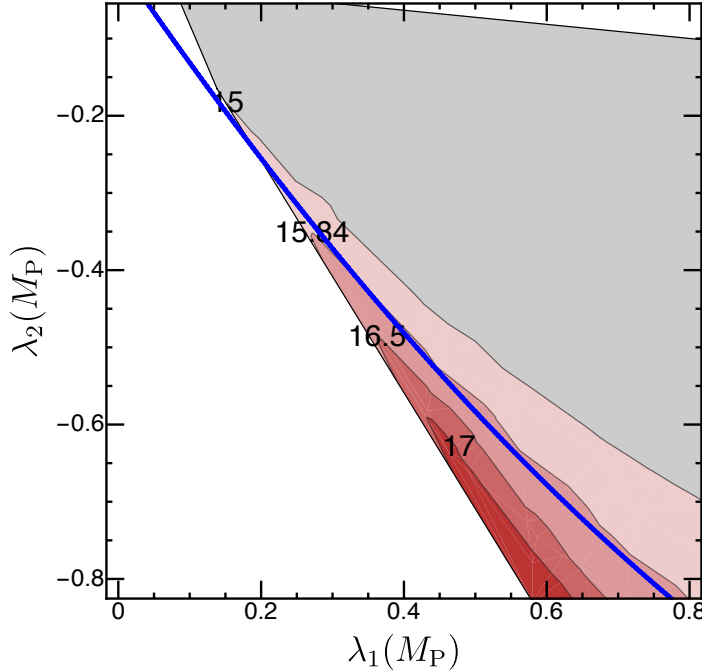


Figure 3.3: The scale of breaking towards $SU(5) \times U(1)$ vacua. The blue line represents Eq. 3.5. In grey we depict the parameter space that does not satisfy (3.4).

3.3.2. The Results: The $\mathbf{16}_H \oplus \mathbf{45}_H$ model

Including the $\mathbf{16}_H$ and $\mathbf{45}_H$ scalar representation, the quartic scalar potential is 6-dimensional, c.f. App. (B.2). We have obtained a random sample of 10^5 points with Planck-scale initial conditions uniformly distributed in the intervals $\lambda_i \in [-0.5, 0.5]$. We exclude roughly $\sim 70,000$ of these points because the respective trajectories exhibit Landau-poles between the Planck and the GUT scale (before any symmetry breaking occurs) or constitute unstable potential already at Planck scale. The remaining parameter space splits up into regions in which radiative VEVs break to the different subgroups of $SO(10)$, cf. Fig. 3.4. The respective regions in the Planck-scale parameter space are non-trivial. While their boundaries in the 6-dimensional parameter space are sharp, projections to two-dimensional slices are not. Note that the same behavior occurs when projecting the 2-dimensional parameter space in the $\mathbf{45}_H$ -model down to 1 dimension, cf. Fig. 3.1.

The possible breaking directions collected in Tab. 3.2 imply that the only possible non-admissible breakings require the $\mathbf{45}_H$ to acquire a vev. This is reflected in the Fig. 3.4 such that the admissibility of breaking is not correlated with any of the λ_6 , λ_7 , λ_8 , λ_9 . If SM-like breaking occurs, it breaks to $SU(5)$, $SU(5) \times U(1)$, or directly to the SM, cf. Fig. 3.5. In particular, we find basically no possibility for breaking in the Pati-Salam-type ($4_c \times 2_l \times 1_R$ or $3_c \times 2_L \times 2_R \times 1_{B-L}$) direction. (In the sample of ~ 30.000 points without Landau poles, we only identify a single such case). Due to stability conditions cf. Tab. 3.1 the quartic couplings λ_2 , λ_8 , and λ_9 serve as good discriminators between the different SM-like VEVs, cf. Fig. 3.5. In particular for $\lambda_2 < 0$ the $SU(5)$ or $SU(5) \times U(1)$ breakings are realized.

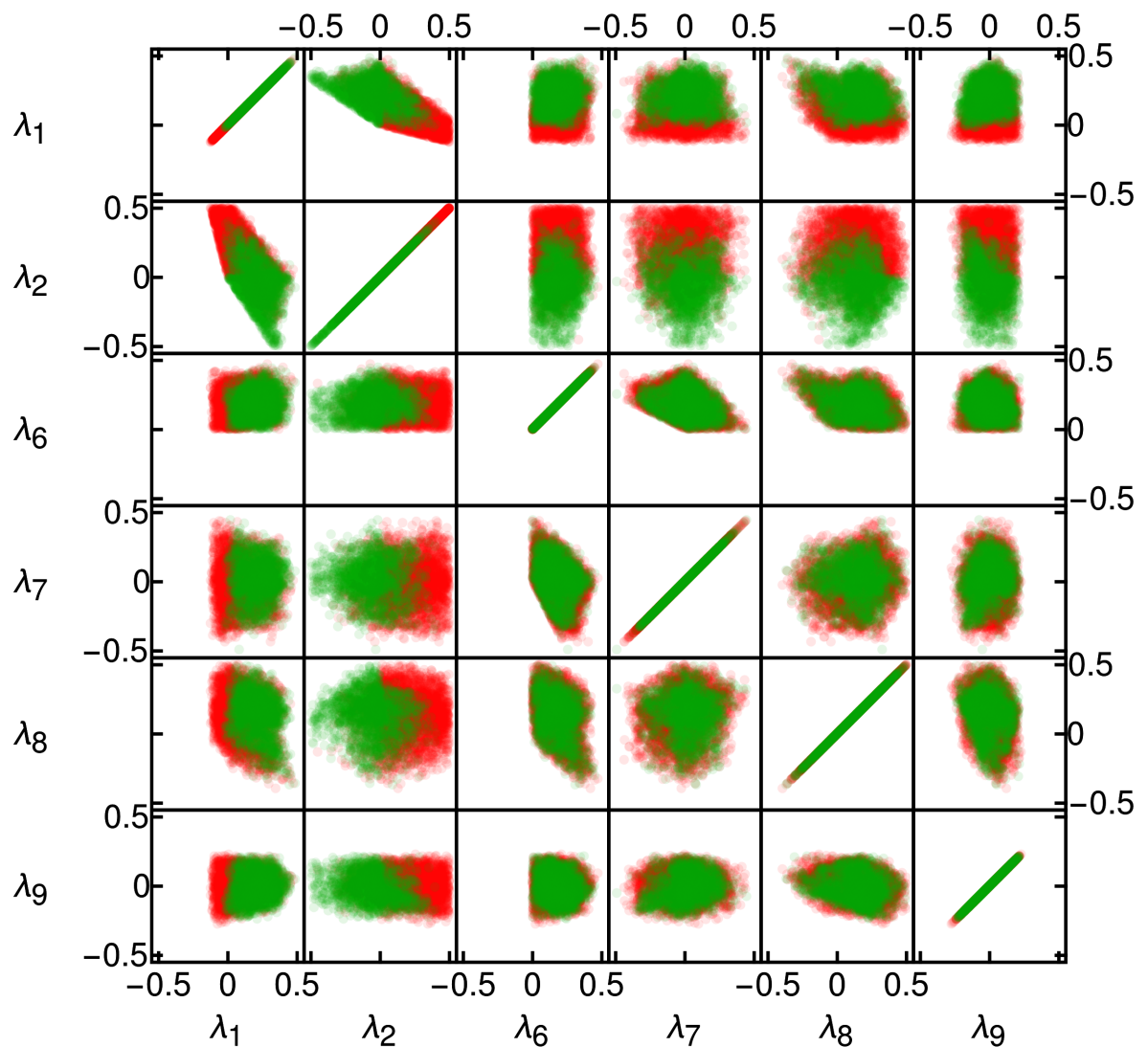


Figure 3.4: The admissible vs non-admissible parameter space for $\mathbf{45}_H \oplus \mathbf{16}_H$ model. The green regions denotes the admissible points, the red non-admissible.

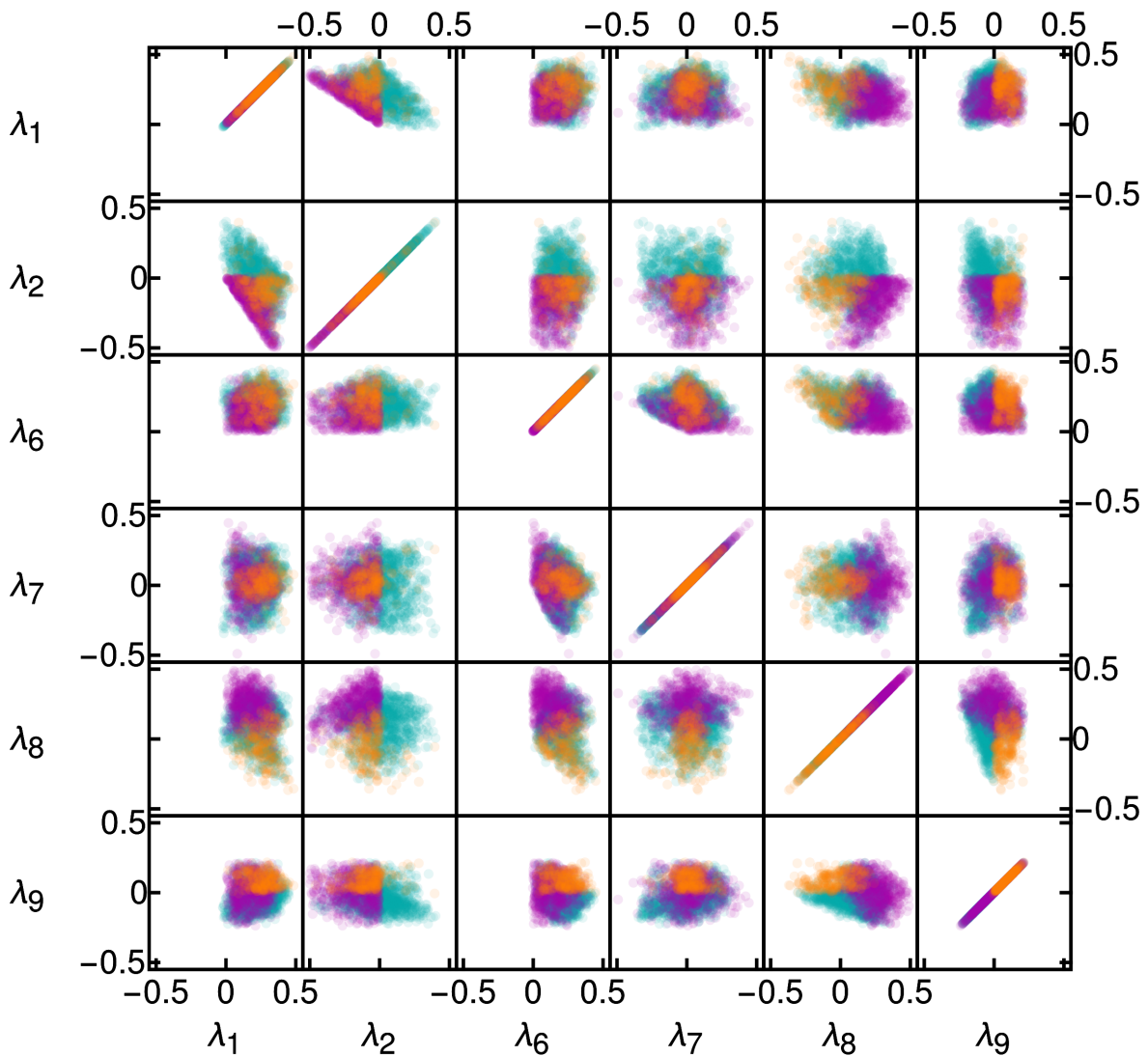


Figure 3.5: Breaking directions in $45_H \oplus 16_H$. The cyan color denotes one step breaking towards the SM. The orange the breaking towards $SU(5)$ and purple towards $SU(5) \times U(1)$.

3.4. Degeneracy of minima and Domain Walls formation

Let us now discuss the dynamics of the domain walls. We shall comment on the connection with the GUT potentials at the end of the section.

3.4.1. Domain walls formation

In systems where specific field ϕ takes different vacuum expectation values throughout the space, such as in the studied GUT model, the topological defects are formed at the boundaries. Analogously to the magnetic domain walls in the materials, those are called the cosmological domain walls. To put it differently, the domains are patches of the Universe where ϕ have reached a certain minimum of the potential, and domain walls are transition regions at which the field smoothly interpolates between these minima.

Evolution of domain walls in the simplest case of degenerate minima (such as the case of $\lambda_2(M_P) = 0$ for the $\mathbf{45}_H$ representation) and symmetric initial distribution leads to the so-called scaling regime. In this regime, the number of domain walls in the horizon stays nearly constant, while average domain size and curvature radius are of the order of Hubble horizon [343]. To maintain the scaling, the domain walls have to interact frequently. On the other hand, for not degenerate minima of the potential, a difference of vevs energy acts as pressure and makes the system unstable.

In general, the formation of the domain walls depends on a fraction of the space occupied by the field strength corresponding to the global minimum of the potential, the variance of initial distribution, the relative depth of the minima, and the steepness of the potential on both sides of the local maximum separating the minima. While the effects of the bias in initial distribution and in the minima have been extensively studied (see [344, 345, 346, 347, 348, 349, 350, 351, 352]), in [4] the other two factors have been studied for the first time. Here we follow the logic of [4] and discuss various factors.

3.4.2. The potential and dynamics

In the past, the studies focused on spontaneous breaking of \mathbb{Z}_2 symmetry in a model given by:

$$\mathcal{L} = \frac{1}{2} \partial_\mu \phi \partial^\mu \phi - V_{\mathbb{Z}_2} := \frac{1}{2} \partial_\mu \phi \partial^\mu \phi - V_0 \left(\frac{\phi^2}{\phi_0^2} - 1 \right)^2. \quad (3.6)$$

To study the potentials of the shape discussed in Sec. 3.2 we have to overcome limitations of the simple model (3.6). Here we take the first step towards that direction and prepare a general set of potentials convenient for further studies in lattice simulations. From the point of view of lattice simulations, it is convenient to define the model's potential by its derivative, which is directly used in simulations. The equation of motion for the symmetry breaking field with the canonical kinetic term and general potential V is of the form:

$$\frac{\partial^2 \phi}{\partial \eta^2} + \frac{2}{a} \left(\frac{da}{d\eta} \right) \frac{\partial \phi}{\partial \eta} - \Delta \phi + a^2 \frac{\partial V}{\partial \phi} = 0, \quad (3.7)$$

assuming the flat Friedman-Robertson-Walker metric background (1.12) with conformal time (such that $d\eta = \frac{1}{a(t)} dt$). The equation (3.7) which depends on the derivative

of the potential $\frac{\partial V}{\partial \phi}$ is solved in lattice simulations using the finite difference scheme. Moreover, the position of the local extrema of the potential are easier to determine from its derivative. We assume the derivative of the potential as

$$\frac{\partial V_{AS}}{\partial \phi}(\phi) := V_0(\phi - a)(\phi - b)(\phi - c) (e^2(\phi - d)^2 + 1), \quad (3.8)$$

where a, b, c determine positions of the extrema of the potential and parameters e, d controls the shape of the potential. Then, the potential V_{AS} takes the complicated form:

$$\begin{aligned} V_{AS}(\phi) = & \frac{V_0}{60} \phi (-60abc(d^2e^2 + 1) + 15\phi^3(e^2(2d(a+b+c) + ab + ac + bc + d^2) + 1) \\ & - 20\phi^2(e^2(d^2(a+b+c) + 2d(a(b+c) + bc) + abc) + a + b + c) \\ & + 30\phi(de^2(ad(b+c) + 2abc + bcd) + ab + ac + bc) - 12e^2\phi^4(a + b + c + 2d) + 10e^2\phi^5). \end{aligned} \quad (3.9)$$

We quantitatively estimate the asymmetry of the potential around the local maximum as a value of the third derivative of the potential:

$$\begin{aligned} \frac{\partial^3 V_{AS}}{\partial \phi^3}(\phi) = & 2V_0(e^2(a - \phi)(\phi - b)(c + 2d - 3\phi) \\ & + (-a - b + 2\phi)(e^2(d - \phi)(2c + d - 3\phi) + 1) + (\phi - c)(e^2(d - \phi)^2 + 1)) \end{aligned} \quad (3.10)$$

At the maximum. In [4] we find a family of potentials of the form (3.9) with given difference of values at minima $V_{AS}(b) - V_{AS}(a)$ (where we assume without loss of generality that b and a are minima of the potential and c is its local maximum) and the value of the third derivative at the maximum $\frac{\partial^3 V_{AS}}{\partial \phi^3}(c)$. However, these conditions are not sufficient to perform simulations whose results will reveal the dependence of domain walls' dynamics on the potential asymmetry. Basing on the results of [349] we chose the value of the width of domain walls to be $w = 5$, for details consult [4]. The considered equations take the simplified form:

$$\begin{aligned} \delta V = & -\frac{V_0}{60}(b+1)^3(5(b-1)d^2 + 2(4-3b)bd \\ & + b(b(2b-3)+8) - 6d - 7), \\ d3V = & 2V_0(-b(d-1)^2 + d^2 + 1), \end{aligned} \quad (3.11)$$

By dividing the first equation by the second, one obtains the equation independent of V_0 , connects b and d , and can be solved in favor of d . The figure 3.6 presents solutions with differences of values of potentials in their minima and with the third derivative vanishing at the local maximum. The figure 3.6 shows solutions for δV and $d3V$.

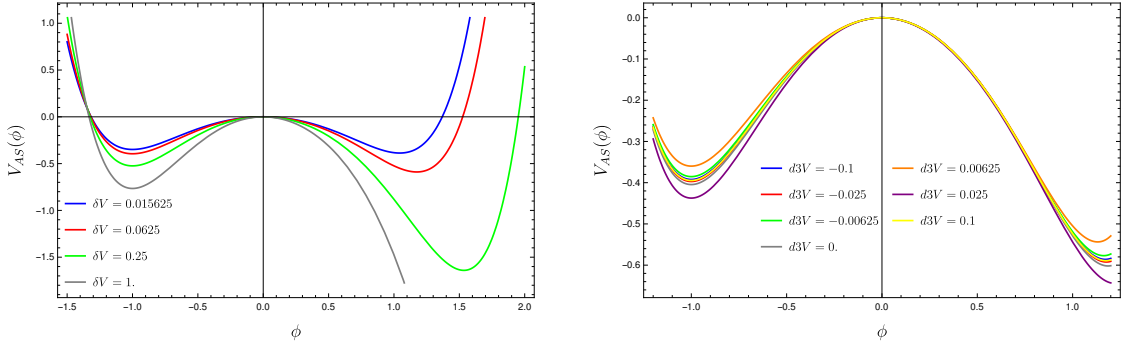


Figure 3.6: Shape of potentials to be studied in the domain wall evolution.
Left panel: various values of δV and $d3V = 0$.
Right panel: various values of $d3V$ and $\delta V = 0.0625$.

3.4.3. Simulation and results

Setting up the simulation The values of parameters b , d and V_0 used in our numerical lattice simulations are presented in appendix of [4]. In our numerical simulation based on PRS algorithm [353] we assumed that

$$a(\eta) = \frac{\eta}{\eta_{start}}, \quad (3.12)$$

according to the fact that scale factor a scales as $a \propto \eta$ with conformal time η during radiation domination. Following [346] initially field follows the Gaussian probability distribution

$$P(\phi) = \frac{1}{\sqrt{2\pi}\sigma} e^{-\frac{(\phi-\theta)^2}{2\sigma^2}}. \quad (3.13)$$

Our simulations were started with three initial conditions:

- initial mean value of the field strength θ ,
- initial standard deviation σ .

The initial conformal time is set to $\eta_{start} = cl$ where l is the lattice spacing. For each set of θ , σ , δV and $d3V$, we run five simulations on the lattice of the size of 512^3 if the decay time of the network is longer than $256 cl$ and only one simulation on the lattice of the size of 512^3 and four on a smaller lattice of the size 256^3 otherwise. This choice is motivated by the fact that conservatively the dynamic range of lattice simulations with periodic boundary conditions is bounded and conformal time needs to be smaller than the size of the lattice (multiplied by the speed of the light). On the other hand, we cannot guarantee that decay times longer than 512 are reliably computed, and networks will not decay later than observed in simulations. Fortunately, only a tiny fraction of simulated cases are touched by this issue. Described five runs were the base for analysis of statistical fluctuations of results obtained from simulations, which proved highly consistent.

Results In the Fig. 3.7 we depict the decay time of networks depending on δV and $d3V$ for unbiased initial distributions with two different values of the standard deviation $\sigma = 1$, $\sigma = 0.25$. Blue regions in these plots denote the parameter space where the evolution of networks ended in the basin of the attraction of the global minimum of

the potential and red ones from networks decaying to the local minimum. The plots in Fig. 3.7 infer that difference of the values of the potential in the respective minima is the main factor determining the lifetime of networks. The potential asymmetry around the local maximum $d3V$ has a much smaller yet visible effect. We observe

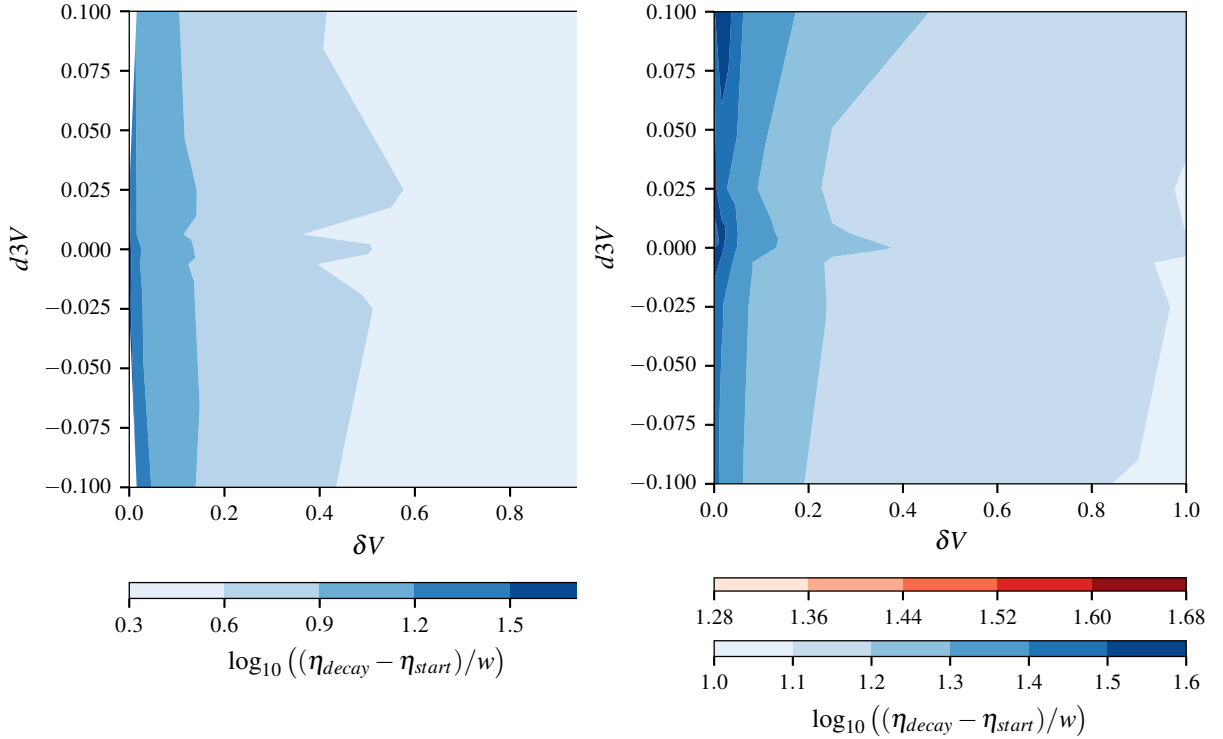


Figure 3.7: Dependence of the decay time $\eta_{dec} - \eta_{start}$ on δV and $d3V$ for initialization distribution with $\theta = 0$, $\sigma = 1$ (left), $\sigma = 0.25$ (right).

that for broad initial distributions ($\sigma = 1$), networks tend to decay to the global minimum of the potential, and only networks in models with $\delta V = 0$ decayed into “unstable” minima. Indeed, it is expected that for broad distributions, the evolution of the network probes the shape of the potential at a considerable distance. Thus the value of $d3V$ will not have much of an effect. Decay times are slightly longer for positive $d3V$, consistently with the naive prediction that steepness of the potential around the maximum opposite in the direction to the evolution of the network may slow down the decay process. This effect increases with decreasing σ . Moreover, the range of parameter δV for which networks decay to the unstable vacuum increases. Plots from Figures 3.8 and 3.9 illustrate influence of bias in the initial distribution on the decay dynamics. In the Fig. 3.8 we depict the estimated decay time of networks as a function of δV of a potential and the mean value θ of the field at the initialization is plotted for two values of the standard deviation of the initialization distribution $\sigma = 1$ (left panel) and $\sigma = 0.0625$ (right panel). The analogous plot for $d3V$ and θ is Fig. 3.9. Both plots infer that the shift of the initial mean value of the field strength from the local maximum of the potential determines the decay dynamics of the network. Even a small initial bias toward an unstable vacuum makes the network decay to this minimum. Moreover, for both wide and narrow initial distributions, the effect is nearly insensitive to values of both δV and $d3V$ if the network decay into the unstable vacuum, thus details of the shape of the potential do not influence the evolution of the network. On the other

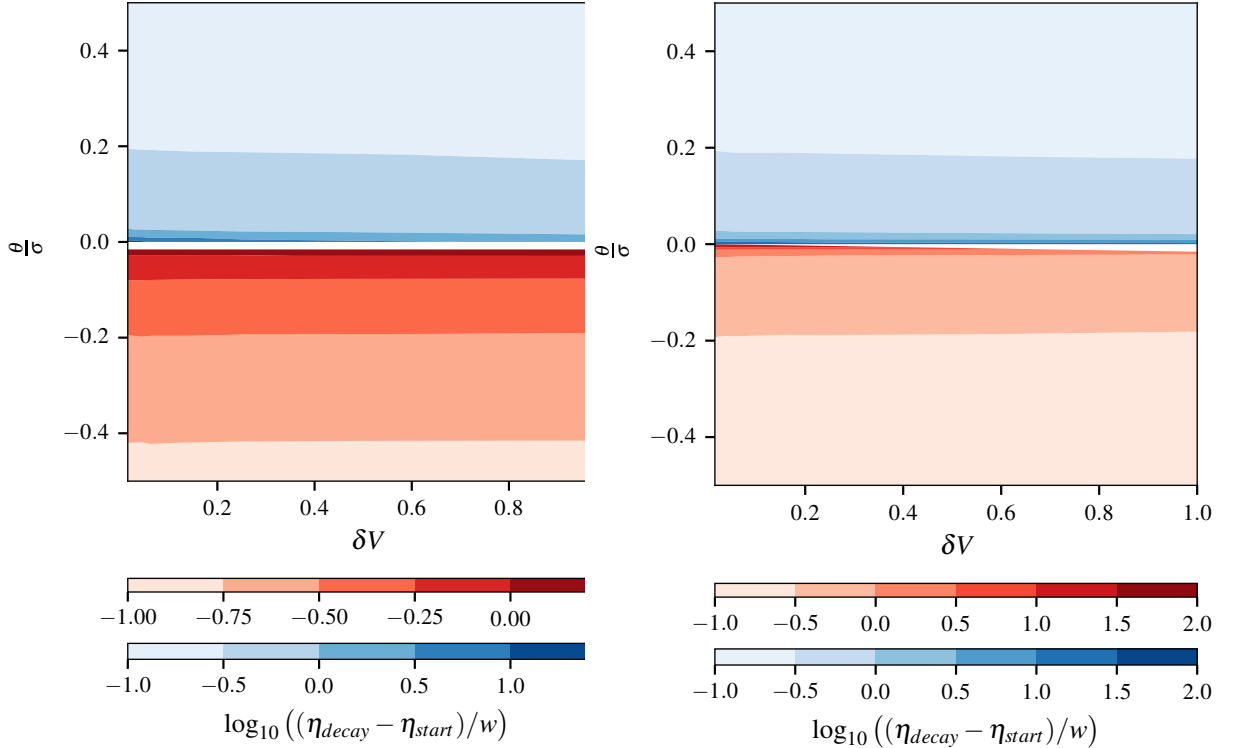


Figure 3.8: Dependence of the decay time $\eta_{decay} - \eta_{start}$ on δV and the mean value of initialization distribution θ with $\sigma = 1$ (left panel) and $\sigma = 0.0625$ (right panel) for models with $d3V = 0$.

hand, if bias is toward the global minimum of the potential and the initial distribution had large standard deviation σ , only potentials with nearly degenerate minima lead to long-living networks. For initial distributions with small standard deviations, this effect is much smaller, and the decay time of networks depends mainly on the initial value of the field strength θ . Finally, distributions with small σ lead to the formation of long-living networks only when they are very weakly biased.

The figure 3.9 shows dependence of the decay conformal time on the scale of asymmetry of the potential $d3V$ and the bias of initial distributions θ for large $\sigma = 1$ and small $\sigma = 0.0625$ standard deviations. For both cases, the final state of the evolution is determined by the mean value of the field θ at the initialization time. Lifetimes of networks are, in both cases, nearly independent of asymmetry of the potential with only a slight increase for nearly symmetric potentials. Formation of long-living networks is possible only with the small bias of the initial field strength distribution.

Comments First of all, strong dependence on the bias we find is consistent with earlier studies [354, 355, 356] of the dynamics of domain walls of the Higgs field. Since we have shown that only a small dominance of lattice sites belonging to the basin of attraction of the corresponding vacuum is needed for ending decay of the network in this vacuum for distributions centered around symmetry preserving field strength equal to 0. Hence, the networks of domain walls can decay into the Pati-Salam vacuum using biased initial distributions even though this vacuum is strongly disfavoured by both differences of values of the effective potential. Then joined results of Sec. 3.2 and

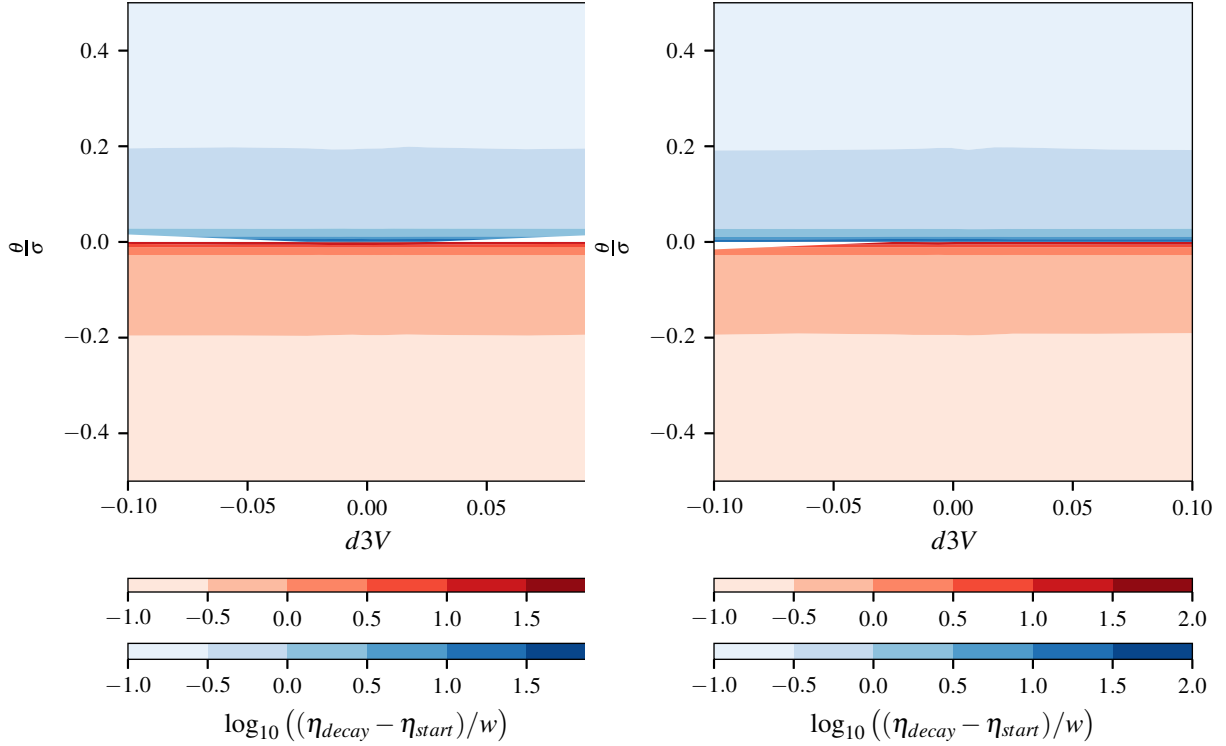


Figure 3.9: Dependence of the decay time $\eta_{decay} - \eta_{start}$ on $d3V$ and the mean value of initialization distribution θ with $\sigma = 1$ (left panel) and $\sigma = 0.0625$ (right panel) for models with $\delta V = 0$.

Sec. 3.4 constraint on the Early Universe dynamics that sets the initial values of the fields, such as inflation.

Secondly, note that the domain walls enter the scaling around $\delta V \approx 0$. The energy density of the network of stable domain walls decreases (with the expansion) slower than the energy density of the radiation and the dust, so long-lived domain walls tend to dominate the energy density of the Universe. Moreover the effective average pressure generated by the network is negative, thus it acts as Dark Energy with the barotropic parameter $-2/3 < w_{DW} < -1/3$ [357, 358]. However, Dark Energy with such an equation of state is ruled out by the present experimental data [359, 360, 361, 362, 363]. Moreover, domain walls that pose a significant fraction of the total energy density of the Universe at recombination would produce unacceptably large fluctuations of the Cosmic Microwave Background Radiation (CMBR). Thus it will be problematic for the studied model. Hence for the model 3.1 to be phenomenologically viable one needs $\lambda_2(M_P) \neq 0$

Chapter 4

Asymptotically safe quantum gravity phenomenology

Where we explore the richness of asymptotically safe phenomenology. On top of the criteria discussed in the previous chapter, namely the absence of Landau poles, stability of the potential, and reduction to the SM in low energies, we further constrain the parameter space by requirements stemming from asymptotically safe gravity. We study the renormalization flows originating from the fixed point structure of quantum gravity. We extend the discussion of GUTs from the previous chapter to the predictions of asymptotic safety and its impact on proton stability. Since AS points towards the “transplanckian” breaking, we focus on the models where the two scales are: electroweak scale and Planck scale.

We discuss whether the SM can be combined with AS within that paradigm. In particular, we focus on the Higgs mass(es) prediction in the SM and beyond.

Then we discuss the U(1) gauge bosons in the context of Weak Gravity Bound. We show that the Weak Gravity Bound allows any number of vector fields within truncation up to 8-mass dimension. In particular, the gauge sector of the SM. We prove that this is an independent gauge statement.

4.1. Unified Asymptotic Safety

Here we discuss the asymptotic safety and Grand Unified Theories. We discuss the SU(5) model and the SO(10) model introduced in the previous Chapter.

4.1.1. A minimal SU(5) model

In the notation introduced above, the minimal SU(5) model reads

$$(\mathcal{G}_{\text{GUT}}, \mathcal{F}_{\text{GUT}}, \mathcal{S}_{\text{GUT}}) = (\text{SU}(5), \bar{\mathbf{5}}_F \oplus \mathbf{10}_F, \mathbf{5}_H \oplus \mathbf{24}_H) \quad (4.1)$$

with a tentative breaking chain of

$$\mathcal{G}_{\text{GUT}} \xrightarrow{\mathbf{24}} \mathcal{G}_{\text{SM}} \xrightarrow{\mathbf{5}} \text{SU}(3)_c \times \text{U}(1)_{\text{em}} . \quad (4.2)$$

Without additional degrees of freedom or super-symmetry, this model is already excluded by (i) slightly measured offset in single-scale gauge-coupling unification [364]. In particular, $\theta_W(M_{\text{GUT}}) = 3/8$ and (ii) the wrong relations between the IR values of

Yukawa couplings [365, 366, 367]. Nevertheless, we will use the model to demonstrate that it can independently be excluded because a Planck-scale quasi fixed-point lead to the scalar potential breaking in the wrong direction, i.e., the above breaking chain cannot be realized. The Lagrangian reads

$$\mathcal{L} = \mathcal{L}_{kin} + \mathcal{L}_Y - V, \quad (4.3)$$

where the \mathcal{L} contains the standard kinetic terms for scalars, fermions in $\mathbf{5}_F$ and $\mathbf{10}_F$ and the gauge bosons in the adjoint representation. The Lagrangian \mathcal{L}_Y is given by [27]:

$$\mathcal{L}_Y = \bar{\mathbf{5}}_F Y_5 \mathbf{10}_F \mathbf{5}_H^* + \frac{1}{8} \epsilon_5 \mathbf{10}_F Y_{10} \mathbf{10}_F \mathbf{5}_H + \text{h.c.}, \quad (4.4)$$

where the internal indices have been suppressed. The potential is given by:

$$\begin{aligned} V(\mathbf{5}_H, \mathbf{24}_H) = & -\mu_{24}^2 \text{Tr} \mathbf{24}_H^2 + \frac{1}{2} \lambda_1 (\text{Tr} \mathbf{24}_H^2)^2 + \lambda_2 \text{Tr} \mathbf{24}_H^4 \\ & - \mu_5^2 (\mathbf{5}_H^\dagger \mathbf{5}_H) + \frac{1}{2} \lambda_3 (\mathbf{5}_H^\dagger \mathbf{5}_H)^2 + \lambda_4 \text{Tr} \mathbf{24}_H^2 (\mathbf{5}_H^\dagger \mathbf{5}_H) + \lambda_5 \mathbf{5}_H^\dagger \mathbf{24}_H^2 \mathbf{5}_H. \end{aligned} \quad (4.5)$$

We assume $\mu_5, \mu_{24} \ll M_P$ and neglect their running in the following discussion.

4.1.2. The asymptotic safety fixed points and potential breaking

The respective leading-order beta-functions for the $SU(5)$ gauge coupling g_5 , Yukawa couplings Y_5 and Y_{10} , as well as quartic couplings $\lambda_{1,2,3,4,5}$ have been obtained by means of Pyr@te3 [368] and are presented in App. C.2. Let us start by looking at the fixed-point structure of the beta functions. Without the gravitational contribution (2.64) the only fixed point of the one-loop beta functions is at

$$g_5 = Y_5 = Y_{10} = \lambda_i = 0 \quad (4.6)$$

In the presence of the non-zero gravity contribution f_λ , the situation changes, while the

$$g_5 = Y_5 = Y_{10} = 0, \quad (4.7)$$

remains, the λ_i can develop a non-trivial fixed point. We summarize all of the possible FP in the Tab. 4.1. For the last fixed point the potential the stability conditions are

$$\lambda_1 > 0, \quad \lambda_3 > 0, \quad 4\lambda_1\lambda_3 < \lambda_4, \quad (4.8)$$

the first two stability conditions are not satisfied, while the final one is satisfied c.f. Fig. 4.1, see discussion in the Appendix A. For all of the non-trivial fixed points the gauge group is broken in such a way that SM gauge group cannot be recovered from the potential breaking at the Planck scale [28, 27]¹.

To investigate the GFP, we assume that the gauge and Yukawa couplings of the

¹Even if one assumes that $SU(2)_L$ is an emergent group and only $SU(3)_c \times U(1)_{em}$ is survives until high energies as a true symmetry of the SM [160] the fermionic content stemming from those breakings cannot reproduce the SM multiplets.

λ_1	λ_2	λ_3	λ_4	λ_5	Stable potential?	Direction of the breaking
0	0	0	0	0	N/A	N/A
negative	0	negative	0	0	unstable	$SU(3) \times U(1)$
negative	0	negative	negative	0	unstable	$SU(3) \times U(1)$
0	0	negative	0	0	unstable	$SU(4) \times U(1)$
negative	0	0	0	0	unstable	$SU(4)$
negative	0	negative	positive	0	unstable	$SU(3) \times U(1)$

Table 4.1: Stability of the SU(5) potential at the Planck scale. The direction of the breaking is assumed to take place towards the deepest minimum, see [28].

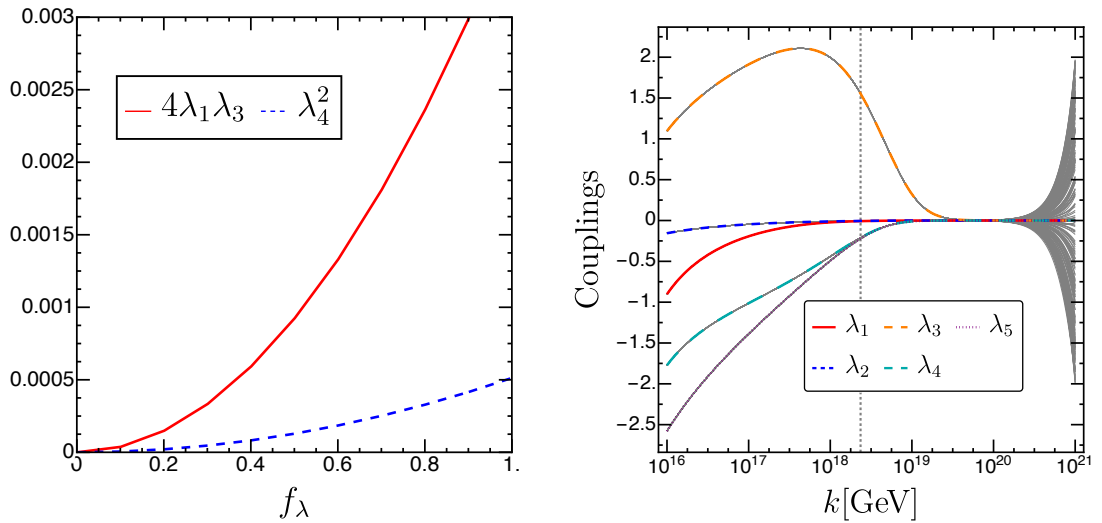


Figure 4.1: Asymptotic safety and SU(5).

Left: Stability condition for (4.8).

Right: The colored lines denote the evolution of the couplings from the gaussian FP, assuming that the scalar couplings reach the GFP at $k = 10^{21}$. The grey lines are the randomly initialized quartic couplings at scale $k = 10^{21}$. We observe that the GFP acts as an IR attractor.

SU(5)-model take viable values as far as possible. To do so the Planck-scale value of the gauge coupling g_5 is inferred from the unification scale of $SU(3)_c$ and $SU(2)_L$. The Yukawa couplings y_5, y_{10} are matched to y_{bottom} and y_{top} respectively since the latter will dominate the contribution to the running of the quartic couplings in comparison to the other fermion Yukawas. Taking that into account these couplings are given by $g_5(M_P) = 0.49, y_5(M_P) = 0.1, y_{10}(M_P) = 0.41$.

Furthermore, for any $f_\lambda > 0$, the set of quartic couplings features a GFP [369]. The latter is fully IR attractive due to the gravitational contribution. The initial value in the trans-Planckian regime is “washed away,” and the IR dynamics resemble those stemming from the GFP [369]. Consequently, all of the quartic couplings except λ_3 are pulled to negative values roughly at the Planck scale, since the contributions from the gauge coupling become dominant over the gravitational contribution [370]. This renders the potential unstable [27]. This is an example of the AS destabilizing the GUT, such that the breaking is realized at the Planck scale. Similar behaviour can be observed for SO(10) with $\mathbf{10}_H \oplus \mathbf{16}_H \oplus \mathbf{45}_H$ representations. For the potential and the beta functions of the model consult App. B and App. C.1 respectively. In the Fig. 4.2 we observe that the theory also breaks at the Planck scale if stemming from the Gaussian FP. This will be discussed in detail in [1].

A few comments are in order. Firstly, implementing the idea that AS will predict

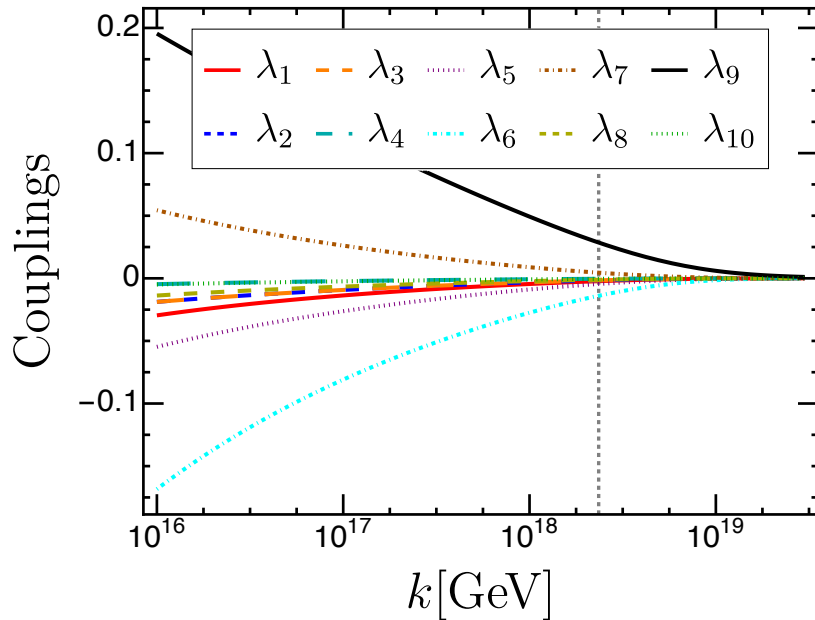


Figure 4.2: Asymptotic safety and SO(10). Evolution of the couplings from the gaussian FP, assuming that the scalar couplings reach the GFP at $k = 10^{21}$.

the breaking chain might be highly non-trivial [370] because realistic GUTs require scalar representations that are not coupled to fermions through Yukawa interactions, resulting in unstable potential if not taking into account higher-order corrections. Our results are reliable as long as the effects of gravity can be approximated as (2.65). This might not be the case. In particular, the arguments in [371, 372] suggest that the scalar potential takes a non-polynomial form beyond the Planck scale. Hence, the calculation of the deepest minimum might be highly non-trivial. In this light, the results discussed above should be taken with a grain of salt.

If trustable, the results obtained here indicate a no-intermediate M_{GUT} scale between the electroweak and Planck scale. Furthermore, the gravitational fluctuations in the context of asymptotic safety render the symmetry breaking of the representations not coupled to Yukawa, resulting in the “transplanckian” breaking and proton stability. This is converse to the conjecture that gravity can further destabilize proton [373, 374]. Finally, let us note that asymptotic safety also has further predictions in the context of GUTs. Depending on the matter sector also the unified gauge group coupling $g(M_{\text{GUT}})$ can also be predicted [375]. In turn, the value of $g(M_{\text{GUT}})$ will specify the SM gauge couplings completely in low energies, compared with experimental results.

4.2. Asymptotic safety and Higgs mass

4.2.1. Higgs mass prediction in the Standard Model

Given assertions from the previous paragraph asymptotic safety breaks the GUT group already close to the Planck scale. Motivated by that fact we now discuss the AS predictions for SM and beyond. In this paragraph, we reevaluate the calculations done in [292] concerning the calculation of the Higgs mass. The “important” couplings for the Higgs stability are y_{top}, g_1, g_2 and g_3 . The two-loop beta function for Higgs self-coupling λ reads for $y_{\text{top}} = g_1 = g_2 = g_3 = 0$ [135]:

$$\beta_\lambda(\mu) = \frac{1}{16\pi^2} \left(24\lambda^2 - \frac{312}{16\pi^2} \lambda^3 \right) + \frac{a_\lambda}{8\pi} \frac{\mu^2}{M_P^2 + 2\xi_0\mu^2} \lambda, \quad (4.9)$$

which has the following fixed points: $\lambda = 0$ (UV repulsive), $\lambda \approx 21$ (UV attractive), $\lambda \approx -9.36$ (UV attractive). The two basins of attraction are separated by the single trajectory going through the repelling fixed point. The numerical calculation confirms that if at any scale below Planck scale $\lambda(\mu) < 0$ then it approaches the negative fixed point. If one assumes that λ has to stay in the perturbative region, then necessarily one gets $\lambda(\mu) \geq 0$ at all scales. Furthermore in order to avoid the attractor in the positive domain one should assume that value of λ is minimal such that the EW vacuum is stable

$$\lambda = \min\{\bar{\lambda} : \forall_\mu \bar{\lambda}(\mu) \geq 0, \bar{\lambda}(M_P) \approx 0 \text{ and } \beta_{\bar{\lambda}}(M_P) \approx 0\} \quad (4.10)$$

which agrees with the arguments of the authors of [292]². To obtain the prediction for λ we perform the two-loop running of the $g_1, g_2, g_3, y_{\text{top}}$ with gravitational contributions of the form (2.65) and find λ satisfying (4.10). For expressions for beta functions consult [380, 381]. The one-loop-matched parameters are given as $g_1(M_{\text{top}}) = 0.35940$, $g_2(M_{\text{top}}) = 0.64754$, $g_3(M_{\text{top}}) = 1.18823$ [135], and due to large error bars we scan over the possible one-loop matched $y_{\text{top}}(M_{\text{top}}) = 0.94759 \pm 0.0022$.

As a result we get $\lambda = 0.15102 \pm 0.00158$ and $m_H \approx 135$ GeV with one-loop beta functions and tree-level matching and $\lambda = 0.13866 \pm 0.00218$ and $m_H \approx 130.5$ GeV with two-loops beta functions and one-loop matching.

The bottom quark and the taon contributions change the predictions for m_H less than 1 keV, far below theoretical and experimental accuracy. This can be expected since $y_b(M_{\text{top}}) \approx 0.015$ [382]. Then to obtain the prediction in accordance with the measured

²This reasoning explains also the Multiple Point Principle postulated in [376]. According to this principle there are two vacuum states with about the same energy density, one at electroweak scale and one at the Planck scale, which can be used to predict the SM couplings [376, 377, 378, 379].

values, it is necessary to introduce the beyond SM fields for Higgs mass to be predicted in the asymptotic safety paradigm at the correct experimental value.

4.2.2. Higgs mass prediction Beyond the Standard Model

Conformal Standard Model Here we analyse the Conformal Standard Model (CSM) [142, 169, 383] in context of asymptotic safety. The fundamental assumption which underlies this model and similar models is that there is no new physics between the weak scale and the Planck scale. This means that for example the masses of heavy neutrinos or vacuum expectation value of new scalars should be of order of 1 TeV. Indeed the observational facts not covered by the SM such as neutrino masses and oscillations, dark matter, dark energy, baryon asymmetry of the Universe and inflation can be understood without introducing an intermediate new scale, see for example [384, 385]. The CSM extends the SM by adding one new complex scalar field and right-handed neutrinos, such that

$$\mathcal{G}_{\text{CSM}} = \mathcal{G}_{\text{SM}}, \quad \mathcal{F}_{\text{CSM}} = \mathcal{F}_{\text{SM}} \oplus \underbrace{(\mathbf{1}, \mathbf{1}, 0)}_{N^{(j)}}, \quad \mathcal{S}_{\text{CSM}} = \mathcal{S}_{\text{SM}} \oplus \underbrace{(\mathbf{1}, \mathbf{1}, 0)}_{\phi} \quad (4.11)$$

The CSM lagrangian reads

$$\mathcal{L} = \mathcal{L}_{\text{kin}} + \mathcal{L}_Y - V, \quad (4.12)$$

the kinetic term is

$$\mathcal{L}_{\text{kin}}^{\text{CSM}} = \mathcal{L}_{\text{kin}}^{\text{SM}} + (\partial_\mu \phi^* \partial^\mu \phi) + i \bar{N}_\alpha^j \bar{\sigma}^{\mu\dot{\alpha}\beta} \partial_\mu N_\beta^j, \quad (4.13)$$

where we use the $\text{SL}(2, \mathbb{C})$ representation for the neutrinos. The potential reads as

$$V(H, \phi) = -m_1^2 H^\dagger H - m_2^2 \phi^* \phi + \lambda_1 (H^\dagger H)^2 + \lambda_2 (\phi^* \phi)^2 + 2\lambda_3 (H^\dagger H) \phi^* \phi. \quad (4.14)$$

For the vacuum expectation values

$$\sqrt{2} \langle H_i \rangle = v_H \delta_{i2}, \quad \sqrt{2} \langle \phi \rangle = v_\phi, \quad (4.15)$$

the tree-level mass parameters are:

$$m_1^2 = \lambda_1 v_H^2 + \lambda_3 v_\phi^2, \quad (4.16)$$

$$m_2^2 = \lambda_3 v_H^2 + \lambda_2 v_\phi^2. \quad (4.17)$$

Hence the model possesses two scalar massive particles, where m_1 is identified with the Higgs particle mass. In particular, the portal interaction can stabilize the Higgs at its current value. In the CSM, the new Yukawa interactions are introduced, which are responsible for interactions of right-chiral neutrinos:

$$\mathcal{L}_Y = \frac{1}{2} Y_{ji}^M \phi N^{j\alpha} N_\alpha^i + Y_{ji}^\nu N^{j\alpha} H^\top \epsilon L_\alpha^i + \mathcal{L}_Y^{\text{SM}} + \text{h.c.}, \quad (4.18)$$

where $\mathcal{L}_Y^{\text{SM}}$ is Yukawa part of the SM Lagrangian part and ϵ is the antisymmetric $SU(2)_L$ metric. Following [383] we assume the degeneracy of Yukawa couplings $Y_{ij}^M = y_M \delta_{ij}$, which amplifies the CP violation and makes the resonant leptogenesis scenario possible, see [169, 383, 386] for details. The masses of right-chiral neutrinos are given by:

$$M_N = y_M v_\phi / \sqrt{2}. \quad (4.19)$$

Furthermore for leptogenesis to take place, one requires: $M_N > m_2$, so that the heavy neutrinos can decay. The phase of ϕ , called minoron, acquire mass v^4/M_P^2 originating from quantum gravity effects, where $v \sim v_\phi$ and can be a potential dark matter candidate. Finally for the electroweak vacuum to be stable one needs

$$\lambda_1(\mu) > 0, \quad \lambda_2(\mu) > 0, \quad \lambda_3(\mu) > -\sqrt{\lambda_2(\mu)\lambda_1(\mu)}. \quad (4.20)$$

In CSM the stability, no Landau poles and successful leptogenesis can be satisfied simultaneously [383]. In order to understand the asymptotic safety consequences for the model let us take a look on the λ_3 , the portal 1-loop beta function

$$\beta_{\lambda_3} = \frac{\lambda_3}{32\pi^2} [24\lambda_1 + 16\lambda_2 + 16\lambda_3 - (9g_2^2 + 3g_1^2) + 6y_M^2 + 12y_{\text{top}}^2], \quad (4.21)$$

under the influence of gravitational dynamics, with $a_{\lambda_3} = +3$, the fixed point at $\lambda_{3,*} = 0$ becomes UV repelling. On the other hand $\lambda_{3,*} = 0$ implies $\lambda_3(\mu) = 0$, hence the coupling vanishes at all scales [9, 387], the same result hold at 2-loops [388]. We would say that CSM lies in asymptotically safe swampland, since it cannot reproduce the correct Higgs mass ³.

Axion-like particles The QCD Lagrangian possess two sources of CP violation ⁴, the θ and θ_q terms [394, 395, 396]

$$\mathcal{L}_{\text{QCD}} = \sum_q \bar{q}(iD^\mu - m_q e^{i\theta_q})q - \frac{1}{4}G_a^{\mu\nu}G_{\mu\nu}^a - \theta \frac{\alpha_s}{8\pi} G_a^{\mu\nu}\tilde{G}_{\mu\nu}^a, \quad (G_{\mu\nu}^a = \frac{1}{2}\epsilon_{\mu\nu\rho\sigma}G^{a,\rho\sigma}). \quad (4.22)$$

The combined $\bar{\theta} = \theta + \sum_q \theta_q$ is invariant under a chiral transformation $U(1)_A$: $q \rightarrow e^{i\gamma_\alpha}q$, with $\alpha = \frac{1}{2N_f} \sum_q \theta_q$. On the other hand $|\bar{\theta}| \leq 10^{-10}$ is constrained by the measurements of the neutron electric dipole moment. This is another source of fine tuning in the SM. Usually it is explained by the Peccei-Quinn (PQ) mechanism [397]. Within this mechanism one assumes a global chiral QCD anomalous $U(1)_{PQ}$ rotating $\bar{\theta} = \theta + \sum_q \theta_q$. The complex field ϕ is spontaneously broken at scale f_a and its Nambu-Goldstone boson, called axion, a couples to the $\bar{\theta}$ term such that

$$\mathcal{L}_{\text{eff}} = \underbrace{\left(\bar{\theta} + \frac{a}{f_a}\right)}_{\langle \theta_{\text{eff}}(x) \rangle \rightarrow 0} \frac{\alpha_s}{8\pi} G_a^{\mu\nu}\tilde{G}_{\mu\nu}^a - \frac{1}{2}\partial_\mu a\partial^\mu a + \dots \quad (4.23)$$

it dynamically “vashes” the $\bar{\theta}$ out ⁵. The case, where $f_a \approx v_H$, called the PQWW model [397, 398, 399] has been ruled out by experimental data. The two “invisible” axion models have been proposed with $f_a \gg v_H$. The DFSZ axion [400, 401] model, where the SM quarks are charged under PQ and require two new scalar particles. Yet, due to prediction $\lambda_3 = 0$, see (4.21) this model will not alleviate the stability problem.

³In [9] we have also studied the case when $a_{\lambda_i} < 0$. Then combining the asymptotic safety bounds together with pheno-bounds the second particle mass lies within $300 < m_2 < 325$ GeV. Nevertheless most of the asymptotic safety calculations points toward $a_\lambda > 0$, see e.g. [389, 390, 391, 392, 393, 287].

⁴CP violation in the QCD sector, should not be confused with weak CP violation.

⁵The name of the axion field is after the Axion dishwashing liquid.

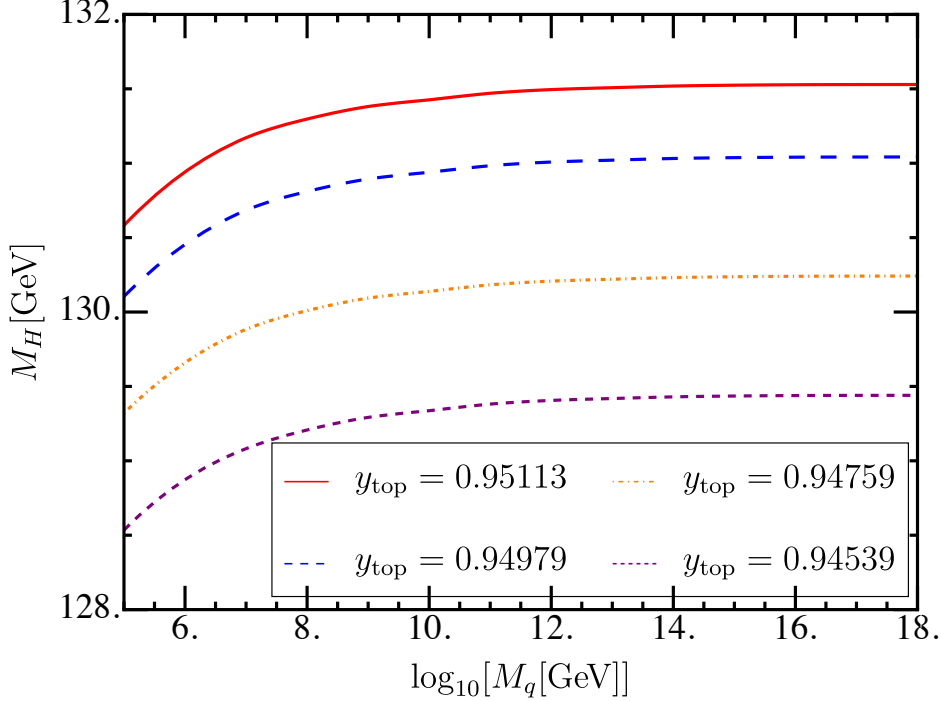


Figure 4.3: The plot depicts optimised $\lambda(M_{\text{top}})$ as a function of M_q (in logarithmic scale) for various y_{top} .

The KSVZ axion [402, 403] model includes new sterile quarks $q_i = (\mathbf{3}, \mathbf{1}, 0)$ charged under $U(1)_{PQ}$ coupled to new complex scalar $\phi = (\mathbf{1}, \mathbf{1}, 0)$:

$$\mathcal{L} = \mathcal{L}_{\text{SM}} + \sum_q (\bar{q} D_\mu \gamma^\mu q - \mathbf{y}_q \phi \bar{q} q + \text{h.c.}) + (\partial_\mu \phi^* \partial^\mu \phi), \quad (4.24)$$

and the potential is given by (4.14). We assume the Yukawa matrix \mathbf{y}_q to be diagonal and the quarks acquire masses $M_i = y_q v_\phi / \sqrt{2}$. Even with $\lambda_3 = 0$, the running of g_3 is affected by the inclusion of the heavy quarks and at one-loop, the modification reads⁶:

$$16\pi^2 \beta(g_3) \rightarrow 16\pi^2 (\beta(g_3)) + \frac{2}{3} \sum_{i=1}^n \Theta(\mu - M_{q_i}) g_3^3, \quad (4.25)$$

which in turn alters the running of y_{top} . The Θ denotes Heaviside theta function. Let us note that if there are many such quarks, then even the asymptotic freedom of the QCD can be spoiled, see discussion below (2.18). However, we focus on adding one or two sterile quarks into the SM in our analysis. The minimal mass for the sterile quark from is $m_q \sim 10$ TeV, otherwise the running hits Landau pole below Planck scale. To avoid it the mass of the second quark has to be of the order of 10^6 TeV giving a huge hierarchy. Hence we focus on the addition of a single quark. We perform the full two-loop analysis with masses in the range $m_q \in [10^5, 10^{18}]$ GeV. The results are shown below in Fig. 4.3. As we can see, the new degrees of freedom have a minor influence on stability. The change in one-loop matched Higgs mass is order 1.5 GeV downwards for $M_q \approx 10$ TeV. There are two reasons for that; first, the addition of q changes only the running of g_3 , which changes the running of y_{top} and has only a slight effect on λ .

⁶At $\mu = M_q$ one has to take into account the threshold corrections, so the coupling becomes discontinuous. Here we neglect those since they will have a marginal effect on the stability.

Secondly, phenomenologically the new degrees of freedom are constrained to have mass far beyond the EW scale [364]. We conclude addition of sterile quarks cannot bring down the Higgs mass to the experimental value.

U(1)_{B-L} model The SM possess one global, not anomalous SM symmetry group, namely U(1)_{B-L}⁷, related to the baryon minus lepton ($B - L$) number. Here the group is gauged and a new Gauge boson Z'_μ [405, 406, 407] is introduced, such that

$$\mathcal{G}_{B-L} = \mathcal{G}_{SM} \oplus U(1)_{B-L}, \quad \mathcal{F}_{B-L} = \mathcal{F}_{SM} \oplus \underbrace{(\mathbf{1}, \mathbf{1}, 0)}_{\nu_R^{(j)}}, \quad \mathcal{S}_{B-L} = \mathcal{S}_{SM} \oplus \underbrace{(\mathbf{1}, \mathbf{1}, 0)}_{\phi}. \quad (4.26)$$

The covariant derivatives receive an additional contribution: $D_\mu \rightarrow D_\mu + i(\tilde{g}Y + g'_1 Y_{B-L})Z'_\mu$, where Y is the hyper-charge and Y_{B-L} is the (B-L)-charge, such that baryons have $Y_{B-L} = +1$ and leptons $Y_{B-L} = -1$. The Z'_μ boson becomes massive due to the non-zero vacuum expectation value of ϕ . The coupling \tilde{g} describes the mixing between Z and Z' after spontaneous symmetry breaking. Following [407] we analyse the “pure” $B - L$ model by assuming that there is no tree level mixing between Z and Z' , hence $(\tilde{g}(M_{top}) = 0)$, which is supported by the current data [408], yet radiative corrections spoil it. Is also one of the most popular way of explaining so called B -anomalies [409, 410, 411, 412], which are the observed inconsistencies of the SM with experimental data in the bottom and strange quark decays. The new terms in the beta functions at the one-loop level are for $\tilde{g} = 0$ [413, 414, 415]:

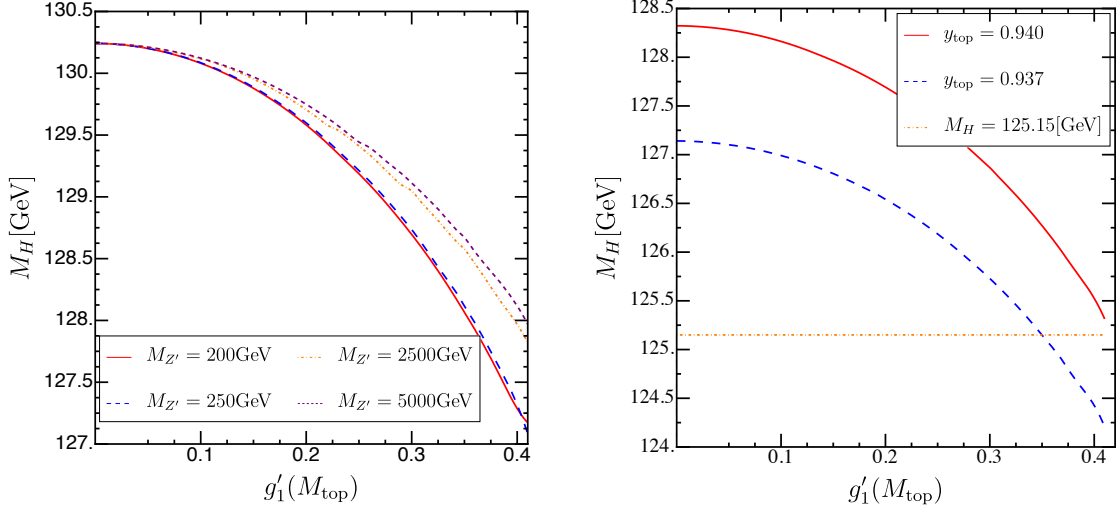
$$\beta_{g'_1} = \frac{12}{16\pi^2} g'^3_1, \quad \beta_{y_{top}} = \beta_{y_{top}}^{SM} - \frac{1}{24\pi^2} y_{top} g'^2_1 \Theta(\mu - M_{Z'}), \quad (4.27)$$

here we perform the two loop runs [413, 414, 415] with $\tilde{g}(M_{top}) = 0, \lambda_3 = 0, \lambda_2 = 0$. Phenomenologically the mass of the Z' boson is restricted to be: $\frac{M_{Z'}}{g'_1} > 7$ TeV or $M_{Z'} \leq 2M_{top}$ [416]. In order to lie within the perturbative range, one needs $g'_1(M_{top}) \in [0.0, 0.4]$. In the left panel of Fig. 4.4 for large g'_1 and small $M_{Z'}$, the Higgs mass is getting close to the experimental value. Furthermore for $M_{top} = 173$ GeV with the two-loop matching [135] the central value for the Yukawa coupling is $y_{top} \approx 0.94$. In the right panel of Fig. 4.4 we perform runs with the two-loop matchings for Higgs and top mass. For $g'_1 > 0.3, 2M_{top} > m_{Z'}$ the Higgs mass is within the observed range $m_H = 125 \pm 1.5$ GeV. Hence the model satisfies asymptotic safety criteria for some parts of the parameter space. The mass of the new gauge boson should be small or coupling g'_1 for be large, which can be verified experimentally. Furthermore our argument is confirmed by other studies of EW stability [388, 413, 404, 417]. The effect of introducing Z' boson can be even more significant if the Higgs boson is also charged under U_{B-L} , see [404]. Yet in such models, Z' is highly constrained observationally with $M_{Z'} > 3$ TeV. Furthermore, we have checked that the \tilde{g} corrections and inclusion of right-handed neutrinos, bottom quark, and taon give negligible contributions. Finally, let us note that there are also other models studied in a similar way. Those include the new fermionic degrees of freedom [191, 418, 419].

4.2.3. The θ_{QCD} and asymptotic safety

Let us note that asymptotic safety can explain the strong CP problem without axions. As we have said, the strong CP-violation consists of two terms $\bar{\theta} = \theta + \sum_q \theta_q$. By

⁷Actually there is a whole group of those symmetries, see [404], which we shall not discuss here.


 Figure 4.4: Higgs mass in the Z' model.

Left: Higgs mass for various g'_1 and $M_{Z'}$ for $M_{\text{top}} = 173$ GeV.

Right: Higgs mass for $M_{Z'} = 200$ GeV and $M_{\text{top}} = 173$, $y_{\text{top}} = 0.94$ corresponds to the two-loop matching, $y_{\text{top}} = 0.936$ corresponds to two-loop matching including the higher order corrections from the QCD [135]. The horizontal line denotes the experimental value of the Higgs mass.

considering the gravitational corrections, the following reasoning can partially explain the smallness of the strong CP-violation effect. Namely, in the case of $\text{Arg det } M_u M_d$ there is no running till at least 7-loops [394]. Despite the fact that the gravitational corrections Eq. (2.65) are extremely small, yet they can overtake the dynamics even in the IR and drop θ_q to zero, since the matter contributions are $\mathcal{O}((\theta_q)^{17})$. For gravitational contributions to be dominant, one needs $0.01 \gtrsim \sum_q \theta_q$, which is far beyond the experimental bounds. However, this argument requires a more detailed analysis.

4.3. U(1) vector bosons and Weak Gravity Bound

4.3.1. Weak gravity bound

Under the impact of gravity, additional matter interactions besides the couplings of the Standard Model have to be taken into account, because these additional interactions are generated by gravitational fluctuations. In particular, all matter interactions that are compatible with the symmetries of the kinetic term of a given matter field are expected to be induced by gravitational fluctuations, such that their GFP gets shifted in presence of gravity and complete asymptotic freedom in the matter sector cannot be achieved [276]. In particular, for gauge fields, the operator $w_2(F_{\mu\nu}F^{\mu\nu})^2$ is induced. Schematically, the scale dependence reads

$$\beta_{w_2} = C_0(G) + w_2 C_1(G) + w_2^2 C_2, \quad (4.28)$$

where $C_0 \rightarrow 0$ as $G \rightarrow 0$ [276, 285]. When gravitational interactions are turned off, there is a GFP $w_{2,*} = 0$. Conversely, in the presence of gravitational fluctuations the $C_0 \neq 0$ and $w_2 = 0$ is no longer a FP. Specifically the interacting, shifted Gaussian

fixed point (sGFP) is given by

$$w_{2,*} = \frac{-C_1(G)}{2C_2} + \sqrt{\frac{C_1(G)^2}{4C_2^2} - \frac{C_0(G)}{C_2}}, \quad (4.29)$$

for $C_2 > 0$. The sGFP collision with the second FP is at

$$C_{0,\text{crit}}(G) = \frac{C_1^2(G)}{4C_2}. \quad (4.30)$$

Therefore, for $C_0 > C_{0,\text{crit}}$, the FP for w_2 becomes complex and UV completion in the gravity-matter system cannot be achieved. Thus scale symmetry conditions can then restrict the gravitational parameter space spanned by the G and Λ . The bound of the region where the UV completion is possible is known as the *weak gravity bound* (WGB) in the literature [291, 276, 285, 288, 420, 421]. The WGB separates the region in the gravitational parameter space, where a UV-completion of the matter sector is possible from the excluded, strong gravity region. Hence, a UV completion for the Abelian gauge sector requires that

$$f_g > 0 \quad \text{and} \quad C_0(G) \leq C_{0,\text{crit}}(G), \quad (4.31)$$

are fulfilled simultaneously. These conditions have been investigated in [285], indicating that asymptotically safe quantum gravity is compatible with a UV-complete Abelian gauge sector. However, the UV completion of the gauge sector might only be available in four or five dimensions [288]. In the following, we extend the studies in [285, 288] in various directions. In particular, we investigate:

- The impact of the second independent, gauge-invariant four-gauge interaction given by the operator $(F\tilde{F})^2$.
- The induced interaction structure of a system containing N_V gauge fields.
- The robustness of the WGB under changes of the gauge parameter β_h .

4.3.2. Single gauge system

We start with the investigation of a single gauge field. The effective action is truncated to the standard kinetic term, and the full basis ⁸ of independent and gauge invariant interactions of mass dimension eight

$$\begin{aligned} \Gamma_k^{\text{U}(1)} = & \frac{1}{4} \int d^4x \sqrt{g} F_{\mu\nu} F^{\mu\nu} + S_{\text{gf},A} \\ & + \frac{w_2 k^{-4}}{8} \int d^4x \sqrt{g} (F_{\mu\nu} F^{\mu\nu})^2 + \frac{v_2 k^{-4}}{8} \int d^4x \sqrt{g} (F_{\mu\nu} \tilde{F}^{\mu\nu})^2 \end{aligned} \quad (4.32)$$

where $F_{\mu\nu} = \partial_\mu A_\nu - \partial_\nu A_\mu$ is the field strength tensor, and $\tilde{F}_{\mu\nu} = \frac{1}{2} \epsilon_{\mu\nu\rho\sigma} F^{\rho\sigma}$ its dual tensor, with the totally antisymmetric tensor $\epsilon_{\mu\nu\rho\sigma}$. The action $\Gamma_k^{\text{U}(1)}$ corresponds to

⁸We neglect an operator $F_{\mu\nu} \square F^{\mu\nu}$ and $F_{\mu\nu} \square^2 F^{\mu\nu}$ here, which would contribute to the momentum-dependent propagator of the gauge field, see [422].

the weak-field expansion of the Euler-Heisenberg Lagrangian [423]. The gauge fixing term is given by

$$S_{\text{gf},A} = \frac{1}{2\alpha_A} \int d^4x \sqrt{\bar{g}} (\bar{D}^\mu A_\mu) (\bar{D}^\mu A_\mu), \quad \alpha_A \rightarrow 0, \quad (4.33)$$

and the corresponding Fadeev-Popov ghosts decouple from the U(1) gauge fields. The calculation of the beta functions has been done in the Landau-gauge limit $\alpha_h = \alpha_A = 0$, $\beta_h = 1$, if not specified otherwise. The diagrammatic representation can be found in [285, 288] and we employ the Mathematica packages *xAct* [424, 425, 426, 427, 428], as well as the *FormTracer* [429], for their evaluation. In a semi-perturbative approximation, where the anomalous dimension stemming from the regulator insertion is neglected, the beta functions reads for $\Lambda = 0$:

$$\eta_A = -\frac{1}{12\pi^2} (6\pi G - v_2 - 4w_2),$$

$$\beta_{w_2} = \left(4 - \frac{7G}{2\pi} + \frac{5v_2}{12\pi^2}\right) w_2 + \left(8G^2 - \frac{Gv_2}{\pi} + \frac{v_2^2}{6\pi^2}\right) + \frac{35}{24\pi^2} w_2^2, \quad (4.34)$$

$$\beta_{v_2} = \left(4 - \frac{25G}{6\pi} + \frac{11w_2}{12\pi^2}\right) v_2 - \left(8G^2 + \frac{7Gw_2}{6\pi} + \frac{w_2^2}{24\pi^2}\right) + \frac{1}{8\pi^2} v_2^2. \quad (4.35)$$

and the full set can be found in ancillary notebook of [2]. The equations (4.34, 4.35) reveal that $C_{0,w_2}(G, v_2 = 0) > 0$ and $C_{0,v_2}(G, w_2 = 0) < 0$. This relation also holds for other values of Λ . Since $C_{0,v_2}(G, w_2 = 0) < 0$ and $C_{2,v_2} > 0$, then in the absence of w_2 there should be no WGB for the v_2 . Similarly for the system (4.32) one can expect the WGB to be qualitatively similar to the WGB of the system only featuring w_2 , see [285, 288]. The reason for this is that the back-coupling of v_2 into β_{w_2} is numerically suppressed by at least a factor of 16π , compared to the pure gravitational contribution to β_{w_2} . Therefore, unless the fixed-point value for v_2 grows very large, the inclusion of v_2 is expected to lead to only quantitative but no qualitative differences, based on Eq. (4.34, 4.35). In the left panel of Fig. 4.5 one can observe that WGB is indeed only slightly alleviated for the full system under the inclusion of v_2 , in comparison to the WGB for w_2 only. The inclusion of the second gauge invariant operator results in a weaker WGB for the full system. This can be understood as the effect of additional contributions to β_{w_2} coming from non-zero v_2 . In particular, $v_{2,*} > 0$, cf. the right panel of Fig. 4.5, results in a reduction of C_{0,w_2} and increment of C_{1,w_2} under the inclusion of v_2 . Finally in the right panel of Figure 4.5 one can observe that for $\Lambda = 0$ the SGFPs are such that $-w_{2,*} \approx v_{2,*}$. This is a consequence of $C_{0,w_2} = -C_{0,v_2}$ holding for $\Lambda = 0$.

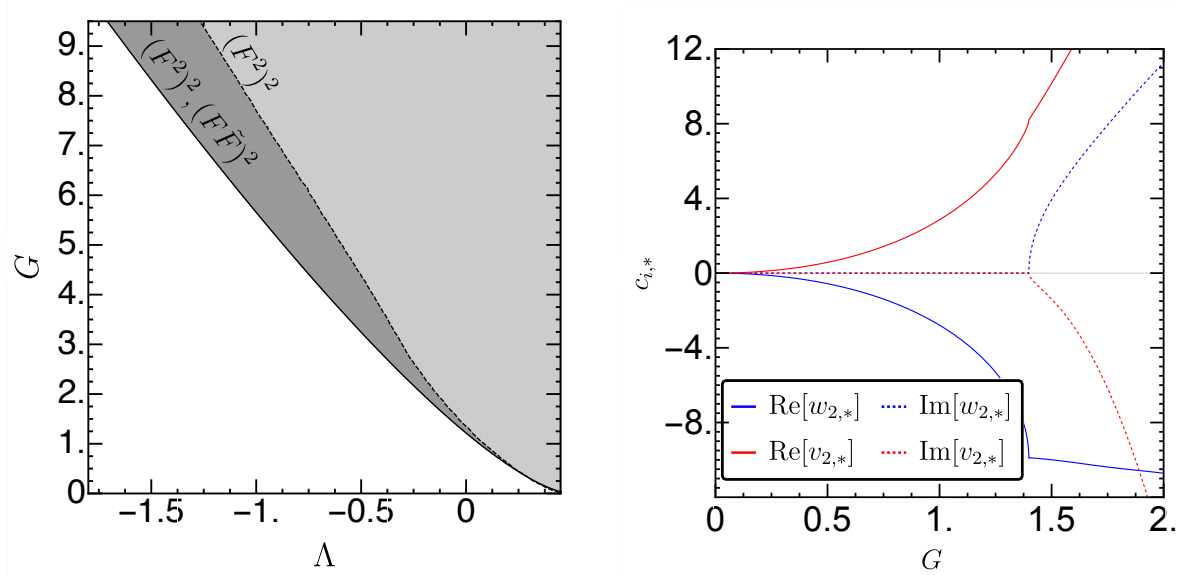


Figure 4.5: To the left: The WGB for the system (4.32).

To the right: The real parts of the fixed point values for w_A and v_A for $\Lambda = 0$.

4.3.3. Weak gravity bound for more than one gauge field

We now study a coupled system of N_V Abelian gauge fields. Gravitational fluctuations preserve asymptotic freedom for the non-abelian gauge bosons within investigated truncations [281, 286, 283]. This indicates that our results are likely relevant for the SM possessing $N_V = 12$ gauge fields 8 gluons, three weak bosons, and one photon. Within AS, there are indications that the SGFP respects the symmetries of the kinetic terms [2, 420], due to the structure of the diagrammatic expansion [279]. Then the system is reduced to the interactions respecting those symmetries and no other interactions are induced. In the case of the N_V gauge fields, this symmetry is $O(N_V)$ rotating the gauge fields. The most general $O(N_V)$ symmetric, \mathbb{Z}_2^N symmetric and gauge invariant effective action up to dimension 8 operators is given

$$\begin{aligned} \Gamma_k(\mathbb{A}) &= \frac{Z_A}{4} \int d^4x \sqrt{g} \mathbb{F}_{\mu\nu}^T \mathbb{F}^{\mu\nu} + S_{\text{gf}, \mathbb{A}} \\ &+ \frac{\bar{w}}{8N_V} \int d^4x \sqrt{g} (\mathbb{F}_{\mu\nu}^T \mathbb{F}^{\mu\nu})(\mathbb{F}_{\rho\sigma}^T \mathbb{F}^{\rho\sigma}) + \frac{\bar{w}'}{8N_V} \int d^4x \sqrt{g} (\mathbb{F}_{\mu\nu}^T \mathbb{F}_{\rho\sigma}) ((\mathbb{F}^{\mu\nu})^T \mathbb{F}^{\rho\sigma}) \\ &+ \frac{\bar{v}}{8N_V} \int d^4x \sqrt{g} (\mathbb{F}_{\mu\nu}^T \tilde{\mathbb{F}}^{\mu\nu})(\mathbb{F}_{\rho\sigma}^T \tilde{\mathbb{F}}^{\rho\sigma}) + \frac{\bar{v}'}{8N_V} \int d^4x \sqrt{g} (\mathbb{F}_{\mu\nu}^T \tilde{\mathbb{F}}_{\rho\sigma}) ((\mathbb{F}^{\mu\nu})^T \tilde{\mathbb{F}}^{\rho\sigma}) \end{aligned} \quad (4.36)$$

where

$$\mathbb{A}_\mu = (A_\mu^1, \dots, A_\mu^{N_V}) \quad \text{and} \quad \mathbb{F} = \partial_\mu \mathbb{A}_\nu - \partial_\nu \mathbb{A}_\mu, \quad (4.37)$$

with $\tilde{\mathbb{F}}_{\mu\nu} = \frac{1}{2} \epsilon_{\mu\nu\rho\sigma} \mathbb{F}^{\rho\sigma}$. In Figure 4.6 one can observe that the addition of new vector fields makes the WGB stronger.

Gravitational fixed point and the weak gravity bound. Thus far, we have treated Λ and G as free input parameters. Yet, as we have discussed in Sec. 2.2 in the

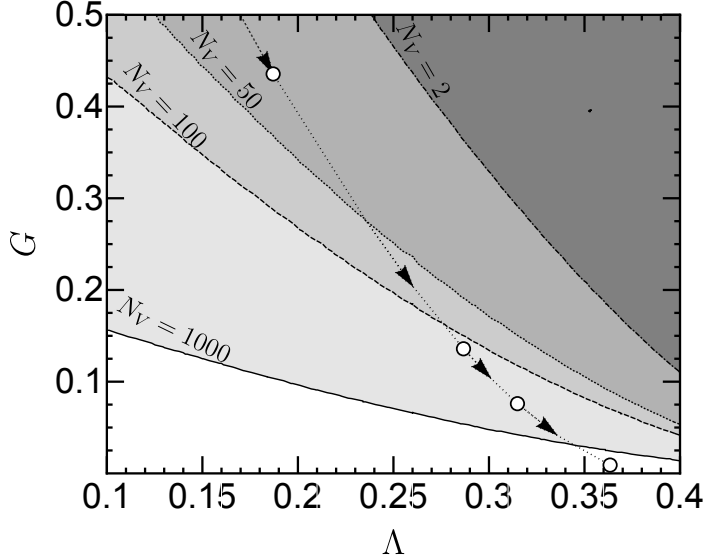


Figure 4.6: The WGB the systems with an increasing number of gauge fields. In the background approximation, the position of the gravitational fixed point, as a function of N_V , is depicted. The circle markers denotes the position of the FP for $N_V = 10$, $N_V = 50$, $N_V = 100$ and $N_V = 1000$, for beta functions consult [274, 275, 22].

asymptotic safety scenario, the fixed point value of G, Λ are not free parameters but depend on the matter content, c.f. Eq. 2.61. In particular, if the gravitational fixed point lies above the bound, then, within the truncation, the combined vector-gravity system cannot realize asymptotic safety.

For the system described by Eq. 4.36 for all N_V the gravity FP lies in the region not excluded by the WGB. This is depicted in Fig. 4.6. This is in the contradistinction to the studies done for the scalar sector [420], where the additional spinning content is required for the system to evade the WGB. To investigate the $N_V \rightarrow \infty$ limit we plug into the matter beta functions the fixed point values for Λ and G . We find that in that limit the matter contributions dominate and the system decouples from gravity

$$\begin{aligned} \beta_{\bar{w}} &= \left(4 + \frac{5\bar{v}'}{24\pi^2} + \frac{5\bar{w}'}{24\pi^2}\right)\bar{w} + \frac{7}{8\pi^2}\bar{w}^2 + \left(\frac{\bar{w}'^2}{192\pi^2} + \frac{\bar{v}'^2}{192\pi^2} + \frac{\bar{w}'\bar{v}'}{192\pi^2}\right), \\ \beta_{\bar{w}'} &= \left(4 + \frac{7\bar{v}'}{96\pi^2} + \frac{\bar{w}}{2\pi^2}\right)\bar{w}' + \frac{23}{192\pi^2}\bar{w}'^2 + \frac{7\bar{v}'}{192\pi^2}, \\ \beta_{\bar{v}} &= \left(4 + \frac{\bar{v}'}{6\pi^2} + \frac{\bar{w}'}{6\pi^2} + \frac{\bar{w}}{\pi^2}\right)\bar{v} - \frac{(\bar{v}' + \bar{w}')^2}{192\pi^2}, \\ \beta_{\bar{v}'} &= \left(4 + \frac{5\bar{w}'}{16\pi^2} + \frac{\bar{w}}{\pi^2}\right)\bar{v}' + \frac{15}{192\pi^2}\bar{v}'^2 - \frac{\bar{w}^2}{192\pi^2} \end{aligned} \quad (4.38)$$

with

$$\eta|_{N_V \rightarrow \infty} = -\frac{\bar{v}' + \bar{w}' + 6\bar{w}}{48\pi^2}. \quad (4.39)$$

4.3.4. Gauge dependence

We study the gauge-dependence of the $O(N_V)$ -symmetric system by computing the WGB at the fixed value of the cosmological constant $\Lambda = 0$. The bound now reduces

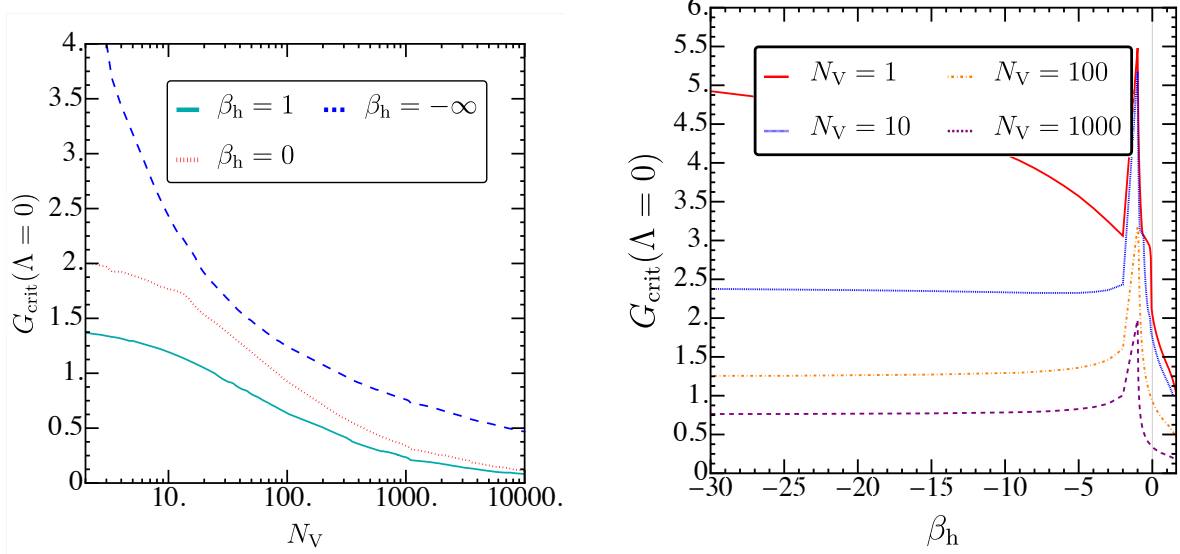


Figure 4.7: The WGB in a function of N_V and β_h . G^{crit} denotes the value of G^* at which the sGFP becomes complex.

To the left: Dependence of the $G_{\text{crit}}(\Lambda = 0)$ on N_V given exemplary values of β_h .

To the right: Dependence of the $G_{\text{crit}}(\Lambda = 0)$ on β_h given exemplary values of N_V .

to a single point, which we denote as G_{crit} . The G_{crit} depends on β_h only quantitatively and remains finite for all displayed values of N_V and β_h , see Fig. 4.7. Specifically, the strongest dependence on β_h is found for $-5 \lesssim \beta_h < 3$, see the right panel of Fig. 4.7. This is a consequence of the incompleteness of the gauge fixing at $\beta_h = 3$. Since these gravitational contributions at $\Lambda = 0$ are functions in $(\beta_h - 3)^{-n}$, where $n \in \mathbb{Z}_+$, their variation with β_h decreases for more negative β_h .

Furthermore, the gauge dependence decreases when the number of gauge fields increases. This is because the contribution from the gauge fields is independent of β_h and starts to become more critical than the gravitational contribution once N_V is large enough. In this matter-dominated regime, the WGB is mostly matter-induced and therefore only weakly dependent on β_h . Thus, the qualitative feature that the inclusion of more gauge fields results in a stronger WGB is independent of the gauge choice.

Weak gravity bound in the $\beta_h \approx 0$ case The $\beta_h \approx 0$ case deserves special attention. Here we discuss it for the representative case of the single species system. As depicted on the right panel of Fig. 4.7 the $G_{\text{crit}}(\Lambda = 0)$ raises sharply around the $\beta \approx 0$. This stems from the fact that the WGB for $\beta_h = 0$ ceases to be a function for $\Lambda \approx 0$, see the left panel of the Fig. 4.8. This is different for other gauge choices, where $G_{\text{crit}}(\Lambda)$ is a function, i.e., there is a single value G_{crit} for a given value of Λ . This behaviour is present only for the full truncation consisting of w_2 and v_2 and absent for truncations consisting of w_2 or v_2 only as depicted in Fig. 4.8.

In particular, for $\Lambda = 0$ there are two allowed intervals, $G < 2.05$ and $2.31 < G < 2.55$. This follows from the form of beta function for w_2 . Let us consider the schematic form of β_{w_2} , which we repeat here for convenience

$$\beta_{w_2} = C_{2,w_2}(G, v_2, \Lambda = 0)w_2^2 + C_{1,w_2}(G, v_2, \Lambda = 0)w_2 + C_{0,w_2}(G, v_2, \Lambda = 0). \quad (4.40)$$

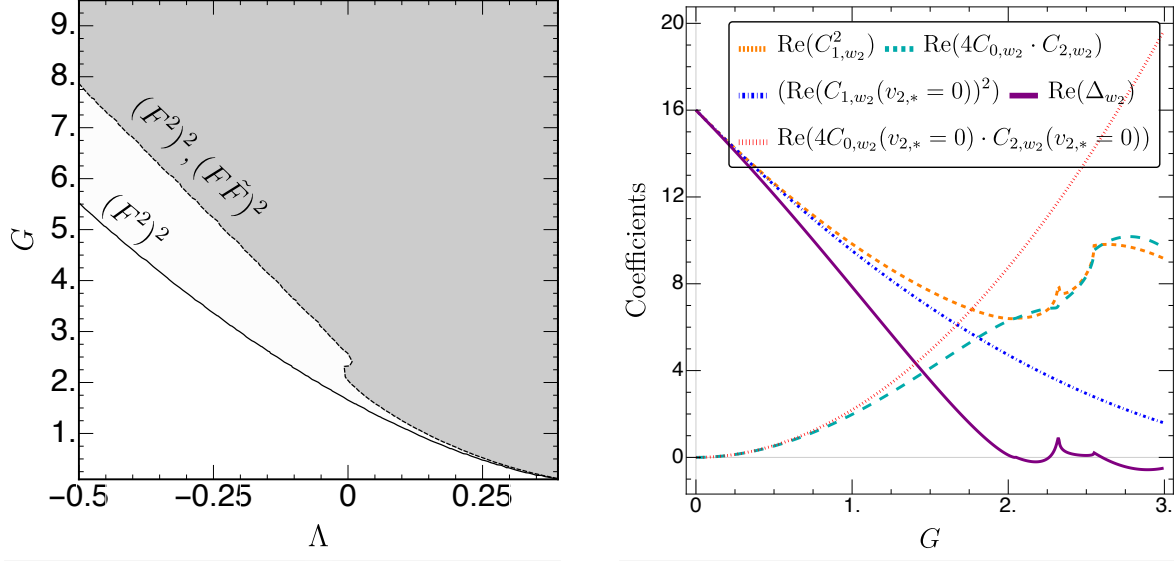


Figure 4.8: In the left panel: Comparison of the WGB for w_2 and w_2 plus v_2 truncations for $\beta_h = 0$. For the full truncation there is a kink at $\Lambda \approx 0$ absent for w_2 truncation only.

In the right panel: The behaviour of coefficients of the coupled w_2 and v_2 system.

As long as the discriminant $\Delta = C_{1,w_2}^2 - 4C_{0,w_2}C_{2,w_2}$ is non-negative, the real sGFP exist. At $\Delta = 0$, there is collision of the FP. For $v_2 \equiv 0$ the $\text{Re}(C_{1,w_2}^2(v_2 = 0))$ decreases with G (the blue dot-dashed line in right panel of Figure 4.8), while $\text{Re}(4C_{0,w_2}C_{2,w_2}(v_2 = 0))$ increases (the red dotted line). As they cross at $G \approx 1.75$ the $\text{Re}(\Delta_{w_2})$ becomes negative and the fixed points are no-longer real. On the other hand, the contribution from v_2 to the C_1 have opposite sign to the one from G

$$\beta_{w_2} = \left(4 - \frac{155G}{54\pi} + \frac{v_2}{12\pi^2} \right) w_2 + \left(\frac{100G^2}{27} - \frac{Gv_2}{\pi} + \frac{v_2^2}{6\pi^2} \right) + \frac{35}{24\pi^2} w_2^2. \quad (4.41)$$

Since $v_{2,*} > 0$, the $\text{Re}(C_{1,w_2}^2)$ starts to grow at $G \approx 2.0$ (in the right panel of Figure 4.8 depicted as the dashed orange line). Furthermore the contributions from $v_{2,*}$ to the $\text{Re}(C_{0,w_2})$ are such that $\text{Re}(C_{0,w_2}) < \text{Re}(C_{0,w_2}(v_{2,*} = 0))$, depicted as the cyan dashed line. This two effects combined results in $\text{Re}(\Delta_{w_2})$ (the purple line) being slightly positive in the interval $2.31 < G < 2.55$, resulting in a second allowed interval. This behaviour is a reminder that one has to be cautious when studying systems with multiple couplings.

Part III

Quantum gravitational cosmology

Chapter 5

Eternal Inflation

Where we study eternal inflation within the exemplary BSM inflation models and the asymptotically safe models. We discuss how the quantum fluctuations of the inflaton field can be translated to the stochastic evolution resulting in eternal inflation. We discuss that tunneling might also lead to eternal inflation. The studied models are non-minimally coupled inflaton in Starobinski inflation, Conformal Standard Model, alpha-attractors, RG-improved Starobinski inflation and scalar, fermion Yang-Mills system in the Veneziano limit.

5.1. Eternal Inflation

5.1.1. How inflation becomes eternal?

In this section we discuss, under what circumstances the inflation becomes eternal. Our discussion follows closely [6, 30, 430]. Consider a scalar field minimally coupled to gravity:

$$S = \int d^4\sqrt{-g} \left(\frac{1}{2}M_{Pl}^2 R + \frac{1}{2}g^{\mu\nu}\partial_\mu\phi\partial_\nu\phi - V(\phi) \right). \quad (5.1)$$

On the FLRW background in the slow roll (1.75) approximation the equations of motion reduce to

$$3H\dot{\phi} + \frac{\partial V}{\partial\phi} \approx 0, \quad H^2 M_P^2 \approx \frac{8\pi}{3}V(\phi). \quad (5.2)$$

Inflation ends once one of the so-called slow-roll parameters becomes of order one and the evolution enters the oscillatory, reheating phase in which all other particles are produced [183]. On the classical level that is the whole story.

On the other hand, the proper treatment of the system requires treating both $g_{\mu\nu}$ and ϕ as quantum operators. This however comes with a number of issues. Firstly we do not know the theory of quantum gravity. Furthermore, the Klein-Gordon equation is highly non-linear and hence quantising it is nontrivial. In the Heisenberg picture it is given as [431]:

$$\left(\frac{\partial^2}{\partial t^2} + 3H\frac{\partial}{\partial t} - \frac{1}{a^2(t)}\Delta \right) \phi(t, \mathbf{x}) + \frac{\partial V}{\partial\phi}(t, \mathbf{x}) = 0. \quad (5.3)$$

The stochastic inflation formalism considers instead the coarse-grained field $\varphi(t, \mathbf{x})$ [431, 432, 433, 434], s.t. it is a spatial average of the ordinary field ϕ over the Hubble

radius H^{-1} , containing the long-wave modes s.t. $k < aH$. Following [430, 435, 436, 437, 438, 439] let us take a look into the problem from the path integral point of view. We split the field into long-wavelength $k \lesssim aH$ classical background and short-wavelength $k \gtrsim aH$ quantum field:

$$\phi(x) = \phi_<(x) + \phi_>(x), \quad (5.4)$$

with short-wavelength being projected as

$$\phi_>(x) = \int dk W(\mathbf{k}, t) \phi_k(x), \quad (5.5)$$

and W being a projection function. Then (5.1) can be casted as

$$S[\phi] = S[\phi_<] + S[\phi_>] + S_{\text{int}}[\phi_<, \phi_>] \quad (5.6)$$

with

$$S_{\text{int}} = \int d^4x a^3 \phi_<(x) \left(\frac{1}{a^3} \partial_\mu a^3 g^{\mu\nu} \partial_\nu - V'' \right) \phi_>(x), \quad (5.7)$$

within the path-integral formalism we wish to integrate out the $\phi_>$, such that we obtain $\Gamma(\phi_<)$. Within the closed-time Schwinger-Keldysh formalism one considers the ϕ being the mean field and ψ signifying the amplitude of quantum fluctuations of $\phi_<$ on top of the mean field value instead of $\phi_<$. For ϕ and ψ the effective action is obtained as

$$\Gamma(\phi, \psi) = - \int dt \psi \left(3H\dot{\phi} + \frac{dV}{d\phi} \right) + i \frac{1}{2} \frac{9H^5}{4\pi^2} \int dt \psi^2. \quad (5.8)$$

The Hubbard-Stratonovich transformation gives

$$e^{-\frac{1}{2} \int dt \frac{9H^5}{4\pi^2} \psi^2} = \int D\xi e^{-\frac{1}{2} \int dt \frac{4\pi^2}{9H^5} \xi^2 + i \int dt \xi \psi}. \quad (5.9)$$

The action is

$$\Gamma[\phi, \psi] = - \int dt \psi \left[3H\dot{\phi} + \frac{dV}{d\phi} - \xi \right], \quad (5.10)$$

The equation of motion stemming from the action is stochastic Langevin equation

$$3H\dot{\phi} + \frac{dV}{d\phi} = \frac{H^{5/2}}{2\pi} \xi(t), \quad (5.11)$$

with noise

$$\langle \xi(t) \rangle = 0, \quad \langle \xi(t) \xi(t') \rangle = \frac{9H^5}{4\pi^2} \delta(t - t'). \quad (5.12)$$

Equivalently the probability density of ϕ field is given by the Fokker-Planck equation [30]:

$$\dot{P}[\phi, t] = \frac{1}{2} \left(\frac{H^3}{4\pi^2} \right) \frac{\partial^2 P[\phi, t]}{\partial \phi \partial \varphi} + \frac{1}{3H} \partial_i (\partial^i V(\phi) P[\phi, t]), \quad (5.13)$$

where $\dot{P}[\phi, t] := \frac{\partial}{\partial t} P[\phi, t]$.

How does inflation become eternal? Given an arbitrary field value ϕ_c , one can ask what is the probability that quantum field $\phi = \phi(t)$ is above this value:

$$\Pr[\phi > \phi_c, t] = \int_{\phi_c}^{\infty} d\phi P[\phi, t]. \quad (5.14)$$

From (5.12) we know that the distribution is Gaussian, centered around the classical evolution of the Langevin equation (5.11). Then (5.14) resembles the error function, which in turn can be approximated by an exponential decay:

$$\Pr[\phi > \phi_c, t] \approx C(t) \exp(-At), \quad (5.15)$$

where $C(t)$ is polynomial in t and all of the dependence on ϕ_c is contained in $C(t)$ with A being the decay rate. Then it seems that inflation cannot last forever since

$$\lim_{t \rightarrow \infty} \Pr[\phi > \phi_c, t] = 0. \quad (5.16)$$

However, there is an additional effect: expansion of the universe during inflation. The size of the universe depends on time according to:

$$U(t) = U_0 e^{3Ht}, \quad (5.17)$$

where U_0 is the initial volume of the pre-inflationary universe. One can interpret the probability $\Pr[\phi > \phi_c, t]$ as fraction of the volume $U_{inf}(t)$ still inflating, that is:

$$U_{inf}(t) = U_0 e^{3Ht} \Pr[\phi > \phi_c, t], \quad (5.18)$$

then in order for the Universe to inflate eternally, the positive exponential factor $3H$ in Eq. (5.18) and the negative exponential factor $-A$ in (5.15) must satisfy:

$$3H > A. \quad (5.19)$$

We shall illustrate this general property on an example of linear potential. For the linear hilltop model the potential is given by

$$V(\phi) = V_0 - \alpha\phi. \quad (5.20)$$

The solution of the Fokker-Planck equation (5.13) is the Gaussian distribution with:

$$\mu(t) = \frac{\alpha}{3H}t, \quad \sigma^2(t) = \frac{H^3}{4\pi^2}t. \quad (5.21)$$

The time-dependence of $\mu(t)$ is due to the classical rolling of the field in the linear potential. The integral for probability density is:

$$\Pr[\phi > \phi_c, t] = \frac{1}{2} \operatorname{erfc} \left(\frac{\frac{\alpha}{3H}t - \phi_c}{\frac{H}{2\pi}\sqrt{2Ht}} \right). \quad (5.22)$$

The error function may be approximated by an exponential:

$$\Pr[\phi > \phi_c, t] = C(t) \exp \left(-\frac{4\pi^2\alpha^2}{18H^5}t \right), \quad (5.23)$$

where $C(t)$ is power-law in t and ϕ_c vanishes from the final approximation of the probability. By comparing the exponents, we can check whether U_{inf} will grow or tend to zero. The condition for eternal inflation to occur becomes:

$$3H > \frac{4\pi^2\alpha^2}{18H^5}. \quad (5.24)$$

For linear potential $\alpha = V'(\phi)$ using the slow-roll equations equation (5.2), above condition can be rewritten:

$$\frac{|V'|}{V^{\frac{3}{2}}} < \frac{\sqrt{2}}{2\pi} \frac{1}{M_P}. \quad (5.25)$$

This can be interpreted as quantum fluctuations dominating over classical field rolling. For linear potential, this is satisfied for a large ϕ . Similarly, the second condition for the eternal inflation may be derived from the quadratic hilltop potential:

$$-\frac{V''}{V} < \frac{3}{M_{Pl}^2}. \quad (5.26)$$

Further necessary conditions on p-th derivative with $p > 2$ have been derived in [30] and give:

$$[-\text{sgn}(\partial^p V)]^{p+1} \frac{|\partial^p V|}{V^{(4-p)/2}} < \mathcal{N}_p M_{Pl}^{p-4}, \quad (5.27)$$

where $\mathcal{N}_p \gg 1$ is numerically determined coefficient. In order to cross check the formulas (5.25, 5.26) the numerical simulation has been developed. To reconstruct the probability distribution one simulates the discretized version of equation (5.11):

$$\phi_n = \phi_{n-1} - \frac{1}{3H} V'(\phi_{n-1}) \delta t + \delta\phi_q(\delta t), \quad (5.28)$$

with $\delta\phi_q(\delta t)$ being random number taken from the gaussian distribution with mean equal zero, and variance $\frac{H^3}{4\pi^2}\delta t$, for details see [6].

5.1.2. Tunelling and eternal inflation

Most of the inflationary potentials are single-minimum, such as Starobinsky inflation and alpha-attractors. There are, however, potentials that are of the type depicted in figure 5.1 and possess various minima. In such models, inflation can become eternal due to tunneling to the inflating vacua. When the vacua are degenerate enough, the tunneling dominates over quantum uphill rolling. As it will turn out, this is the dominant effect for the model discussed in section 5.3.2, where the tunneling goes in the opposing direction to the old inflation scenario [440].

The eternal inflation mechanism discussed in the previous sections relies on the local shape of the potential and cannot provide an accurate description in that case. In order to quantitatively derive predictions for this new effect one can rely on the first passage formalism [441, 442] instead, and apply it to the eternal inflation considerations [6]. Given the initial value of the field ϕ_0 being between ϕ_- and ϕ_+ , the probability that it reaches ϕ_+ before ϕ_- and ϕ_- before ϕ_+ , denoted respectively $p_+(\phi_0)$ and $p_-(\phi_0)$, obeys the following equation:

$$v p''_{\pm}(\phi) - \frac{v'}{v} p'_{\pm}(\phi) = 0, \quad (5.29)$$

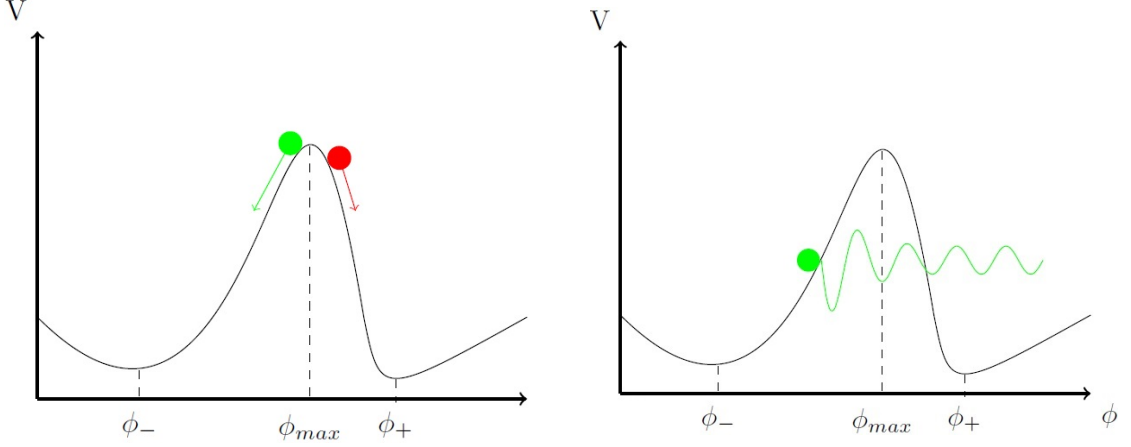


Figure 5.1: Left: field initially placed at the maximum of the potential may decay towards one of the two vacua: at ϕ_- with probability p_- and at ϕ_+ with probability p_+ . Right: field initially placed at $\phi_0 < \phi_{\max}$ may tunnel through the barrier towards ϕ_+ with probability $p_+(\phi_0)$. Analogous tunnelling from "plus" to "minus" side is also possible.

with initial conditions: $p_{\pm}(\phi_{\pm}) = 1$, $p_{\pm}(\phi_{\mp}) = 0$, where $v = v(\phi)$ is the dimensionless potential $v(\phi) := \frac{V(\phi)}{24\pi^2 M_{Pl}^4}$. The analytical solution is:

$$p_{\pm}(\phi_0) = \pm \frac{\int_{\phi_{\pm}}^{\phi_0} e^{-\frac{1}{v(\phi)}} d\phi}{\int_{\phi_{-}}^{\phi_{+}} e^{-\frac{1}{v(\phi)}} d\phi}. \quad (5.30)$$

One may also define the probability ratio R :

$$R(\phi_0) := \frac{p_+(\phi_0)}{p_-(\phi_0)} = \frac{\int_{\phi_{-}}^0 e^{-\frac{1}{v(\phi)}} d\phi}{\int_{\phi_0}^{\phi_{+}} e^{-\frac{1}{v(\phi)}} d\phi}. \quad (5.31)$$

The above integrals may be evaluated numerically. Within the steepest descent approximation, the probability ratio R may be evaluated approximately, where the leading contributions to (5.31) come from the values of the field in the neighborhood of ϕ_{\max} ¹:

$$R(\phi_{\max}) \approx 1 - \frac{2\sqrt{2}}{3\pi} \frac{v(\phi_{\max})v'''(\phi_{\max})}{|v''(\phi_{\max})|^{3/2}}. \quad (5.32)$$

In this regime, the probability of descending into each of the minima ϕ_- and ϕ_+ is similar, giving $|1 - R| \ll 1$. It is possible to start the inflation in the subset of $[\phi_-, \phi_+]$ that would lead to the violation of the slow-roll conditions and tunnel through the potential barrier to the sector dominated by eternal inflation. We further analyze this possibility in Sec. 5.3.2 for a particular effective potential with two vacua, stemming from an asymptotically safe theory. We use Eq. (5.32) to find the dependence of R on the parameters of the theory and compare the result with direct numerical simulation of the Eq (5.11) given set of parameters.

¹For the details of the calculation consult [442].

5.1.3. Starobinski eternal inflation

In 1980 Starobinsky proposed [443] a model where the addition of the R^2 term to the action can cause non-singular evolution of the Universe:

$$S = \frac{1}{2} \int d^4x \sqrt{-g} \left(M_{\text{P}}^2 R + \frac{1}{6M^2} R^2 \right), \quad (5.33)$$

where M is some “mass” parameter. The action (5.33) can be transformed into equivalent linear representation:

$$S_l = \frac{1}{2} \int d^4x \sqrt{-g} \left(\frac{M_{\text{P}}^2}{2} R + \frac{1}{M} R\psi - 3\psi^2 \right), \quad (5.34)$$

with equations of motion for ψ :

$$\frac{1}{M} R = 6\psi,$$

being equivalent to (5.33). Then if we use a following conformal transformation [444]:

$$g_{\mu\nu} \rightarrow e^{-\sqrt{2/3}\phi/M_{\text{P}}} g_{\mu\nu} = \left(1 + \frac{2\psi}{MM_{\text{P}}^2} \right) g_{\mu\nu}, \quad (5.35)$$

we get action with scalar field coupled to gravity:

$$S = \frac{1}{2} \int d^4x \sqrt{-g} \left[\frac{M_{\text{P}}^2}{2} R + \frac{1}{2} \partial_\mu \phi \partial^\mu \phi - V(\phi) \right], \quad (5.36)$$

with the potential given by

$$V(\phi) = V_0 \left(1 - \exp \left(-\sqrt{\frac{2}{3}} \frac{\phi}{M_{\text{P}}} \right) \right)^2. \quad (5.37)$$

The resulting dynamics is almost the same as for the non-minimally coupled scalar field a.k.a. Higgs inflation [445] with $M^2 = \frac{\lambda}{9\xi^2}$. According to Planck data, Starobinski model and its descendants are the main class of models which having correct tensor to scalar ratio and scalar-tilt:

$$n_s - 1 \approx -\frac{2}{N}, \quad r \approx \frac{12}{N^2}, \quad (5.38)$$

with N being the number of e-folds, hence are of high interest. Usually it is assumed that $N \approx 60$, hence:

$$n_s \approx 0.96, \quad r \approx 0.003, \quad (5.39)$$

which are within the range of the 3- σ Planck data [203, 204]. The 60 e-folds corresponds to the initial condition $\phi_0 = 5.5 M_{\text{P}}$. The value $V_0 = 8.12221 \times 10^{-11} M_{\text{P}}^4$ is fixed by (1.84) resulting in $M \simeq 10^{-5}$ [444]. Applying the analytical eternal inflation conditions (5.25, 5.26) to the Starobinski potential, the initial value of the field, above which the eternal inflation occurs, has been estimated to be $\phi_0 = 16.7 M_{\text{P}}$ [30]. It has been found, that decay rate A decreases approximately exponentially with ϕ_0 . The numerical simulation of the Langevin dynamics within a sample of 10000 simulations confirms the analytical prediction.

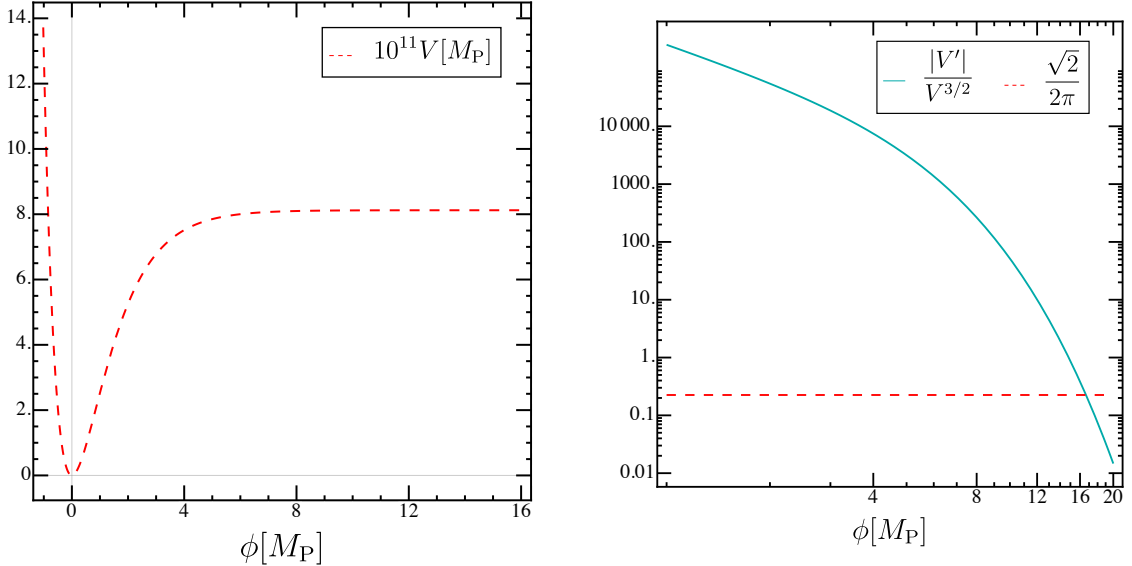


Figure 5.2: Left: The Starobinski potential (5.37).
Right: Eternal inflation condition for Starobinski potential.

5.2. Eternal inflation beyond the Standard Model

5.2.1. Inflation in Conformal Standard Model

After Planck results [203, 204] a wide spectrum of models have been discarded [446], leaving Starobinski model and its descendants together with alpha-attractors² as viable models. To accommodate inflation in the Conformal Standard Model (or other multi-scalar models) [142, 169, 383], see also Sec. 4.2.2, we modify the CSM Lagrangian (4.12) as [10]:

$$\mathcal{L} = \mathcal{L}_{\text{CSM}} - \frac{(M_P^2 + 2\xi_1 H^\dagger H + 2\xi_2 \phi^* \phi)}{2} R, \quad (5.40)$$

with $\xi_i > 0$. We introduce the unitary gauge $H^T = (0, h/\sqrt{2})$ and $\phi = s/\sqrt{2}$ ³. We proceed in the scheme of [445, 447, 448]. Since the calculations in the Jordan and Einstein frames are equivalent [449] we make the following convenient conformal transformation:

$$\tilde{g}_{\mu\nu} = \Omega^2 g_{\mu\nu}, \quad \Omega^2 = 1 + \frac{\xi_1 h^2 + \xi_2 s^2}{M_P^2}. \quad (5.41)$$

In the Einstein frame the scalar part of the Lagrangian is given by

$$\mathcal{L}_E = -\frac{R}{2} + \frac{3}{4} [\partial_\mu \log(\Omega^2)]^2 + \frac{1}{2\Omega^2} [(\partial_\mu h)^2 + (\partial_\mu s)^2] - \frac{1}{\Omega^4} V(h, s). \quad (5.42)$$

We consider the large field values:

$$\xi_1 h^2 + 2\xi_2 s^2 \gg M_P^2 \gg v_i^2, \quad (5.43)$$

²To be discussed in Sec. 5.2.2.

³In the case of [169] we assume that ϕ_{ij} reduces to its trace part and take $\lambda_4 = 0$, for non-zero value of λ_4 study see [10].

Table 5.1: Minimal values of the radial part of inflation potential.

τ_0 values	stable minimum condition	U_0
$\tau_0 = 0$	$a > 0$ and $b < 0$	$\frac{\lambda_1}{4\xi_1^2}$,
$\tau_0 = +\infty$	$a < 0$ and $b > 0$	$\frac{\lambda_p}{4\xi_2^2}$,
$\tau_0 = \pm\sqrt{\frac{b}{a}}$	$a > 0$ and $b > 0$	$\frac{\lambda_1\lambda_2 - \lambda_3^2}{4(\lambda_1\xi_2^2 + \lambda_p\xi_1^2 - 2\lambda_3\xi_1\xi_2)}$,
$\tau = 0$ or $\tau_0 = +\infty$	$a < 0$ and $b < 0$	$\frac{\lambda_1}{4\xi_1^2}$ or $\frac{\lambda_2}{4\xi_2^2}$.

and redefine the fields as:

$$\begin{aligned} \chi &= \sqrt{\frac{3}{2}} \log(\xi_1 h^2 + \xi_2 s^2), \\ \tau &= \frac{h}{s}. \end{aligned} \quad (5.44)$$

The kinetic part of the lagrangian is:

$$\begin{aligned} \mathcal{L}_{\text{kin}} &= \frac{1}{2} \left(1 + \frac{1}{6} \frac{\tau^2 + 1}{\xi_1 \tau^2 + \xi_2} \right) (\partial_\mu \chi)^2 + \frac{1}{\sqrt{6}} \frac{(\xi_2 - \xi_1)\tau}{(\xi_1 \tau^2 + \xi_2)^2} (\partial_\mu \chi)(\partial^\mu \tau) \\ &\quad + \frac{1}{2} \frac{\xi_1^2 \tau^2 + \xi_2^2}{(\xi_1 \tau^2 + \xi_2)^3} (\partial_\mu \tau)^2, \end{aligned} \quad (5.45)$$

furthermore considering the limit (5.43) it reduces to

$$\mathcal{L}_{\text{kin}} \simeq \frac{1}{2} (\partial_\mu \chi)^2 + \frac{1}{2} \frac{\xi_1^2 \tau^2 + \xi_2^2}{(\xi_1 \tau^2 + \xi_2)^3} (\partial_\mu \tau)^2, \quad (5.46)$$

and the potential is given by

$$V_E(\tau, \chi) = U(\tau)W(\chi) = \frac{\lambda_1 \tau^4 + \lambda_2 + 2\lambda_3 \tau^2}{4(\xi_1 \tau^2 + \xi_2)^2} \left(1 + e^{-2\chi/\sqrt{6}} \right)^{-2}. \quad (5.47)$$

Field τ settles in the stable minimum, see Tab. 5.1 and evolution of χ follows. In the case $\xi_i = 0$ for $i \in \{1, 2\}$ the field associated with i 'th coupling decouples [448], which results in $\tau = 0, +\infty$. For $\xi \neq 0$ the τ still settles in the on of the minimas [447, 448], such that

$$m_\tau^2 \gg H^2 \quad (5.48)$$

and the τ field can be integrated out, resulting in the single field χ evolution in the effective potential of the same shape as Starobinski inflation

$$V(\chi) = \frac{\lambda_{\text{eff}}}{4\xi^2} W(\chi), \quad (5.49)$$

with $\xi = \xi_1 \tau_0^2 + \xi_2$ and $\lambda_{\text{eff}} = \lambda_1 + \lambda_2 \tau_0^4 + 2\lambda_3 \tau_0^2$. There are two possibilities. For τ_0 equal to zero or infinity the single inflaton case: Higgs or single “shadow” Higgs inflation. Secondly the multi-inflaton scenario for $\tau_0 = \sqrt{\frac{b}{a}}$. The multi-inflaton scenario to occur requires:

$$\begin{aligned} a &= \lambda_1 \xi_2 - \lambda_3 \xi_1 > 0, \\ b &= \lambda_2 \xi_1 - \lambda_3 \xi_2 > 0, \\ \lambda_1 \lambda_2 - \lambda_3^2 &> 0, \end{aligned} \quad (5.50)$$

where the last one is the vacuum stability requirement, that is not satisfied for the pure Standard Model. The calculation of n_s and r gives the same predictions as the Starobinski model and similar conclusions for the eternal inflation. The amplitude fitting gives

$$\xi \simeq 49000 \sqrt{\lambda_{eff}}, \quad (5.51)$$

our reasoning can also be applied to other models described in Chapter 4.

5.2.2. Alpha-attractors

The α -attractor models are a general class of the inflationary models, initially introduced in the context of supergravity, see [450, 451] and references therein. They are consistent with the Planck CMB data [452], and their preheating phase has been studied on a lattice in [453]. The Lagrangian is given by:

$$\frac{1}{\sqrt{-g}} \mathcal{L}_T = \frac{1}{2} R - \frac{1}{2} \frac{\partial \phi^2}{\left(1 - \frac{\phi^2}{6\alpha}\right)^2} - V(\phi) \quad (5.52)$$

and α can take any real, positive value. At the limit $\alpha \rightarrow \infty$ the scalar field becomes canonically normalized, and the theory coincides with the chaotic inflation. The transformation:

$$\phi = \sqrt{6\alpha} \tanh \frac{\varphi}{\sqrt{6\alpha}}, \quad (5.53)$$

results in the canonical kinetic term and the potential is given by:

$$V(\phi) = \alpha \mu^2 \tanh^{2n} \frac{\varphi}{\sqrt{6\alpha}}, \quad (5.54)$$

where parameter μ is of order 10^{-5} . The shape of the potential for exemplary values of n and α is plotted on figure 5.3. At large field values the potential (5.54) is asymptotically flat, resulting in eternal inflation. The condition (5.25) implies, above certain ϕ_{EI} for all initial values of the ϕ_0 the inflation is eternal, see Fig 5.3. The second eternal condition (5.26) as well as the higher order conditions are satisfied for almost all values of ϕ_0 above 0, providing no new information. This is a generic feature for all of the models we investigate.

For every α , $n = 1$, the ϕ_0 necessary to produce 60 e-folds is safely below ϕ_{EI} . It is shown on Fig. 5.3. We found that the values of ϕ_{EI} change only slightly with n .

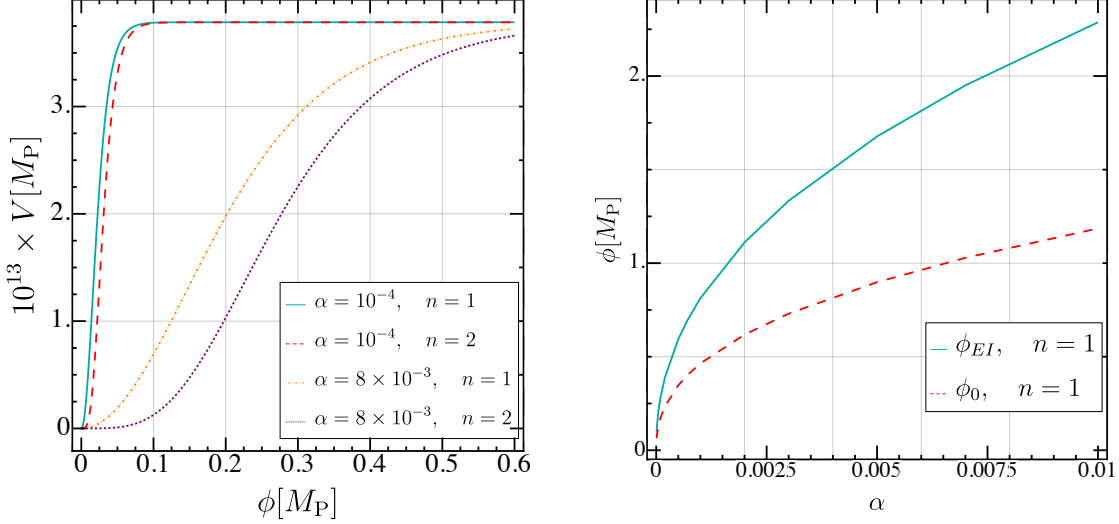


Figure 5.3: Left: the T-model potential with various n and various α were depicted. Right: plot of the initial value ϕ_0 necessary for 60 e-folds, as a function of α , as well as the lowest initial value ϕ_{EI} of the field required for the eternal inflation to occur.

5.3. Can Asymptotically Safe Inflation be eternal?

5.3.1. Renormalisation group improved Starobinski

In this section, we analyze the renormalisation group improvement of the Starobinski action in context of eternal inflation. Action is given by [313, 309]:

$$\mathcal{L}_k = \frac{1}{16\pi g_k} (R - 2\lambda_k k^2) - \beta_k R^2, \quad (5.55)$$

with the running dimensionless couplings g_k , λ_k , β_k being the three relevant directions of the theory, and their running is considered in [313, 454]. By the virtue of the Bianchi identities [309] in the cosmological setting $k^2 \sim R$ is the unique RG improvement. Then the RG-improved quadratic gravity Lagrangian is [313, 309]:

$$S^{\text{eff}} = \frac{1}{2\kappa^2} \int d^4x \sqrt{-g} \left\{ R - 2\tilde{\Lambda} + \frac{R^2}{6m^2} + \tilde{\alpha} R^{3/2} \right\}, \quad (5.56)$$

where κ , $\tilde{\Lambda}$, m are measurable parameters, while $\tilde{\alpha}$ denotes the speed of departure from the non-gaussian fixed point. In the Einstein frame the action is given by

$$V_{\pm} = \frac{m^2 e^{-2\sqrt{\frac{2}{3}}\kappa\phi}}{256\kappa} \left\{ 192(e^{\sqrt{\frac{2}{3}}\kappa\phi} - 1)^2 - 3\alpha^4 + 128\Lambda - \sqrt{32}\alpha \left[(\alpha^2 + 8e^{\sqrt{\frac{2}{3}}\kappa\phi} - 8) \pm \alpha \sqrt{\alpha^2 + 16e^{\sqrt{\frac{2}{3}}\kappa\phi} - 16} \right]^{\frac{3}{2}} - 3\alpha^2(\alpha^2 + 16e^{\sqrt{\frac{2}{3}}\kappa\phi} - 16) \mp 6\alpha^3 \sqrt{\alpha^2 + 16e^{\sqrt{\frac{2}{3}}\kappa\phi} - 16} \right\}, \quad (5.57)$$

with $\Lambda = m^{-2}\tilde{\Lambda}$ and $\alpha = 3\sqrt{3}m\tilde{\alpha}$. The V_0 is the constant part of the potential at infinity $V_0 = V(\phi \rightarrow \infty) = \frac{3m^2}{4\kappa^2}$ and is fixed by the relation (1.84). The α, Λ are free

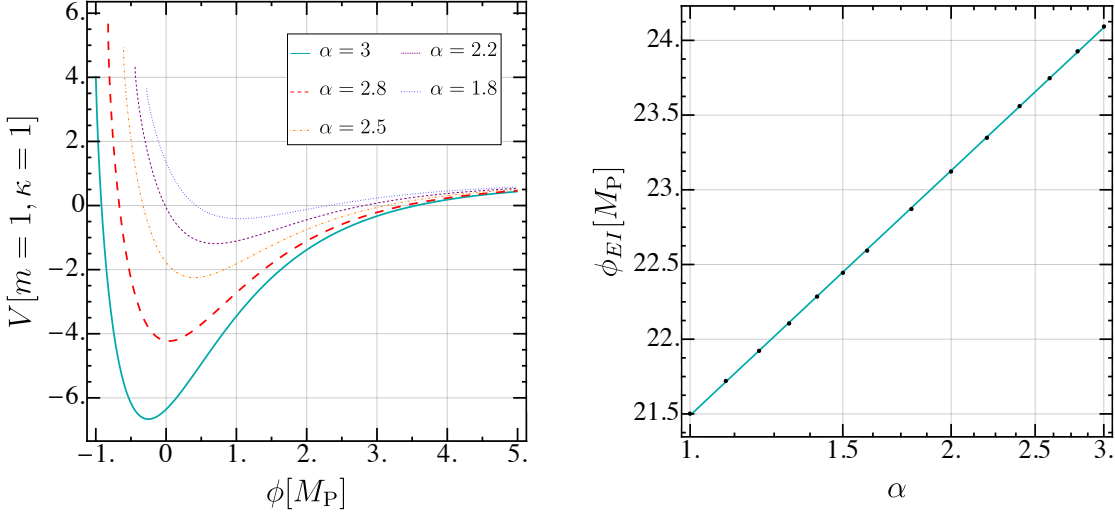


Figure 5.4: RG improved Starobinski and eternal inflation.

Left: $V_+(\phi)$ plot for various α and fixed $\Lambda = 5$.

Right: the logarithmic dependence of initial field value ϕ_{EI} above which eternal inflation occurs on parameter α has been found. Black points were evaluated via the numerical simulation.

parameters, for example, given $\alpha = 2.8$, $\Lambda = 1$ one gets $V_0 = 1.99 \times 10^{-10} M_P^4$ and $m = 2 \times 10^{14}$ GeV. Only the V_+ branch gives minimum required for the reheating to occur. The potential is depicted in the left panel of the Fig. 5.4 for various α . Now we shall investigate the eternal inflation conditions given by (5.25, 5.26). We search for ϕ_{EI} above which the eternal inflation occurs as a function of the theory parameters. First, the initial value above which eternal inflation occurs does not depend on the cosmological constant. Parameter Λ only shifts the minimum of the potential and does not affect the large-field behavior of the system. Secondly, in the large field expansion:

$$V_{\pm}(\phi) = V_{plateau} - 128V_0\alpha e^{-\frac{1}{2}\sqrt{\frac{3}{2}}\phi}, \quad (5.58)$$

and by the substitution $\tilde{\phi} = e^{-\frac{1}{2}\sqrt{\frac{3}{2}}\phi}$ the potential reduces to the linear hilltop model (5.20):

$$V_{\pm}(\phi) = V_{plateau} - 128V_0\alpha\tilde{\phi}, \quad (5.59)$$

justifying the usage of analytical condition (5.25). The behavior is depicted as a straight line on the Log-Linear Plot in the right panel of Fig. 5.4. The numerical simulations confirm these results, and the analytical formulas converge to the Langevin dynamics results. Let us note that the plateau of (5.57) at large field values is a characteristic feature of effective inflationary potentials stemming from the asymptotically safe theories⁴.

⁴Interestingly, eternal inflation has been studied [92] with the Finite Action Principle, which we discuss in Chapter 6. The investigation showed that when inflation becomes eternal, the action diverges, and hence the field configuration resulting in eternal inflation does not enter the amplitude process.

5.3.2. Inflation in the Veneziano limit

In this section, we investigate model in which inflation is driven by an ultraviolet asymptotically safe fixed point without gravity. We consider a $SU(N_C)$ gauge theory, with N_F Dirac fermions interacting with an $N_F \times N_F$ complex scalar matrix H_{ij} , for details we refer to [455, 456, 457]. We consider the Veneziano limit $N_F \rightarrow +\infty$, $N_C \rightarrow +\infty$ taken such that the $\delta = N_F/N_C - 11/2$ becomes a continuous parameter [455, 456, 457]. In this limit the theory possess a non-trivial asymptotically safe fixed point in all the couplings. The inflaton action in Jordan frame has the following form:

$$S_J = \int d^4x \sqrt{-g} \left\{ -\frac{M_P^2 + \xi\phi^2}{2} R + \frac{g^{\mu\nu}}{2} \partial_\mu \phi \partial_\nu \phi - V_{\text{iUVFP}} \right\}, \quad (5.60)$$

where ϕ is the real scalar field along the diagonal of $H_{ij} = \phi \delta_{ij} / \sqrt{2N_f}$. The leading logarithmically resummed potential V_{iUVFP} is given by:

$$V_{\text{iUVFP}}(\phi) = \frac{\lambda_* \phi^4}{4N_f^2 (1 + W(\phi))} \left(\frac{W(\phi)}{W(\mu_0)} \right)^{\frac{18}{13\delta}}, \quad (5.61)$$

where $\lambda_* = \delta \frac{16\pi^2}{19} (\sqrt{20 + 6\sqrt{23}} - \sqrt{23} - 1)$ is positive quartic coupling at the fixed point and $W(\phi)$ is the Lambert function solving the transcendent equation

$$z = W \exp W, \quad (5.62)$$

with

$$z(\mu) = \left(\frac{\mu_0}{\mu} \right)^{\frac{4}{3}\delta\alpha_*} \left(\frac{\alpha_*}{\alpha_0} - 1 \right) \exp \left[\frac{\alpha_*}{\alpha_0} - 1 \right]. \quad (5.63)$$

The parameter $\alpha_* = \frac{26}{57}\delta + O(\delta^2)$ is the gauge coupling at its UV fixed point value and $\alpha_0 = \alpha(\mu_0)$ is the same coupling at the scale μ_0 , where the theory reaches a fixed point scaling. We take $\mu_0 = 10^{-3}M_P$, around the Grand Unification Scale.

We rewrite the action in the Einstein frame with $U = V_{\text{iUVFP}}/\Omega^4$, with $\Omega^2 = (M_P^2 + \xi\phi^2)/M_P^2$ being the conformal transformation of the metric. The potential U is given by:

$$U = \frac{V_{\text{iUVFP}}}{\Omega^4} \approx \frac{\lambda_* \phi^4}{4N_f^2 \left(1 + \frac{\xi\phi^2}{M_P^2} \right)^2} \left(\frac{\phi}{\mu_0} \right)^{-\frac{16}{19}\delta}, \quad (5.64)$$

in the limit $\phi \gg M_P/\sqrt{\xi}$ it reduces to

$$\frac{\lambda_* M_P^4}{4N_f^2 \xi^2} \left(\frac{\phi}{\mu_0} \right)^{-\frac{16}{19}\delta}. \quad (5.65)$$

The potential 5.64 has one local maximum and two minima. The overall height of the potential decreases with increasing N_F, ξ and with decreasing δ , see Fig. 5.5. The region to the left of the maximum is where the inflation can be brought to an end, and the reheating takes place [458]. To the right of the maximum, the inflation becomes classically eternal due to the run-away solution. The potential flattens out for large values of ϕ , and the slow-roll conditions are not violated. Let us now investigate the analytical eternal inflation conditions. Similarly, as in the Starobinsky model,

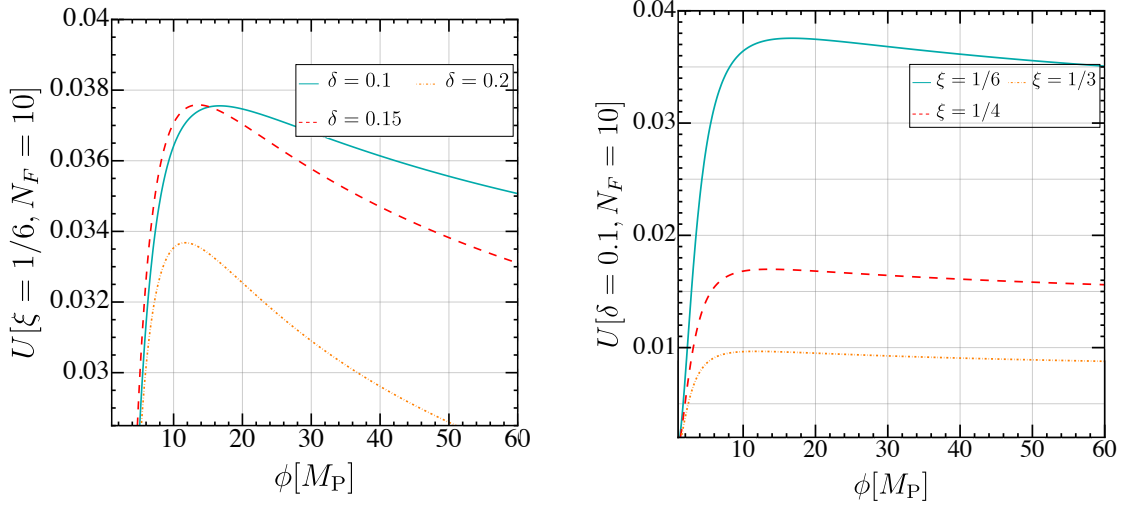


Figure 5.5: Left: the non-minimally coupled potential as a function of ϕ for, $\xi = 1/6$ and $\mu_0 = 10^{-3} M_P$ for various values of δ . For $\delta = 0.1$ there is a maximum at $\phi_{\max} = 16.7 M_P$.

Right: the non-minimally coupled potential as a function of ϕ for, $\delta = 0.1$ and $\mu_0 = 10^{-3} M_P$ for various values of ξ .

the second condition (5.26) is always satisfied. The first condition (5.25) allows for eternal inflation in the close neighbourhood of maximum ϕ_{\max} , since at the maximum one has $V'(\phi_{\max}) = 0$. Nevertheless, numerical solutions to the FP equation show no eternal inflation in that region due to the potential steepness around the maximum. Nevertheless, eternal inflation may still occur due to the quantum tunneling through the potential barrier.

Tunnelling and eternal inflation In general, if a potential has multiple vacua, quantum tunneling through the potential barrier is expected. The non-minimal coupling potential (5.64) belongs in this class. The question is, whether tunnelling from the non-eternal inflation region of $\phi < \phi_{\max}$ to the region of classical eternal inflation $\phi > \phi_{\max}$ is possible.

We start with investigating the fate of the field initially placed at the peak $\phi_0 = \phi_{\max}$ of the potential depicted on figure 5.5. At the maximum of the potential, the steepest descent approximation, cf. Eq. (5.32), may be employed. It is presented in the left panel of Figure 5.6. Due to the complexity of the potential (5.64), its maximum was found numerically and then employed in (5.32). The right panel of Figure 5.6 shows how the maximum changes with parameters. As expected, the ratio $R(\delta, \xi)$ is close to 1 and favours the right-side (left-side) of the potential for large (small) values of the parameters. The biggest ratio emerges at large parameters ξ and δ since the potential is “step-like” and highly asymmetric. It is monotonically decreasing with the values of ϕ_{\max} , for which the potential has a maximum. In order to verify the accuracy of the relation (5.32), we have performed numerical simulation of the discretized Langevin equation (5.28) with initial condition $\phi_0 = \phi_{\max}$. For example it was found, that for the set of the parameters $N_F = 10$, $\mu = 10^{-3} M_{Pl}$, $\xi = \frac{1}{6}$, $\delta = 0.1$ the steepest descent approximation yields $R = 0.92$, and the numerical analysis results in $R = 0.97$, which proves good accuracy of the analytical formula.

One may wonder, how does the probability $p_{\pm}(\phi_0)$ depends on the departure from the

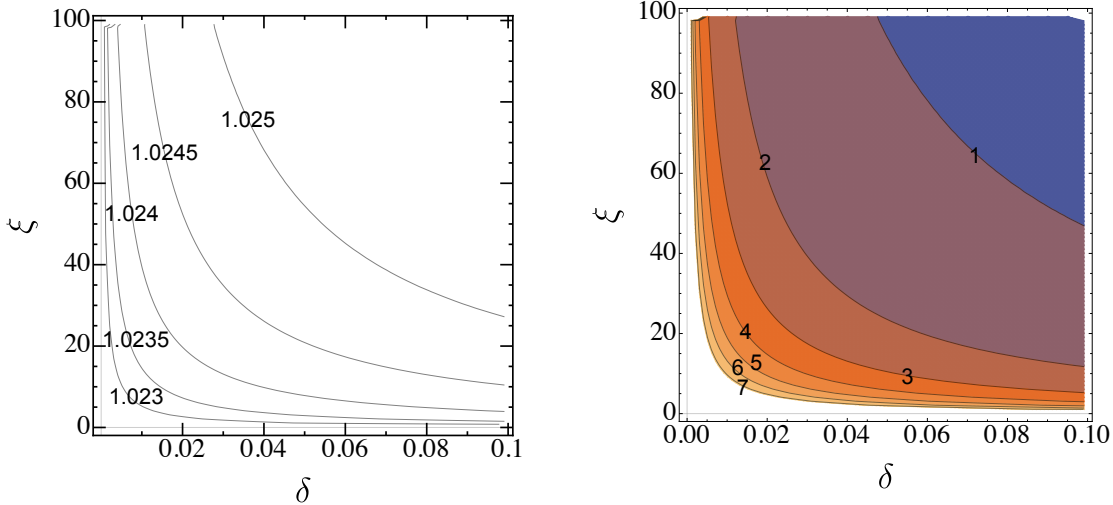


Figure 5.6: Tunnelling in eternal inflation: parameter dependence.

Left: probability ratio $R = \frac{p_+}{p_-}$ of descending from the maximum towards the right minimum (p_+) and the left minimum (p_-), as a function of theory parameters ξ and δ . For the small values of the parameters, it is more probable to fall from the maximum towards $\phi_- = 0$ with non-eternal inflation. In contrast, for the large values of parameters, minimum at $\phi_+ = \infty$ is favored, resulting in an eternally inflating universe.
 Right: the value of the field at which the potential is maximal. The above figures are qualitatively similar because for the small values of ϕ_{\max} , the effective potential is highly asymmetric (“step-like”). This is the origin of asymmetry between right and left descend probability.

maximum $\phi_0 \neq \phi_{\max}$. The analytical answer is given by (5.30). As we have checked numerically, inflation becomes eternal when tunneling probability is non-zero, as depicted in Figure 5.7.

To bypass the numerical calculation of the integral (5.30), we employ the direct numerical simulation of the Langevin equation. However, this time, we do not seek the time evolution of the inflaton. Rather than creating histograms of the count of inflationary events at a given time-step, we simply track the probabilities p_+ and p_- . We say that the particle tunneled through the potential barrier contributing to p_+ if the evolution starts at $\phi_0 < \phi_{\max}$ and proceeds to arbitrarily large field values after a long time. For each point at figure 5.7, the probability has been calculated on the sample of 10000 simulations. As expected, choosing values of ϕ_0 smaller than ϕ_{\max} lowers the probability of the tunneling to the right side of the barrier. Moreover, tunneling probability decreases linearly with the distance to the maximum. The result of the simulation for the set of parameters

$$N_F = 10, \quad \mu = 10^{-3} M_{Pl}, \quad \xi = \frac{1}{6}, \quad \delta = 0.1 \quad (5.66)$$

is shown on figure 5.7. The green line shows the probability of tunneling through the barrier as a function of proximity to the maximum $\phi_0 \neq \phi_{\max}$. The red line shows the probability of rolling towards the minimum at infinity.

The rolling is also a stochastic process, as tunneling in the opposite direction is possible. The probability distribution of tunneling in either direction is not an asymmetric process. Notice, that the initial condition, for which $p_+ = \frac{1}{2}$ is shifted to the right

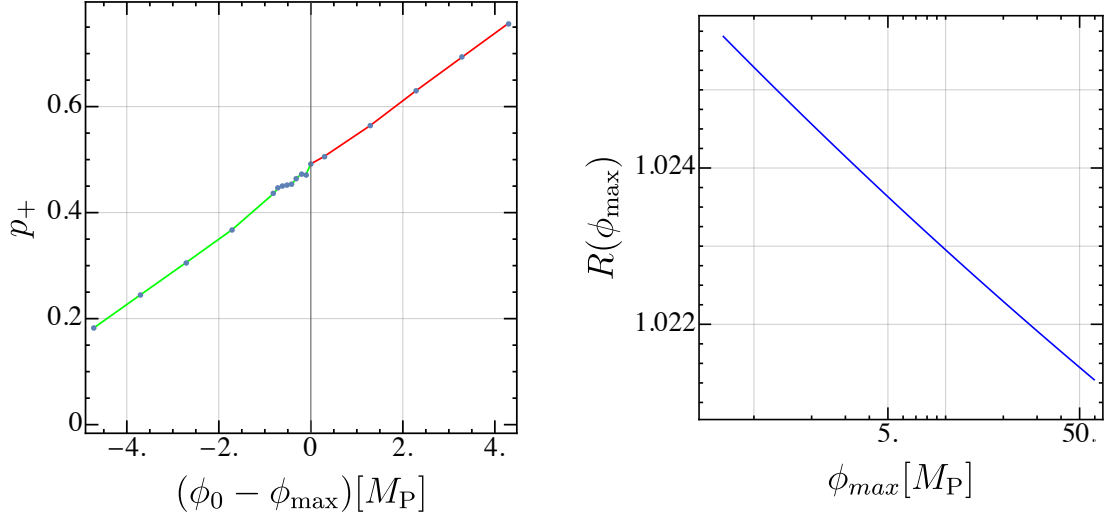


Figure 5.7: Tunnelling in eternal inflation: probabilities.

Left: Linear probability distribution of tunneling (green side) and rolling (red side) towards the minimum at infinity as. The data points have been directly simulated. Right: Probability ratio R , evaluated with (5.32), is a monotonically decreasing with the value of the maximum of the potential in the steepest descent approximation.

of ϕ_{\max} . This means that starting from the maximum; it is slightly more probable to land in ϕ_- . For the set of parameters given by (5.66) there is a field value, below which the field cannot tunnel $p_+ = 0$, at $9.2 M_{Pl}$, and starting from $24.8 M_P$, the $p_- = 0$. Hence, for every initial value of the field above $9.2 M_{Pl}$, there is a non-zero probability of tunneling and hence eternal inflation. On the other hand, for $\phi_0 = 9.2 M_P$ and parameters are given by (5.66), the inflation classically produces roughly 54 e-folds, depending on the reheating time [458], and agrees with CMB data. This shows that the model is on the verge of being eternally inflating, pointing out the interesting phenomenology.

To sum up, the critical point of our analysis is that the analytical conditions (5.25, 5.26) did not allow for eternal inflation and the tunneling process has to be taken into account. This shows that conditions (5.25, 5.26) are not well suited for the multiple minima models and cannot contain the complete information of the global influence of quantum fluctuations in the early universe.

Chapter 6

Finite Action Principle

Where we discuss the implications of the Finite Action Principle (FAP) for the Early Universe dynamics, black holes, and wormholes in the context of Hořava-Lifshyc (H-L) gravity. Assuming the Finite Action Principle, we show that the universe's beginning is flat and homogeneous. Furthermore, we offer that the H-L gravity action selects only the regular black-hole spacetimes since the singular black holes possess infinite action. We also comment on the wormholes in theories with higher curvature invariants.

The path integral

$$Z[J] = \int \mathcal{D}\Phi e^{iS[\Phi]+J\Phi} \quad (6.1)$$

sums over all possible configurations of a field(s) Φ weighted by $e^{iS[\Phi]}$, where $S[\Phi]$ is the classical action of the theory. In the Minkowski path integral, when the classical action approaches infinity, it causes fast oscillations in the path integral and the destructive interference of the neighboring field configurations [33]. In Euclidean, Wick rotated path integral, the field configuration is weighted by $e^{-S[\Phi]}$, and the field(s) configurations on which the action is infinite do not contribute at all. Hence Finite Action Principle (FAP) has been put forward [31], saying that action is the fundamental entity and should be finite. Recently this principle has been applied to quantum gravity understood within the path integral paradigm

$$Z[J] = \int \mathcal{D}g_{\mu\nu} e^{iS[g_{\mu\nu}]+J_{\mu\nu}g^{\mu\nu}}. \quad (6.2)$$

This quantum perspective gave new insight into the cosmological solutions [459, 460], see also Finite Amplitudes Principle [92], black holes [5, 33, 461, 462] and wormholes [5, 12]. As it turned out, once the higher curvature invariants are concerned [459], in the isotropic and flat Universe emerges naturally, and the black hole singularities problem can be solved. Yet it is not known whether considered R^2 term can constitute fundamental action, see discussion in [5, 92], due presence of the particles with the negative mass-squared spectrum, known as *ghosts*, which makes theory non-unitary. It is the consequence of the Ostrogradsky Theorem [67] and the presence of the higher than second-order time derivatives in the terms beyond R in action. Furthermore, in asymptotic safety, one is concerned with the “integrated out” effective action, and so-called reconstruction of the microscopic action constitutes part of the ongoing research within the field [72, 463, 34, 464].

Here we explore another possibility. Namely, we investigate H-L gravity [73], where the Lorentz Invariance (LI) is broken at the fundamental level, see discussion in Sec. 1.2.1. In Sec. 6.1 we show that the Finite Action arguments applied to the H-L gravity result

in isotropic, homogeneous, UV-complete, and ghost-free beginning of the universe. In Sec. 6.2 we demonstrate that the finite action selection principle [33] works for H-L gravity in the context of black-holes (the action is finite for non-singular BH and conversely for the singular). Finally in Sec. 6.3, we discuss the wormhole solutions.

6.1. Cosmological Singularities and Finite Action Principle

Flatness The FLRW metric is given by the formula

$$N \rightarrow N(t), \quad N_i \rightarrow 0, \quad {}^{(3)}g_{ij} \rightarrow a^2(t)\gamma_{ij}, \quad (6.3)$$

where γ_{ij} is a maximally symmetric constant curvature metric, with $k = +1$ for the metric on the sphere, $k = 0$ for flat space time and $k = -1$ for the hyperbolic metric. The relevant quantities are given by

$${}^{(3)}R_{ij} = 2k\gamma_{ij}, \quad {}^{(3)}R = \frac{6k}{a(t)^2}, \quad \mathcal{K} = 3(1 - 3\lambda) \left(\frac{\dot{a}}{a}\right)^2, \quad (6.4)$$

and $N\sqrt{{}^{(3)}g} = Na^3(t)$. For $a(t) = t^s$ the kinetic part of the action (1.23) gives us:

$$N\sqrt{{}^{(3)}g}\mathcal{K} \sim t^{3s-2}, \quad (6.5)$$

since $N\sqrt{{}^{(3)}g}\mathcal{K} \sim t^{-1}$ leads to a logarithmic divergence at $t \rightarrow 0$ after integrating over time, hence the exponent of t in the integrand should be greater than -1 giving $s > 1/3$. In the potential part we have exemplary terms

$$\begin{aligned} N\sqrt{{}^{(3)}g}{}^{(3)}R &\sim kt^s, \\ N\sqrt{{}^{(3)}g}{}^{(3)}R^2 &\sim k^2t^{-s}, \\ N\sqrt{{}^{(3)}g}{}^{(3)}R^3 &\sim k^3t^{-3s}. \end{aligned} \quad (6.6)$$

For $k \neq 0$ equations (6.5, 6.6) give rise to the following set of contradicting inequalities:

$$s > 1/3, \quad s > -1, \quad s < 1, \quad s < 1/3, \quad (6.7)$$

this shows that for $k \neq 0$ in there is the no-FLRW-like beginning of the Universe for the projectable action with potential given by (1.26). This means that in this version of H-L gravity, the Big Bang with power-law time dependence of the scale factor cannot be realized (similar behavior has been observed in [92] for the R^3 gravity). Rejecting the cubic R^3 terms from the potential responsible for the contradictory inequalities yields the action to be finite. None of the anisotropic non-flat solutions are allowed in action with terms cubic in Ricci curvature, as we discuss below.

Anisotropies We consider Bianchi IX metric as a representative model of non-flat anisotropic spacetimes (in this paragraph $k = 1$):

$$ds_{IX}^2 = -N^2dt^2 + h_{ij}\omega^i\omega^j, \quad (6.8)$$

where $h_{ij} = \text{diag}(M^2, Q^2, R^2)$ and M, Q, R are functions of the time only. The connection is

$$d\omega^a = \Gamma_c^a \wedge \omega^c = \Gamma_{cb}^a \omega^b \wedge \omega^c. \quad (6.9)$$

The Bianchi IX one forms satisfy:

$$d\omega^a = \frac{1}{2}\epsilon^{abc}\omega^b \wedge \omega^c, \quad (6.10)$$

hence $\Gamma_{bc}^a = -\frac{1}{2}\epsilon^{abc}$. The usual closed FRLW universe is obtained when $R(t) = M(t) = Q(t) = \frac{a(t)}{2}$, where $a(t)$ is the scale factor. The explicit form of the curvature invariants was calculated in [80]:

$$\begin{aligned} {}^{(3)}R &= \frac{-1}{2M^2Q^2R^2} \left(M^4 + Q^4 + R^4 - (R^2 - Q^2)^2 \right. \\ &\quad \left. - (R^2 - M^2)^2 - (M^2 - Q^2)^2 \right), \end{aligned} \quad (6.11)$$

$$\begin{aligned} {}^{(3)}R_j^i {}^{(3)}R_i^j &= \frac{1}{4(MQR)^4} \left[3M^8 - 4M^6(Q^2 + R^2) \right. \\ &\quad - 4M^2(Q^2 - R^2)^2(Q^2 + R^2) \\ &\quad + 2M^4(Q^2 + R^2)^2 + (Q^2 - R^2)^2(3Q^4) \\ &\quad \left. + (Q^2 - R^2)^2(2Q^2R^2 + 3R^4) \right], \end{aligned} \quad (6.12)$$

$$\begin{aligned} {}^{(3)}R_j^i {}^{(3)}R_k^j {}^{(3)}R_i^k &= \frac{1}{8(MQR)^6} \left([(M^2 - Q^2)^2 - R^4]^3 \right. \\ &\quad + [(M^2 - R^2)^2 - Q^4]^3 \\ &\quad \left. + [(Q^2 - R^2)^2 - M^4]^3 \right). \end{aligned} \quad (6.13)$$

The kinetic and the potential part are respectively:

$$\begin{aligned} N\sqrt{{}^{(3)}g}\mathcal{K} &= \frac{MQR}{N} \left[(1 - \lambda) \left(\frac{\dot{M}^2}{M^2} + \frac{\dot{Q}^2}{Q^2} + \frac{\dot{R}^2}{R^2} \right) \right. \\ &\quad \left. - 2\lambda \left(\frac{\dot{M}\dot{Q}}{MQ} + \frac{\dot{Q}\dot{R}}{QR} + \frac{\dot{M}\dot{R}}{MR} \right) \right], \\ N\sqrt{{}^{(3)}g}V &= -N(MQR)V. \end{aligned} \quad (6.14)$$

For the Bianchi IX metric we use the following ansatz:

$$M(t) \sim t^m, \quad Q(t) \sim t^q, \quad R(t) \sim t^r. \quad (6.15)$$

With such solutions, the kinetic term is proportional to

$$N\sqrt{{}^{(3)}g}\mathcal{K} \sim t^{m+q+r-2}. \quad (6.16)$$

This results in an inequality:

$$m + q + r > 1. \quad (6.17)$$

Similar reasoning is applied to all of the curvature scalars in the potential. Ricci scalar terms lead to conditions:

$$\begin{aligned} 3m - q - r &> -1, & 3q - m - r &> -1, & 3r - m - q &> -1, \\ r + q - m &> 1, & r + m - q &> -1, & m + q - r &> -1. \end{aligned} \quad (6.18)$$

Quadratic terms are numerous and we provide explicit conditions only for the $R_{ij}R^{ij}$ terms:

$$\begin{aligned} 5m - 3q - 3r &> -1, & 3m - q - 3r &> -1, & 3m - 3q - r &> -1, \\ 3r - m - 3q &> -1, & r - m - q &> -1, & q - m - r &> -1, \\ 3q - m - 3r &> -1, & m + q - 3r &> -1, & m - q - r &> -1, \\ m + r - 3q &> -1, & 5q - 3m - 3r &> -1, & 3q - 3 - r &> -1, \\ q + r - 3m &> -1, & 3r - q - 3m &> -1, & -3m - 3q + 5r &> -1. \end{aligned} \quad (6.19)$$

These are such that the kinetic part and scalars up to the quadratic order in curvature do not lead to contradictory conditions [5]. However, including the R^3 term, we have:

$$N\sqrt{(3)g}(3)R^3 \ni \frac{N}{MQR} \sim t^{-m-q-r} \implies m + q + r < 1. \quad (6.20)$$

This is in clear contradiction with (6.17). This means, that also Bianchi IX anisotropic spacetime leads to infinite action. Notice, that taking the isotropic limit $m = q = r$ also leads to infinite action, as discussed in the previous paragraph.

Inhomogeneities Unlike the anisotropies, the finiteness of the action suppresses the inhomogeneities already at the second-order of the spatial Ricci scalar curvature. Investigation of the inhomogeneities concerns following isotropic metric tensor [459]:

$$ds^2 = -dt^2 + \frac{A'^2}{F^2}dr^2 + A^2(d\theta^2 + \sin^2\theta d\phi^2), \quad (6.21)$$

where $A = A(t, r)$, $F = F(r)$ and $A' = \partial_r A$. The homogeneous FRLW metric is retrieved, when $F \rightarrow 1$. The resulting Ricci scalar and Ricci scalar squared contribution to the action are:

$$\sqrt{(3)g}(3)R \sim 2AF' + \frac{A'(-1+F)^2}{F}, \quad (6.22)$$

$$\sqrt{(3)g}(3)R^2 \sim \frac{2AFF' + A'(F^2 - 1)}{A^2A'F}. \quad (6.23)$$

Again, we suppose that each term should be convergent as $t \rightarrow 0$. By the ansatz $A(t) \sim t^s$, inequalities stemming from $(3)R$ and $(3)R^2$ are contradictory. This means that $F(r) \rightarrow 1$, hence the metric of the early universe was homogeneous.

6.2. Black holes and Finite Action Principle

As we have discussed in Chapter 1, it is expected that quantum gravity should resolve the black-hole singularity problem. One may ask which microscopic actions remain finite for non-singular black holes and conversely interfere destructively with the singular ones. This we shall call the Finite Action selection principle. As it turns out, only after the inclusion of higher-curvature operators, beyond the Einstein-Hilbert term, such a selection principle can be satisfied [33].

In this section, we show that H-L gravity satisfies the Finite Action selection principle. We study both the singular solutions of H-L gravity and the known regular black holes spacetimes, yet there are no known regular BH solutions in the H-L gravity. Nevertheless, keep in mind that a metric does not need to be a solution to the equations of motion to enter the path integral.

6.2.1. Singular black holes

First of all, the coordinate singularities of General Relativity may become scalar singularities in the H-L gravity [465]. The spacetime diffeomorphism of GR is a broader symmetry than the foliation-preserving diffeomorphism of H-L gravity. As an example, consider the Schwarzschild black hole, discussed in Sec. 1.1. In GR, the Schwarzschild coordinates (1.8) and Painleve-Gullstrand ones ((1.10)) describe the same spacetime with a singularity at $r = 0$. Notice, however, that the coordinate transformation (1.9) does not preserve the spacetime foliation, breaking the projectability condition. Hence, in the framework of H-L gravity, metric tensors (1.8) and (1.10) describe different spacetimes. Moreover, Schwarzschild's metric singularity at $r = r_s$ becomes a spacetime singularity. Hence due to the nature of the foliation-preserving diffeomorphism, investigating the singularities in H-L gravity is a delicate matter.

Here, we consider representative solutions: the Schwarzschild solution [465] and the H-L solution found by Lu, Mei, and Pope (LMP) [466]. Further solutions have been investigated in [5], including Kerr and the (anti-) de-Sitter Schwarzschild solution¹.

The Schwarzschild solution The most general spherically symmetric, static metric in the Arnowitt-Deser-Misner (ADM) [467] form respecting the projectability condition is given by

$$ds^2 = -dt^2 + e^{2\nu}(dr + e^{\mu-\nu}dt)^2 + r^2d\Omega^2, \quad (6.24)$$

where $\mu = \mu(r)$, $\nu = \nu(r)$. In particular, the Schwarzschild solution is obtained for [465]: $\mu = \frac{1}{2}\ln\left(\frac{M}{r}\right)$, $\nu = 0$.

$${}^{(3)}R = 0, \quad K = 3\left(\frac{3M}{12r^3}\right)^{\frac{1}{2}}, \quad K_{ij}K^{ij} = \frac{81M}{4r^3}. \quad (6.25)$$

To test the Finite Action selection principle we investigate the finiteness of the function:

$$S_s(r_{UV}, r_{IR}) := \int_{r_{UV}}^{r_{IR}} dr N\sqrt{g} (K_{ij}K^{ij} - \lambda K^2 + {}^{(3)}R). \quad (6.26)$$

¹For the (anti-de-Sitter Schwarzschild there is additional cosmological scalar singularity at $r = \left(\frac{3M}{|\Lambda|}\right)^{1/3}$, which cannot be remove by coordinate transformation. This might be an indication that H-L gravity “prefers” positive cosmological constant from the FAP point of view.

The r_{IR} is chosen so that the volume integral is finite. Hence, we do not consider singularities stemming from the spacetime boundary and time integration's IR behavior (large distances). In particular, which we investigate the $r_{UV} \rightarrow 0$ limit. Explicitly we have:

$$S_s(r_{UV}, r_{IR}) \propto (1 - \lambda) \left(\frac{9M}{4} \right) \ln r_{UV} + \text{IR terms.} \quad (6.27)$$

When $\lambda \neq 1$ the singular solution is suppressed in the gravitational path integral. On the other hand, λ is the running parameter [468, 74, 76, 469, 77] and its UV fixed point value is away from $\lambda^* = 1$ indicating that $\lambda \neq 1$ at the regime where curvatures become significant.

In contradistinction to GR, the Schwarzschild metric (1.8) in the usual (orthogonal) frame constitutes a different solution in the H-L gravity. For (1.8) the components of the metric tensor do not depend on the time coordinate. Then the kinetic part vanishes $K_{ij} = 0$. Furthermore the Ricci scalar is ${}^{(3)}R = 0$. However, this time the higher-order curvature terms are divergent at the origin:

$${}^{(3)}R_{ij} {}^{(3)}R^{ij} = \frac{6M^2}{r^6}, \quad {}^{(3)}R_j^i {}^{(3)}R_k^j {}^{(3)}R_i^k = -\frac{6M^3}{r^9}, \quad (6.28)$$

yielding an infinite action and suppressing the singularity. We conclude that both Schwarzschild solutions result in divergent action and do not appear in the path integral.

Kerr spacetime Kerr spacetime corresponds to an axially symmetric, rotating black hole with mass M and angular momentum J . It is a solution to the Einstein Equations in GR. However, it has been shown order by order in the parameter $a = J/M$ that it is not a solution to the H-L field equations [470], nevertheless see [471]. Yet, it can still enter the path integral as an off-shell metric. The line element in the Boyer-Lindquist coordinates is given by:

$$ds^2 = -\frac{\rho^2 \Delta_r}{\Sigma^2} dt^2 + \frac{\rho^2}{\Delta_r} dr^2 + \rho^2 d\theta^2 + \frac{\Sigma^2 \sin^2 \theta}{\rho^2} (d\phi - \xi dt)^2, \quad (6.29)$$

where

$$\rho^2 = r^2 + a^2 \cos^2 \theta, \quad \Delta_r = r^2 + a^2 - 2Mr, \quad \Sigma^2 = (r^2 + a^2)^2 - 2Mr, \quad \xi = \frac{2Mar}{\Sigma^2}. \quad (6.30)$$

We are interested in the singularity on equator plane $\cos \theta = 0$, $r = 0$, described in detail in [460]. For the explicit form of the extrinsic curvature scalars and Ricci scalar refer to [470]. The 3-dimensional Ricci scalar on the $\cos \theta = 0$ plane is:

$${}^{(3)}R = -\frac{2a^2 m^2 (a^2 + 3r^2)^2}{r^4 (r^3 + a^2 (2M + r))^2}, \quad (6.31)$$

and it is singular at $r = 0$. Integrating ${}^{(3)}R$ with the measure $N\sqrt{g} = r^2$ results in the infinite action in the UV limit, and the Kerr spacetime does not contribute the path integral. On the other hand, the 4-dimensional Ricci scalar vanishes in the LI limit $\lambda = 1$, and similar reasoning holds as for the Schwarzschild case. It is then necessary to include the Kretschmann scalar to resolve the singularity as discussed in [33].

6.2.2. Regular black holes

Following [33], we shall discuss Hayward metric [472] and Dymnikova spacetime [473]. The Hayward metric is an example of the regular black hole solution in GR:

$$\begin{aligned} ds^2 &= -f(r)dt^2 + f(r)^{-1}dr^2 + r^2d\Omega^2, \\ f(r) &= 1 - \frac{2Mr^2}{(r^3 + 2g^3)}, \end{aligned} \quad (6.32)$$

where g is an arbitrary positive parameter. The metric is non-singular in $r \rightarrow 0$. It is not a solution to H-L theory, however, we consider it as an off-shell metric present in the path integral.

The kinetic tensor vanishes $K_{ij} = 0$, while the Ricci scalar and the second-order curvature scalars are regular:

$$\begin{aligned} {}^{(3)}R &= \frac{24g^3GM}{(2g^3 + r^3)^2}, \\ {}^{(3)}R_{ij}{}^{(3)}R^{ij} &= \frac{6M^2(32g^6 + r^6)}{(2g^3 + r^3)^4}, \end{aligned} \quad (6.33)$$

leading to finite action. The Dymnikova spacetime is another regular solution in GR. It is constructed with the line element (6.32) with:

$$f(r) = 1 - \frac{2M(r)}{r}, \quad M(r) = M \left(1 - e^{-\frac{r^3}{2g^3}} \right). \quad (6.34)$$

The corresponding curvature scalars are non-singular:

$$\begin{aligned} {}^{(3)}R &= \frac{6M}{g^3}e^{-\frac{r^3}{2g^3}}, \quad {}^{(3)}R_{ij}{}^{(3)}R^{ij} = \frac{3M^2}{2g^6r^6}e^{-\frac{r^3}{g^3}} \left(4g^6 \left(e^{\frac{r^3}{2g^3}} - 1 \right)^2 - 4g^3r^3 \left(e^{\frac{r^3}{2g^3}} - 1 \right) + 9r^6 \right) \end{aligned} \quad (6.35)$$

and the action is finite in the limit $r_{UV} \rightarrow 0$. In particular, in this limit we have ${}^{(3)}R_{ij}{}^{(3)}R^{ij} \rightarrow 12M^2/g^6$.

6.3. Wormholes and Finite Action Principle

Wormholes (WH) constitute another class of interesting solutions of General Relativity, linking disparate spacetime points. The wormholes may be characterized in two classes: traversable and non-traversable. The traversable WH, colloquially speaking, are such that one can go through it to the other side, see [474] for specific conditions. Conversely, the non-transversable cannot be crossed. The pioneering Einstein-Rosen bridge [475] has been found originally as a non-static, non-traversable solution to GR. Within GR, the traversable solutions are unstable. However, they might be stabilized by an exotic matter or inclusion of the higher curvature scalar gravity [476]. This is important in the context of finite action. Usually, the divergences of black holes do appear in the curvature squared terms, yet see [461]. Hence, due to the inclusion of the higher-order terms in the actions, the traversable wormholes are solutions to the equations of motions without the exotic matter. The exemplary wormhole spacetimes investigated here are the Einstein-Rosen bridge proposed in [475], the Morris-Thorne (MT) wormhole [474],

the traversable exponential metric wormhole [477] and the wormhole solution discussed in the H-L gravity [478]. All of them have a finite action. Here, we shall discuss the exponential metric WH. The for the other exemplary wormholes are similar, and we discuss them in the [5, 12]. For the exponential metric WH, the line element is given by:

$$ds^2 = -e^{-\frac{2M}{r}} dt^2 + e^{\frac{2M}{r}} (dr^2 + r^2 d\Omega^2). \quad (6.36)$$

This spacetime consists of two regions: “our universe” with $r > M$ and the “other universe” with $r < M$ and $r = M$ corresponds to the wormhole’s throat. The spatial volume of the “other universe” is infinite when $r \rightarrow 0$. Hence, such volume divergence is irrelevant to our discussion since it describes large distances in the “other universe”. Hence, we further consider only $r \geq M$. The resulting Ricci and Kretschmann scalars calculated in [477] and the measure are non-singular everywhere:

$$\begin{aligned} R &= -\frac{2M^2}{r^4} e^{\frac{-2M}{r}}, \\ R_{\mu\nu\sigma\rho} R^{\mu\nu\sigma\rho} &= \frac{4M^2(12r^2 - 16Mr + 7M^2)}{r^8} e^{-4\frac{M}{r}}, \end{aligned} \quad (6.37)$$

resulting in the finite action for the R^2 gravity. Similarly for the H-L gravity:

$$\begin{aligned} {}^{(3)}R &= R, \quad K^2 = K_{ij}K^{ij} = 0, \\ {}^{(3)}R_{ij} {}^{(3)}R^{ij} &= \frac{2M^2(M^2 - 2Mr + 3r^2)}{r^8} e^{-\frac{4M}{r}}, \end{aligned} \quad (6.38)$$

we get the finite invariants.

Chapter 7

Conclusions, future directions

Where we summarize the results on the Beyond Standard Model Physics and beyond the Λ -CDM physics from the quantum gravity perspective. We give an outlook on our results.

7.1. Conclusions

Beyond the Standard Model, physics is a vast subject. A plethora of models have been proposed, to mention grand unified theories, supersymmetry, and scale / conformal invariant models¹. Most of the Standard Model extensions propose the introduction of new particles and interactions. However, we cannot predict the free parameters of these models theoretically. So, for example, the masses of particles might be arbitrary, much too big for us to measure them in particle accelerators.

On the other hand, the amount of inflationary models quickly inflates². Furthermore, some of those models have enough free parameters that they are compatible with any measurement of n_s , A_s , A_t and r [479]. There is also quite a few models that are an alternative to inflation. Those such as string gas cosmology [480], slow contraction cosmology [481], or Conformal Cyclic Cosmology (CCC) [482].

The main idea of the research presented in this thesis is *it is not only challenging to quantize gravity, but it is also challenging to combine matter with gravity*. This notion is heavily utilized in string theory in the swampland program. However, the idea of the compatibility of gravity with QFT is not unique to string theory. In the thesis, we have mainly adopted two perspectives: the asymptotic safety one in Chapter 5 and Chapter 4 and the cross-approaches one, utilizing basic features of quantum gravity, in Chapter 3 and Chapter 6. Furthermore, we have studied the Finite Action Principle in H-L gravity to see whether the predictions for the higher derivative gravities carry over to the theory where the Lorentz symmetry is broken. We showed that string theory fulfills the AS requirements. We also discussed the criteria to be fulfilled for well-defined AS amplitudes. In other words, in this thesis, we have shown that quantum gravity can narrow down the possible space of models' parameters and the cosmological evolution. Conversely, the quantum gravity models are significantly constrained by the connection with the matter.

¹The scale /conformal invariance has to be broken at some scale, but one usually assumes that it is broken “softly” [171].

²The amount of articles with inflation in the title is estimated to be $N_{infl} \approx 4000$ in 2013 [479]. From that time, the number has significantly increased. We also have contributed to that number.

For the Grand Unified Theories in Chapter 3, we have shown that the requirement of stability of the potential at the Planck scale, absence of Landau poles constrains possible microscopic dynamics. To investigate the broken potential minima, we have calculated the beta functions for model c.f. App. C.1 as well as introduced a new method to calculate the effective potential and calculate it, c.f. App. A. The resulting deepest minima in the considered model are either non-SM-like or require large threshold corrections for the model to reconcile with the running of the gauge couplings and the proton stability bound. In particular, as we have discussed in Sec. 4.1, the microscopic dynamics stemming from asymptotic safety does not satisfy those criteria (under the discussed assumptions) and result in “transplanckian” breaking and proton stability, such that the two scales remain: Planck and electroweak one.

Furthermore, the broken phases of global and local symmetries result in the domain wall evolution. In this thesis, we have investigated the longevity of the domain walls depending on the initial conditions and the shape of potential. We found that two dominant factors are the mean of the initial field distribution and the bias between the minima. Yet, those initial conditions and the shape of potential for the cosmological evolution cannot be deduced from the dynamics of domain walls by itself and must be derived from a model of the evolution of the early Universe. Hence, our results can also be thought of as a further constraint on the microscopic dynamics.

We discussed the Higgs mass prediction in the Standard Model and beyond within the asymptotic safety paradigm. We pointed out that the prediction is roughly 5 GeV up from the experimental value within the Standard Model. Hence, we discussed the extensions such that the correct mass is predicted. We've shown that the inclusion of the Abelian gauge group with a massive boson can result in an accurate prediction. Finally, we have explored the Weak Gravity Bound in systems with more than one gauge field for the first time to discover whether systems with 12 gauge fields (like the Standard Model) exhibit a weak-gravity bound and whether the gravitational fixed point evades it. Further, we have tested the robustness of the present and previous results on the Weak Gravity bound by exploring their dependence on a gravitational gauge parameter.

In the cosmological part of the thesis, we have discussed two principles:

- (i) No eternal inflation principle,
- (ii) Finite Action Principle.

The first one stems from the string theory considerations and the de-Sitter conjecture. In this thesis, we have investigated whether a similar principle holds in the asymptotically safe paradigm. As we found out generically, the existence of an asymptotically safe fixed point flattens the potential for large field values, where eternal inflation is inevitable. We illustrated this viewpoint by calculating RG-improved Starobinski inflation and the Yang-Mills theory in the Veneziano limit. We showed that tunneling to the false vacua might also be a source of eternal inflation, which is not usually discussed. Furthermore, we've introduced an inflationary dynamics for the Conformal Standard Model that matches the current data.

In Chapter 6, we have discussed the consequences of the Finite Action Principle in the framework of H-L gravity. Following this principle, we show that the beginning of the Universe is flat and homogeneous when approaching the initial singularity. Furthermore, we show that the H-L gravity action selects only the regular black-hole space-times since the singular black holes possess infinite action. The H-L gravity, therefore,

satisfies the selection principle proposed in [33]. We also comment on the wormhole solutions being an attractive alternative to black holes in light of this principle. Similar conclusions can be drawn for the higher derivative gravity. Yet, due to ghost states in the theory, the path integral might be not well defined; see discussion in [92]. For possible resolutions of the ghost issue, see discussion in [5] and references therein.

We have also argued that contemporary particle physics and cosmology problems can “find answers” combined with quantum gravity. This might be the case of the Landau pole in the U(1) sector, discussed in Sec. 2.2, the strong CP problem in Sec. 4.2.3 and initial conditions for inflation in Chapter 6.

Finally, we have discussed the asymptotic safety program and its caveats in Chapter 2. We discussed the Wilsonian renormalization approach on the exactly solvable $1/r^2$ model. We proposed three criteria that asymptotically safe amplitudes should satisfy to constitute a UV fundamental theory. We have illustrated our viewpoint with string theory amplitude.

All in all, our results demonstrate that while various approaches stem from different philosophies and rely on different model building, some results are quantum gravity model-independent (Finite Action Principle, viable not fine-tuned non-SUSY GUT breakings). The other, such as the No-Eternal Inflation Principle, proton stability, and Higgs mass prediction models, are specific for string theory and asymptotic safety.

7.2. Outlook

Is that the end? Quite the opposite this the beginning! Much of the work presented here is about sharpening the tools used in further work. In favor of concreteness, let us present projects we are currently undertaking.

(i) Quantum gravity and baryon asymmetry In the Early Universe, matter dominance over antimatter cannot be explained in the Standard Model. The successful baryogenesis at the GUT scale is usually considered one of the arguments favoring GUTs. However, asymptotic safety indicates that “transplanckian” breaking might occur and thus spoiling this mechanism as well. On the other hand, models, such as Conformal Standard Model, are naturally supplemented with the mechanism which can create such asymmetry. This mechanism is called resonant leptogenesis [483]. Since sterile scalar ϕ has a non-vanishing vacuum expectation value, the lepton number symmetry L of the Conformal Standard Model is spontaneously broken. This property allows us to explain the amount of CP violation, which is too small in the Standard Model, to provide the observed baryon to photon ratio. In [383] the authors describe how the Conformal Standard Model can provide the desired baryon asymmetry via resonant leptogenesis scenario [483]. This provides non-trivial sets of constraints on the investigated model that can be combined with the requirements stemming from asymptotic safety.

Together with the authors of [383] we are planning to study the Standard Model extended by new U(1) symmetry. We will check whether the constraints on the Higgs mass stemming from AS and those resulting from successful leptogenesis form a non-empty parameter space.

(ii) Unified quantum gravity The research program we have started in [3] has various possible developments. One is to extend the programme towards the realistic

models such as $\mathbf{10}_H \oplus \mathbf{126}_H \oplus \mathbf{45}_H$ or $\mathbf{10}_H \oplus \mathbf{126}_H \oplus \mathbf{54}_H$ and also include the models containing supersymmetry. Another possible development is to explicitly calculate the higher-order $1/M_P^2$ contributions to the GUT models stemming from quantum gravity and check their influence on the parameter space. Finally, both string theory and asymptotic safety give specific predictions on the values on the scalar couplings. In the case of AS, it may seem that the GUTs with representations not coupled to the Yukawa sector enjoy the “transplanckian” breaking, yet to confirm it, we have to perform the calculation within the FRG setting, taking into account the higher-order operators. Finally in the non-supersymmetric, non-tachyonic $SO(16) \times SO(16)$ string theory model, the $SO(10)$ with $\mathbf{45}_H$ is realized in the compactification to 4 dimensions [484].

(iii) Towards the non-perturbative quantum gravity cosmology Recently the de-Sitter conjecture has been under scrutiny. Yet, the swampland research still lacks non-perturbative methods that would allow for the transformation of hypotheses into mathematical evidence.

Potentially the symmetries and dualities (symmetries between two different theories) can provide such methods. In the cosmological context, their practical implementation is the symmetry $O(d, d)$ proposed by Meissner and Veneziano in a series of works [68, 103]. The $O(d, d)$ symmetry considerations classifies the α' corrections for purely time-dependent (cosmological) backgrounds and the non-perturbative solutions featuring string-frame de Sitter vacua can be constructed [102, 101]. Furthermore, the un-truncated action can be studied with the Functional Renormalization Group techniques [485, 486, 487]. The tentative results indicate absence of de-Sitter vacua in string theory [485, 486, 487].

In our work, we plan to check under what general assumptions the de-Sitter solutions can be constructed and whether they can be realized dynamically. We are also planning to apply the same reasoning as [101, 102], based on other space-time (and field configurations) such as non-planar FLRW spacetime, BKL singularity, or D-dimensional black hole. The existence of $O(d, d)$ symmetry to all orders in string corrections allows for a complete understanding of the string theory in a given range, thus allowing for confirmation or refutation of the existing criteria related to the swampland. This symmetry will also allow for a complete description of the Hartle-Hawking state (previously described semi-classically) or alternative cosmologies to the theory of inflation.

Appendices

A. Effective potential and the breaking scale

This section is taken from [3] and only slightly modified. This has been done with the other author's consent.

A.1. Renormalisation group-improved 1-loop potential

In Chapter 3 we are interested in the radiative minima of the potential generated due to the renormalization group flow of the quartic couplings. Hence the renormalization group equations (RGEs) constitute the principal tool in our analysis. The schematic form of the one-loop RGEs are given in the seminal papers [380, 488, 489], see also the recent discussion [490, 491].

In the absence of mass terms in the tree-level potential, any nontrivial minimum must be generated by higher-order corrections to the scalar potential. The dependence of loop corrections on the arbitrary renormalization scale can be alleviated using techniques of RG-improvement of the scalar potential. Such techniques generally allow a better approximation of the all-order quantum potential already in the one-loop truncation. For these reasons, we have used in this work the RG-improved 1-loop potential to study the breaking patterns of a GUT model in a formalism that we now briefly review.

Considering a gauge theory with a scalar multiplet noted ϕ , and using the conventions of [305], the one-loop contributions to the effective potential can be put in the form

$$V^{(1)} = \mathbb{A} + \mathbb{B} \log \frac{\varphi^2}{\mu_0^2} \quad (\text{A.1})$$

where μ_0 is the arbitrary renormalisation scale and where $\varphi = \sqrt{\phi_i \phi^i}$. The quantities \mathbb{A} and \mathbb{B} receive contributions from the scalar, gauge and Yukawa sectors of the theory. In the $\overline{\text{MS}}$ scheme and working in the Landau gauge, they may be expressed as

$$\mathbb{A} = \frac{1}{64\pi^2} \sum_{i=s,g,f} n_i \text{Tr} \left[M_i^4 \left(\log \frac{M_i^2}{\varphi^2} - C_i \right) \right], \quad (\text{A.2})$$

$$\mathbb{B} = \frac{1}{64\pi^2} \sum_{i=s,g,f} n_i \text{Tr} (M_i^4). \quad (\text{A.3})$$

where the numerical constants n_i and C_i take the values

$$\begin{aligned} n_s &= 1, & n_g &= 3, & n_f &= -2, \\ C_s &= \frac{3}{2}, & C_g &= \frac{5}{6}, & C_f &= \frac{3}{2}, \end{aligned} \quad (\text{A.4})$$

and where $M_{s,g,f}$ respectively stand for the field-dependent mass matrices of the scalars, gauge bosons and fermions of the model. The first two matrices can be straightforwardly computed once the scalar potential and the gauge generators of the scalar representations have been fixed:

$$(M_s^2)_{ij} = \frac{\partial^2 V^{(0)}}{\partial \phi^i \partial \phi^j} \quad (\text{A.5})$$

$$(M_g^2)_{AB} = g^2 \{T_A, T_B\}_{ij} \phi^i \phi^j \quad (\text{A.6})$$

The $\mathbf{16}_H \oplus \mathbf{45}_H$ sector of the model considered in this work contains no Yukawa interactions; hence the M_f mass matrix will be taken to vanish.

The dependence of $V^{(1)}$ on the renormalization scale μ_0 is an artifact of working at fixed order in perturbation theory and introduces arbitrariness in the computations. In some circumstances, simple prescriptions on the value of μ_0 may be appropriate for computations involving the quantum potential. Such prescriptions are particularly suitable for single-scale models, thus giving a reasonable approximation of the effective potential around this one scale. For computations involving a more comprehensive range of energy scales, or in theories with multiple characteristic scales (*e.g.* several vevs, possibly spanning over orders of magnitude), one inevitably encounters large logarithms indicating the breakdown of perturbation theory. Various renormalization group techniques were developed to resum those large logarithms, yielding a well-behaved quantum potential over large energy ranges. Such a procedure is generally referred to as renormalization group improvement of the scalar potential.

The SO(10) model considered in this work (and generally any GUT model) enters the category of multi-scale theories, requiring an appropriate procedure of RG-improvement. Here we briefly review the method developed in [305] and further extended in [492] in the case of classically scale-invariant potentials. The starting point is to consider the Callan-Symanzik equation satisfied by the all-order quantum potential, stating that the total derivative of the effective potential concerning the renormalization scale vanishes:

$$\frac{dV^{\text{eff}}}{d \log \mu_0} = \left(\frac{\partial}{\partial \log \mu_0} + \sum_i \beta(g_i) \frac{\partial}{\partial g_i} - \phi^i \gamma^{ij} \frac{\partial}{\partial \phi^j} \right) V^{\text{eff}} = 0. \quad (\text{A.7})$$

The above relation describes the invariance of the quantum potential on the renormalisation scale, given that the couplings of the theory are evolved according to their β -functions, and the field strength renormalisation values according to their anomalous dimension matrix γ . Following [305, 492] and using (A.7), we may simultaneously promote the RG-scale μ_0 to a field-dependent quantity $\mu(\phi^i)$, and the couplings and fields to μ -dependent quantities. Formally, we have

$$\begin{aligned} \mu_0 &\longrightarrow \mu(\phi^i), \\ \lambda &\longrightarrow \lambda(\mu(\phi^i)), \\ \phi &\longrightarrow \phi(\mu(\phi^i)). \end{aligned} \quad (\text{A.8})$$

The cornerstone of the RG-improvement procedure presented in [305] is to note that for each point in the field space, and as long as perturbation theory holds, there exists a renormalization scale μ_* such that the one-loop corrections $V^{(1)}$ vanish³:

$$V^{(1)}(\phi^i, \lambda^i; \mu_*) = \mathbb{A}(\phi^i(\mu_*), \lambda^i(\mu_*)) + \mathbb{B}(\phi^i(\mu_*), \lambda^i(\mu_*)) \log \frac{\varphi^2}{\mu_*^2} = 0. \quad (\text{A.9})$$

³In presence of negative eigenvalues in the mass matrices, one may instead require the real part of the one-loop corrections to vanish.

The above relation gives the implicit definition of the field-dependent scale $\mu_*(\phi^i)$, and is shown in [305] to allow for a proper treatment of large logarithms. Going on, the full 1-loop effective potential is simply given by its tree-level contribution, with the couplings and fields evaluated at the scale μ_* :

$$V^{\text{eff}}(\phi^i) = V^{(0)}(\phi^i; \mu_*(\phi^i)) . \quad (\text{A.10})$$

That the RG-improved effective potential takes its tree-level form provides valuable insight on the conditions of radiative symmetry breaking in classically scale-invariant models [305, 493, 492]. In particular, a necessary condition for symmetry breaking is that the scalar potential's tree-level stability conditions must be violated at some scale along with the RG flow. As illustrated in the next sections, this observation crucially allows us to determine whether the breaking of the SO(10) symmetry towards a specific subgroup will happen at all, given some initial conditions for the quartic couplings at the initial scale.

A.2. Minimisation of the RG-improved potential

To identify the breaking patterns of the model, one needs to evaluate the depth of the RG-improved potential at the minimum for each relevant vacuum configuration. The set of stationary point equations of the RG-improved potential, in principle, need to be solved numerically to determine the position of its global minimum. However, such a numerical minimization procedure can be computationally costly and therefore rather inappropriate in this work, where a scan over a large number of points is to be performed. Instead, we propose in this section a simple procedure allowing to estimate (somewhat accurately) the position and depth of the minimum of the RG-improved potential. In [3], we derive the radial stationary point equation satisfied by the RG-improved potential at a minimum, in the $\mathcal{O}(\hbar)$ approximation:

$$4V^{\text{eff}} + 2\mathbb{B} = 0, \quad \frac{d\mathbb{A}}{dt} \approx 0 \quad \text{and} \quad \frac{d\mathbb{B}}{dt} \approx 0 . \quad (\text{A.11})$$

The quantity \mathbb{B} must be strictly positive at a minimum, thus implying

$$V^{\text{eff}} < 0 . \quad (\text{A.12})$$

Recalling that for all field values, V^{eff} takes its classically scale invariant tree-level form, this means in turn that the tree-level stability conditions must not hold at the RG-scale μ_*^{\min} , defined such that

$$\frac{\partial V^{\text{eff}}}{\partial \langle \phi \rangle^i} \left(\langle \phi \rangle^i; \mu_*^{\min}(\langle \phi \rangle^i) \right) = 0 \quad \text{and} \quad V^{(1)} \left(\langle \phi \rangle^i; \mu_*^{\min}(\langle \phi \rangle^i) \right) = 0 . \quad (\text{A.13})$$

More concretely, μ_*^{\min} is the value of the RG-improved scale μ_* evaluated at the vacuum $\langle \phi \rangle$. Letting μ_0 be some arbitrary high scale at which the tree-level potential is assumed to be stable, one can identify a scale μ_{GW} characterising the breaking of tree-level stability, such that

$$\mu_*^{\min} < \mu_{\text{GW}} < \mu_0 . \quad (\text{A.14})$$

Hence at the RG-scale μ_{GW} the tree-level potential (without RG-improvement) develops flat directions, along which a minimum will be radiatively generated through the Gildener-Weinberg mechanism [494]. A first important observation is that μ_{GW} gives

an upper bound on the value of μ_* at the minimum, as well as a rough estimate of it. This bound may be further refined observing that an additional scale $\tilde{\mu}$ can be identified, at which the quantity $\tilde{V}^{(0)}$ defined as

$$\tilde{V}^{(0)} \equiv V^{\text{eff}} + \frac{1}{2}\mathbb{B} \quad (\text{A.15})$$

develops flat directions, see [3]. Since $\mathbb{B} > 0$ near the minimum, one has

$$\mu_*^{\min} < \tilde{\mu} < \mu_{\text{GW}}, \quad (\text{A.16})$$

so $\tilde{\mu}$ provides an improved upper bound for μ_*^{\min} . In practice, the former scale provides in most cases a remarkably accurate estimation of μ_*^{\min} , for reasons detailed and exemplified in [3]. Based on this observation, we have used for the present analysis a simplified procedure to identify and characterize the minima of RG-improved potentials in an algorithmic, fast, and efficient way — the only other alternative being the minimization via numerical methods, increasingly costly for vacuum structure with many vevs. For a given vacuum configuration, this minimization procedure may be summarised as follows:

1. Starting with random values for the quartic couplings at some large scale μ_0 , the stability of the tree-level potential is asserted, and unstable configurations are discarded.
2. Evolution of the quartic couplings according to their RG running is performed down to some lower scale μ_1 . A natural choice for this scale is $\mu_1 \approx 10^{11} \text{ GeV}$, where the gauge coupling usually runs into a Landau pole⁴.
3. The scale $\tilde{\mu}$ at which $\tilde{V}^{(0)}$ develops flat directions is identified. To determine it in practice, one only needs to assert the tree-level stability conditions at each integration step over the considered energy range.
4. At the scale $\tilde{\mu}$, depending on the considered vacuum structure, the flat direction \vec{n} is identified. Along this flat direction, the field values take the form

$$\phi = \varphi \vec{n} \quad (\text{A.17})$$

5. The unique value of $\langle \varphi \rangle$ such that

$$V^{(1)}(\langle \varphi \rangle \vec{n}; \tilde{\mu}) = 0 \quad (\text{A.18})$$

is identified. The field vector $\langle \phi \rangle = \langle \varphi \rangle \vec{n}$ constitutes an estimation of the exact position of the minimum.

6. Finally, the depth of the RG-improved potential at the minimum, *i.e.* the quantity

$$V^{\text{eff}}(\langle \phi \rangle) = V^{(0)}(\langle \phi \rangle; \tilde{\mu}) \quad (\text{A.19})$$

is evaluated.

⁴The precise value of μ_1 is anyways rather arbitrary since in practice one observes either the breakdown of SO(10) or the occurrence of Landau poles along the way from μ_0 to μ_1 .

In this form, the above procedure is essentially equivalent to a Gildener-Weinberg minimization (see [494] and [3]). However, as explained in [3], it can be straightforwardly extended to include $\mathcal{O}(\hbar^2)$ corrections characteristic of the 1-loop RG-improvement procedure. From an algorithmic point of view, our method proves remarkably more efficient, particularly for multidimensional vacuum structures. The reason behind this is rather simple: Here, one avoids the numerical minimization of a multivariate function, whose evaluation at a point $\phi \in \mathbb{R}^N$ is itself rather costly (evaluating the potential at some given field values involves a root-finding algorithm to determine the RG-improved scale μ_*). Instead, two 1-dimensional numerical scans are performed, respectively, to find the value of $\tilde{\mu}$ at step 3, then the value of $\langle\varphi\rangle$ at step 5.

A.3. Breaking patterns triggered by the RG-flow

As stated above, the spontaneous breakdown of $\text{SO}(10)$ — *i.e.* the occurrence of a non-trivial minimum of the RG-improved potential — is triggered around the RG-scale at which the tree-level potential turns unstable. While the knowledge of necessary stability conditions allows discarding points from the parameter space for which the scalar potential is unstable, the determination of the breaking patterns of the considered model requires additional information. In particular, given some vacuum manifold, there are several qualitatively different ways of violating the stability conditions. When the RG-improved potential develops a nontrivial minimum, the resulting symmetry breaking pattern depends on how the stability conditions get violated along with the RG flow. More precisely, the set of stability conditions for a given vacuum structure can, in general, be expressed as the conjunction of n individual constraints:

$$S = S_1 \wedge \cdots \wedge S_n. \quad (\text{A.20})$$

Defining \bar{S} as the condition of an unstable potential, one clearly has

$$\bar{S} = \bar{S}_1 \vee \cdots \vee \bar{S}_n, \quad (\text{A.21})$$

and therefore the violation of any one of the S_i will trigger spontaneous symmetry breaking, in general towards different subgroups of original symmetry group. To illustrate this rather general statement, let us consider a concrete example. Namely, for the $\mathbf{16}_H \oplus \mathbf{45}_H$ $\text{SO}(10)$ model considered in the next section, a possible vacuum configuration leading to a $\text{SU}(5)$ breaking is obtained as

$$\langle V \rangle_{\text{SU}(5)} = \left(\lambda_1 + \frac{13}{20} \lambda_2 \right) \omega^4 + \left(2\lambda_8 + \frac{5}{2} \lambda_9 \right) \omega^2 \chi^2 + \lambda_6 \chi^4, \quad (\text{A.22})$$

and matches the definition of a general 2-vev vacuum manifold given in [3]. Directly using the results from this appendix, we derive the following tree-level stability conditions:

$$S_1 : \lambda_1 + \frac{13}{20} \lambda_2 > 0, \quad (\text{A.23})$$

$$S_2 : \lambda_6 > 0, \quad (\text{A.24})$$

$$S_3 : 2\lambda_8 + \frac{5}{2} \lambda_9 + 2\sqrt{\lambda_6 \left(\lambda_1 + \frac{13}{20} \lambda_2 \right)} > 0. \quad (\text{A.25})$$

With these definitions at hand, the sufficient and necessary stability condition for this vacuum manifold is given by

$$S = S_1 \wedge S_2 \wedge S_3. \quad (\text{A.26})$$

We note that (A.26) constitutes a set of necessary conditions for the stability of the full SO(10) potential. Starting at a RG-scale μ_0 were S is satisfied, spontaneous symmetry breaking will occur around the scale $\mu_{\text{GW}} < \mu_0$ at which any one of the S_i gets violated. This can happen in three distinct ways, generating in each case different vacuum configurations along the flat directions appearing at μ_{GW} :

$$\bar{S}_1 : \lambda_1(\mu_{\text{GW}}) + \frac{13}{20}\lambda_2(\mu_{\text{GW}}) = 0 \quad \rightarrow (\omega, \chi) = (\langle \omega \rangle, 0) \quad (\text{A.27})$$

$$\bar{S}_2 : \lambda_6(\mu_{\text{GW}}) = 0 \quad \rightarrow (\omega, \chi) = (0, \langle \chi \rangle) \quad (\text{A.28})$$

$$\bar{S}_3 : \left[2\lambda_8 + \frac{5}{2}\lambda_9 + 2\sqrt{\lambda_6 \left(\lambda_1 + \frac{13}{20}\lambda_2 \right)} \right] (\mu_{\text{GW}}) = 0 \quad \rightarrow (\omega, \chi) = (\langle \omega \rangle, \lambda \langle \omega \rangle) \quad (\text{A.29})$$

Finally, the residual symmetry group can be determined for each vacuum configuration based on group theoretical arguments. Here, \bar{S}_2 and \bar{S}_3 do generate a SU(5) minimum, although in the former case ω vanishes. In contrast, the minimum associated with \bar{S}_1 preserves an additional U(1) gauge factor, so the residual symmetry group is $\text{SU}(5) \times \text{U}(1)$.

The above example shows how to determine the residual gauge symmetry associated with a flat direction of the tree-level potential in a specific vacuum configuration. In addition, one must determine the location and depth of the minimum of the effective potential. For this purpose, the procedure described in the previous section can be used in practice, allowing to estimate the position and depth of the minimum based on the study of the flat directions of \tilde{V}_0 . Such a procedure is reiterated for every relevant vacuum configuration to identify the deepest minimum. The corresponding residual symmetry gives the only allowed breaking pattern among the various subgroups initially identified.

B. $SO(10)$ appendix

B.1. Conventions

Spinor conventions:

$$S_{ij} = \frac{1}{4\sqrt{2}i} [\Gamma_i, \Gamma_j] = \frac{1}{2\sqrt{2}} \begin{pmatrix} \sigma_{ij} & 0 \\ 0 & \tilde{\sigma}_{ij} \end{pmatrix} \quad (\text{B.30})$$

Note that the additional $\sqrt{2}$ factor allows to match the convention where the Dynkin index of the 16 equals 2 (as compared to 4 in LDL and some other works in the literature).

- 32-dimensional spinor: Ξ
- 32-dimensional projected spinors:

$$\chi_+ = P_+ \Xi = \begin{pmatrix} \chi \\ 0 \end{pmatrix}, \quad \chi_- = P_- \Xi = \begin{pmatrix} 0 \\ \chi^c \end{pmatrix}, \quad (\text{B.31})$$

Adjoint rep conventions:

- Adjoint field: ϕ_{ij}
- Adjoint field in the 16×16 spinor space (LDL): $\Phi_{16} = \frac{1}{4}\sigma^{ij}\phi_{ij}$
- Adjoint field in the 32×32 spinor space: $\Phi_{32} = \frac{1}{2}S^{ij}\phi_{ij}$

Fundamental rep conventions:

- 10 field (real): H_i

B.2. Potential for $10_H \oplus 16_H \oplus 45_H$ model

The potential is given by (we assume the \mathbb{Z}_2 for all of the scalar fields).

$$\begin{aligned}
V &= V_{10} + V_{45} + V_{1045} + V_{16} + V_{1645} + V_{1016} \\
V_{45} &= -\frac{\mu_{45}^2}{2} \text{Tr}45_H^2 + \frac{1}{8}\lambda_1 (\text{Tr}45_H^2)^2 + \frac{1}{4}\lambda_2 (\text{Tr}45_H^4) \\
V_{10} &= -\frac{\mu_{10}^2}{2} (\mathbf{10}_H^\dagger \mathbf{10}_H) + \frac{1}{8}\lambda_3 (\mathbf{10}_H^\dagger \mathbf{10}_H)^2 \\
V_{1045} &= \frac{1}{4}\lambda_4 \text{Tr}45_H^2 (\mathbf{10}_H^\dagger \mathbf{10}_H) + \frac{1}{8}\lambda_5 \mathbf{10}_H \mathbf{45}_H \mathbf{45}_H \mathbf{10}_H \\
V_{16} &= -\frac{\mu_{16}^2}{2} (\mathbf{16}_H^+ \mathbf{16}_H) + \frac{1}{4}\lambda_6 (\mathbf{16}_H^+ \mathbf{16}_H)^2 + \frac{1}{4}\lambda_7 (\mathbf{16}_H^+ \Gamma_i \mathbf{16}_H) (\mathbf{16}_H^+ \Gamma^i \mathbf{16}_H) \\
V_{1645} &= \frac{1}{4}\lambda_8 (\mathbf{16}_H^+ \mathbf{16}_H) (\text{Tr}45_H^2) + \frac{1}{4}\lambda_9 \mathbf{16}_H^+ \mathbf{45}_H \mathbf{45}_H \mathbf{16}_H \\
V_{1016} &= \frac{1}{4}\lambda_{10} (\mathbf{16}_H^+ \mathbf{16}_H) (\mathbf{10}_H^\dagger \mathbf{10}_H)
\end{aligned}$$

C. Beta functions

Convention of presenting the beta functions is the following:

$$\beta(X) \equiv \mu \frac{dX}{d\mu} \equiv \frac{1}{(4\pi)^2} \beta^{(1)}(X) + \frac{1}{(4\pi)^4} \beta^{(2)}(X)$$

C.1. Beta functions of the $SO(10)$ $10_H \oplus 45_H \oplus 16_H$ model**Gauge couplings**

$$\beta^{(1)}(g) = -\frac{139}{6}g^3$$

Yukawa couplings

$$\beta^{(1)}(Y_{10}) = -\frac{3}{8}Y_{10}Y_{10}^*Y_{10} + \text{Tr}(Y_{10}Y_{10}^*)Y_{10} - \frac{135}{4}g^2Y_{10}$$

Quartic couplings

$$\beta^{(1)}(\lambda_1) = +53\lambda_1^2 + 38\lambda_1\lambda_2 + 6\lambda_2^2 + 10\lambda_4^2 + \lambda_4\lambda_5 + 8\lambda_8^2 + 2\lambda_8\lambda_9 + \frac{3}{8}\lambda_9^2 - 48g^2\lambda_1 + 9g^4$$

$$\beta^{(1)}(\lambda_2) = +12\lambda_1\lambda_2 + 19\lambda_2^2 + \frac{1}{8}\lambda_5^2 - \frac{1}{4}\lambda_9^2 - 48g^2\lambda_2 + 3g^4$$

$$\begin{aligned} \beta^{(1)}(\lambda_3) = & +18\lambda_3^2 + 45\lambda_4^2 + \frac{9}{2}\lambda_4\lambda_5 + \frac{9}{16}\lambda_5^2 + 8\lambda_{10}^2 - 27g^2\lambda_3 + \frac{27}{4}g^4 \\ & + 4\lambda_3 \text{Tr}(Y_{10}Y_{10}^*) - \frac{1}{2} \text{Tr}(Y_{10}Y_{10}^*Y_{10}Y_{10}^*) \end{aligned}$$

$$\begin{aligned} \beta^{(1)}(\lambda_4) = & +47\lambda_1\lambda_4 + \frac{9}{4}\lambda_1\lambda_5 + 19\lambda_2\lambda_4 + \frac{1}{2}\lambda_2\lambda_5 + 12\lambda_3\lambda_4 + \frac{1}{2}\lambda_3\lambda_5 + 4\lambda_4^2 + \frac{1}{8}\lambda_5^2 \\ & + 8\lambda_{10}\lambda_8 + \lambda_{10}\lambda_9 - \frac{75}{2}g^2\lambda_4 + \frac{3}{2}g^4 + 2\lambda_4 \text{Tr}(Y_{10}Y_{10}^*) \end{aligned}$$

$$\beta^{(1)}(\lambda_5) = +2\lambda_1\lambda_5 + 9\lambda_2\lambda_5 + 2\lambda_3\lambda_5 + 8\lambda_4\lambda_5 + \frac{5}{2}\lambda_5^2 - \frac{75}{2}g^2\lambda_5 + 18g^4 + 2\lambda_5 \text{Tr}(Y_{10}Y_{10}^*)$$

$$\beta^{(1)}(\lambda_6) = +10\lambda_6^2 + 20\lambda_6\lambda_7 + 40\lambda_7^2 + 45\lambda_8^2 + \frac{45}{4}\lambda_8\lambda_9 + \frac{105}{64}\lambda_9^2 + 10\lambda_{10}^2 - \frac{135}{4}g^2\lambda_6 + \frac{315}{16}g^4$$

$$\beta^{(1)}(\lambda_7) = +3\lambda_6\lambda_7 + \frac{3}{16}\lambda_9^2 - \frac{135}{4}g^2\lambda_7 + \frac{9}{4}g^4$$

$$\begin{aligned} \beta^{(1)}(\lambda_8) = & +47\lambda_1\lambda_8 + \frac{45}{8}\lambda_1\lambda_9 + 19\lambda_2\lambda_8 + \frac{21}{8}\lambda_2\lambda_9 + \frac{17}{2}\lambda_6\lambda_8 + \lambda_6\lambda_9 + 10\lambda_7\lambda_8 + \lambda_7\lambda_9 \\ & + 2\lambda_8^2 + \frac{3}{8}\lambda_9^2 + 10\lambda_{10}\lambda_4 + \frac{1}{2}\lambda_{10}\lambda_5 - \frac{327}{8}g^2\lambda_8 + \frac{9}{2}g^4 \end{aligned}$$

$$\beta^{(1)}(\lambda_9) = +2\lambda_1\lambda_9 - 2\lambda_2\lambda_9 + \frac{1}{2}\lambda_6\lambda_9 + 2\lambda_7\lambda_9 + 4\lambda_8\lambda_9 + \frac{17}{4}\lambda_9^2 - \frac{327}{8}g^2\lambda_9 + 12g^4$$

$$\begin{aligned} \beta^{(1)}(\lambda_{10}) = & +45\lambda_4\lambda_8 + \frac{45}{8}\lambda_4\lambda_9 + \frac{9}{4}\lambda_5\lambda_8 + \frac{9}{32}\lambda_5\lambda_9 + 12\lambda_{10}\lambda_3 + \frac{17}{2}\lambda_{10}\lambda_6 + 10\lambda_{10}\lambda_7 + 2\lambda_{10}^2 \\ & - \frac{243}{8}g^2\lambda_{10} + \frac{27}{8}g^4 + 2\lambda_{10} \text{Tr}(Y_{10}Y_{10}^*) \end{aligned}$$

C.2. Beta functions of the $SU(5)$ model

Gauge couplings

$$\beta^{(1)}(g_5) = -\frac{40}{3}g_5^3$$

Yukawa couplings

$$\begin{aligned}\beta^{(1)}(Y_5) &= +3Y_5Y_5^\dagger Y_5 - \frac{9}{32}Y_5Y_{10}^*Y_{10} + 4\text{Tr}\left(Y_5Y_5^\dagger\right)Y_5 \\ &\quad + \frac{3}{16}\text{Tr}(Y_{10}Y_{10}^*)Y_5 - 18g^2Y_5 \\ \beta^{(1)}(Y_{10}) &= -3Y_5^TY_5^*Y_{10} - 3Y_{10}Y_5^\dagger Y_5 + \frac{3}{16}Y_{10}Y_{10}^*Y_{10} + 4\text{Tr}\left(Y_5Y_5^\dagger\right)Y_{10} \\ &\quad + \frac{3}{16}\text{Tr}(Y_{10}Y_{10}^*)Y_{10} - \frac{108}{5}g_5^2Y_{10}\end{aligned}$$

Quartic couplings

$$\begin{aligned}\beta^{(1)}(\lambda_1) &= +32\lambda_1^2 + \frac{188}{5}\lambda_1\lambda_2 + \frac{336}{25}\lambda_2^2 + 10\lambda_4^2 + 4\lambda_4\lambda_5 - 60g_5^2\lambda_1 + 18g_5^4 \\ \beta^{(1)}(\lambda_2) &= +12\lambda_1\lambda_2 + \frac{64}{5}\lambda_2^2 + \lambda_5^2 - 60g_5^2\lambda_2 + 15g_5^4 \\ \beta^{(1)}(\lambda_3) &= +18\lambda_3^2 + 24\lambda_4^2 + \frac{48}{5}\lambda_4\lambda_5 + \frac{66}{25}\lambda_5^2 - \frac{144}{5}g_5^2\lambda_3 + \frac{198}{25}g_5^4 \\ &\quad + 16\lambda_3\text{Tr}\left(Y_5Y_5^\dagger\right) + \frac{3}{4}\lambda_3\text{Tr}(Y_{10}Y_{10}^*) - 16\text{Tr}\left(Y_5Y_5^\dagger Y_5 Y_5^\dagger\right) - \frac{3}{64}\text{Tr}(Y_{10}Y_{10}^*Y_{10}Y_{10}^*) \\ \beta^{(1)}(\lambda_4) &= +26\lambda_1\lambda_4 + \frac{24}{5}\lambda_1\lambda_5 + \frac{94}{5}\lambda_2\lambda_4 + \frac{56}{25}\lambda_2\lambda_5 + 12\lambda_3\lambda_4 + 2\lambda_3\lambda_5 \\ &\quad + 4\lambda_4^2 + \lambda_5^2 - \frac{222}{5}g_5^2\lambda_4 + 3g_5^4 + 8\lambda_4\text{Tr}\left(Y_5Y_5^\dagger\right) + \frac{3}{8}\lambda_4\text{Tr}(Y_{10}Y_{10}^*) \\ \beta^{(1)}(\lambda_5) &= +2\lambda_1\lambda_5 + \frac{38}{5}\lambda_2\lambda_5 + 2\lambda_3\lambda_5 + 8\lambda_4\lambda_5 + \frac{21}{5}\lambda_5^2 - \frac{222}{5}g_5^2\lambda_5 + 15g_5^4 \\ &\quad + 8\lambda_5\text{Tr}\left(Y_5Y_5^\dagger\right) + \frac{3}{8}\lambda_5\text{Tr}(Y_{10}Y_{10}^*)\end{aligned}$$

Bibliography

- [1] Aaron Held, Jan Henryk Kwapisz, and Lohan Sartore, 2022.
- [2] Astrid Eichhorn, Jan Henryk Kwapisz, and Marc Schiffer. The weak-gravity bound in asymptotically safe gravity-gauge systems, 12 2021.
- [3] Aaron Held, Jan Henryk Kwapisz, and Lohan Sartore, 2021.
- [4] Tomasz Krajewski, Jan Henryk Kwapisz, Zygmunt Lalak, and Marek Lewicki. Stability of domain walls in models with asymmetric potentials. *Phys. Rev. D*, 104(12):123522, 2021.
- [5] Jan Chojnacki and Jan Kwapisz. Finite action principle and Hořava-Lifshitz gravity: Early universe, black holes, and wormholes. *Phys. Rev. D*, 104(10):103504, 2021.
- [6] Jan Chojnacki, Julia Krajecka, Jan Henryk Kwapisz, Oskar Slowik, and Artur Strag. Is asymptotically safe inflation eternal? *JCAP*, 04:076, 2021.
- [7] Jan Henryk Kwapisz and Krzysztof Antoni Meissner. Asymptotic safety and quantum gravity amplitudes. *Nucl. Phys. B*, 965:115341, 2021.
- [8] Jan Henryk Kwapisz. Asymptotic safety, the Higgs boson mass, and beyond the standard model physics. *Phys. Rev. D*, 100(11):115001, 2019.
- [9] Frederic Grabowski, Jan Henryk Kwapisz, and Krzysztof Antoni Meissner. Asymptotic safety and conformal standard model. *Phys. Rev. D*, 99:115029, Jun 2019.
- [10] Jan Henryk Kwapisz and Krzysztof Antoni Meissner. Conformal Standard Model and Inflation. *Acta Phys. Polon. B*, 49:115, 2018.
- [11] Sebastian M. Dawid, Rafa Gonsior, Jan Henryk Kwapisz, Kamil Serafin, Mariusz Tobolski, and Stanisaw D. Gazek. Renormalization group procedure for potential $-g/r^2$. *Phys. Lett.*, B777:260–264, 2018.
- [12] Jan Chojnacki and Jan Henryk Kwapisz. Finite Action Principle and wormholes. In *16th Marcel Grossmann Meeting on Recent Developments in Theoretical and Experimental General Relativity, Astrophysics and Relativistic Field Theories*, 11 2021.
- [13] Jan H. Kwapisz and Leszek Z. Stolarczyk. Applications of Hückel-Su-Schrieffer-Heeger method. *Structural Chemistry*, 32:1393–1406, 2021.

- [14] Jan Kwapisz and Frederic Grabowski. Asymptotic safety, cosmology and Conformal Standard Model. In *15th Marcel Grossmann Meeting on Recent Developments in Theoretical and Experimental General Relativity, Astrophysics, and Relativistic Field Theories*, 2018.
- [15] Nima Arkani-Hamed, Savas Dimopoulos, and G. R. Dvali. The Hierarchy problem and new dimensions at a millimeter. *Phys. Lett. B*, 429:263–272, 1998.
- [16] Lisa Randall and Raman Sundrum. A Large mass hierarchy from a small extra dimension. *Phys. Rev. Lett.*, 83:3370–3373, 1999.
- [17] Lisa Randall and Raman Sundrum. An Alternative to compactification. *Phys. Rev. Lett.*, 83:4690–4693, 1999.
- [18] Juan Martin Maldacena. The Large N limit of superconformal field theories and supergravity. *Int. J. Theor. Phys.*, 38:1113–1133, 1999.
- [19] S. S. Gubser, Igor R. Klebanov, and Alexander M. Polyakov. Gauge theory correlators from noncritical string theory. *Phys. Lett. B*, 428:105–114, 1998.
- [20] Edward Witten. Anti-de Sitter space and holography. *Adv. Theor. Math. Phys.*, 2:253–291, 1998.
- [21] Zachary Feinstein. It’s a trap: Emperor palpatine’s poison pill. *arXiv preprint arXiv:1511.09054*, 2015.
- [22] Pietro Donà, Astrid Eichhorn, and Roberto Percacci. Matter matters in asymptotically safe quantum gravity. *Phys. Rev. D*, 89(8):084035, 2014.
- [23] William H. Kinney. The Swampland Conjecture Bound Conjecture. 3 2021.
- [24] John F. Donoghue. A Critique of the Asymptotic Safety Program. *Front. in Phys.*, 8:56, 2020.
- [25] Weinberg Steven. Critical phenomena for field theorists. Lectures presented at Int. School of Subnuclear Physics, Ettore Majorana, Erice, Sicily, Jul 23 - Aug 8, 1976.
- [26] Steven Weinberg. *The Quantum Theory of Fields*, volume 1,2. Cambridge University Press, 1995.
- [27] Luca Di Luzio. *Aspects of symmetry breaking in Grand Unified Theories*. PhD thesis, SISSA, Trieste, 2011.
- [28] Ling-Fong Li. Group Theory of the Spontaneously Broken Gauge Symmetries. *Phys. Rev. D*, 9:1723–1739, 1974.
- [29] Kateřina Jarkovská, Michal Malinský, Timon Mede, and Vasja Susič. Quantum guts of the minimal potentially realistic SO(10) Higgs model. 9 2021.
- [30] Tom Rudelius. Conditions for (No) Eternal Inflation. *JCAP*, 08:009, 2019.
- [31] John D. Barrow and Frank J. Tipler. Action principles in nature. *Nature*, 331(6151):31–34, 1988.

- [32] Jean-Luc Lehners and K.S. Stelle. A Safe Beginning for the Universe? *Phys. Rev. D*, 100(8):083540, 2019.
- [33] Johanna N. Borissova and Astrid Eichhorn. Towards black-hole singularity-resolution in the Lorentzian gravitational path integral. *Universe*, 7(3):48, 2021.
- [34] Elisa Manrique and Martin Reuter. Bare versus Effective Fixed Point Action in Asymptotic Safety: The Reconstruction Problem. *PoS*, CLAQG08:001, 2011.
- [35] Richard P. Feynman. There's plenty of room at the bottom. 1959.
- [36] Lord Rayleigh F.R.S. Liii. remarks upon the law of complete radiation. *Philosophical Magazine Series 1*, 49:539–540.
- [37] J.H. Jeans M.A. Xi. on the partition of energy between matter and \mathcal{A} ether. *The London, Edinburgh, and Dublin Philosophical Magazine and Journal of Science*, 10(55):91–98, 1905.
- [38] Max Planck. On the theory of the energy distribution law of the normal spectrum. 1900.
- [39] J. J. Thomson M.A. F.R.S. Xl. cathode rays. *The London, Edinburgh, and Dublin Philosophical Magazine and Journal of Science*, 44(269):293–316, 1897.
- [40] Professor E. Rutherford F.R.S. Lxxix. the scattering of α and β particles by matter and the structure of the atom. *The London, Edinburgh, and Dublin Philosophical Magazine and Journal of Science*, 21(125):669–688, 1911.
- [41] N. Bohr. Lxxiii. on the constitution of atoms and molecules, November 1913.
- [42] Louis Victor Pierre Raymond de Broglie. Recherches sur la théorie des quanta. *Annals Phys.*, 2:22–128, 1925.
- [43] W. Heisenberg. On the quantum reinterpretation of kinematical and mechanical relationships. *Z. Phys.*, pages 879–893, 1925.
- [44] E. Schrödinger. Quantisierung als eigenwertproblem. *Annalen der Physik*, 384(4):361–376, 1926.
- [45] S.W. Hawking and G.F.R. Ellis. *The Large Scale Structure of Space-Time*. Cambridge Monographs on Mathematical Physics. Cambridge University Press, 1973.
- [46] G.F.R. Ellis and B.G. Schmidt. Singular space-times. *Gen. Rel. Grav.*, 8:915–953, 1977.
- [47] Richard C. Tolman. Effect of inhomogeneity on cosmological models. *Proceedings of the National Academy of Sciences*, 20(3):169–176, 1934.
- [48] J. R. Oppenheimer and H. Snyder. On continued gravitational contraction. *Phys. Rev.*, 56:455–459, Sep 1939.
- [49] Roger Penrose. Gravitational collapse and space-time singularities. *Phys. Rev. Lett.*, 14:57–59, 1965.
- [50] S. Hawking and R. Penrose. *The Nature of space and time*. 1996.

- [51] R. Penrose. Gravitational collapse: The role of general relativity. *Riv. Nuovo Cim.*, 1:252–276, 1969.
- [52] A. Friedman. On the curvature of space. *Z. Phys.*, 10:377386, 1922.
- [53] Abbé G. Lemaître. A Homogeneous Universe of Constant Mass and Increasing Radius accounting for the Radial Velocity of Extra-galactic Nebulæ. *Monthly Notices of the Royal Astronomical Society*, 91(5):483–490, 03 1931.
- [54] H. P. Robertson. Kinematics and World-Structure. *Astrophys. J.*, 82:284–301, 1935.
- [55] A. G. Walker. On milne’s theory of world-structure*. *Proceedings of the London Mathematical Society*, s2-42(1):90–127, 1937.
- [56] S. W. Hawking and R. Penrose. The Singularities of gravitational collapse and cosmology. *Proc. Roy. Soc. Lond. A*, 314:529–548, 1970.
- [57] Gerard ’t Hooft and M.J.G. Veltman. One loop divergencies in the theory of gravitation. *Ann. Inst. H. Poincaré Phys. Theor. A*, 20:69–94, 1974.
- [58] S.M. Christensen and M.J. Duff. Quantizing Gravity with a Cosmological Constant. *Nucl. Phys. B*, 170:480–506, 1980.
- [59] Marc H. Goroff and Augusto Sagnotti. The Ultraviolet Behavior of Einstein Gravity. *Nucl. Phys.*, B266:709–736, 1986.
- [60] A.E.M. van de Ven. Two loop quantum gravity. *Nucl. Phys. B*, 378:309–366, 1992.
- [61] John F. Donoghue. General relativity as an effective field theory: The leading quantum corrections. *Phys. Rev. D*, 50:3874–3888, 1994.
- [62] I. B. Khriplovich and G. G. Kirilin. Quantum power correction to the Newton law. *J. Exp. Theor. Phys.*, 95(6):981–986, 2002.
- [63] N. E. J Bjerrum-Bohr, John F. Donoghue, and Barry R. Holstein. Quantum gravitational corrections to the nonrelativistic scattering potential of two masses. *Phys. Rev. D*, 67:084033, 2003. [Erratum: Phys.Rev.D 71, 069903 (2005)].
- [64] John F. Donoghue. The effective field theory treatment of quantum gravity. *AIP Conf. Proc.*, 1483(1):73–94, 2012.
- [65] K.S. Stelle. Renormalization of Higher Derivative Quantum Gravity. *Phys. Rev. D*, 16:953–969, 1977.
- [66] E.S. Fradkin and A.A. Tseytlin. Renormalizable asymptotically free quantum theory of gravity. *Nuclear Physics B*, 201(3):469–491, 1982.
- [67] Richard P. Woodard. Ostrogradsky’s theorem on Hamiltonian instability. *Scholarpedia*, 10(8):32243, 2015.
- [68] K. A. Meissner and G. Veneziano. Symmetries of cosmological superstring vacua. *Phys. Lett. B*, 267:33–36, 1991.

- [69] Damiano Anselmi and Marco Piva. Quantum Gravity, Fakeons And Microcausality. *JHEP*, 11:021, 2018.
- [70] John F. Donoghue and Gabriel Menezes. Arrow of Causality and Quantum Gravity. *Phys. Rev. Lett.*, 123(17):171601, 2019.
- [71] Neil Barnaby and Niky Kamran. Dynamics with infinitely many derivatives: The Initial value problem. *JHEP*, 02:008, 2008.
- [72] Alessia Platania and Christof Wetterich. Non-perturbative unitarity and fictitious ghosts in quantum gravity. *Phys. Lett. B*, 811:135911, 2020.
- [73] Petr Hoava. Quantum gravity at a lifshitz point. *Physical Review D*, 79(8), Apr 2009.
- [74] Giulio D’Odorico, Frank Saueressig, and Marrit Schutten. Asymptotic Freedom in Hořava-Lifshitz Gravity. *Phys. Rev. Lett.*, 113(17):171101, 2014.
- [75] Giulio D’Odorico, Jan-Willem Goossens, and Frank Saueressig. Covariant computation of effective actions in Hořava-Lifshitz gravity. *JHEP*, 10:126, 2015.
- [76] Andrei O. Barvinsky, Diego Blas, Mario Herrero-Valea, Sergey M. Sibiryakov, and Christian F. Steinwachs. Hořava Gravity is Asymptotically Free in $2 + 1$ Dimensions. *Phys. Rev. Lett.*, 119(21):211301, 2017.
- [77] Andrei O. Barvinsky, Alexander V. Kurov, and Sergey M. Sibiryakov. Beta functions of (3+1)-dimensional projectable Horava gravity. 10 2021.
- [78] Richard Arnowitt, Stanley Deser, and Charles W. Misner. Republication of: The dynamics of general relativity. *General Relativity and Gravitation*, 40(9):19972027, Aug 2008.
- [79] Anzhong Wang. Hoava gravity at a lifshitz point: A progress report. *International Journal of Modern Physics D*, 26(07):1730014, Mar 2017.
- [80] Rodrigo Maier and Ivano Damião Soares. Hoava-lifshitz bouncing bianchi ix universes: A dynamical system analysis. *Physical Review D*, 96(10), Nov 2017.
- [81] Petr Horava. General Covariance in Gravity at a Lifshitz Point. *Class. Quant. Grav.*, 28:114012, 2011.
- [82] Christos Charmousis, Gustavo Niz, Antonio Padilla, and Paul M. Saffin. Strong coupling in Horava gravity. *JHEP*, 08:070, 2009.
- [83] Miao Li and Yi Pang. A Trouble with Hořava-Lifshitz Gravity. *JHEP*, 08:015, 2009.
- [84] D. Blas, O. Pujolas, and S. Sibiryakov. On the Extra Mode and Inconsistency of Horava Gravity. *JHEP*, 10:029, 2009.
- [85] Marc Henneaux, Axel Kleinschmidt, and Gustavo Lucena Gómez. A dynamical inconsistency of Horava gravity. *Phys. Rev. D*, 81:064002, 2010.
- [86] Petr Horava and Charles M. Melby-Thompson. General Covariance in Quantum Gravity at a Lishitz Point. *Phys. Rev. D*, 82:064027, 2010.

- [87] Diego Blas, Oriol Pujolas, and Sergey Sibiryakov. Models of non-relativistic quantum gravity: The Good, the bad and the healthy. *JHEP*, 04:018, 2011.
- [88] Sante Carloni, Emilio Elizalde, and Pedro J. Silva. Matter couplings in Horava-Lifshitz and their cosmological applications. *Class. Quant. Grav.*, 28:195002, 2011.
- [89] James W. York. Role of conformal three-geometry in the dynamics of gravitation. *Phys. Rev. Lett.*, 28:1082–1085, Apr 1972.
- [90] G. W. Gibbons and S. W. Hawking. Action integrals and partition functions in quantum gravity. *Phys. Rev. D*, 15:2752–2756, May 1977.
- [91] Chethan Krishnan and Avinash Raju. A Neumann Boundary Term for Gravity. *Mod. Phys. Lett. A*, 32(14):1750077, 2017.
- [92] Caroline Jonas, Jean-Luc Lehners, and Jerome Quintin. Cosmological consequences of a principle of finite amplitudes. *Phys. Rev. D*, 103(10):103525, 2021.
- [93] Guillermo Lara, Mario Herrero-Valea, Enrico Barausse, and Sergey M. Sibiryakov. Black holes in ultraviolet-complete Hořava gravity. *Phys. Rev. D*, 103(10):104007, 2021.
- [94] Ali H. Chamseddine, Viatcheslav Mukhanov, and Tobias B. Russ. Mimetic Hořava gravity. *Phys. Lett. B*, 798:134939, 2019.
- [95] Ola Malaeb and Chireen Saghir. Mimetic Horava Gravity and Surface terms. 5 2020.
- [96] David Tong. String Theory. 1 2009.
- [97] Michael B. Green, John H. Schwarz, and Edward Witten. *Superstring Theory: 25th Anniversary Edition*, volume 1,2 of *Cambridge Monographs on Mathematical Physics*. Cambridge University Press, 2012.
- [98] Joseph Polchinski. *String Theory*, volume 1 of *Cambridge Monographs on Mathematical Physics*. Cambridge University Press, 1998.
- [99] G. Veneziano. Construction of a crossing - symmetric, Regge behaved amplitude for linearly rising trajectories. *Nuovo Cim. A*, 57:190–197, 1968.
- [100] D. Friedan. Nonlinear Models in Two Epsilon Dimensions. *Phys. Rev. Lett.*, 45:1057, 1980.
- [101] Olaf Hohm and Barton Zwiebach. Non-perturbative de Sitter vacua via α' corrections. *Int. J. Mod. Phys. D*, 28(14):1943002, 2019.
- [102] Olaf Hohm and Barton Zwiebach. Duality invariant cosmology to all orders in α' . *Phys. Rev. D*, 100(12):126011, 2019.
- [103] K. A. Meissner and G. Veneziano. Manifestly $O(d,d)$ invariant approach to space-time dependent string vacua. *Mod. Phys. Lett. A*, 6:3397–3404, 1991.
- [104] Krzysztof A. Meissner. Symmetries of higher order string gravity actions. *Phys. Lett. B*, 392:298–304, 1997.

- [105] Petr Horava and Edward Witten. Heterotic and type I string dynamics from eleven-dimensions. *Nucl. Phys. B*, 460:506–524, 1996.
- [106] Petr Horava and Edward Witten. Eleven-dimensional supergravity on a manifold with boundary. *Nucl. Phys. B*, 475:94–114, 1996.
- [107] M. J. Duff. M theory (The Theory formerly known as strings). *Int. J. Mod. Phys. A*, 11:5623–5642, 1996.
- [108] S. Weinberg. Ultraviolet divergences in quantum theories of gravitation. In S. W. Hawking and W. Israel, editors, *General Relativity: An Einstein centenary survey*, pages 790–831, 1979.
- [109] Steven Weinberg. *Ultraviolet divergences in quantum theories of gravitation*, pages 790–831. 1 1980.
- [110] Graham M. Shore. *The c and a-theorems and the Local Renormalisation Group*. SpringerBriefs in Physics. Springer, Cham, 2017.
- [111] David J. Gross and Frank Wilczek. Ultraviolet behavior of non-abelian gauge theories. *Phys. Rev. Lett.*, 30:1343–1346, Jun 1973.
- [112] H. David Politzer. Reliable perturbative results for strong interactions? *Phys. Rev. Lett.*, 30:1346–1349, Jun 1973.
- [113] R. Gastmans, R. Kallosh, and C. Truffin. Quantum Gravity Near Two-Dimensions. *Nucl. Phys.*, B133:417–434, 1978.
- [114] S. M. Christensen and M. J. Duff. Quantum Gravity in Two + ϵ Dimensions. *Phys. Lett.*, 79B:213–216, 1978.
- [115] I. Jack and D.R.T. Jones. The Epsilon expansion of two-dimensional quantum gravity. *Nucl. Phys. B*, 358:695–712, 1991.
- [116] Hikaru Kawai, Yoshihisa Kitazawa, and Masao Ninomiya. Renormalizability of quantum gravity near two-dimensions. *Nucl. Phys. B*, 467:313–331, 1996.
- [117] Lee Smolin. A Fixed Point for Quantum Gravity. *Nucl. Phys.*, B208:439–466, 1982.
- [118] Ch. Wetterich. Exact evolution equation for the effective potential. *Phys. Lett. B*, 301:90–94, 1993.
- [119] T. R. Morris. The Exact renormalization group and approximate solutions. *Int. J. Mod. Phys. A*, 9:2411–2450, 1994.
- [120] Ulrich Ellwanger. FFlow equations for N point functions and bound states. pages 206–211, 9 1993.
- [121] M. Reuter. Nonperturbative evolution equation for quantum gravity. *Phys. Rev. D*, 57:971–985, 1998.
- [122] O. Lauscher and M. Reuter. Ultraviolet fixed point and generalized flow equation of quantum gravity. *Phys. Rev. D*, 65:025013, 2001.

- [123] M. Reuter and F. Saueressig. Renormalization group flow of quantum gravity in the einstein-hilbert truncation. *Phys. Rev. D*, 65:065016, Feb 2002.
- [124] Hermann Nicolai. Talk at quantum gravity 2020.
- [125] Abhay Ashtekar. New variables for classical and quantum gravity. *Phys. Rev. Lett.*, 57:2244–2247, Nov 1986.
- [126] Sheldon L. Glashow. Partial-symmetries of weak interactions. *Nuclear Physics*, 22(4):579–588, 1961.
- [127] Abdus Salam. Elementary particle physics: Relativistic groups and analyticity. In N. Svartholm, editor, *Eighth Nobel Symposium*, page 367. Almqvist and Wiksell, Stockholm, 1968.
- [128] Steven Weinberg. A model of leptons. *Phys. Rev. Lett.*, 19:1264–1266, Nov 1967.
- [129] Krzysztof A. Meissner. *Classical field theory*. Wydawnictwo Naukowe PWN, 2013. Title of original: Klasyczna Teoria Pola.
- [130] Stefan Pokorski. *Gauge Field Theories*. Cambridge Monographs on Mathematical Physics. Cambridge University Press, 2 edition, 2000.
- [131] Nakarin Lohitsiri and David Tong. Hypercharge Quantisation and Fermat’s Last Theorem. *SciPost Phys.*, 8(1):009, 2020.
- [132] An anomaly-free version of weinberg’s model. *Physics Letters B*, 38(7):519–523, 1972.
- [133] Reinhard Alkofer, Astrid Eichhorn, Aaron Held, Carlos M. Nieto, Roberto Percacci, and Markus Schröfl. Quark masses and mixings in minimally parameterized UV completions of the Standard Model. *Annals Phys.*, 421:168282, 2020.
- [134] Aaron Held. From particle physics to black holes: The predictive power of asymptotic safety, 2019. PhD thesis, private communication.
- [135] Dario Buttazzo, Giuseppe Degrassi, Pier Paolo Giardino, Gian F. Giudice, Filippo Sala, Alberto Salvio, and Alessandro Strumia. Investigating the near-criticality of the Higgs boson. *JHEP*, 12:089, 2013.
- [136] Fedor Bezrukov, Mikhail Yu. Kalmykov, Bernd A. Kniehl, and Mikhail Shaposhnikov. Higgs Boson Mass and New Physics. *JHEP*, 10:140, 2012. [,275(2012)].
- [137] Giuseppe Degrassi, Stefano Di Vita, Joan Elias-Miro, Jose R. Espinosa, Gian F. Giudice, Gino Isidori, and Alessandro Strumia. Higgs mass and vacuum stability in the Standard Model at NNLO. *JHEP*, 08:098, 2012.
- [138] Fedor Bezrukov and Mikhail Shaposhnikov. Why should we care about the top quark Yukawa coupling? *J. Exp. Theor. Phys.*, 120:335–343, 2015. [Zh. Eksp. Teor. Fiz.147,389(2015)].
- [139] Takehiko Asaka, Steve Blanchet, and Mikhail Shaposhnikov. The nuMSM, dark matter and neutrino masses. *Phys. Lett. B*, 631:151–156, 2005.

- [140] Takehiko Asaka and Mikhail Shaposhnikov. The ν MSM, dark matter and baryon asymmetry of the universe. *Phys. Lett. B*, 620:17–26, 2005.
- [141] M. Shaposhnikov and I. Tkachev. The nuMSM, inflation, and dark matter. *Phys. Lett. B*, 639:414–417, 2006.
- [142] K. A. Meissner and H. Nicolai. Conformal symmetry and the Standard Model. *Phys. Lett. B*, 648(4):312 – 317, 2007.
- [143] Tsutomu Yanagida. Horizontal Symmetry and Masses of Neutrinos. *Progress of Theoretical Physics*, 64(3):1103–1105, 09 1980.
- [144] Rabindra N. Mohapatra and Goran Senjanović. Neutrino mass and spontaneous parity nonconservation. *Phys. Rev. Lett.*, 44:912–915, Apr 1980.
- [145] J. Schechter and J. W. F. Valle. Neutrino decay and spontaneous violation of lepton number. *Phys. Rev. D*, 25:774–783, Feb 1982.
- [146] P. Binétruy and S. Lavignac. 25 years of seesaw (summary of seesaw'25). *Nuclear Physics B - Proceedings Supplements*, 143:175–183, 2005. NEUTRINO 2004.
- [147] S. F. King. Neutrino mass models. *Rept. Prog. Phys.*, 67:107–158, 2004.
- [148] Andrei D Sakharov. Violation of cp invariance, c asymmetry, and baryon asymmetry of the universe. 34(5):392–393, may 1991.
- [149] V.A. Kuzmin, V.A. Rubakov, and M.E. Shaposhnikov. On anomalous electroweak baryon-number non-conservation in the early universe. *Physics Letters B*, 155(1):36–42, 1985.
- [150] V. A. Rubakov and M. E. Shaposhnikov. Electroweak baryon number nonconservation in the early universe and in high-energy collisions. *Usp. Fiz. Nauk*, 166:493–537, 1996.
- [151] M.E. Shaposhnikov. Structure of the high temperature gauge ground state and electroweak production of the baryon asymmetry. *Nuclear Physics B*, 299(4):797–817, 1988.
- [152] M. E. Shaposhnikov. Possible Appearance of the Baryon Asymmetry of the Universe in an Electroweak Theory. *JETP Lett.*, 44:465–468, 1986.
- [153] M.E. Shaposhnikov. Baryon asymmetry of the universe in standard electroweak theory. *Nuclear Physics B*, 287:757–775, 1987.
- [154] Jan Ambjorn, M. L. Laursen, and M. E. Shaposhnikov. Baryon Asymmetry Generation in the Electroweak Theory: A Lattice Study. *Nucl. Phys. B*, 316:483–508, 1989.
- [155] M. B. Gavela, P. Hernandez, J. Orloff, O. Pene, and C. Quimbay. Standard model CP violation and baryon asymmetry. Part 2: Finite temperature. *Nucl. Phys. B*, 430:382–426, 1994.
- [156] Patrick Huet and Eric Sather. Electroweak baryogenesis and standard model CP violation. *Phys. Rev. D*, 51:379–394, 1995.

- [157] Tomas Brauner, Olli Taanila, Anders Tranberg, and Aleksi Vuorinen. Temperature Dependence of Standard Model CP Violation. *Phys. Rev. Lett.*, 108:041601, 2012.
- [158] A.E. Nelson, D.B. Kaplan, and A.G. Cohen. Why there is something rather than nothing: Matter from weak interactions. *Nuclear Physics B*, 373(2):453–478, 1992.
- [159] Andrew G. Cohen, D. B. Kaplan, and A. E. Nelson. Progress in electroweak baryogenesis. *Ann. Rev. Nucl. Part. Sci.*, 43:27–70, 1993.
- [160] Krzysztof A. Meissner and Hermann Nicolai. Standard Model Fermions and N=8 supergravity. *Phys. Rev. D*, 91:065029, 2015.
- [161] Krzysztof A. Meissner and Hermann Nicolai. Standard Model Fermions and Infinite-Dimensional R-Symmetries. *Phys. Rev. Lett.*, 121(9):091601, 2018.
- [162] R. Percacci. *An Introduction to Covariant Quantum Gravity and Asymptotic Safety*. World Scientific, 2017.
- [163] H. Georgi and S. L. Glashow. Unity of all elementary-particle forces. *Phys. Rev. Lett.*, 32:438–441, Feb 1974.
- [164] John C. Baez and John Huerta. The Algebra of Grand Unified Theories. *Bull. Am. Math. Soc.*, 47:483–552, 2010.
- [165] Stefano Bertolini, Luca Di Luzio, and Michal Malinsky. Seesaw Scale in the Minimal Renormalizable SO(10) Grand Unification. *Phys. Rev. D*, 85:095014, 2012.
- [166] Howard Georgi and S. L. Glashow. Unity of all elementary-particle forces. *Phys. Rev. Lett.*, 32:438–441, Feb 1974.
- [167] Harald Fritzsch and Peter Minkowski. Unified Interactions of Leptons and Hadrons. *Annals Phys.*, 93:193–266, 1975.
- [168] G.G. Ross and Benjamin/Cummings Publishing Company. *Grand Unified Theories*. Benjamin/Cummings Series in the Life Sciences. Benjamin/Cummings Publishing Company, 1984.
- [169] A. Latosinski, A. Lewandowski, K. A. Meissner, and H. Nicolai. Conformal standard model with an extended scalar sector. *JHEP*, 2015(10):170, Oct 2015.
- [170] Krzysztof A. Meissner and Hermann Nicolai. Effective action, conformal anomaly and the issue of quadratic divergences. *Phys. Lett. B*, 660:260–266, 2008.
- [171] P. H. Chankowski, A. Lewandowski, K. A. Meissner, and H. Nicolai. Softly broken conformal symmetry and the stability of the electroweak scale. *Mod. Phys. Lett. A*, 30(02):1550006, 2015.
- [172] K. A. Meissner, H. Nicolai, and J. Plefka. Softly broken conformal symmetry with quantum gravitational corrections. *Phys. Lett.*, B791:62–65, 2019.

- [173] Li-Sheng Geng, Benjamín Grinstein, Sebastian Jäger, Jorge Martin Camalich, Xiu-Lei Ren, and Rui-Xiang Shi. Towards the discovery of new physics with lepton-universality ratios of $b \rightarrow s\ell\ell$ decays. *Phys. Rev. D*, 96:093006, Nov 2017.
- [174] Gregory Ciezarek, Manuel Franco Sevilla, Brian Hamilton, Robert Kowalewski, Thomas Kuhr, Vera Lüth, and Yutaro Sato. A Challenge to Lepton Universality in B Meson Decays. *Nature*, 546:227–233, 2017.
- [175] Georges Aad et al. Test of the universality of τ and μ lepton couplings in W -boson decays with the ATLAS detector. *Nature Phys.*, 17(7):813–818, 2021.
- [176] B. Abi et al. Measurement of the positive muon anomalous magnetic moment to 0.46 ppm. *Phys. Rev. Lett.*, 126:141801, Apr 2021.
- [177] Sz. Borsanyi et al. Leading hadronic contribution to the muon magnetic moment from lattice QCD. *Nature*, 593(7857):51–55, 2021.
- [178] Cumrun Vafa. The String landscape and the swampland. 9 2005.
- [179] Nima Arkani-Hamed, Lubos Motl, Alberto Nicolis, and Cumrun Vafa. The String landscape, black holes and gravity as the weakest force. *JHEP*, 06:060, 2007.
- [180] Shamit Kachru, Renata Kallosh, Andrei D. Linde, and Sandip P. Trivedi. De Sitter vacua in string theory. *Phys. Rev. D*, 68:046005, 2003.
- [181] Georges Obied, Hirosi Ooguri, Lev Spodyneiko, and Cumrun Vafa. De Sitter Space and the Swampland. 6 2018.
- [182] Prateek Agrawal, Georges Obied, Paul J. Steinhardt, and Cumrun Vafa. On the Cosmological Implications of the String Swampland. *Phys. Lett. B*, 784:271–276, 2018.
- [183] V. Mukhanov. *Physical Foundations of Cosmology*. Cambridge University Press, Oxford, 2005.
- [184] Wendy L. Freedman. Cosmology at a Crossroads. *Nature Astron.*, 1:0121, 2017.
- [185] Eleonora Di Valentino. Crack in the cosmological paradigm. *Nature Astron.*, 1(9):569–570, 2017.
- [186] Adam G. Riess. The Expansion of the Universe is Faster than Expected. *Nature Rev. Phys.*, 2(1):10–12, 2019.
- [187] L. Verde, T. Treu, and A. G. Riess. Tensions between the Early and the Late Universe. *Nature Astron.*, 3:891, 7 2019.
- [188] Eleonora Di Valentino et al. Snowmass2021 - Letter of interest cosmology intertwined II: The hubble constant tension. *Astropart. Phys.*, 131:102605, 2021.
- [189] Eleonora Di Valentino, Olga Mena, Supriya Pan, Luca Visinelli, Weiqiang Yang, Alessandro Melchiorri, David F. Mota, Adam G. Riess, and Joseph Silk. In the realm of the Hubble tension—a review of solutions. *Class. Quant. Grav.*, 38(15):153001, 2021.

- [190] V. Rubakov. Introduction to Cosmology, 2014. Lectures given at ICTP on Summer School on Cosmology in 2014.
- [191] Manuel Reichert and Juri Smirnov. Dark Matter meets Quantum Gravity. *Phys. Rev. D*, 101(6):063015, 2020.
- [192] John F. Donoghue. Cosmological constant and the use of cutoffs. *Phys. Rev. D*, 104(4):045005, 2021.
- [193] Xiangdong Zhang, Gaoping Long, and Yongge Ma. Loop quantum gravity and cosmological constant. 1 2021.
- [194] Astrid Eichhorn. An asymptotically safe guide to quantum gravity and matter. *Front. Astron. Space Sci.*, 5:47, 2019.
- [195] Alfio Bonanno, Astrid Eichhorn, Holger Gies, Jan M. Pawłowski, Roberto Percacci, Martin Reuter, Frank Saueressig, and Gian Paolo Vacca. Critical reflections on asymptotically safe gravity. 4 2020.
- [196] J. Ambjorn, A. Gorlich, J. Jurkiewicz, and R. Loll. Planckian Birth of the Quantum de Sitter Universe. *Phys. Rev. Lett.*, 100:091304, 2008.
- [197] J. Ambjorn, A. Gorlich, J. Jurkiewicz, and R. Loll. The Nonperturbative Quantum de Sitter Universe. *Phys. Rev. D*, 78:063544, 2008.
- [198] S. Jordan and R. Loll. De Sitter Universe from Causal Dynamical Triangulations without Preferred Foliation. *Phys. Rev. D*, 88:044055, 2013.
- [199] J. Ambjørn, J. Gizbert-Studnicki, A. Görlich, J. Jurkiewicz, N. Klitgaard, and R. Loll. Characteristics of the new phase in CDT. *Eur. Phys. J. C*, 77(3):152, 2017.
- [200] L. Glaser and R. Loll. CDT and Cosmology. *Comptes Rendus Physique*, 18:265–274, 2017.
- [201] Rafael D. Sorkin. Forks in the road, on the way to quantum gravity. *Int. J. Theor. Phys.*, 36:2759–2781, 1997.
- [202] Leonardo Senatore. Lectures on Inflation. In *Theoretical Advanced Study Institute in Elementary Particle Physics: New Frontiers in Fields and Strings*, pages 447–543, 2017.
- [203] P. A. R. Ade et al. Planck 2015 results. XX. Constraints on inflation. *Astron. Astrophys.*, 594:A20, 2016.
- [204] Y. Akrami et al. Planck 2018 results. X. Constraints on inflation. *Astron. Astrophys.*, 641:A10, 2020.
- [205] Jan Henryk Kwapisz. Conformal standard model and inflation. 11 2019.
- [206] Daniel Baumann. Primordial Cosmology. *PoS*, TASI2017:009, 2018.
- [207] James E. Lidsey, Andrew R. Liddle, Edward W. Kolb, Edmund J. Copeland, Tiago Barreiro, and Mark Abney. Reconstructing the inflaton potentialan overview. *Reviews of Modern Physics*, 69(2):373410, Apr 1997.

- [208] Alan H. Guth. Inflation and eternal inflation. *Phys. Rept.*, 333:555–574, 2000.
- [209] Alan H. Guth. Eternal inflation and its implications. *J. Phys. A*, 40:6811–6826, 2007.
- [210] Matthew C. Johnson and Jean-Luc Lehners. Cycles in the Multiverse. *Phys. Rev. D*, 85:103509, 2012.
- [211] Jean-Luc Lehners. Eternal Inflation With Non-Inflationary Pocket Universes. *Phys. Rev. D*, 86:043518, 2012.
- [212] Gabriel León. Eternal inflation and the quantum birth of cosmic structure. *Eur. Phys. J. C*, 77(10):705, 2017.
- [213] Hiroki Matsui and Fuminobu Takahashi. Eternal Inflation and Swampland Conjectures. *Phys. Rev. D*, 99(2):023533, 2019.
- [214] Ziwei Wang, Robert Brandenberger, and Lavinia Heisenberg. Eternal Inflation, Entropy Bounds and the Swampland. *Eur. Phys. J. C*, 80(9):864, 2020.
- [215] Jose J. Blanco-Pillado, Heling Deng, and Alexander Vilenkin. Eternal Inflation in Swampy Landscapes. *JCAP*, 05:014, 2020.
- [216] Chia-Min Lin. Topological Eternal Hilltop Inflation and the Swampland Criteria. *JCAP*, 06:015, 2020.
- [217] Tom Banks. On the Limits of Effective Quantum Field Theory: Eternal Inflation, Landscapes, and Other Mythical Beasts. 10 2019.
- [218] Min-Seok Seo. Eternal inflation in light of Wheeler-DeWitt equation. *JCAP*, 11:007, 2020.
- [219] Ana Achúcarro and Gonzalo A. Palma. The string swampland constraints require multi-field inflation. *JCAP*, 02:041, 2019.
- [220] William H. Kinney, Sunny Vagnozzi, and Luca Visinelli. The zoo plot meets the swampland: mutual (in)consistency of single-field inflation, string conjectures, and cosmological data. *Class. Quant. Grav.*, 36(11):117001, 2019.
- [221] S. Weinberg. *Cosmology*. Oxford University Press 10001 Derekwood Lane, Suite 100 Lanham, MD 20706-4876 United States of America, 2008.
- [222] Piotr Chankowski. Quantum field theory lecture notes.
- [223] H. Lehmann, Kurt Symanzik, and W. Zimmermann. Zur formulierung quantisierter feldtheorien. *Il Nuovo Cimento (1955-1965)*, 1:205–225, 1955.
- [224] Piotr H. Chankowski, Adrian Lewandowski, and Krzysztof A. Meissner. Two-loop RGE of a general renormalizable Yang-Mills theory in a renormalization scheme with an explicit UV cutoff. *JHEP*, 11:105, 2016.
- [225] Curtis G. Callan. Broken scale invariance in scalar field theory. *Phys. Rev. D*, 2:1541–1547, Oct 1970.

- [226] K. Symanzik. Small distance behavior in field theory and power counting. *Commun. Math. Phys.*, 18:227–246, 1970.
- [227] R. Slansky. Group Theory for Unified Model Building. *Phys. Rept.*, 79:1–128, 1981.
- [228] S. D. Drell. Quantum electrodynamics at small distances. *Annals Phys.*, 4:75–80, 1958.
- [229] M. Gockeler, R. Horsley, V. Linke, Paul E. L. Rakow, G. Schierholz, and H. Stüber. Is there a Landau pole problem in QED? *Phys. Rev. Lett.*, 80:4119–4122, 1998.
- [230] Holger Gies and Joerg Jaeckel. Renormalization flow of QED. *Phys. Rev. Lett.*, 93:110405, 2004.
- [231] Leo P. Kadanoff. Scaling laws for ising models near T_c . *Physics Physique Fizika*, 2:263–272, Jun 1966.
- [232] K. M. Case. Singular potentials. *Phys. Rev.*, 80:797–806, Dec 1950.
- [233] S. R. Beane, P. F. Bedaque, L. Childress, A. Kryjevski, J. McGuire, and U. van Kolck. Singular potentials and limit cycles. *Phys. Rev. A*, 64:042103, Sep 2001.
- [234] M. Bawin and S. A. Coon. The Singular inverse square potential, limit cycles and selfadjoint extensions. *Phys. Rev. A*, 67:042712, 2003.
- [235] Sidney A. Coon and Barry R. Holstein. Anomalies in quantum mechanics: The $1/r^2$ potential. *American Journal of Physics*, 70(5):513–519, 2002.
- [236] Eric Braaten and Demian Phillips. Renormalization-group limit cycle for the $1/r^2$ potential. *Phys. Rev. A*, 70:052111, Nov 2004.
- [237] H. W. Hammer and Brian G. Swingle. On the limit cycle for the $1/r^{**2}$ potential in momentum space. *Annals Phys.*, 321:306–317, 2006.
- [238] H. W. Hammer and R. Higa. A model study of discrete scale invariance and long-range interactions. *The European Physical Journal A*, 37(2):193–200, 2008.
- [239] B. Long and U. van Kolck. Renormalization of Singular Potentials and Power Counting. *Annals Phys.*, 323:1304–1323, 2008.
- [240] Sidney R. Coleman and Erick J. Weinberg. Radiative Corrections as the Origin of Spontaneous Symmetry Breaking. *Phys. Rev.*, D7:1888–1910, 1973.
- [241] David B. Kaplan, Jong-Wan Lee, Dam T. Son, and Mikhail A. Stephanov. Conformality Lost. *Phys. Rev. D*, 80:125005, 2009.
- [242] Kenneth G. Wilson. Model hamiltonians for local quantum field theory. *Phys. Rev.*, 140:B445–B457, Oct 1965.
- [243] Kenneth G. Wilson. The Renormalization Group and Strong Interactions. *Phys. Rev. D*, 3:1818, 1971.

- [244] Stanislaw D. Glazek and Kenneth G. Wilson. Limit cycles in quantum theories. *Phys. Rev. Lett.*, 89:230401, 2002. [Erratum: Phys.Rev.Lett. 92, 139901 (2004)].
- [245] Stanislaw D. Glazek and Kenneth G. Wilson. Universality, marginal operators, and limit cycles. *Phys. Rev. B*, 69:094304, 2004.
- [246] Kenneth G. Wilson, Timothy S. Walhout, Avaroth Harindranath, Wei-Min Zhang, Robert J. Perry, and Stanislaw D. Glazek. Nonperturbative QCD: A Weak coupling treatment on the light front. *Phys. Rev. D*, 49:6720–6766, 1994.
- [247] Stanislaw D. Glazek. Limit cycles of effective theories. *Phys. Rev. D*, 75:025005, 2007.
- [248] David Skinner. Lecture notes: Quantum Field Theory II.
- [249] Joseph Polchinski. Renormalization and Effective Lagrangians. *Nucl. Phys. B*, 231:269–295, 1984.
- [250] Jan M. Pawłowski. Aspects of the functional renormalisation group. *Annals Phys.*, 322:2831–2915, 2007.
- [251] Holger Gies. Introduction to the functional RG and applications to gauge theories. *Lect. Notes Phys.*, 852:287–348, 2012.
- [252] Manuel Reichert. Lecture notes: Functional Renormalisation Group and Asymptotically Safe Quantum Gravity. *PoS*, 384:005, 2020.
- [253] C. Wetterich. Quantum scale symmetry. 2019.
- [254] N. Dupuis, L. Canet, A. Eichhorn, W. Metzner, J.M. Pawłowski, M. Tissier, and N. Wschebor. The nonperturbative functional renormalization group and its applications. 6 2020.
- [255] B. de Wit and H. Nicolai. N=8 Supergravity. *Nucl. Phys. B*, 208:323, 1982.
- [256] R.E. Kallosh. Counterterms in extended supergravities. *Phys. Lett. B*, 99:122–127, 1981.
- [257] Renata Kallosh. The Ultraviolet Finiteness of N=8 Supergravity. *JHEP*, 12:009, 2010.
- [258] Z. Bern, J. J. Carrasco, Lance J. Dixon, Henrik Johansson, D. A. Kosower, and R. Roiban. Three-Loop Superfiniteness of N=8 Supergravity. *Phys. Rev. Lett.*, 98:161303, 2007.
- [259] Z. Bern, J. J. M. Carrasco, and H. Johansson. Progress on Ultraviolet Finiteness of Supergravity. *Subnucl. Ser.*, 46:251–276, 2011.
- [260] Zvi Bern, John Joseph Carrasco, Wei-Ming Chen, Henrik Johansson, and Radu Roiban. Gravity Amplitudes as Generalized Double Copies of Gauge-Theory Amplitudes. *Phys. Rev. Lett.*, 118(18):181602, 2017.
- [261] Z. Bern, J. J. M. Carrasco, and Henrik Johansson. New Relations for Gauge-Theory Amplitudes. *Phys. Rev. D*, 78:085011, 2008.

- [262] Zvi Bern, John Joseph M. Carrasco, and Henrik Johansson. Perturbative Quantum Gravity as a Double Copy of Gauge Theory. *Phys. Rev. Lett.*, 105:061602, 2010.
- [263] Nemanja Kaloper and Krzysztof A. Meissner. Duality beyond the first loop. *Phys. Rev. D*, 56:7940–7953, 1997.
- [264] Wataru Souma. Nontrivial ultraviolet fixed point in quantum gravity. *Prog. Theor. Phys.*, 102:181–195, 1999.
- [265] M. Reuter and Frank Saueressig. Renormalization group flow of quantum gravity in the Einstein-Hilbert truncation. *Phys. Rev. D*, 65:065016, 2002.
- [266] Dario Benedetti, Pedro F. Machado, and Frank Saueressig. Asymptotic safety in higher-derivative gravity. *Mod. Phys. Lett. A*, 24:2233–2241, 2009.
- [267] Yannick Kluth and Daniel F. Litim. Fixed Points of Quantum Gravity and the Dimensionality of the UV Critical Surface. 8 2020.
- [268] Astrid Eichhorn. Faddeev-Popov ghosts in quantum gravity beyond perturbation theory. *Phys. Rev. D*, 87(12):124016, 2013.
- [269] Kai Groh and Frank Saueressig. Ghost wave-function renormalization in Asymptotically Safe Quantum Gravity. *J. Phys. A*, 43:365403, 2010.
- [270] Holger Gies. Running coupling in Yang-Mills theory: A flow equation study. *Phys. Rev. D*, 66:025006, 2002.
- [271] Dario Benedetti, Kai Groh, Pedro F. Machado, and Frank Saueressig. The Universal RG Machine. *JHEP*, 06:079, 2011.
- [272] Holger Gies, Benjamin Knorr, and Stefan Lippoldt. Generalized Parametrization Dependence in Quantum Gravity. *Phys. Rev. D*, 92(8):084020, 2015.
- [273] D. F. Litim. Optimized renormalization group flows. *Phys. Rev.*, D64:105007, 2001.
- [274] Astrid Eichhorn and Stefan Lippoldt. Quantum gravity and Standard-Model-like fermions. *Phys. Lett. B*, 767:142–146, 2017.
- [275] Pietro Dona and Roberto Percacci. Functional renormalization with fermions and tetrads. *Phys. Rev. D*, 87(4):045002, 2013.
- [276] Astrid Eichhorn and Aaron Held. Viability of quantum-gravity induced ultraviolet completions for matter. *Phys. Rev. D*, 96(8):086025, 2017.
- [277] Astrid Eichhorn, Stefan Lippoldt, and Marc Schiffer. Zooming in on fermions and quantum gravity. *Phys. Rev. D*, 99(8):086002, 2019.
- [278] A. Eichhorn. Status of the asymptotic safety paradigm for quantum gravity and matter. In *Black Holes, Gravitational Waves and Spacetime Singularities Rome, Italy, May 9-12, 2017*, 2017.
- [279] Astrid Eichhorn. Asymptotically safe gravity. In *57th International School of Subnuclear Physics: In Search for the Unexpected*, 2 2020.

- [280] Holger Gies, Benjamin Knorr, Stefan Lippoldt, and Frank Saueressig. Gravitational Two-Loop Counterterm Is Asymptotically Safe. *Phys. Rev. Lett.*, 116(21):211302, 2016.
- [281] Jan-Eric Daum, Ulrich Harst, and Martin Reuter. Running Gauge Coupling in Asymptotically Safe Quantum Gravity. *JHEP*, 01:084, 2010.
- [282] U. Harst and M. Reuter. QED coupled to QEG. *JHEP*, 05:119, 2011.
- [283] Sarah Folkerts, Daniel F. Litim, and Jan M. Pawłowski. Asymptotic freedom of Yang-Mills theory with gravity. *Phys. Lett. B*, 709:234–241, 2012.
- [284] Astrid Eichhorn and Fleur Versteegen. Upper bound on the Abelian gauge coupling from asymptotic safety. *JHEP*, 01:030, 2018.
- [285] Nicolai Christiansen and Astrid Eichhorn. An asymptotically safe solution to the $U(1)$ triviality problem. *Phys. Lett. B*, 770:154–160, 2017.
- [286] Nicolai Christiansen, Daniel F. Litim, Jan M. Pawłowski, and Manuel Reichert. Asymptotic safety of gravity with matter. *Phys. Rev. D*, 97(10):106012, 2018.
- [287] Astrid Eichhorn and Aaron Held. Mass difference for charged quarks from asymptotically safe quantum gravity. *Phys. Rev. Lett.*, 121(15):151302, 2018.
- [288] Astrid Eichhorn and Marc Schiffer. $d = 4$ as the critical dimensionality of asymptotically safe interactions. *Phys. Lett. B*, 793:383–389, 2019.
- [289] O. Zanusso, L. Zambelli, G. P. Vacca, and R. Percacci. Gravitational corrections to Yukawa systems. *Phys. Lett. B*, 689:90–94, 2010.
- [290] Kin-ya Oda and Masatoshi Yamada. Non-minimal coupling in Higgs–Yukawa model with asymptotically safe gravity. *Class. Quant. Grav.*, 33(12):125011, 2016.
- [291] Astrid Eichhorn, Aaron Held, and Jan M. Pawłowski. Quantum-gravity effects on a Higgs–Yukawa model. *Phys. Rev. D*, 94(10):104027, 2016.
- [292] M. Shaposhnikov and Ch. Wetterich. Asymptotic safety of gravity and the Higgs boson mass. *Phys. Lett. B*, 683:196–200, 2010.
- [293] L. Laulumaa. Higgs mass predicted from the standard model with asymptotically safe gravity. Master’s thesis, Jyväskylä U., 2016.
- [294] R. Percacci and D. Perini. Asymptotic safety of gravity coupled to matter. *Phys. Rev. D*, 68:044018, Aug 2003.
- [295] G. Narain and R. Percacci. Renormalization Group Flow in Scalar-Tensor Theories. I. *Class. Quant. Grav.*, 27:075001, 2010.
- [296] A. Eichhorn and A. Held. Top mass from asymptotic safety. *Phys. Lett.*, B777:217–221, 2018.
- [297] A. Eichhorn and A. Held. Mass difference for charged quarks from asymptotically safe quantum gravity. *Phys. Rev. Lett.*, 121(15):151302, 2018.

- [298] Yu Hamada, Koji Tsumura, and Masatoshi Yamada. Scalegenesis and fermionic dark matters in the flatland scenario. *Eur. Phys. J. C*, 80(5):368, 2020.
- [299] Artur R. Pietrykowski. Gauge dependence of gravitational correction to running of gauge couplings. *Phys. Rev. Lett.*, 98:061801, 2007.
- [300] David J. Toms. Quantum gravity and charge renormalization. *Phys. Rev. D*, 76:045015, 2007.
- [301] Dietmar Ebert, Jan Plefka, and Andreas Rodigast. Absence of gravitational contributions to the running Yang-Mills coupling. *Phys. Lett. B*, 660:579–582, 2008.
- [302] David J. Toms. Quantum gravitational contributions to quantum electrodynamics. *Nature*, 468:56–59, 2010.
- [303] Mohamed M. Anber, John F. Donoghue, and Mohamed El-Houssieny. Running couplings and operator mixing in the gravitational corrections to coupling constants. *Phys. Rev. D*, 83:124003, 2011.
- [304] S. Mandelstam. Determination of the pion - nucleon scattering amplitude from dispersion relations and unitarity. General theory. *Phys. Rev.*, 112:1344–1360, 1958.
- [305] Leonardo Chataignier, Tomislav Prokopec, Michael G. Schmidt, and Bogumila Swiezewska. Single-scale Renormalisation Group Improvement of Multi-scale Effective Potentials. *JHEP*, 03:014, 2018.
- [306] Anders Andreassen, William Frost, and Matthew D. Schwartz. Consistent Use of Effective Potentials. *Phys. Rev. D*, 91(1):016009, 2015.
- [307] Anders Andreassen, William Frost, and Matthew D. Schwartz. Consistent Use of the Standard Model Effective Potential. *Phys. Rev. Lett.*, 113(24):241801, 2014.
- [308] Tom Draper, Benjamin Knorr, Chris Ripken, and Frank Saueressig. Graviton-Mediated Scattering Amplitudes from the Quantum Effective Action. *JHEP*, 11:136, 2020.
- [309] Alessia Platania. From renormalization group flows to cosmology. *Front. in Phys.*, 8:188, 2020.
- [310] Alfio Bonanno and Martin Reuter. Quantum gravity effects near the null black hole singularity. *Phys. Rev. D*, 60:084011, 1999.
- [311] A. Bonanno and M. Reuter. Spacetime structure of an evaporating black hole in quantum gravity. *Phys. Rev. D*, 73:083005, 2006.
- [312] Carlo Pagani and Martin Reuter. Finite Entanglement Entropy in Asymptotically Safe Quantum Gravity. *JHEP*, 07:039, 2018.
- [313] Alfio Bonanno and Alessia Platania. Asymptotically safe inflation from quadratic gravity. *Phys. Lett. B*, 750:638–642, 2015.

- [314] Jan M. Pawłowski and Manuel Reichert. Quantum Gravity: A Fluctuating Point of View. *Front. in Phys.*, 8:551848, 2021.
- [315] Tobias Denz, Jan M. Pawłowski, and Manuel Reichert. Towards apparent convergence in asymptotically safe quantum gravity. *Eur. Phys. J. C*, 78(4):336, 2018.
- [316] Astrid Eichhorn, Peter Labus, Jan M. Pawłowski, and Manuel Reichert. Effective universality in quantum gravity. *SciPost Phys.*, 5(4):031, 2018.
- [317] Astrid Eichhorn, Stefan Lippoldt, Jan M. Pawłowski, Manuel Reichert, and Marc Schiffer. How perturbative is quantum gravity? *Phys. Lett. B*, 792:310–314, 2019.
- [318] Nicolai Christiansen, Benjamin Knorr, Jan M. Pawłowski, and Andreas Rodigast. Global Flows in Quantum Gravity. *Phys. Rev. D*, 93(4):044036, 2016.
- [319] Nicolai Christiansen, Benjamin Knorr, Jan Meibohm, Jan M. Pawłowski, and Manuel Reichert. Local Quantum Gravity. *Phys. Rev. D*, 92(12):121501, 2015.
- [320] Nicolai Christiansen, Kevin Falls, Jan M. Pawłowski, and Manuel Reichert. Curvature dependence of quantum gravity. *Phys. Rev. D*, 97(4):046007, 2018.
- [321] Benjamin Bürger, Jan M. Pawłowski, Manuel Reichert, and Bernd-Jochen Schaefer. Curvature dependence of quantum gravity with scalars. 12 2019.
- [322] Benjamin Knorr, Chris Ripken, and Frank Saueressig. Form Factors in Asymptotic Safety: conceptual ideas and computational toolbox. *Class. Quant. Grav.*, 36(23):234001, 2019.
- [323] Tom Draper, Benjamin Knorr, Chris Ripken, and Frank Saueressig. Finite Quantum Gravity Amplitudes: No Strings Attached. *Phys. Rev. Lett.*, 125(18):181301, 2020.
- [324] Benjamin Knorr, Chris Ripken, and Frank Saueressig. Form Factors in Quantum Gravity - contrasting non-local, ghost-free gravity and Asymptotic Safety. 11 2021.
- [325] Benjamin Knorr and Marc Schiffer. Non-Perturbative Propagators in Quantum Gravity. *Universe*, 7(7):216, 2021.
- [326] Marcel Froissart. Asymptotic behavior and subtractions in the mandelstam representation. *Phys. Rev.*, 123:1053–1057, Aug 1961.
- [327] D.J. Gross and J. Wess. Scale invariance, conformal invariance, and the high-energy behavior of scattering amplitudes. *Phys. Rev. D*, 2:753–764, 1970.
- [328] Y. Nambu. Quark model and the factorization of the Veneziano amplitude. In Ramesh Chand, editor, *Symmetries and Quark Models*, page 269, January 1970.
- [329] D. Amati, M. Ciafaloni, and G. Veneziano. Superstring Collisions at Planckian Energies. *Phys. Lett. B*, 197:81, 1987.
- [330] David J. Gross and Paul F. Mende. String Theory Beyond the Planck Scale. *Nucl. Phys. B*, 303:407–454, 1988.

- [331] D. Amati, M. Ciafaloni, and G. Veneziano. Classical and Quantum Gravity Effects from Planckian Energy Superstring Collisions. *Int. J. Mod. Phys. A*, 3:1615–1661, 1988.
- [332] Corinne De Lacroix, Harold Erbin, and Ashoke Sen. Analyticity and Crossing Symmetry of Superstring Loop Amplitudes. *JHEP*, 05:139, 2019.
- [333] D. Friedan. Nonlinear models in $2+\epsilon$ dimensions. *Phys. Rev. Lett.*, 45:1057–1060, Sep 1980.
- [334] Jr. Callan, Curtis G., E.J. Martinec, M.J. Perry, and D. Friedan. Strings in Background Fields. *Nucl. Phys. B*, 262:593–609, 1985.
- [335] Sidney R. Coleman. The Fate of the False Vacuum. 1. Semiclassical Theory. *Phys. Rev. D*, 15:2929–2936, 1977. [Erratum: Phys.Rev.D 16, 1248 (1977)].
- [336] Stefano Bertolini, Luca Di Luzio, and Michal Malinsky. Intermediate mass scales in the non-supersymmetric SO(10) grand unification: A Reappraisal. *Phys. Rev.*, D80:015013, 2009.
- [337] Tommy Ohlsson, Marcus Pernow, and Erik Sönerlind. Realizing unification in two different SO(10) models with one intermediate breaking scale. *Eur. Phys. J. C*, 80(11):1089, 2020.
- [338] Borut Bajc, Alejandra Melfo, Goran Senjanovic, and Francesco Vissani. Yukawa sector in non-supersymmetric renormalizable SO(10). *Phys. Rev. D*, 73:055001, 2006.
- [339] Masaki Yasuè. Symmetry breaking of so(10) and constraints on the higgs potential: Adjoint 45 and spinorial 16 representations. *Phys. Rev. D*, 24:1005–1013, Aug 1981.
- [340] Masaki Yasue. HOW TO BREAK SO(10) VIA SO(4) x SO(6) DOWN TO SU(2)(L) x SU(3)(C) x U(1). *Phys. Lett. B*, 103:33–38, 1981.
- [341] G. Anastaze, J. P. Derendinger, and F. Buccella. INTERMEDIATE SYMMETRIES IN THE SO(10) MODEL WITH (16+16) + 45 HIGGSES. *Z. Phys. C*, 20:269–273, 1983.
- [342] K. S. Babu and Ernest Ma. Symmetry Breaking in SO(10): Higgs Boson Structure. *Phys. Rev. D*, 31:2316, 1985.
- [343] Mark Hindmarsh. Analytic scaling solutions for cosmic domain walls. *Phys. Rev. Lett.*, 77:4495–4498, 1996.
- [344] Graciela B. Gelmini, Marcelo Gleiser, and Edward W. Kolb. Cosmology of biased discrete symmetry breaking. *Phys. Rev. D*, 39:1558–1566, Mar 1989.
- [345] Z. Lalak, S. Lola, Burt A. Ovrut, and Graham G. Ross. Large scale structure from biased nonequilibrium phase transitions: Percolation theory picture. *Nucl. Phys.*, B434:675–696, 1995.

- [346] D. Coulson, Z. Lalak, and Burt A. Ovrut. Nonequilibrium phase transitions and domain walls. In *Particles, strings and cosmology. Proceedings, 19th Johns Hopkins Workshop and 5th PASCOS Interdisciplinary Symposium, Baltimore, USA, March 22–25, 1995*, pages 429–444, 1995.
- [347] D. Coulson, Z. Lalak, and Burt A. Ovrut. Biased domain walls. *Phys. Rev. D*, 53:4237–4246, 1996.
- [348] Sebastian E. Larsson, Subir Sarkar, and Peter L. White. Evading the cosmological domain wall problem. *Phys. Rev. D*, 55:5129–5135, 1997.
- [349] Z. Lalak, S. Lola, and P. Magnowski. Dynamics of domain walls for split and runaway potentials. *Phys. Rev.*, D78:085020, 2008.
- [350] P. P. Avelino, D. Bazeia, R. Menezes, and J. C. R. E. Oliveira. Bifurcation and pattern changing with two real scalar fields. *Phys. Rev. D*, 79:085007, Apr 2009.
- [351] J. R. C. C. C. Correia, I. S. C. R. Leite, and C. J. A. P. Martins. Effects of Biases in Domain Wall Network Evolution. *Phys. Rev.*, D90(2):023521, 2014.
- [352] J. R. C. C. C. Correia, I. S. C. R. Leite, and C. J. A. P. Martins. Effects of biases in domain wall network evolution. II. Quantitative analysis. *Phys. Rev. D*, 97(8):083521, 2018.
- [353] William H. Press, Barbara S. Ryden, and David N. Spergel. Dynamical Evolution of Domain Walls in an Expanding Universe. *Astrophys. J.*, 347:590–604, 1989.
- [354] Tomasz Krajewski, Zygmunt Lalak, Marek Lewicki, and Paweł Olszewski. Domain walls and gravitational waves in the Standard Model. *JCAP*, 1612(12):036, 2016.
- [355] Tomasz Krajewski, Zygmunt Lalak, Marek Lewicki, and Paweł Olszewski. Domain walls in the extensions of the Standard Model. *JCAP*, 1805(05):007, 2018.
- [356] Tomasz Krajewski, Zygmunt Lalak, Marek Lewicki, and Paweł Olszewski. Higgs domain walls in the thermal background. *Phys. Dark Univ.*, 26:100347, 2019.
- [357] Edward W. Kolb and Michael S. Turner. *The Early Universe*, volume 69. 1990.
- [358] Alexander Friedland, Hitoshi Murayama, and Maxim Perelstein. Domain walls as dark energy. *Phys. Rev. D*, 67:043519, 2003.
- [359] Alessandro Melchiorri, Laura Mersini, Carolina J. Ödman, and Mark Trodden. The state of the dark energy equation of state. *Phys. Rev. D*, 68:043509, Aug 2003.
- [360] D. N. Spergel et al. First year Wilkinson Microwave Anisotropy Probe (WMAP) observations: Determination of cosmological parameters. *Astrophys. J. Suppl.*, 148:175–194, 2003.
- [361] Max Tegmark et al. Cosmological parameters from SDSS and WMAP. *Phys. Rev. D*, 69:103501, 2004.
- [362] Luca Conversi, Alessandro Melchiorri, Laura Mersini-Houghton, and Joseph Silk. Are domain walls ruled out? *Astropart. Phys.*, 21:443–449, 2004.

- [363] P. P. Avelino, V. M. C. Ferreira, J. Menezes, and L. Sousa. Phantom Domain Walls. *Phys. Rev. D*, 96(4):043506, 2017.
- [364] P.A. Zyla et al. Review of Particle Physics. *PTEP*, 2020(8):083C01, 2020.
- [365] Michael S. Chanowitz, John R. Ellis, and Mary K. Gaillard. The Price of Natural Flavor Conservation in Neutral Weak Interactions. *Nucl. Phys.*, B128:506–536, 1977.
- [366] A. J. Buras, John R. Ellis, M. K. Gaillard, and Dimitri V. Nanopoulos. Aspects of the Grand Unification of Strong, Weak and Electromagnetic Interactions. *Nucl. Phys.*, B135:66–92, 1978.
- [367] Howard Georgi and C. Jarlskog. A New Lepton - Quark Mass Relation in a Unified Theory. *Phys. Lett.*, 86B:297–300, 1979.
- [368] Lohan Sartore and Ingo Schienbein. PyR@TE 3. 7 2020.
- [369] Aaron Held. Effective asymptotic safety and its predictive power: Gauge-Yukawa theories. *Front. in Phys.*, 8:341, 2020.
- [370] Astrid Eichhorn, Aaron Held, and Christof Wetterich. Predictive power of grand unification from quantum gravity. *JHEP*, 08:111, 2020.
- [371] C. Wetterich and M. Yamada. Variable Planck mass from gauge invariant flow equation. 2019.
- [372] C. Wetterich. Effective scalar potential in asymptotically safe quantum gravity. *Universe*, 7(2):45, 2021.
- [373] Pran Nath and Pavel Fileviez Perez. Proton stability in grand unified theories, in strings and in branes. *Phys. Rept.*, 441:191–317, 2007.
- [374] Cosimo Bambi and Katherine Freese. Dangerous implications of a minimum length in quantum gravity. *Class. Quant. Grav.*, 25:195013, 2008.
- [375] Astrid Eichhorn, Aaron Held, and Christof Wetterich. Quantum-gravity predictions for the fine-structure constant. *Phys. Lett. B*, 782:198–201, 2018.
- [376] D. L. Bennett and Holger Bech Nielsen. Predictions for nonAbelian fine structure constants from multicriticality. *Int. J. Mod. Phys.*, A9:5155–5200, 1994.
- [377] C. D. Froggatt and Holger Bech Nielsen. Standard model criticality prediction: Top mass 173 ± 5 -GeV and Higgs mass 135 ± 9 -GeV. *Phys. Lett.*, B368:96–102, 1996.
- [378] C. D. Froggatt and H. B. Nielsen. Trying to understand the standard model parameters. *Surveys High Energ. Phys.*, 18:55–75, 2003.
- [379] B. G. Sidharth, C. R. Das, C. D. Froggatt, H. B. Nielsen, and Larisa Laperashvili. Degenerate Vacua of the Universe and What Comes Beyond the Standard Model. 2018.

- [380] Marie E. Machacek and Michael T. Vaughn. Two Loop Renormalization Group Equations in a General Quantum Field Theory. 3. Scalar Quartic Couplings. *Nucl. Phys. B*, 249:70–92, 1985.
- [381] H. Arason, D. J. Castano, B. Kesthelyi, S. Mikaelian, E. J. Piard, Pierre Ramond, and B. D. Wright. Renormalization group study of the standard model and its extensions. 1. The Standard model. *Phys. Rev.*, D46:3945–3965, 1992.
- [382] A. V. Bednyakov, B. A. Kniehl, A. F. Pikelner, and O. L. Veretin. On the b -quark running mass in QCD and the SM. *Nucl. Phys.*, B916:463–483, 2017.
- [383] A. Lewandowski, K. A. Meissner, and H. Nicolai. Conformal Standard Model, Leptogenesis and Dark Matter. *Phys. Rev. D*, 97(3):035024, 2018.
- [384] A. Boyarsky, O. Ruchayskiy, and M. Shaposhnikov. The Role of sterile neutrinos in cosmology and astrophysics. *Ann. Rev. Nucl. Part. Sci.*, 59:191–214, 2009.
- [385] M. Shaposhnikov. Is there a new physics between electroweak and Planck scales? In *Astroparticle Physics: Current Issues, 2007 (APCI07) Budapest, Hungary, June 21-23, 2007*, 2007.
- [386] A. Pilaftsis and T. E. J. Underwood. Resonant leptogenesis. *Nuc. Phys. B*, 692(3):303 – 345, 2004.
- [387] Astrid Eichhorn, Yuta Hamada, Johannes Lumma, and Masatoshi Yamada. Quantum gravity fluctuations flatten the Planck-scale Higgs potential. *Phys. Rev. D*, 97(8):086004, 2018.
- [388] C. Coriano and R. L. Delle and C. Marzo. Constraints on abelian extensions of the Standard Model from two-loop vacuum stability and $U(1)_{B-L}$. *JHEP*, 02:135, 2016.
- [389] L. Griguolo and R. Percacci. The Beta functions of a scalar theory coupled to gravity. *Phys. Rev. D*, 52:5787–5798, 1995.
- [390] R. Percacci and D. Perini. Asymptotic safety of gravity coupled to matter. *Phys. Rev. D*, 68:044018, 2003.
- [391] Alberto Salvio and Alessandro Strumia. Agravity. *JHEP*, 06:080, 2014.
- [392] A. Salvio and A. Strumia. Agravity up to infinite energy. *Eur. Phys. J.*, C78(2):124, 2018.
- [393] Astrid Eichhorn and Aaron Held. Top mass from asymptotic safety. *Phys. Lett. B*, 777:217–221, 2018.
- [394] John Ellis and Mary K. Gaillard. Strong and weak cp violation. *Nuclear Physics B*, 150:141–162, 1979.
- [395] Luca Di Luzio, Federico Mescia, and Enrico Nardi. Redefining the Axion Window. *Phys. Rev. Lett.*, 118(3):031801, 2017.
- [396] Luca Di Luzio, Federico Mescia, and Enrico Nardi. Window for preferred axion models. *Phys. Rev. D*, 96(7):075003, 2017.

- [397] R. D. Peccei and Helen R. Quinn. CP Conservation in the Presence of Instantons. *Phys. Rev. Lett.*, 38:1440–1443, 1977.
- [398] F. Wilczek. Problem of strong p and t invariance in the presence of instantons. *Phys. Rev. Lett.*, 40:279–282, Jan 1978.
- [399] Steven Weinberg. A new light boson? *Phys. Rev. Lett.*, 40:223–226, Jan 1978.
- [400] A P Zhitnitskii. Possible suppression of axion-hadron interactions. *Sov. J. Nucl. Phys. (Engl. Transl.); (United States)*, 31:2, 2 1980.
- [401] Michael Dine, Willy Fischler, and Mark Srednicki. A simple solution to the strong cp problem with a harmless axion. *Physics Letters B*, 104(3):199–202, 1981.
- [402] J. E. Kim. Weak-interaction singlet and strong CP invariance. *Phys. Rev. Lett.*, 43:103–107, Jul 1979.
- [403] M. A. Shifman, A. Vainshtein, and V. I. Zakharov. Can confinement ensure natural cp invariance of strong interactions? *Nuclear Physics B*, 166:493–506, apr 1980.
- [404] Stefano Di Chiara, Venus Keus, and Oleg Lebedev. Stabilizing the Higgs potential with a Z' . *Phys. Lett.*, B744:59–66, 2015.
- [405] Paul Langacker. The Physics of Heavy Z' Gauge Bosons. *Rev. Mod. Phys.*, 81:1199–1228, 2009.
- [406] P. H. Chankowski, S. Pokorski, and J. Wagner. Z -prime and the Appelquist-Carrazzone decoupling. *Eur. Phys. J.*, C47:187–205, 2006.
- [407] L. Basso. *Phenomenology of the minimal B-L extension of the Standard Model at the LHC*. PhD thesis, Southampton U., 2011.
- [408] M. Tanabashi et al. Review of particle physics. *Phys. Rev. D*, 98:030001, Aug 2018.
- [409] Roel Aaij et al. Angular analysis of the $B^0 \rightarrow K^{*0}\mu^+\mu^-$ decay using 3 fb^{-1} of integrated luminosity. *JHEP*, 02:104, 2016.
- [410] R. Aaij et al. Test of lepton universality with $B^0 \rightarrow K^{*0}\ell^+\ell^-$ decays. *JHEP*, 08:055, 2017.
- [411] Aristizabal D. Sierra, Florian Staub, and Avelino Vicente. Shedding light on the $b \rightarrow s$ anomalies with a dark sector. *Phys. Rev.*, D92(1):015001, 2015.
- [412] Wolfgang Altmannshofer and David M. Straub. New physics in $b \rightarrow s$ transitions after LHC run 1. *Eur. Phys. J.*, C75(8):382, 2015.
- [413] Arindam Das, Nobuchika Okada, and Nathan Papapietro. Electroweak vacuum stability in classically conformal B-L extension of the Standard Model. *Eur. Phys. J.*, C77(2):122, 2017.
- [414] F. del Aguila, G. D. Coughlan, and M. Quiros. Gauge Coupling Renormalization With Several U(1) Factors. *Nucl. Phys.*, B307:633, 1988. [Erratum: Nucl. Phys.B312,751(1989)].

- [415] Ming-xing Luo and Yong Xiao. Renormalization group equations in gauge theories with multiple U(1) groups. *Phys. Lett.*, B555:279–286, 2003.
- [416] Cheng-Wei Chiang, Takaaki Nomura, and Kei Yagyu. Phenomenology of E_6 -Inspired Leptophobic Z' Boson at the LHC. *JHEP*, 05:106, 2014.
- [417] Zhi-Wei Wang, Frederick S. Sage, T. G. Steele, and R. B. Mann. Asymptotic Safety in the Conformal Hidden Sector? *J. Phys. G*, 45(9):095002, 2018.
- [418] Astrid Eichhorn and Martin Pauly. Constraining power of asymptotic safety for scalar fields. *Phys. Rev. D*, 103(2):026006, 2021.
- [419] Astrid Eichhorn, Martin Pauly, and Shouryya Ray. Towards a Higgs mass determination in asymptotically safe gravity with a dark portal. *JHEP*, 10:100, 2021.
- [420] Gustavo P. de Brito, Astrid Eichhorn, and Rafael Robson Lino dos Santos. The weak-gravity bound and the need for spin in asymptotically safe matter-gravity models. *JHEP*, 11:110, 2021.
- [421] Marc Schiffer. *Probing Quantum Gravity: Theoretical and phenomenological consistency tests of asymptotically safe quantum gravity*. PhD thesis, U. Heidelberg (main), 2021.
- [422] Benjamin Knorr. The derivative expansion in asymptotically safe quantum gravity: general setup and quartic order. *SciPost Phys.*, 4(3):020, 2021.
- [423] W. Heisenberg and H. Euler. Consequences of Dirac’s theory of positrons. *Z. Phys.*, 98(11-12):714–732, 1936.
- [424] David Brizuela, Jose M. Martin-Garcia, and Guillermo A. Mena Marugan. xPert: Computer algebra for metric perturbation theory. *Gen. Rel. Grav.*, 41:2415–2431, 2009.
- [425] Jose M. Martin-Garcia, Renato Portugal, and Leon R. U. Manssur. The Invar Tensor Package. *Comput. Phys. Commun.*, 177:640–648, 2007.
- [426] Jose M. Martin-Garcia, David Yllanes, and Renato Portugal. The Invar tensor package: Differential invariants of Riemann. *Comput. Phys. Commun.*, 179:586–590, 2008.
- [427] José M. Martín-García. xperm: fast index canonicalization for tensor computer algebra. *Computer Physics Communications*, 179(8):597–603, 2008.
- [428] Teake Nutma. xTras : A field-theory inspired xAct package for mathematica. *Comput. Phys. Commun.*, 185:1719–1738, 2014.
- [429] Anton K. Cyrol, Mario Mitter, and Nils Strodthoff. FormTracer - A Mathematica Tracing Package Using FORM. *Comput. Phys. Commun.*, 219:346–352, 2017.
- [430] Tomislav Prokopec and Gerasimos Rigopoulos. Functional renormalization group for stochastic inflation. *JCAP*, 08:013, 2018.

- [431] Ken-ichi Nakao, Yasusada Nambu, and Misao Sasaki. Stochastic Dynamics of New Inflation. *Progress of Theoretical Physics*, 80(6):1041–1068, 12 1988.
- [432] Alexander Vilenkin. The Birth of Inflationary Universes. *Phys. Rev. D*, 27:2848, 1983.
- [433] Alexei A. Starobinsky. STOCHASTIC DE SITTER (INFLATIONARY) STAGE IN THE EARLY UNIVERSE. *Lect. Notes Phys.*, 246:107–126, 1986.
- [434] Jerome Martin and Marcello Musso. Solving stochastic inflation for arbitrary potentials. *Phys. Rev. D*, 73:043516, 2006.
- [435] Masahiro Morikawa. Dissipation and fluctuation of quantum fields in expanding universes. *Phys. Rev. D*, 42:1027–1034, Aug 1990.
- [436] Björn Garbrecht, Gerasimos Rigopoulos, and Yi Zhu. Infrared correlations in de Sitter space: Field theoretic versus stochastic approach. *Phys. Rev. D*, 89:063506, 2014.
- [437] Ian Moss and Gerasimos Rigopoulos. Effective long wavelength scalar dynamics in de Sitter. *JCAP*, 05:009, 2017.
- [438] Gerasimos Rigopoulos. Thermal Interpretation of Infrared Dynamics in de Sitter. *JCAP*, 07:035, 2016.
- [439] Xingang Chen, Yi Wang, and Zhong-Zhi Xianyu. Schwinger-Keldysh Diagrammatics for Primordial Perturbations. *JCAP*, 12:006, 2017.
- [440] Alan H. Guth. The Inflationary Universe: A Possible Solution to the Horizon and Flatness Problems. *Adv. Ser. Astrophys. Cosmol.*, 3:139–148, 1987.
- [441] Vincent Vennin and Alexei A. Starobinsky. Correlation functions in stochastic inflation. *The European Physical Journal C*, 75(9), Sep 2015.
- [442] Mahdiyar Noorbala, Vincent Vennin, Hooshyar Assadullahi, Hassan Firouzjahi, and David Wands. Tunneling in stochastic inflation. *Journal of Cosmology and Astroparticle Physics*, 2018(09):032032, Sep 2018.
- [443] A.A. Starobinsky. A new type of isotropic cosmological models without singularity. *Physics Letters B*, 91(1):99 – 102, 1980.
- [444] Alexandros Kehagias, Azadeh Moradinezhad Dizgah, and Antonio Riotto. Remarks on the Starobinsky model of inflation and its descendants. *Phys. Rev. D*, 89:043527, Feb 2014.
- [445] F. L. Bezrukov and M. Shaposhnikov. The Standard Model Higgs boson as the inflaton. *Phys. Lett. B*, 659:703–706, 2008.
- [446] Anna Ijjas, Paul J. Steinhardt, and Abraham Loeb. Inflationary paradigm in trouble after Planck2013. *Phys. Lett. B*, 723:261–266, 2013.
- [447] O. Lebedev and H. M. Lee. Higgs Portal Inflation. *Eur. Phys. J. C*, 71:1821, 2011.

- [448] Jinn-Ouk Gong, Hyun Min Lee, and Sin Kyu Kang. Inflation and dark matter in two Higgs doublet models. *Journal of High Energy Physics*, 2012(4):128, 2012.
- [449] Marieke Postma and Marco Volponi. Equivalence of the Einstein and Jordan frames. *Phys. Rev. D*, 90:103516, 2014.
- [450] Andrei Linde. Single-field α -attractors. *JCAP*, 05:003, 2015.
- [451] John Joseph M. Carrasco, Renata Kallosh, and Andrei Linde. Cosmological attractors and initial conditions for inflation. *Physical Review D*, 92(6), Sep 2015.
- [452] Renata Kallosh and Andrei Linde. Planck, LHC, and α -attractors. *Phys. Rev. D*, 91:083528, 2015.
- [453] Tomasz Krajewski, Krzysztof Turzyski, and Micha Wieczorek. On preheating in α -attractor models of inflation. *The European Physical Journal C*, 79(8), Aug 2019.
- [454] A. Bonanno and M. Reuter. Proper time flow equation for gravity. *JHEP*, 02:035, 2005.
- [455] Daniel F. Litim and Francesco Sannino. Asymptotic safety guaranteed. *Journal of High Energy Physics*, 2014(12), Dec 2014.
- [456] Daniel F. Litim, Matin Mojaza, and Francesco Sannino. Vacuum stability of asymptotically safe gauge-Yukawa theories. *JHEP*, 01:081, 2016.
- [457] Niklas Grønlund Nielsen, Francesco Sannino, and Ole Svendsen. Inflation from Asymptotically Safe Theories. *Phys. Rev. D*, 91:103521, 2015.
- [458] Ole Svendsen, Hossein Bazrafshan Moghaddam, and Robert Brandenberger. Preheating in an Asymptotically Safe Quantum Field Theory. *Phys. Rev. D*, 94(8):083527, 2016.
- [459] Jean-Luc Lehners and K. S. Stelle. Safe beginning for the universe? *Physical Review D*, 100(8), Oct 2019.
- [460] John D. Barrow. Finite Action Principle Revisited. *Phys. Rev. D*, 101(2):023527, 2020.
- [461] Breno L. Giacchini, Tibério de Paula Netto, and Leonardo Modesto. Action principle selection of regular black holes. *Phys. Rev. D*, 104(8):084072, 2021.
- [462] Akihiro Ishibashi, Nobuyoshi Ohta, and Daiki Yamaguchi. Quantum improved charged black holes. *Phys. Rev. D*, 104(6):066016, 2021.
- [463] Elisa Manrique and Martin Reuter. Bare Action and Regularized Functional Integral of Asymptotically Safe Quantum Gravity. *Phys. Rev. D*, 79:025008, 2009.
- [464] Tim R. Morris and Zoë H. Slade. Solutions to the reconstruction problem in asymptotic safety. *JHEP*, 11:094, 2015.

- [465] Rong-Gen Cai and Anzhong Wang. Singularities in horava lifshitz theory. *Physics Letters B*, 686(2-3):166174, Mar 2010.
- [466] H. Lü, Jianwei Mei, and C. N. Pope. Solutions to horava gravity. *Physical Review Letters*, 103(9), Aug 2009.
- [467] R. Arnowitt, S. Deser, and C. W. Misner. Dynamical structure and definition of energy in general relativity. *Phys. Rev.*, 116:1322–1330, Dec 1959.
- [468] Adriano Contillo, Stefan Rechenberger, and Frank Saueressig. Renormalization group flow of Hořava-Lifshitz gravity at low energies. *JHEP*, 12:017, 2013.
- [469] Andrei O. Barvinsky, Mario Herrero-Valea, and Sergey M. Sibiryakov. Towards the renormalization group flow of Horava gravity in $(3 + 1)$ dimensions. *Phys. Rev. D*, 100(2):026012, 2019.
- [470] Hyung Won Lee and Yun Soo Myung. The absence of the kerr black hole in the horava lifshitz gravity. *The European Physical Journal C*, 72(1), Jan 2012.
- [471] Anzhong Wang. Stationary axisymmetric and slowly rotating spacetimes in Hořava lifshitz gravity. *Phys. Rev. Lett.*, 110(9):091101, 2013.
- [472] Sean A. Hayward. Formation and evaporation of regular black holes. *Phys. Rev. Lett.*, 96:031103, 2006.
- [473] I. Dymnikova. Vacuum nonsingular black hole. *Gen. Rel. Grav.*, 24:235–242, 1992.
- [474] M. S. Morris and K. S. Thorne. Wormholes in space-time and their use for interstellar travel: A tool for teaching general relativity. *Am. J. Phys.*, 56:395–412, 1988.
- [475] A. Einstein and N. Rosen. The particle problem in the general theory of relativity. *Phys. Rev.*, 48:73–77, Jul 1935.
- [476] Francis Duplessis and Damien A. Easson. Traversable wormholes and non-singular black holes from the vacuum of quadratic gravity. *Physical Review D*, 92(4), Aug 2015.
- [477] Petarpa Boonserm, Tritos Ngampitipan, Alex Simpson, and Matt Visser. Exponential metric represents a traversable wormhole. *Physical Review D*, 98(8), Oct 2018.
- [478] Marcelo Botta Cantcheff, Nicolás E. Grandi, and Mauricio Sturla. Wormhole solutions to hoava gravity. *Physical Review D*, 82(12), Dec 2010.
- [479] Jerome Martin, Christophe Ringeval, and Vincent Vennin. Encyclopædia Inflationaris. *Phys. Dark Univ.*, 5-6:75–235, 2014.
- [480] Robert H. Brandenberger. String Gas Cosmology. 8 2008.
- [481] Justin Khoury, Burt A. Ovrut, Paul J. Steinhardt, and Neil Turok. The Ekpyrotic universe: Colliding branes and the origin of the hot big bang. *Phys. Rev. D*, 64:123522, 2001.

- [482] Roger Penrose. The basic ideas of conformal cyclic cosmology. *AIP Conf. Proc.*, 1446(1):233–243, 2012.
- [483] A. Pilaftsis. Resonant CP violation induced by particle mixing in transition amplitudes. *Nucl. Phys. B*, 504:61–107, 1997.
- [484] Michael McGuigan. Dark Horse, Dark Matter: Revisiting the $SO(16) \times SO(16)$ ' Nonsupersymmetric Model in the LHC and Dark Energy Era. 7 2019.
- [485] Ivano Basile and Alessia Platania. Cosmological α' -corrections from the functional renormalization group. *JHEP*, 21:045, 2021.
- [486] Ivano Basile and Alessia Platania. String tension between de Sitter vacua and curvature corrections. *Phys. Rev. D*, 104(12):L121901, 2021.
- [487] Ivano Basile and Alessia Platania. Asymptotic Safety: Swampland or Wonderland? *Universe*, 7(10):389, 2021.
- [488] Marie E. Machacek and Michael T. Vaughn. Two Loop Renormalization Group Equations in a General Quantum Field Theory. 1. Wave Function Renormalization. *Nucl. Phys. B*, 222:83–103, 1983.
- [489] Marie E. Machacek and Michael T. Vaughn. Two Loop Renormalization Group Equations in a General Quantum Field Theory. 2. Yukawa Couplings. *Nucl. Phys. B*, 236:221–232, 1984.
- [490] Ingo Schienbein, Florian Staub, Tom Steudtner, and Kseniia Svirina. Revisiting RGEs for general gauge theories. *Nucl. Phys. B*, 939:1–48, 2019. [Erratum: Nucl.Phys.B 966, 115339 (2021)].
- [491] Lohan Sartore. General renormalization group equations for dimensionful couplings in the $\overline{\text{MS}}$ scheme. *Phys. Rev. D*, 102(7):076002, 2020.
- [492] Kristjan Kannike, Kaius Loos, and Luca Marzola. Minima of Classically Scale-Invariant Potentials. 11 2020.
- [493] Leonardo Chataignier, Tomislav Prokopec, Michael G. Schmidt, and Bogumiła Świeżewska. Systematic analysis of radiative symmetry breaking in models with extended scalar sector. *JHEP*, 08:083, 2018.
- [494] Eldad Gildener and Steven Weinberg. Symmetry Breaking and Scalar Bosons. *Phys. Rev. D*, 13:3333, 1976.